Characterisation of Particulate Matter Originating from Automotive Occupant Restraints

Ryan Wood

Department of Mechanical Engineering and Mathematical Sciences

Oxford Brookes University

December 2013

Table of Contents

List of Figures

List of Tables

List of Equations

Nomenclature

ACI	Andersen cascade impactor
ATF	Authorised treatment facility
CI	Cascade impactor
CoD	Certificate of Destruction
CPC	Condensation particle counter
COSHH	Control of Substances Hazardous to Health
CCIS	Co-operative crash injury study
DAB	Driver airbag
DASA	Driver anti-submarining airbags
db	Decibel
DEFRA	Department for Environment Food and Rural Affairs
DfT	Department for Transport
DMS	Differential mobility spectrometer
DMA	Differential mobility analyser
EA	Environment Agency
ECU	Electronic control unit
ELPI	Electrical low pressure impactor
ELV	End of life vehicle
EM	Electron microscopy
EOL	End of life
ESC	Electronic stability control
EU	European Union
EuroNCAP	European New Car Assessment Programme
FBP	Front belt pre-tensioner
FMVSS	Federal Motor Vehicle Safety Standard
FPS	Frames per seconds
FT-IR	Fourier transform infrared
GF	Gravimetric filtration
GMD	Geometric mean diameter
GSD	Geometric standard deviation
GSR	Gunshot residue
HSE	Health and Safety Executive
HSF	High speed film
IC	Inflatable curtain
ICRP	International Commission on Radiological Protection

IDLH	Immediately dangerous to life or health
KAB	Knee airbag
LSLP	Light scattering laser photometer
LEV	Local exhaust ventilation
mg	Milligram
NIOSH	National Institute of Safety and Health
NCAP	New car assessment programme
NHTSA	National Highways and Transport Safety Administration
nm	Nanometre
OPC	Optical particle counter
OOP	Out of position
PAB	Passenger airbag
PPM	Parts per million
PASA	Passenger anti-submarining airbags
PBP	Pyrotechnic belt pre-tensioner
PEL	Permissible exposure limit
PM	Particulate matter
PT	Pressure testing
px	Pixels
QCM	Quartz crystal microbalance
RFCSS	Rear facing child safety seat
RH	Relative humidity
SAB	Side airbag
SEM	Scanning electron microscopy
SMPS	Scanning mobility particle sizer
STEL	Short term exposure limit
SAE	Society of Automotive Engineers
SRS	Supplementary restraint system
SUV	Sports utility vehicle
TEOM	Tapered element oscillating microbalance
TWA	Time weighted average
TEM	Transmission electron microscopy
TM	Tympanic membrane
UK	United Kingdom
USA	United States of America
USCAR	United States Council for Automotive Research
WEL	Workplace exposure limit

Glossary of Terms and Abbreviations

ATF	=	Authorised Treatment Facility. These facilities are permitted to accept end of life motor vehicles and process them in-line with legislation. The compliance of these facilities is enforced by the Environment Agency in the United Kingdom.
Aerosol	=	Solid or liquid particles suspended in gas or air.
CCIS	=	The Cooperative Crash Injury Study (http://www.ukccis.com/). CCIS was one of the world's largest studies of car occupant injury causation. Each year the project investigated more than twelve hundred crashes involving cars or car derived vans. CCIS came to an end in 2010.
ELV	=	End of Life Vehicle. A vehicle that has reached the end of its useful life and is to be disposed of.
Effluent	=	Terminology used by the automotive restraint industry to describe particulate matter and gaseous emissions released during airbag or associated safety system deployment.
FMVSS	=	The National Highway Traffic Safety Administration has a legislative mandate under Title 49 of the United States Code, Chapter 301, Motor Vehicle Safety, to issue Federal Motor Vehicle Safety Standards (FMVSS) and Regulations to which manufacturers of motor vehicle and equipment items must conform and certify compliance (http://www.fmvss.com/).
GMD	=	The geometric mean diameter is defined as the *n*th root of the product of *n* values. For particle distributions this measurand is equivalent to the mean calculated with logarithmic diameters
EuroNCAP	=	European New Car Assessment Programme provides consumers with information regarding the safety of a potential car purchase. Tests generally complement existing regulations.
NHTSA	=	National Highway Traffic Safety Administration. Part of the U.S. Department of Transportation. It was established by the Highway Safety Act of 1970 to carry out safety programs (http://www.nhtsa.gov/About).
OOP	=	Out-of-position. This relates to an occupant being away from the standard position in a seat. An example of this would be if a person is leaning forward in their seat. The implication of this example is that the person could be subjected to the full force of a deploying airbag if its deployment wasn't adapted in some way for such a condition.
PM	=	Particulate Matter. Solid or liquid particles suspended in gas or air
STATS19	=	The national, standardised, form for reporting road traffic accidents (http://www.dft.gov.uk/pgr/statistics/committeesusergroups/scras/2008reviewstats19/stats19repform.pdf).

USCAR	=	United States Council for Automotive Research. Umbrella organization of DaimlerChrysler, Ford and General Motors, formed to conduct cooperative, pre-competitive research.

Acknowledgments

For their help and patience throughout my studies I would like to thank my supervisors Dr. Patricia Winfield and Dr. Stephen Samuel. I would also like to thank all my colleagues at the Transport Research Laboratory, Colas UK and the SAE IRSC.

Further thanks go to Dr. Louise Hughes for assistance with microscopy and Warwick Major and Kieron Tew for technical support. In addition the support and humour from Dr. Ryan McCurdy, Dr. Matthew Clarke, Dr. Nick Hooper and Walter Sweeting was very much appreciated.

Finally and most importantly I'd like to thank Hayley and Isla and all of my family for their love, support and patience throughout this project.

Abstract

In 2012, in the UK, it was estimated that 6.5 million airbags required deployment at end of life. This process poses hazards such as that of occupational respiratory exposure to solid particulate matter (PM) effluents produced during the production of inflation gases for airbag deployment. To date methods for assessing effluent exposure has focused on vehicle occupants and not occupational exposures and has mainly centred on direct and static measurement of particle mass.

This research programme evaluated existing methods of assessment and defined novel methods for more comprehensive characterisation. The methods were employed to characterise sub-micron PM effluents from driver airbags using non-azide, solid propellant and hybrid inflators. Testing was undertaken using a differential mobility spectrometer (DMS), gravimetric filtration, high speed photography and electron microscopy.

A comparison of an effluent test tank and a vehicle of a comparable volume showed that the tank was able to replicate a vehicle environment and provide measurements with acceptable levels of inter-test variability with test duration of >900s.

Characterisation of particle geometric mean diameter (GMD) and number concentration for airbag effluents showed that dominant particles were below 150nm in size, with smaller particles being emitted by hybrid airbags. Particle concentrations were also lower for hybrid airbags. By assessing transient behaviour it was identified that as time elapsed, concentration reduced whilst particle mean size increased.

This data allowed identification of propellants used in airbags and a mathematical model was defined to describe effluent characteristics for each propellant employed.

The particle sizes measured by DMS compared well with those obtained from TEM images which identified generally spherical particles, commonly accumulated as agglomerates. TEM also identified large concentrations of particles below the lower measurement range of the DMS, <5nm, and lower concentrations of larger particles >1μm.

This research has provided verification of existing test methodologies and allowed a more comprehensive assessment of airbag effluents than previously presented in the literature.

Chapter 1

Introduction

With motor vehicle accidents claiming many lives worldwide the implementation of safety systems to provide protection for vehicle occupants and other road users remains a high priority for governments, legislators, manufacturers and consumers alike. Although efforts to avoid collisions are gaining momentum, a truly autonomous vehicle community is still a significant number of years distant. Therefore, systems designed to mitigate the severity of injuries in collisions remain a high priority and continue to develop at pace. One option for mitigation that has been employed extensively is the use of airbags that are designed to operate in conjunction with safety belts. These are designed to decelerate a vehicle occupant at a reduced rate in a collision, whilst preventing interaction between an occupant and the vehicle interior and ejection from a vehicle during a roll-over. The airbag cushion is inflated with a gas that is commonly generated by the burning of a solid propellant and is designed to be fully inflated by the time it is impacted by a vehicle occupant.

Where these systems are not consumed during collisions they remain as an environmental and health hazard at a vehicle's end of life (EOL) and must be neutralised (by deployment or disabling) to minimise their impact and to ensure compliance with legislation (European Commission, 2000). Large numbers of these airbags are neutralised by a relatively small population of staff at treatment facilities with generally simple techniques and equipment. Of the hazards posed to the staff tasked with neutralisation, the exposure to the solid particle matter output, (referred to in the literature and within this thesis as an effluent), which is created by the burning of a solid propellant is less well understood and documented than others.

This thesis is therefore concerned with the methodologies used for assessment of these effluents and the measurement, definition and understanding of their characteristics. To achieve this aim the following objectives were required to be met:

- Review occupant restraint technologies and their uptake in passenger cars.
- Identify the scale of un-deployed airbags reaching the end-of-life vehicle depollution industry and define legislative and technical requirements and common practice associated with their neutralisation.
- Identify airbag test samples representative of those likely to be encountered at end-of-life vehicle depollution facilities.
- Robustly assess and compare existing test methodologies for airbag effluent characterisation and construct suitable test facilities to facilitate comparisons and characterisation of airbag particle effluents.
- Define the effects of ventilation of a test vehicle after airbag deployment on particle effluent characteristics.
- Define new test methodologies for airbag particle effluent testing where required.
- Characterise the particulate effluents emitted during airbag deployments.
- Define a test methodology for collecting particle effluents for assessment of morphology and characterise the tested effluents.

A research programme was devised to achieve these objectives and the structure of the programme and thesis is defined in Figure 1.1.

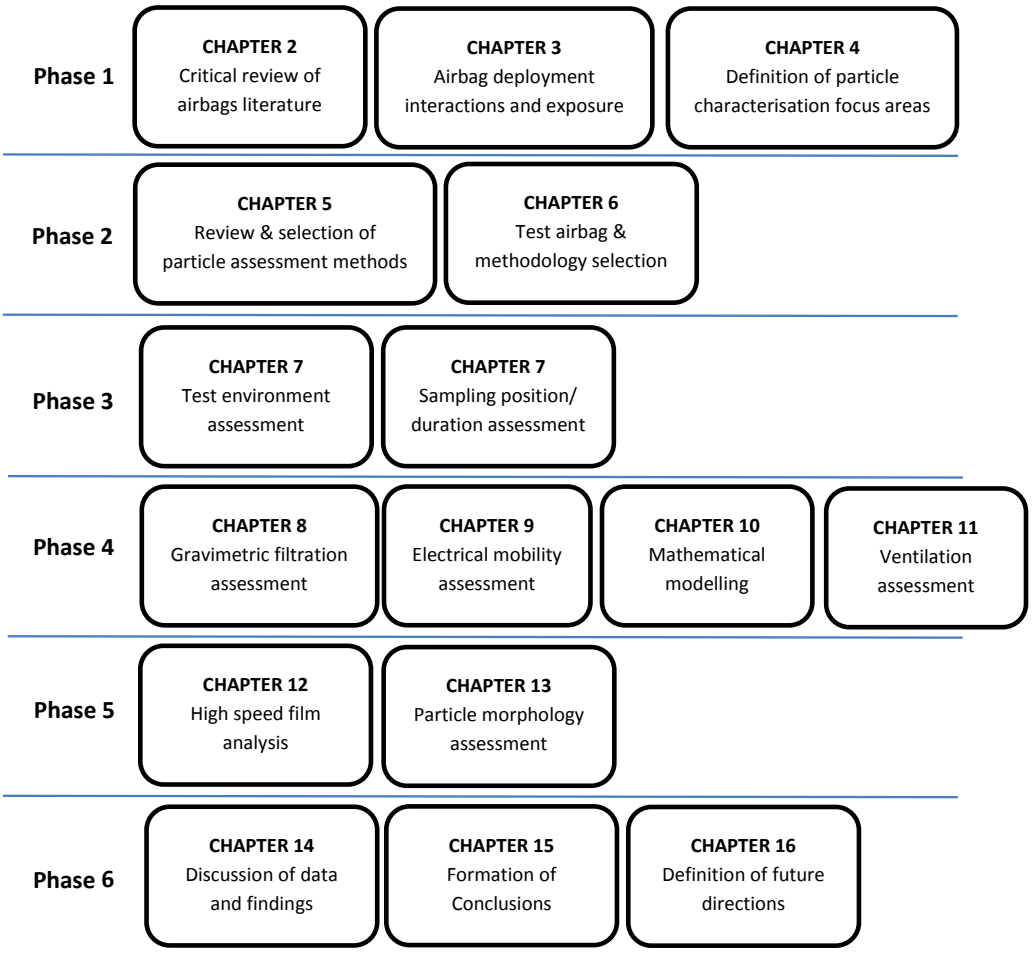

Figure 1.1: Research Programme Structure

As illustrated in Figure 1.1 the research programme and therefore thesis is divided into 6 phases made up of a number of stages. A summary of these follows:

Phase 1: Critical review of literature, assessment of airbag exposure and interaction and definition of PM characteristics focus areas

The initial Phase starts with Chapter 2, detailing the purpose of occupant restraint systems such as airbags and safety belts and provides a detailed summary of key airbag system characteristics. This includes a review of the various airbag types and applications, such as driver front, passenger and curtain; the inflator type, including solid propellants, hybrids and compressed gas and the compositions of these propellants and gases as previously summarised by Chan et al., (2000). Other characteristics including inflator staging, cushion volumes and shapes, filtration, tethering and venting are also discussed. This introduction to the review has shown an increase in the capabilities and complexities of airbag systems and their effectiveness at reducing injury risk for occupants (Hynd et

al., 2011). The uptake of these systems within vehicles is also documented to provide an indication of scale.

Whilst airbags offer great advantages to vehicle occupants in a collision, they also pose hazards not only to occupants but others interacting with these systems at end of life and this is explored in Chapter 3. A summary of the requirements for neutralisation of airbags at the end of a vehicle's life is described in Chapter 3, alongside a calculation of the number to be neutralised in the United Kingdom (UK) and a brief summary of current practices and likely exposure scenarios.

The initial phase is concluded in Chapter 4 with a review of key particulate matter (PM) characteristics and their effect on human health and definition of those characteristics investigated within the research programme.

Phase 2: Review and selection of PM assessment methods, test samples and methodologies

Phase 2 details the key characteristics of PM and their influence on human health and selects those characteristics to be investigated, within the research programme, in Chapter 5. Airbag test samples and methodologies are evaluated in Chapter 6 and suitable options chosen.

Phase 3: Test environment and methodology assessment

As identified in Phase 1 that there is little data in the literature to define the capabilities of test methodologies to provide robust and representative data from tests of airbag effluents. Consequently an assessment of test methodologies was conducted in Chapter 7 and it considered the interior of a car and an effluent test tank specially constructed by the author. The assessment used a DMS to define test durations, inter-test variability, the variation attributed to differences in sampling location and any differences between the test vehicle and effluent test tank. The assessment ultimately yielded a methodology that was utilised to undertake a large element of the assessment of airborne airbag effluents conducted in Phase 4. A test matrix is also presented.

Phase 4: Effluent Characterisation, mathematical modelling and ventilation assessment

Phase 4 is composed of Chapters 8 to 11, which detail the results of practical tests and assessments. Chapter 8 details the characterisation of the solid particle effluents produced during airbag deployment by means of gravimetric filtration (GF) assessment. A substantial element of this research, which demonstrated a novel assessment of effluent characteristics by measuring the electrical mobility of particles, is reported in Chapter 9.

From this data a mathematical model of key characteristics of the effluents is also presented and evaluated in Chapter 10. To provide information regarding the exposure condition, a further assessment of the effluent was conducted to define the effect of ventilation of a test vehicle on the particle effluent and this is presented in Chapter 11.

Phase 5: Morphology assessment and high speed film analysis

An assessment of airbag deployment by means of high speed photography and any association with effluent test data is presented in Chapter 12. To provide further information regarding particle characteristics and to allow size distribution comparisons with the data collected by DMS in Phase 4, a morphological assessment was conducted using Transmission Electron Microscopy (TEM) and Scanning Electron Microscopy (SEM) and the data and associated analysis is presented in Chapter 13.

Phase 6: Discussion of data and findings and formation of conclusions

Chapter 14 provides a discussion of the review conducted in Phases 1 and 2 and the experimental test data and analysis from Phases 3 – 5. Conclusions were drawn from this data and analysis and were compared against the project objectives as a metric for achievement and these are presented in Chapter 15. Whilst the presented research was comprehensive, opportunities for further work to expand knowledge further in the field are also presented in Chapter 16.

Chapter 2

Automotive Restraint Systems

2.1 Introduction to occupant restraint systems

In Great Britain fatalities and injuries occurring during vehicle collisions have been reducing since the implementation of a governmental 'Road Safety Strategy' in 1987 (DfT, 2011a). This has been attributed to improvements in driver training, road infrastructure, increased testing requirements and vehicle development. Changes to legislation, the development of improved driver safety systems by manufacturers and consumer testing programmes such as the European New Car Assessment Programme (EuroNCAP, n.d.) have all contributed to the improvements in protection offered to vehicle occupants. These improvements have resulted in significant changes to vehicle structures and through the provision of airbags, which has resulted in improved injury outcomes and a reduction in fatalities occurring in collisions (DfT, 2011a). However, during 2011 alone, 203,950 casualties were still reported on the roads of Great Britain and of these, 1,901 were fatally injured and 23,122 sustained serious injuries (DfT, 2012a).

Occupant restraint systems are designed to reduce these injuries and allow the vehicle occupant to decelerate inside the vehicle at a reduced and controlled rate, whilst minimising the possibility of contact between the occupant and the vehicle's interior. These systems are also used to ensure that a vehicle occupant is positioned in the optimum position during a collision and not ejected from the vehicle. Occupant restraints form part of the complex and comprehensive safety systems of a modern vehicle, as shown in Figure 2.1.

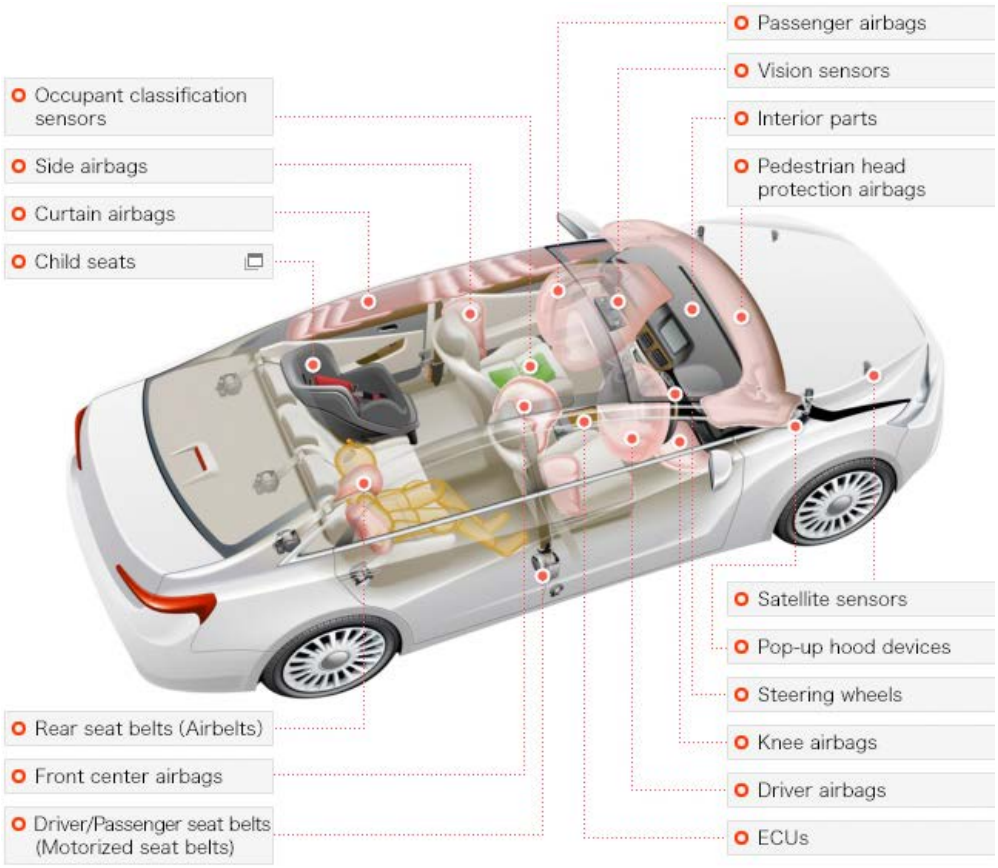

Figure 2.1: Occupant safety systems (Takata, 2013)

The level of protection and effectiveness provided by a restraint system will vary depending on (a) impact characteristics, (b) vehicle size and mass, (c) vehicle occupant characteristics (mass, physical size, age, bone density etc.), and (d) seating position (Hynd et al., 2011).

Although occupant restraints (including airbags and safety belts) are predominantly designed to minimise the injuries to vehicle occupants in collisions, systems using similar technologies have now been developed to protect pedestrian in vehicle impacts (pedestrian airbags and actuators) (Jaguar, 2011; Volvo, 2013) and for pre-collision safety systems such as emergency brake actuation (Volkswagen, 2008).

The combined efforts of legislators (European Commission, n.d.), manufacturers and consumer testing programmes such as Euro NCAP (EuroNCAP, n.d.) has led to rapid developments in vehicle safety over the past two decades, with substantial improvements in sectors such as vehicle structures and active safety systems, designed to prevent a collision, yet none more so than in occupant restraint systems.

The greatest and most effective developments in the field of vehicle occupant restraints have been realised through the use of pyrotechnic and compressed gas (released by pyrotechnics) systems. The use of such technologies allows a safety system to react to a

collision and provide injury mitigation within the extremely short timeframe of an impact. These restraints can be simply divided into four main segments, which are detailed further in the following sections:

1. Inflatable restraints (airbags)
2. Safety belts
3. Actuators
4. Airbag control

2.1.1 Inflatable restraints

The essentials of an airbag system described by Chan (2000), are the sensors, inflator, cushion and vehicle interior (comprising of a module and compliant vehicle interior). Sensors identify an impact occurrence and its severity and determine the need for airbag deployment. The decision, based on a pre-set algorithm is used as the 'trigger' for deployment of not only airbags but other restraint systems such as seatbelt pre-tensioners. Whereas early systems simply initiated deployment, an increase in sensor technology now allows adaptive systems to react to specific crash pulses and vehicle occupants, altering the behaviour of the restraints to suit.

The inflator provides gas volume to the airbag cushion, releasing it from its position of rest and inflating it to the desired shape and size. The inflator's initiator will react to either mechanical stimulus, in early systems, or more commonly a signal from the Electronic Control Unit (ECU) and sensors and in the case of a solid propellant inflator, rapidly burn a compound to generate gas. Hybrid inflators use a combination of a compressed gas and a solid propellant to provide an often larger, cooler and 'cleaner' gas volume, whilst compressed gas inflators provide inflation from a stored inert gas. These systems are discussed in further detail within section 2.2.5.

A fabric (ordinarily Polyamide) bag filled by the inflation gases provides a cushion that allows the controlled deceleration of a vehicle occupant during an impact, whilst preventing interaction with other interior surfaces and ejection from the vehicle. The cushion can incorporate tear-seam stitching or tethers to control the forward inflation distance, whilst venting voids (positioned to the rear) allow simplistic control of internal cushion pressure. This careful control of cushion pressure and timing allows the force of the airbag and that of the vehicle occupant (impacting the cushion) to be balanced, limiting the risk of the airbag injuring the occupant or not being sufficiently stiff to prevent the bag from not sufficiently cushioning the occupant (known as 'bottoming-out').

The vehicle interior, engineered in tandem with the airbag allows the module to be positioned in a position commensurate with the expected occupant seating and interaction

position. For some interiors and airbag positions a deflection plate will guide the inflating cushion to the correct position and provide support during the impact (Hynd et al., 2011). The airbag mounting must be capable of withstanding both the force from deployment and that exerted by the vehicle occupant as the cushion is compressed and ridden down during an impact.

Airbags were first used in vehicles as an injury mitigation system for frontal impacts, as these incidents account for the majority of collisions (Hynd et al., 2011). These airbags are fitted within the steering wheel for the driver and generally within the upper dashboard for the passenger and are designed to dissipate the occupant's kinetic energy and provide a low deceleration rate whilst preventing interaction with hard surfaces inside the vehicle (Richert et al., 2007; Figure 2.2). It should be noted that there are different requirements for drivers airbags fitted in Europe and the US, the former being 30litres of gas and the latter 50litres.

Figure 2.2: Ford driver frontal airbag (Ford, 2013)

Working in conjunction with the frontal airbag system, a knee airbag, which is usually only fitted on the driver side, is used to reduce the severity of knee, leg and hip injuries received during a collision.

Whilst frontal impacts are likely to be the most common collision types, side impacts carry an increased probability of serious injuries (Braver and Kyrychenko, 2004). In these incidents, side airbags, generally fitted to the outer flank of the seat back, provide protection against impact and intrusion injuries for vehicle occupants, Figure 2.3. Side airbags, sometimes referred to as torso airbags are commonly fitted to the first seating row but are now becoming increasingly prominent for both second and third row seats.

Figure 2.3: Side and curtain airbag (NSW Centre for Road Safety, n.d.)

In rollover incidents and some side impacts an Inflatable Curtain (IC) airbag, commonly fitted to the vehicle pillars and roof, provides protection to the vehicle occupant and minimises the risk of ejection from the vehicle. Where curtain airbags cannot easily be incorporated into the roof, such as in convertible vehicles, the side airbag may provide protection for the head in addition to the thorax. These airbags are commonly fitted for front and rear outer seat positions and are inflated and held at full inflation for extended periods to provide protection and prevent ejection from the vehicle during protracted collision events, such as rollovers.

In vehicles where passenger access to the rear seats (via a tipping front seat) prevents the easy fitment of outboard safety belt pre-tensioners, anti-submarining airbags may be fitted within the base of the front seats (Renault, n.d.). These airbags mounted internally within the seat deform the front portion of the seat base to prevent occupants from sliding below the safety belt, an instance commonly referred to as 'submarining'.

In addition to these more commonplace airbags, there are a number of others that are beginning to be utilised for occupant protection in mainstream vehicles. Examples include the rear seat interaction airbag, designed to prevent interaction between inboard and outboard rear passengers during a collision and the rear impact protection airbag that inflates behind the rear seats of vehicles with seating close to the rear of the vehicle body, to improve the protection offered in a rear impact (Toyota, 2010).

Airbags (and pyrotechnic actuators) are now also finding use as protection for pedestrians and are likely to be fitted to mass production vehicles by manufacturers including Volvo in the near future, Figure 2.4.

Figure 2.4: Volvo Pedestrian Airbag System (Volvo, 2013)

Prior to the introduction of these systems, protection for pedestrians was limited to a more compliant impact area and amendments to traditional materials and designs, which provide much improved yet ultimately limited results. The inclusion of pedestrian impact performance within the Euro NCAP crash testing programme provides the likely impetus for the implementation of external airbag systems and is likely to continue to influence their implementation.

2.1.2 Safety belts

Approximately 65 years prior to the conception of the airbag system, safety belts were first patented for those working at height, and by the 1950's they had begun to be fitted to vehicles. During 1959 the automotive, three point safety belt was first conceived by Nils Bohlin whilst working at Volvo and the widespread success of the system and an open patent resulted in their proliferation as a standard safety feature from this date (Volvo, 2009). They are likely to be the most significantly effective occupant restraint system fitted to vehicles, having been directly responsible for the prevention of in excess of 143,000 fatalities in the US alone between 1999 and 2009 (NHTSA, 2009a). Safety belts are generally manufactured from woven polyester and are designed to limit the movement of a vehicle occupant during a collision. They significantly minimise the risk of interaction with the interior of the vehicle and also the possibility of ejection in roll-over collisions. Belts spread the load caused by the inertia of the body when the vehicle they are travelling in is decelerated quickly during a collision across stronger parts of the body, such as the pelvis. Safety belts are now designed to work in conjunction with airbags, although some airbags in use outside of Western Europe are also designed to operate without a safety belt, to account for collisions involving unbelted occupants.

Early safety belt systems used a simple mechanical retractor that allows the fabric belt to be 'payed-out' and tightened when an occupant attaches or releases the safety belt and in the event of a collision a mechanical locking device prevents the belt from being payed-

out again. The locking mechanism either reacts to the speed of rotation of the spool holding the coiled belt, or is activated by a pendulum that locks into place when a specific level of acceleration is experienced. These basic safety belts have now been supplemented by other systems such as load limiters, pre-tensioners and inflatable belts that are capable of further reducing the injury risk in a collision.

A load limiter is designed to limit the load transmitted through the shoulder belt to a tolerable level by allowing the belt to pay-out a predefined amount and to allow the torso of the occupant to move forward within the vehicle. With too high a load limit the presence of the belt is still likely to result in injury to the occupant (Mertz and Dalmotas, 2007), yet with too low a limit the occupant may move forward too far and actually 'bottom-out' the airbag, striking the steering wheel or surrounding fascia. Most load limiters are mechanical devices set with a pre-defined, constant load limit level, but others can adapt to the amount and duration of force being applied to the device and some using a small pyrotechnic are able to 'switch' to a lower secondary load limit (TRW, n.d.).

Safety belt pre-tensioners are designed to retract and apply tension to the belt and remove any slack in response to a collision. This limits the amount of forward movement of the occupant during a collision and minimises the risk of the occupant sliding below the belt (submarining) in a frontal impact. This reduction in forward motion is able to provide an associated reduction in load upon the occupant of over 20% and also to increase the airbag ride-down time (Müller and Linn, 1998). For occupants who may be slightly out of position, the application of tension to the safety belt may also help to ensure that a vehicle occupant is held within the optimum position during a collision.

These pre-tensioners utilise a pyrotechnic sub-system commonly fired at the same time as the airbag to tension the belt at the shoulder or lap positions. Conventional systems will use a dual pre-tensioning system at the reel (shoulder belt), Figure 2.5, and at the inboard lap belt anchoring point (buckle), Figure 2.6, but both systems may be used independently.

Figure 2.5: Reel Pre-tensioner

Figure 2.6: Buckle Pre-tensioner

Early systems predominantly used a mechanical sensing system that responded to deceleration during an impact (CDX, 2010), whilst most contemporary pre-tensioners react to electrical stimulus from satellite sensors (Autoliv, n.d.). Upon receiving a signal from the sensors, an initiator will ignite a larger pyrotechnic charge that in turn generates gas and operates the pre-tensioner. Buckle pre-tensioners commonly use a piston and cable arrangement where the generated gas pushes against a piston connected to a cable and the safety belt buckle. This movement pulls the buckle downwards and creates tension in the belt. A reel pre-tensioner works in a similar manner, but commonly uses the generated gas to push a ratchet connected to the spool (holding the belt) or by directly rotating the spool to tension the belt. Figure 2.7 shows this operation and schematic 'A' shows the pre-deployment configuration of the pre-tensioner. Schematic 'B' shows the stage where the gas generator has been initiated and has forced the ball bearings around a ratchet that in turn has rotated th A actor spool and retracted the belt.

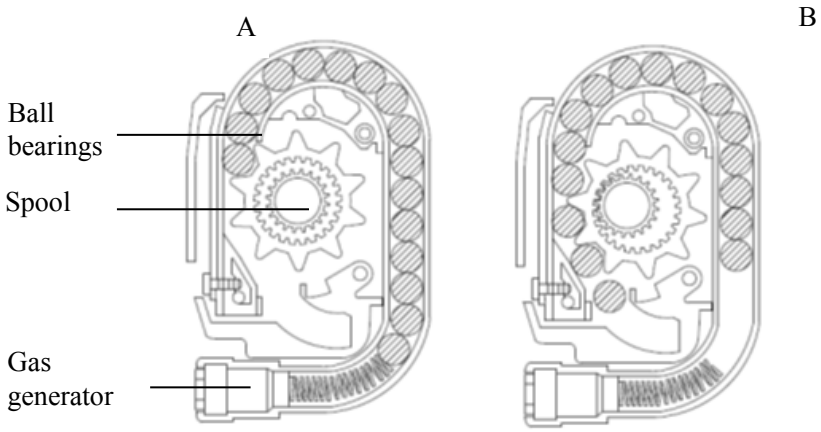

Figure 2.7: Safety Belt Reel Pre-Tensioner Schematic (Hamaue et al., 2004)

Inflatable seatbelts, as first demonstrated upon the Ford Explorer during 2011, provide greater head, neck and chest protection in rear seat positions. The system uses a modified belt and buckle arrangement and a compressed gas inflator, which on impact inflates a cushion similar to an airbag within the transverse element of the belt. This inflation provides a surface area five times greater than that of a standard belt, helping to distribute the force across the body (Ford, 2013).

Figure 2.8: Ford Inflatable Safety Belt (Ford, 2013)

2.1.3 Actuators

Recent developments in occupant and pedestrian safety have resulted in a proliferation of 'small' solid propellant actuators in modern vehicles (EuroNCAP, 2011; BMW, 2013) for relatively small operations within safety systems, such as the following:

- Rollover Protection Systems
- Active head restraints
- Bonnet actuation
- Battery isolation

Rollover protection systems fitted to convertible vehicles limit collapse of the vehicle structure in the absence of a fixed roof and thus increase protection for occupants. Where vehicle sensors detect a rollover situation, two small pyrotechnic actuators are mechanically or more commonly electrically initiated and operate small piston actuators, releasing a high potential energy spring, pushing up a strengthened rollover hoop to protect vehicle occupants.

In many significant collisions, such as rollovers, the presence of a live battery connection poses a post-collision risk of fire to occupants and emergency service personnel from short circuits and arcing (aei, 2007) In response to these risks vehicle manufacturers developed a pyrotechnic battery isolation device to split the main vehicle positive battery

connection (BMW, 2013). The presence of high currents passing through this cable means that a fuse does not provide a suitable solution and therefore a small pyrotechnic, contained within a housing upon the main battery lead, Figure 2.9, is able to split the connection at a pre-defined point, thus isolating the battery and reducing the post-collision injury risk (aei, 2007).

Figure 2.9: Pyrotechnic battery isolator

Figure 2.10: Pyrotechnic active head restraint

Most companies use passive rear impact seating and in some cases actuators are now also starting to be utilised as part of mitigation measures against whiplash injuries in rear impacts. Active head restraints use a pyrotechnic actuator (Figure 2.10) to release a spring loaded mechanism, moving the head restraint in the direction of the impact and therefore reducing the distance to the rear of the occupants head. This movement minimises the risk of hyperextension of the neck and associated whiplash injuries.

Aside from those systems using pyrotechnic actuators to provide protection to vehicle occupants, a number of vehicles are now being equipped with multiple actuators to elevate a vehicle's bonnet in a collision with a pedestrian as a means of reducing injury risk. This elevation provides a void between the bonnet and engine block and any other rigid components within the engine bay and allows deformation and thus a degree of 'cushioning' for the impacting pedestrian.

There are a number of other uses for small pyrotechnic actuators within vehicle safety, such as for emergency braking systems (Volkswagen, 2008) and as a means of controlling airbag performance, and their usage can be expected to increase in the future.

2.1.4 Airbag control

Airbags are generally optimised to provide protection for a mid-sized, young male occupant with EuroNCAP currently using 50th percentile Hybrid III male dummies (Hynd et al., 2011). For many individuals the occupant energy will differ to that of the tested occupant, which may result in a less than optimal restraint system performance and a subsequent inequality in protection. In the case of high occupant energies (during severe/high speed impacts and for higher mass occupants) there is a possibility that the

airbag is not stiff enough (filled with enough pressure), resulting in 'bottoming out', where the occupant compresses the airbag and impacts the surfaces below. For lower occupant energies (low speed/severity and smaller, lighter occupants) the airbag may be too stiff or large and result in avoidable injuries to the neck, upper limbs, chest or face. Mackay et al. (1998) described these occupant energies:

- "A 100-pound [45 kg], 70-year-old woman who is a front seat passenger is sitting well back and is involved in a 20-mph [32 km/h] frontal collision with no intrusion: she would be best protected by a relatively soft restraint system and a soft air bag.
- … a 25-year-old 220-pound [100 kg] man sitting close to the steering wheel in a 40-mph [64 km/h] offset frontal collision. He would need an early deploying stiff airbag.

Mackay et al. (1998) identified the requirements of restraint performance for occupants of different gender, age, mass, stature and seating position. To provide an optimal and equal level of protection for these different occupant types, these factors need to be considered. Systems are now available that are able to adjust performance, but currently are not widely implemented due to the cost of the systems.

The simplest and earliest form of control may well be the dual stage inflator, which is able to provide two levels of inflation performance and was originally created in response to fatalities caused by occupants in close proximity to the airbag. Whilst dual stage inflators are limited to only two performance levels, variable output inflators allow real-time adjustment of inflator mass flow rate in response to sensory inputs and afford even greater control of airbag pressure and volume

Aside from these staged and variable inflators, inflatable restraint systems are now able to vary airbag cushion venting and tethering to control airbag performance and these are discussed further within section 2.5. Daimler-Chrysler demonstrated the '*Continuously Adaptive Restraint*' system which combined systems capable of adapting airbag shape and volume and inflator performance into a single package capable of responding to the requirements of a diverse range of occupants and collisions, indicating the continuing intent of mainstream manufacturers to utilise adaptive restraint technologies, (Richert et al., 2007).

2.2 Inflator and actuator types

Three basic options exist for producing or providing inflation or actuation gases for automotive safety systems. These gases are used to inflate airbags or operate actuation systems and can be generated by rapidly burning a solid propellant, releasing a

compressed gas and 'augmenting' with a solid or liquid propellant or by just releasing a compressed gas. Each technology offers both advantages and disadvantages that are considered by vehicle manufacturers when selecting technologies for occupant protection applications. These parameters include cost, size, gas mass flow rate, uptime capability, inflation speed, pressure and temperature amongst others.

These options for provision of inflation gases can be divided into three main types; solid propellants, hybrids and compressed gas systems. Each of these types is generally suited to specific restraint system applications and typical utilisation is identified in Figure 2.11 with their operation discussed within the following sections.

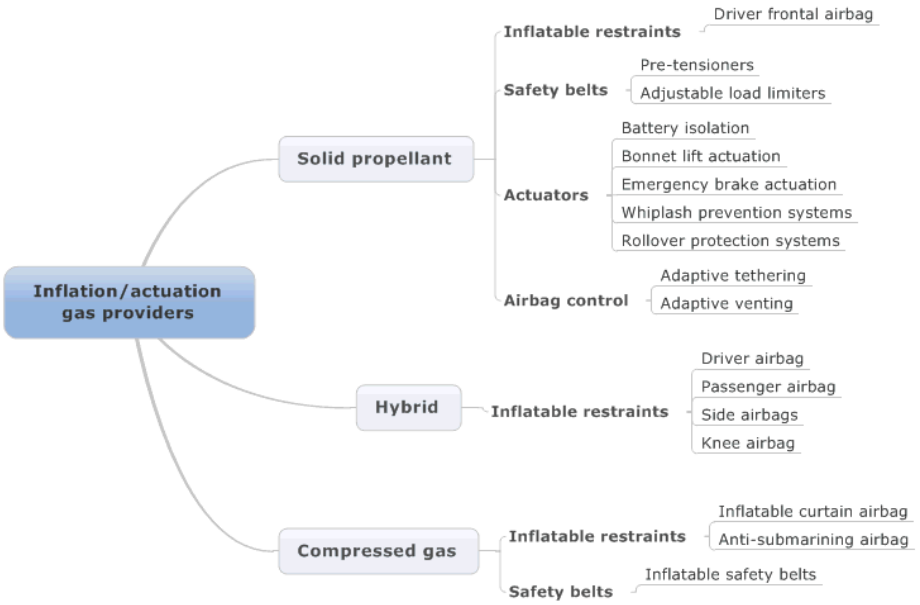

Figure 2.11: Restraint system 'inflation/actuation gas providers'

2.2.1 Solid propellants

The rapid burning of a solid propellant generates gas which provides the capability to inflate airbags and operate actuators within the short timescales required for protecting occupants during motor vehicle accidents. In most cases the inflator's initiator (a smaller propellant charge that ignites the main propellant) will react to a signal from the Electronic Control Unit (on instruction from the sensors) and rapidly burn a compound to generate gas. The initiator is heated by means of a supplied current from the source and this ignites a small propellant load, which in turn ignites a larger propellant mass, creating the gas output required to inflate an airbag or operate a seatbelt pre-tensioner or actuator. For dual stage systems (Figure 2.12) the propellant mass is divided into two sections and allows simplistic gas output control.

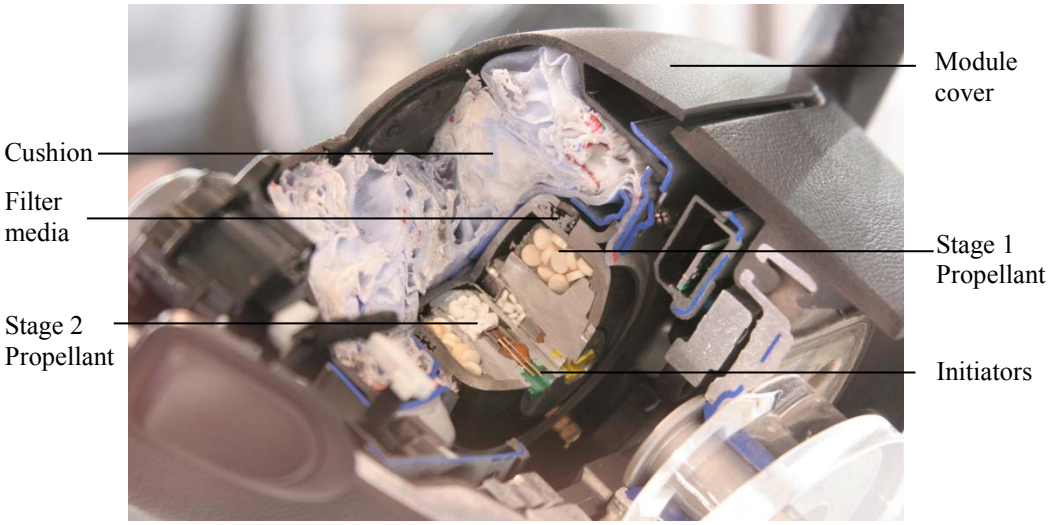

Figure 2.12: Dual-stage solid propellant airbag module

The initiator receives the signal from the crash sensor and a bridgewire in direct contact with the initiator charge is heated by the current from the firing circuit, (Figure 2.13 and 2.14). The increase in temperature created by the bridgewire is sufficient to ignite or initiate a charge, typically composed of titanium or zirconium powder as the fuel and potassium perchlorate as an oxidiser (Little, 1992). The burning of this charge initiates the burn of the main solid propellant load producing inflation gases. In some cases a secondary or booster charge within the initiator is ignited and this in turn initiates the burn of the main solid propellant load.

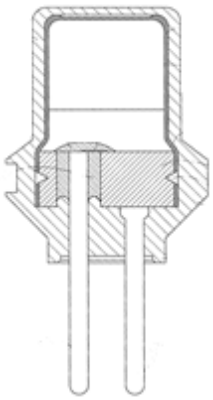

Figure 2.13: Typical airbag initiator (Avetisian et al., 2006)

Figure 2.14: Initiator within inflator assembly

The combustion of these solid propellants produces inflation gases and also undesirable products of combustion such as high temperature solid and gaseous emissions. The temperature of these inflation gases typically ranges between 200°C and 700°C (Reed, 1994; Wallis and Greaves, 2002). These high temperature gases may compromise the

integrity of the airbag cushion or pose hazards to vehicle occupants and therefore filter devices are used in mitigation. These increase the complexity of the inflator design and thus also increase the cost (Green et al., 1999). In addition to the use of a filter to reduce the temperature of inflation gases, cushions for solid propellant (and some hybrid) airbags are coated with neoprene or silicone to ensure cushion integrity (Green et al., 1999).

2.2.2 Solid propellant inflator compositions

While most of the earliest airbag systems (Hetrick, 1952) used compressed air or gases such as Freon and Nitrogen to inflate the airbag cushion, the first utilisation of a deflagrating substance was that of 'black powder', used to heat Freon to inflate a driver's airbag. Heating Freon produces phosgene gas, ($COCl_2$), an extremely hazardous substance (Hollembeak, 2010) and therefore its use for occupant protection was short lived. During the 1950's and early 60's some advances in propellant design were made, but John Pietz's (1975) demonstration of a nitrogen producing solid propellant for airbag inflators in 1968 proved to be the solution to the generation of inflation gases for restraint systems. The propellant made from a composition of sodium azide (NaN_3) and a metallic oxide and initiated by a primary 'initiator' became the widest utilised propellant composition for automotive airbags for many years.

The oxidising agents used in sodium azide propellants included copper oxide, iron oxide and silicon dioxide amongst others (Chan et al., 1989). The oxidation of sodium azide predominantly produces nitrogen gas (N_2), heat and sodium oxide (Gross et al., 1999) and other solid and gaseous outputs discussed further within Chapter 3. The balanced equation for the decomposition of sodium azide alone is shown in Equation 1 (Kubota, 2002).

$$\mathbf{2\ NaN_3 \rightarrow 2\ Na + 3\ N_2} \qquad \textbf{(Equation 1)}$$

The addition of potassium nitrate (KNO_3) as an oxidant and silicon dioxide (SiO_2) as a fuel results predominantly in the production of nitrogen as the inflation gas, potassium oxide (K_2O), sodium oxide (Na_2O) and silicon dioxide (SiO_2). Equation 2 summarises the decomposition or deflagration of the propellant, (Kubota, 2002).

$$\mathbf{2Na + 2KNO_3 + SiO_2 \rightarrow K_2O + Na_2O + N_2 + SiO_2} \qquad \textbf{(Equation 2)}$$

Sodium azide as a propellant in its solid form poses a number of hazards to both the environment, those involved in its manufacture and to the environment (Lee, 1982). This has resulted in almost complete removal of sodium azide as a propellant for restraints in European and American vehicles.

The reduced utilisation of sodium azide mixtures as a solid propellant has resulted in the development of alternative 'non-azide' propellants that provide comparable or increased performance and reduced environmental hazards. These propellants predominantly use oxidisers such as potassium nitrate and ammonium perchlorate, which decompose at moderate to high temperatures. A metallic, such as aluminium, serving as the fuel and a binder is added to provide stability and longevity (Names withheld, 2000; 2002; 2003; 2006; 2008).

The addition of heat to ammonium perchlorate yields nitrogen (the inflation gas), water, hydrochloric acid and Oxygen, Equation 3.

$$\mathbf{2NH_4ClO_4 + heat \rightarrow N_2 + 3H_2O + 2HCl + 2.5\,O_2} \quad \textbf{(Equation 3)}$$

In addition to an oxidiser, such as ammonium perchlorate, a pyrotechnic mixture will contain one or more fuels (electron donors), these react with the oxygen released by the oxidiser (for an airbag system) to produce a *large volume of low molecular weight gas* and a rapid burning rate (Conkling, 2011). Common fuels used for automotive propellant applications include, 5-Amino Tetrazole (CH_3N_5), Guanidine Nitrate ($C(NH_2)_3NO_3$) and Aluminium (Al) (Name withheld; 2002; 2004; 2005; 2008; 2008; 2010).

The use of an energetic metallic fuel, such as aluminium, in propellant mixtures does not enhance the production of output gases, as required for airbag systems, but does increase the burn rate of the propellant, which results in the production of solid metal oxides as a product of combustion (Conkling, 2011).

To bind all elements of the pyrotechnic mixture together and provide mechanical strength to the propellant, an organic polymer is added to act as a binder. The strength and durability provided by this is a key requirement for an airbag or restraint system, as the propellant is subjected to sustained vibration and movement throughout its life, which could affect the burn rate if its integrity cannot be maintained. Typical binder materials include Polybutadiene, Polyvinyl acetate and Viton (Conkling, 2011).

In addition to the binder, ballistic additives may be added to modify the burn rate characteristics of the propellant and optimise the rate of inflation of the airbag cushion or actuation of other restraint systems (Assovskiy et al., 1997; Fogelzang et al., 1998).

Aside from those common propellants using nitrates and perchlorates, single base nitrocellulose propellants, based on nitrocellulose alone, are used widely for micro gas generators (MGG) within seatbelt pre-tensioner assemblies (Perotto and Banes, 2002). Although limited in terms of thermal stability and oxygen balance, nitrocellulose propellants provide high gas outputs, good auto-ignition properties and considerable performance adaptability whilst remaining at a low cost and producing lower outputs of toxic gas (Nitrochemie Wimmis AG, 2005).

2.2.3 Solid propellant mass and size

The mass of solid propellants used in airbag applications varies by the application and thus cushion volume, inflator type (hybrid/solid) and propellant type and characteristics. Indicative propellant masses calculated from manufacturer data for solid propellant driver airbag inflators and solid and hybrid passenger airbags are shown within Table 2.1.

Fitment	Type	Mean mass (g)	Min. mass (g)	Max. mass (g)
Driver Airbag	Solid propellant	42.8	25	51.9
Passenger Airbag		65	60	73.4
Passenger Airbag	Hybrid	22.5	9	36.5

Table 2.1: Solid propellant inflator mass

Propellant masses of solid propellant passenger airbags are higher than for driver airbags, reflecting the larger volumes of passenger airbag cushions and therefore the requirement for higher inflation gas volumes from deflagration of propellants. Hybrid systems for passenger airbags however require lower propellant masses than their solid propellant counterparts, due to the provision of a proportion of inflation gases from a stored compressed gas.

Most solid propellants are press formed into pellets of varying sizes and shapes with the surface area of the tablets affecting the burn rate of the propellant and thus its performance. Assessment of propellant pellets by the author, from various airbags identified only disc shaped forms with similar thicknesses and varying diameters, Table 2.2. Although not a statistically robust assessment, this data may be considered indicative of the propellant pellet characteristics used in airbag inflator applications.

Pellet	Diameter (mm)	Thickness (mm)
1	8	1.7
2	8	2
3	4	1.2
Mean	6.7	1.6

Table 2.2: Solid propellant pellet dimensions

2.2.4 Hybrid inflators

The use of hybrid inflators extends to driver, passenger, side and curtain positions and these offer a number of advantages over the solid propellant base inflators discussed previously, which include:

- reduced gas temperatures
- an anticipated reduction in gaseous and particulate effluent concentration
- increased ability to stay inflated (uptime capability)
- the ability to provide greater inflation volume.

Hybrid inflators were first used for passenger airbags but are now used in many other systems/positions and can provide inflation gases for airbags of between 3 and 150 litres (ARC Automotive Inc., 2009), Figure 2.15. These inflators utilise inert gases, typically Argon, with Helium, Oxygen or N_2O, held under high pressure (up to 4000psi) in conjunction with a solid propellant. A large proportion of the inflation gas is produced by the stored gas and therefore a reduced mass of pyrotechnic material is required in comparison to solid fuelled inflators.

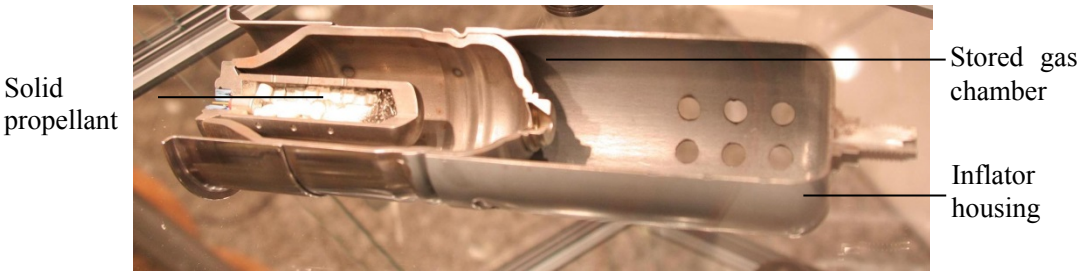

Figure 2.15: Hybrid inflator assembly cutaway

An initiator similar to those used in solid propellant airbags ignites the solid propellant, increasing the pressure inside the primary inflator housing. This increase in pressure causes a disc, which separates the solid propellant from the compressed gas, to rupture. The burning solid propellant heats the compressed gas, compensating for the cooling effect resulting from its expansion and provides sufficient inflation gases to inflate the airbag cushion.

As high storage pressures are required for the large volume of gas required to inflate most airbags, the inflator body must be produced from a relatively high thickness material to increase strength and ensure structural integrity. This requirement for the higher mass materials for gas storage and a large inflator size increases the overall size and mass of the airbag module (Green et al., 1999).

Information presented by the National Highway and Transport Safety Administration (NHTSA) stated that hybrid inflators were first introduced within passenger side frontal

airbags in 1994 and by 1998 they accounted for ~46% of all inflators in this position, with their prominence appearing to have increased since that date (NHTSA, 2001). Whilst for driver airbags, the uptake appears to have been slower, with only ~5% using a hybrid inflator by 1998. An assessment of 30 driver inflators from 12 of the top selling vehicles in the UK between 1996 and 2006, (conducted by the author), identified that 17% of these operated a hybrid inflator, with only one being fitted to a vehicle produced before 2002. Although not statistically robust, the assessment supports the expectation that since the 1990's their uptake has continued to increased.

2.2.5 Compressed gas inflators

The first iterations of vehicle airbag systems in the 1950's used a reservoir of compressed air released by an electrically operated valve to inflate the airbag cushion. These early systems, first patented by John W. Hetrick in 1952 and Walter Linderer in 1953 (Hetrick, 1952; Linderer, 1953) were unable to rapidly provide the required inflation volume and suffered from pressure losses. The concept of release of a stored gas to inflate an airbag continues today, although considerable advances in technology have been made. These inflators are known as compressed, stored or cold gas inflators and use an inert gas, commonly argon or helium in place of compressed air. These compressed gas inflators use a small pyrotechnic device to release a rupture disc allowing the gas, held under high pressure, to be released and inflate the airbag, Figure 2.16.

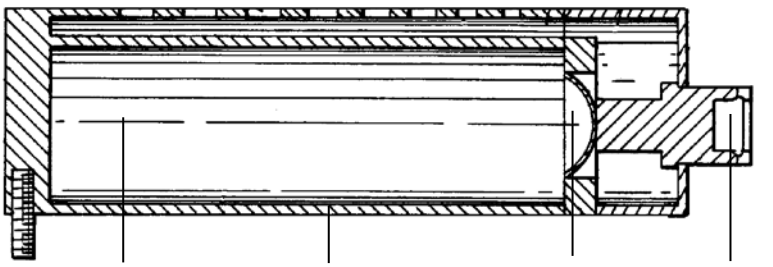

Figure 2.16: Compressed gas inflator assembly (Ellis et al., 1998)

As the pyrotechnic element of the inflator is only used to release the stored gas, solid propellant mass is significantly lower than that of a full solid propellant or hybrid inflator.

Whilst those early systems from the 1950's were intended for use in driver front positions, contemporary compressed gas systems are mainly utilised for curtain airbags (Figure 2.17), where increased uptime capability is required. An increased uptime is needed in a rollover incident, where the impact and therefore risk to the occupant can continue for a number of seconds. This can only be achieved by use of a cold gas inflator where inflation gas temperatures are lower, allowing them to be held within the airbag cushion.

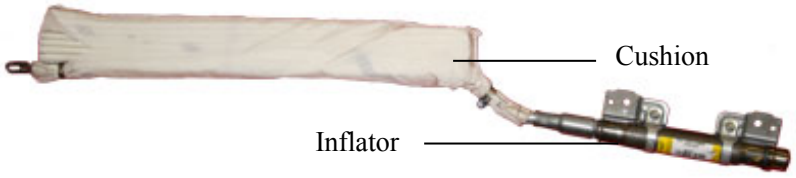

Figure 2.17: Inflatable curtain airbag module

2.2.6 Liquid propellants

Liquid propellants are beginning to be utilised within inflators similar to the more common hybrid system. Inflators using a liquid propellant, as detailed by both Hollembeak (2010) and Richardson et al. (1997) use a dual chamber inflator with the fluid fuel and an oxidant in the first chamber, and a pressurised gas in the second (Figure 2.18). These liquid fuels, such as ethanol, require lower ignition temperatures and offer reduced concentrations of solid particle effluents than their solid propellant equivalents (VOI, 2010). An initiator starts the combustion of the fluid fuel within the combustion chamber and as pressure increases, the heated inflation gas created is released to the stored, compressed gas in the gas chamber, Figure 2.18. The increase in temperature and pressure created by the combustion of the liquid fuels and entry into the second chamber, releases the inflation gases from the inflator into the airbag cushion (Green et al., 1999).

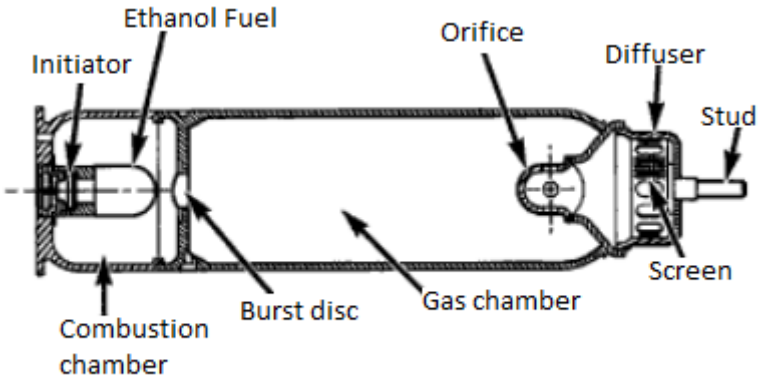

Figure 2.18: Liquid propellant inflator (Hollembeak, 2010)

2.3 Inflator staging

Frontal airbags, both for the driver and front seat passenger are currently operated by either a single or dual stage airbag inflator. A dual stage inflator is capable of deploying at either a low or high power in response to any one of a number of sensory inputs; although initially they simply provided a response to the Federal Motor Vehicle Safety Standard (FMVSS) 208 (NHTSA, 1998) requirements for out-of-position occupants (Clemo et al., 2006).

Dual stage inflators provide two levels of inflation performance, with the primary being generated by the first stage, at approximately 70% of available inflation performance and the secondary being provided by the first and second simultaneously at 100%. Where only the first stage is required, inflators may deploy the second stage up to 160ms after deployment. This delayed deployment ensures that additional inflation gases are not directed into the airbag during the crash phase and ensures complete neutralisation of the pyrotechnic and propellant within the airbag (Hollembeak, 2010).

The implementation of dual-stage inflation in the vehicle fleet has been increasing since 1998, with staging data from six vehicle manufacturers (sample size = 169) identifying that since 1988, 91.4% of inflators have used a single stage inflator and prior to 1998 no vehicles used a dual stage inflator (IDIS, 2011) Although dual staging of inflation has become more prevalent since 1998, it currently remains considerably less common than single stage inflation, Figure 2.19. The analysis supports the findings of a 2001 NHTSA study which assessed characteristics of airbag systems, such as staging. (NHTSA, 2001)

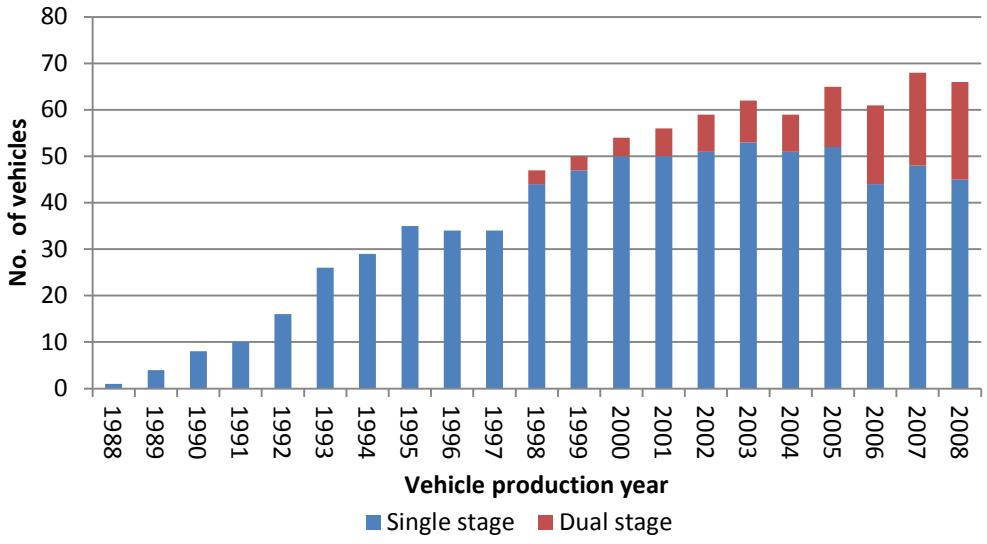

Figure 2.19: Driver airbag inflator staging by vehicle production year

While single and dual stage inflators are limited to providing pre-set inflation force and pressure, variable output inflators are able to tailor the output from the inflator to different impact types, scenarios and occupants. These inflators are capable of continuously adjusting inflator output during deployment and are controlled by an electronic control unit (ECU) responding to an array of sensors (VOI, 2010). This control of inflation allows airbag performance to be varied depending on factors including impact type and severity, seat track and recline, occupant position and characteristics and safety belt usage.

In addition to increased adaptability and variance in restraint performance, the use of a liquid propellant within a variable output inflator is able to significantly reduce gaseous and particulate effluents (VOI, 2010). However, although variable output inflators offer distinct advantages over single and dual stage inflators, they are yet to infiltrate mainstream vehicles where the traditional inflator types dominate. Dual stage and variable output inflators provide a means of controlling airbag inflation. However, the use of variable venting and adaptive tethering (section 2.5) allows the use of a single stage inflator and therefore a shift back toward these inflators may occur in the future.

2.4 Inflator filter media

Whilst the rapid burning of a solid propellant creates gas to inflate the airbag cushion, it also produces a solid particle effluent that can include large heated particles potentially able to compromise the integrity of the cushion. This risk is controlled by the use of metallic wound wire or knitted mesh filters within the airbag inflator, Figure 2.20 and 2.21. This media is also capable of reducing output temperatures and minimising the risk of thermal injuries to vehicle occupants as the heated output exits the cushion during inflation and 'ride-down'.

Where there is a reduced output from the inflator a dedicated filter may not be used, such as in cooler gas inflator technologies such as hybrid and compressed gas inflators.

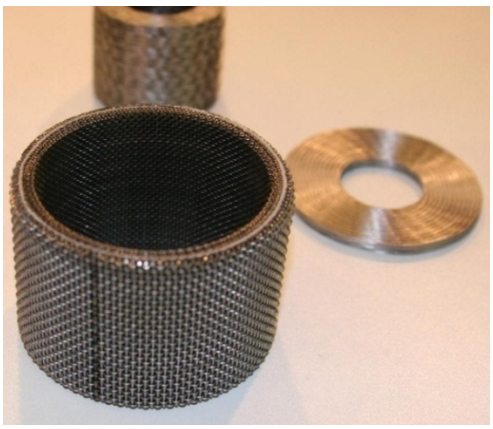

Figure 2.20: Wire mesh filter media

Figure 2.21: Filter media within airbag inflator assembly

Minimal information is presented in the literature regarding the efficacy of filter media and its ability to remove particulate from airbag inflation output.

2.5 Airbag shape and volume

Airbag shape and volume varies by purpose, vehicle interior geometric size and shape and airbag technology type. Driver airbags are generally spherical, although some vehicles utilise fixed airbag modules (Citroen C4) allowing a shaped airbag to be used. This shaped airbag can be larger and provide greater coverage of the outer extents of the vehicle interior such as the A-pillar. Passenger airbags are more complex in their shape, yet generally appear as rectangular prisms when viewed from the occupant position, as do side, knee bolster and inflatable curtain airbags.

As with shape, airbag volumes vary depending on the application and type and size of vehicle. Table2.3, conducted from research conducted by the author, details indicative

airbag volumes for the most common airbags currently fitted to vehicles in the UK. The airbags assessed were from mid-sized vehicles such as the Volkswagen Passat (sample size=10) and, although not statistically robust, are expected to be broadly representative of most vehicles currently in use in the UK. Volume varies from 12-18L for a side thorax airbag to 65-95L for a passenger front airbag.

Airbag Type	Indicative Volume (litres)
Driver front	30-45
Passenger front	65-95
Side thorax airbag	12-18
Knee bolster	14-20
Inflatable curtain	20-40

Table2.3: Indicative airbag volumes - UK vehicles

Airbag volumes in the UK are generally lower than those in the USA, reflecting the difference in mean vehicle interior size and the tendency of a higher proportion of vehicle occupants to wear safety belts in the UK. Airbags that must also provide protection for unbelted occupants are generally larger and stiffer than those intended for belted occupants. These airbags provide a greater area of protection for unbelted drivers who will travel with greater inertia and in a less controlled manner. Although offering improved protection for unbelted occupants, these stiffer and larger airbags are likely to increase the risk of airbag associated injuries to smaller and other more susceptible individuals. Between 1990 and 1998 in the USA the mean driver airbag volume remained broadly steady at approximately 56 litres, whilst the passenger airbag volumes have reduced from over 200 litres to 120 during the same time period reflecting a reduction in inflation mass flow rate and therefore risk to OOP occupants, (NHTSA, 2001).

Although the information presented regarding volume represents standard airbags with passive tethering and venting, the volume, size and shape of airbags may be controlled or varied by adaptive systems. These provide greater performance variability and improvements in protection and are discussed further within the following sections.

2.5.1 Airbag cushion tethering

The control of airbag shape and volume allows greater adaptability to variations in crash type and severity, and occupant characteristics, allowing optimisation of airbag deployment behaviour. Internal cushion tethers are used to control cushion shape, forward displacement and volume either passively and defined prior to the collision by use of fixed tethers, or as an active system responding to information provided by vehicle sensors. Controlling the cushion's forward displacement and volume limits the risks to occupants situated in close proximity (out of position) to the airbag and to occupants of different sizes and statures. A "passive" tether made of fabric, (Figure 2.22) is attached to a secondary panel stitched to the front, (Figure 2.23), and rear of the airbag cushion close to the inflator. Adaptive tethers are attached to the cushion in the same general manner but operate in a comparatively complex manner, as discussed in section 2.5.

Figure 2.22: Tether connection to front panel (internal view)

Figure 2.23: Airbag B: Front tether panel

Assessment of airbag characteristics from NHTSA data, (2001) identified that in the early 1990's the great majority of driver airbags were not equipped with internal tethers, but by 1998, 88% of driver airbags were equipped with two or more. In comparison to driver airbags the increased forward displacement required of passenger airbags results in a reduced requirement for tethering and thus utilisation rates are lower.

Whilst passive tethers and venting control forward displacement and cushion pressure to pre-defined levels, adaptive systems are able to respond to crash and occupant characteristics. An adaptive tether system is able to release tethers and increase the amount of forward displacement of the airbag by using a small pyrotechnic release device. In situations where sensors detect that the occupant is seated further from the airbag module, tethers are released by a 'cutter', allowing increased forward displacement and a reduction of the gap between the vehicle occupant and airbag, aiding "ride-down". The cutter usually mounted close to the inflator and operated by a small pyrotechnic,

responds to a sensory signal and either rotates or displaces a sharpened cutter blade, severing the tether and releasing the airbag cushion. As programmes assessing the safety performance of passenger cars increase in complexity and start to consider even more variance in occupant types, the requirement for adaptive systems including those that control venting and tethering will increase, and therefore such systems are likely to become commonplace in inflatable restraint systems.

2.5.2 Airbag cushion venting

Vent voids positioned to the rear of airbag cushions (Figure 2.24) are used to allow controlled deflation of an airbag cushion when impacted by a vehicle occupant during a collision. In some cases these vents have been replaced by the use of a permeable airbag fabric, which upon impact (by an occupant) or when reaching 'design pressure' releases pressure within the airbag and controls occupant 'ride-down'.

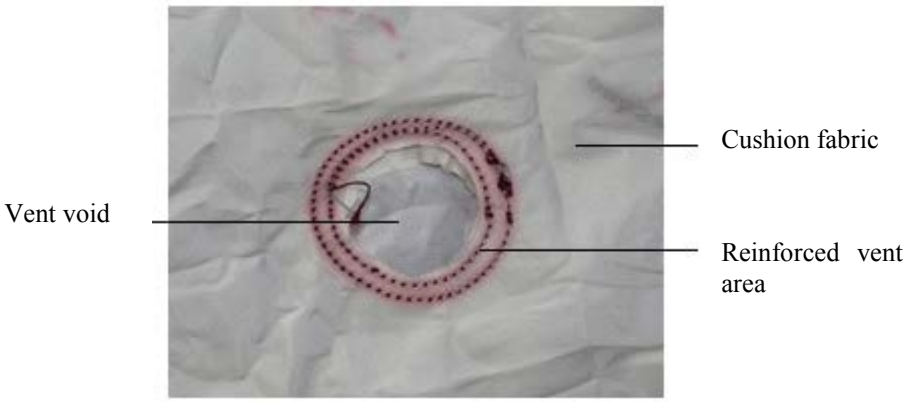

Figure 2.24: Driver airbag rear vent

Adaptive or active venting adds to the fixed venting offered by the simple vent voids shown in Figure 2.24. This ability to open greater vent areas or to vent inflation gases away from the inflating airbag allows a greater degree of control over cushion pressure and stiffness and thus provides a benefit for those occupants and scenarios that do not require the full performance of the restraint (Bauberger, 2007). Self-adaptive venting systems react to information regarding a vehicle occupant's position and distance from the airbag to control cushion pressure (TRW, 2011). The system uses a pyrotechnic actuator to either open or close vents and can be used to fulfil the requirements of FMVSS 208 for passenger OOP testing, negating the requirement to use a dual stage inflator (Hynd et al., 2011).

As an alternative to opening or closing vents within the cushion, inflation gases can be directly vented from the module by means of a shutter or hinged door that directs the flow

of inflation gases away from the airbag cushion, reducing the cushion pressure and stiffness.

As with other adaptive systems, it can be expected that these methods and systems of controlling venting will be used in greater numbers over the next decade to provide equalised protection during different collisions and for occupants with differing characteristics.

2.6 Airbag materials, permeability and coating

Airbag cushions are a key element of the airbag system and provide an inflated fabric surface that allows deceleration of occupant energy in a controlled manner, whilst preventing interaction between the occupant and vehicle interior and in the case of curtain airbags, prevent ejection from the vehicle. These fabric cushions must be capable of containing the heat and pressure created by the inflator, whilst providing energy absorption during the crash phase when an occupant impacts the cushion. The airbag cushion must also be capable of providing reliable and predictable performance as per its design after substantial in vehicle ageing. Many airbag systems are designed to perform as per their specification for up to 20 years and must perform in a wide range of environments across the globe.

The material that best fulfils these performance requirements is Nylon 6, 6, which has remained the material of choice for airbag cushions since the 1970's (CITA, 2002) albeit with some modifications, that may include:

- Multi layers of fabric around high temperature areas such as the inflator body and vent voids
- Increased number of yarns in the fabric
- Application of a coating, either loose or adhered

In earlier airbag systems a 'loose' coating of cornstarch or talcum powder was used to aid the release of the airbag from the module assembly (Chan et al., 1989). Upon deployment these 'loose' coatings were ejected from the outer surfaces of the airbag into the interior of vehicles as the airbag unfurled and inflated. These particles were clearly visible within the vehicle and many anecdotal accounts (unreferenced) of a 'cloud' of particles invoking concern in vehicle occupants (as they associated a visible smoke with fire) led to the development of an alternative adhered coating. This adhered coating not only prevented the dispersal of coating particles into the vehicle but also provided improved thermal performance when used with a solid propellant inflator, Figure 2.25.

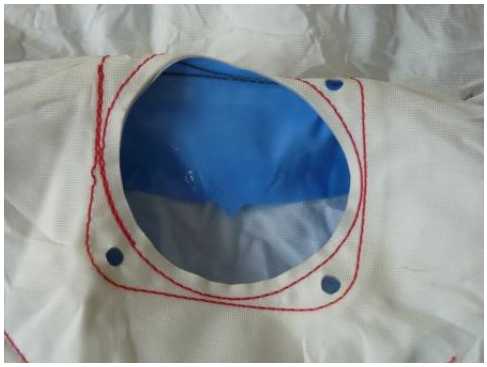

Figure 2.25: Coated polyamide surrounding inflator

Other materials have been considered as an alternative to Nylon and recent research into polyester fibres has identified that whilst a suitable material in some aspects, its 'specific heat capacity' and 'energy to melt' performance remains inferior to that of Nylon 6, 6. Even with the increased use of systems that provide lower temperature inflation gases (hybrid/compressed gas); polyester is yet to have made any ingress into the sector. This may be in part associated with the lack of a specific improvement in performance and an increase in material density and therefore mass. It is therefore anticipated that nylon will remain the material of choice for airbag applications for the foreseeable future.

2.7 Fitment rates for restraint systems

Whilst restraint systems were originally conceived in the 1950's, their uptake into the vehicle fleet remained slow until the 1990's. The literature presents little information regarding the introduction of the broad variety of restraint systems, yet some studies have indicated fitment rates for European and UK vehicles. The analysis of Co-operative Crash Injury Study (CCIS) accident cases conducted by Carroll et al., (2009) defined restraint system fitment for occupants in a sample of frontal impact accidents. Only incidents involving vehicles produced in the year 2000 or later were assessed and a sample of 1899 occupants (approximately 475-1000 incidents) was used, Table 2.4.

Restraint type	Fitment proportion %		
	Driver	Front seat passenger	Rear seat passenger
Airbag	97	78	0
Safety belt pre-tensioner	85	87	7

Table 2.4: Occupant restraint system feature by seating position (Carroll et al. 2009)

This data suggests that by the year 2000 driver airbags were fitted to nearly all new vehicles and that relatively high fitment rates were reported for front safety belt pre-

tensioners and passenger airbags. It is not clear however, how fitment rates vary by vehicle production year or if any bias toward vehicle production years existed within the study.

Indications of restraint fitment data were also presented by Frampton et al. (2005) from an analysis of EuroNCAP data. Approximately 200 passenger cars, from a number of classes, produced between 1996 and 2005 were assessed, although the data were not summarised within the study. Analysis conducted by the author of a subset of the same data (sample size=128) identified mean restraint system fitment rates for vehicles produced between 1997 and 2004, Table 2.5, which provided similar results to that of Carroll et al. (2009).

Vehicle Class	Mean restraint system fitment rates %				
	Driver airbag	Passenger airbag	Side airbags	Curtain airbags	Front safety belt pre-tensioners
Supermini	97.6	68.3	31.7	12.2	97.6
Small family	96.9	71.9	62.5	37.5	90.6
Large family	97.9	75.0	60.4	50.0	97.9

Table 2.5: Restraint system mean fitment rates (derived from Frampton et al., 2005)

Although some variance between vehicle classes can be established, this may be in part associated with the relatively small sample size and a reported bias within the accident data toward collisions involving older vehicles, (Carroll et al., 2009), but it may also reflect the generally improved safety protection provided in larger vehicles. This data is however not sufficiently robust to provide a clear understanding of restraint fitment rates for vehicles in the UK and provides little information regarding changes in rates over time. Therefore, a comprehensive assessment of restraint fitment data from vehicles produced between 1993 and 2011 has been conducted by the author, Figure 2.26, from manufacturer data provided by JATO (JATO, 2011). This analysis was limited to driver and passenger front airbags (DAB/PAB), knee airbags (KAB), front seatbelt pre-tensioners (FBP) and driver and passenger anti-submarining airbags (DASA/PASA).

Data regarding restraints for rear seat positions and side impact and rollover protection were not readily available, therefore, rear seat restraint systems have not been considered in this review but front seat side airbag (SAB) fitment has been estimated.

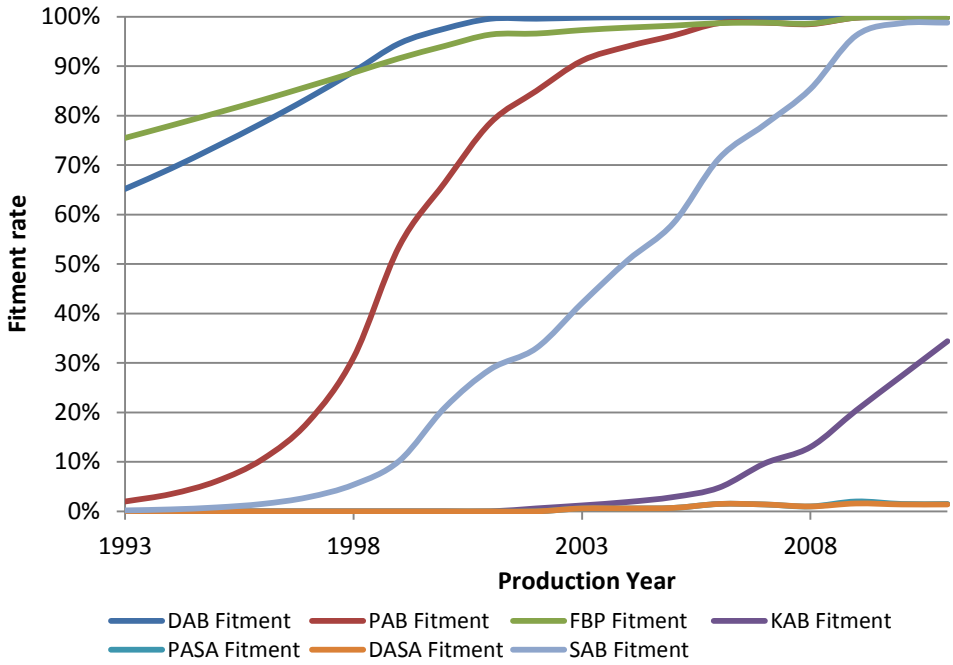

Figure 2.26: UK Passenger car restraint system fitment rates

The data presented in Figure 2.26 details restraint system fitment rates weighted by sales volume for all EU vehicle classes from 'superminis' to luxury SUVs. Fitment rate variances between vehicle types can be found, with most of the prestige and luxury vehicles being fitted with restraint system components first (Appendix A). This bias toward these vehicle types has limited effect on the overall data presented, as the lower cost vehicle classes account for the great majority of vehicles sold in the United Kingdom. The data provides a considerably more robust understanding of fitment rates than that presented by either Carroll et al. (2009) or Frampton et al. (2005) as data has been assessed for all mainstream passenger cars sold in the UK between 1993 and 2011. The data therefore indicates that nearly 100% of vehicles produced after 2005 contained a driver and passenger front airbag and front safety belt pre-tensioners.

Whilst data is presented as proportions for all system types, it is important to note that equal fitment rates exist for both driver and front seat passenger side airbags and safety belt pre-tensioners. As such, calculations of total restraint system component numbers (as presented within section 2.7) must account for the presence of two of each of these components.

2.8 Restraint system effectiveness

The rapid increases in restraint system fitment rates seen across the vehicle parc, Figure 2.26, can be attributed to a number of factors including; consumer testing programmes such as EuroNCAP, the drive of manufacturers and legislators and the increased mindfulness of the consumer. The awareness of these stakeholders to the effectiveness of restraint systems at preventing fatalities and injuries in vehicle collisions has not only driven their uptake but continues to fuel the development of innovative systems and the fine tuning of those that already exist.

Safety belts are regarded as the single most effective type of occupant restraint and are now considered the primary occupant restraint mechanism within a vehicle, with their fitment and use being mandated in most of the Western world. In a 10 year period between 1999 and 2009, they have been attributed to the prevention of in excess of 143,000 front seat fatalities in the USA alone (NHTSA, 2010), equating to the prevention of millions of fatalities and serious injuries worldwide. Aside from safety belts, the first inflatable restraint systems to be introduced; driver airbags, have been subject to the greatest research and assessment regarding their effectiveness. The effectiveness of driver airbags is rather clearer than that of other systems and during the same 10 year period from 1999 to 2009, frontal airbags are estimated to have prevented over 24,000 fatalities in the USA; an additional 17% of the figure for safety belts (NHTSA, 2010). Estimates of the absolute effectiveness of the driver airbag suggest they are effective at reducing fatal injury risk by 7% for belted occupants and 9% for those unbelted (Cummings et al., 2002). Whilst other studies estimated fatal injury prevention for belted occupants at 11% (NHTSA, 2001) and as high as 20%, (Cuerden, 2006) reflecting substantial variance in the methodologies and datasets used for such calculations.

Estimates of the effectiveness of passenger frontal airbags suggest that the ability of these systems to prevent fatal injuries are broadly comparable to those of driver airbags, with reductions of 7% (NHTSA, 2009a) and 11% in crashes of all types (IIHS, 1996) suggested within the literature.

In contrast to driver and passenger airbags, estimates of fatality risk reduction for knee airbags do not appear to be currently available within the literature and instead focus upon reductions in specific injury mechanisms. The data suggests that knee airbags are capable of substantially reducing chest injury mechanisms and therefore collision injury risk, especially when an occupant is using a safety belt (Mitsubishi, 2012).

Aside from those frontal impact restraints, side airbags, designed to minimise the high risk of injury to occupants in side impacts, are key to reducing fatalities and serious injuries. Side airbags with integral head protection are capable of reducing fatal injury

risk for drivers by between 37% and 45%, and for side airbags with torso only protection, reductions of between 11% and 30% have been reported (Braver and Kyrychenko, 2004) and (McCartt and Kyrychenko, 2007). Although some variance in their reported efficacy exists, it is clear that side airbags are capable of substantially reducing risk in side impacts, where the effectiveness of safety belts is reduced. These systems have become standard fitment for many vehicles (Figure 2.26) reflecting their value in reducing injury risk.

2.9 Summary

A general overview of automotive restraint systems has been provided with a description of the function of each system, how they operate and where they are employed in vehicles.

A comprehensive study of fitment rates for these restraint systems up to 2012 is also presented.

Whilst some disparities exist between the reporting methods and the effectiveness estimates for occupant restraints, it remains clear that these systems are extremely important in driving down the risk of injury in vehicle collisions across the globe. These capabilities, coupled with the drive of manufacturers and legislators to reduce fatalities and injuries in vehicles has resulted in a proliferation of occupant restraint systems. In addition, consumer testing programme EuroNCAP has provided vehicle buyers with independent information regarding the type and efficacy of safety systems; undoubtedly resulting in improvements to vehicle safety and increased provision of restraint systems.

Although it is clear from this data that occupant restraints provide significant benefits in many collision scenarios they also pose hazards to vehicle occupants and to those involved in their manufacture and disposal. A number of fatalities and a larger number of injuries sustained by vehicle occupants have been reported in the literature and these hazards and a broad overview of the potential risks are defined within Chapter 3, with particular reference to the hazards experienced by vehicle dismantlers at EOL.

Chapter 3

Airbag deployment interactions and exposure

3.1 Introduction

Occupant restraints have provided significant benefits in many collision scenarios and therefore are widely considered to be a crucial element in protection against injuries in collisions. However, they can also pose hazards to vehicle occupants and to those involved in their manufacture and disposal.

The short durations involved in most vehicle collisions require airbags and other occupant restraints to work rapidly to control the high inertial forces of an occupant's body, when the vehicle they are travelling in is rapidly decelerated in a collision. These short duration crash phases require the use of systems such as pyrotechnics to inflate airbags and operate other restraints to reduce occupant injury risk. The use of these energetic systems poses hazards to vehicle occupants and those involved in their manufacture, disposal and replacement. For vehicle occupants these are generally outweighed by their ability to minimise injuries and fatalities in most scenarios and in addition significant effort is being expended to reduce their prevalence and the hazards posed (Hynd et al., 2011). However, for occupational exposures, such as during manufacture, repair and arguably most importantly for those tasked with disposal, there are no direct advantages of the exposure to the deployment of these restraint systems and exposure frequency will be far greater than that experienced by vehicle occupants. It is therefore the occupational exposure at vehicle end-of-life treatment that is the primary stimulus for the work presented in this thesis.

3.2 Airbag Deployment Interactions

The physical force of movement of a deploying airbag is the most commonly reported injury mechanism for those in close proximity to an inflating airbag (Wallis and Greaves, 2002) The high speed inflation of the airbag cushion (Schreck et al. 1995) poses a risk of impact injury as the airbag inflates, and may also result in less injurious friction burns as an airbag cushion interacts with exposed skin (Ulrich et al., 2001). In the United States of America (USA) between 1990 and 2009, 296 fatal injuries were confirmed as being associated with an airbag (NHTSA, 2010). The majority, 55% (162), of these involved children who were also commonly unrestrained, with 10% (29) involving those seated in a rear facing child safety seat (RFCSS). Many of these injuries are linked to misuse, with occupants not using safety belts or positioning child restraints in positions where they are at the lowest risk from airbag deployments. These injuries appear more prevalent in the USA but there are also less frequent reports of fatal injuries being sustained by vehicle occupants in the UK (Cunningham et al., 2000; BBC News, 2010). However, in these instances it appears likely that the occupants assumed a position too close to the deploying airbag, where injury risk levels are known to be higher (Morris et al., 1998). Assessment of injuries recorded in the UK CCIS database between 2006 and 2009, identified that of all injuries sustained in a collision, only 1.1% could be attributed to airbags (DfT, 2012). These injuries are therefore rare and their prevalence and severity is reducing as airbag technologies are refined. (Hynd et al., 2011)

Whilst injuries caused by the physical force and motion of the airbag may be the most likely to occur for vehicle occupants, the specific risks are generally well characterised and understood by the industry, the medical profession and legislators, and considerable effort has been expended to reduce the injurious potential of these systems (Hynd et al., 2011). However, with regards to occupational exposures when undertaking airbag neutralisation as part of the depollution process, the use of a remote deployment system (Autodrain, 2012; Vortex, 2013) allows the operative to assume a position substantially away from the motion of a deploying airbag. For these reasons the potential hazard posed by the physical force of deployment is not considered here in any further detail.

Aside from the motion of a deploying airbag, the production of a short impulse sound wave during deployment (Hickling, 1996 and 2002; Davila and Nombela, 2011) has the potential to cause long and short term otological injury (Huelke and Moore, 1999; Mittal, 2006; McFeely et al., 1998) to those in close proximity. Sound levels of greater than 160dB have been measured, at the ear position, during dynamic tests, with exposure times of 1ms or less (Davila and Nombela, 2011) and these have been attributed to auditory injury. Employing a remote deployment system during airbag neutralisation will again reduce the risk associated with exposure to this deployment noise and therefore whilst

consideration may be given to this in future work by the industry it does not form the focus of this research programme.

Alongside deployment noise, deflagration of a solid propellant and airbag deployment creates heat, which is reported to have caused some instances of thermal burn injuries to vehicle drivers (Ulrich et al., 2001). These burn injuries commonly sustained on the hands and lower arms are associated with vehicle occupants coming into contact with heated gases and particles as they are expelled from the cushion, as it deploys, and is subsequently compressed in a collision (Reed and Schneider, 1994). The injury mechanism associated with a driver's hands being in close proximity to the heat source is unlikely to be replicated during airbag neutralisation as it has been considered that the use of a remote deployment system will allow an operative to assume a safe position sufficiently far from the airbag during deployment.

Another more serious effect of the heated gaseous and solid particle effluent produced on airbag deployment is that the effluent is released into the environment after airbag deployment (Chan et al., 1989, Gross 1994; 1995; 1999) and unlike the noise and heat emission, will remain in the vehicle environment over extended time periods (Chan et al., 1989). These effluents are therefore more likely to be encountered by deployment operatives tasked with airbag neutralisation. These operatives are required to re-enter end-of-life vehicles after airbag deployment to retrieve remote deployment equipment (European Commission, 2000; Autodrain, 2012; Vortex, 2013) or continue depollution and therefore become exposed to these effluents each time a vehicle is depolluted. Whilst there is little information in the literature specifically regarding exposures during neutralisation, for vehicle occupants, exposure has resulted in instances of ocular, dermal and respiratory responses and injuries.

Ocular injury associated with airbags most commonly originates from contact between vehicle occupants and an airbag cushion (Duma et al., 2005; Stein et al., 1999; Gault et al., 1995); however, exposure to alkali materials produced by the deflagration of a solid propellant (to provide inflation gases) also poses a risk of damage to the eye. The risk of severe injury to the eye is comparably higher than for the dermis and such instances associated with airbag deployments have been recorded in the literature (Smally et al., 1992; De Vries, 2007). If ocular exposure to such alkali materials is diagnosed (by pH measurement of ocular secretions) early and subsequently treated by saline irrigation, permanent vision loss and severe damage to the cornea can however be prevented (Subash et al., 2010).

Dermal burn injuries and skin desquamation (peeling) from exposure to alkaline materials emitted during airbag deployment have also been reported in the literature (Conover, 1992; Epperley, 1997; Swanson-Biearman, 1993) but, in stark comparison to ocular

exposure to alkali materials, dermal injuries are ordinarily minor and require only basic treatment (Tinitinalli, 2003). It is possible that on re-entry to a vehicle during depollution that operatives may be at risk of dermal or ocular injury from exposure to alkali material within the solid PM effluent.

Respiratory responses to exposure to airbag effluents are detailed in a number of case reports (Epperley, 1997) and whilst controlled testing has focused on individuals with pre-existing conditions (Gross 1994; 1995; 1999; Linn and Gong, 2005), exposure to airbags has elicited a response in those with and without existing respiratory conditions (Mazieres et al., 2000; Perez-Camarero, 2002). Exposure of these individuals to airbag effluents after a collision has resulted in reports of dyspnea, wheezing, bronchoconstriction and subsequent bronchospasms when exposed to other agents which did not occur before. Sinusitis (inflammation of the paranasal sinuses) and pneumonitis (inflammation of lung tissues) have also been reported. In addition a recent fatality in the UK was attributed to exposure to effluents from airbag deployment, with the coroner stating that 'this man died as a result of this incident (the car crash) and more pointedly because of the explosion of his airbag and exposure to noxious substances' (The Northern Echo, 2012). It is understood that the driver airbag cushion ruptured and the victim was exposed to an effluent and the fatal injury was attributed to bronchial pneumonia and pulmonary fibrosis, yet little is known about the victim's medical past and the presence of any underlying illness. Whilst individual case studies exist, an assessment of collision injury data (DfT, 2012b) provides little evidence of respiratory injuries, yet this may be explained by a bias towards serious and fatal injuries where a self-reported respiratory injury or reaction is less likely to be reported.

There is a generally good understanding of ocular and dermal injuries in the literature and the mechanisms in which these occur. However, there is a lack of information in the literature relating to the characteristics of airbag effluents likely to elicit respiratory responses. Consequently, the latter has formed the focus of the assessment reported in this thesis. There are many opportunities to expand knowledge in this field and increase understanding of the characteristics of airbag effluents and the considerable exposure occurring during airbag neutralisation.

The following sections define the characteristics of these effluents and provide detailed information about exposure during end of life vehicle (ELV) depollution processes.

3.3 Effluent assessment methods and characterisation

During airbag deployment both a gaseous and solid particle effluent is produced and released from the deflagration of a solid propellant providing inflation gases. Characterisation studies have provided a generally robust understanding of the gaseous

effluents from airbags, with early assessments (Chan et al., 1989; Wheatley et al., 1997) identifying low concentrations of ammonia (NH_3), nitrogen dioxide (NO_2) and sulphur dioxide (SO2), and higher concentrations of carbon monoxide (CO). Although higher than other gaseous elements, average CO concentrations remained below recommended short term exposure limits (STEL). Later studies of non-azide airbag systems suggested that CO concentrations were broadly comparable, yet in some cases exceeded these same limits. (Gross et al., 1999). The assessment of the PM element of the effluent is comparably more complex with particle mass concentration, size distribution and composition being investigated in the literature.

Studies assessing PM concentrations from sodium azide airbags reported varying concentrations from as low as 83 mg/m^3 to as high as 684 mg/m^3 (Chan et al., 1989; Wheatley et al., 1997), whilst assessments of non-azide inflator airbags suggested a similarly variable situation albeit with substantially lower concentration values, which ranged from 12-133 mg/m^3 (Gross et al., 1999; Linn and Gong, 2005). However, there is yet to be a controlled study that compares sodium azide airbags with non-azide airbags, and since various elements of airbag performance, such as inflator pressure and vent hole area are known to affect effluent concentration, simple comparisons are not easily drawn (Starner, 1998).

In addition to concentration assessment, some characterisation of solid particle effluent spectral density has been presented, with many samples exhibiting a bimodal distribution, with the primary mode occurring at around 1 micron (Chan et al., 1989; Schreck et al., 1995), and in some cases a secondary mode is also apparent at around 10 microns (Wheatley et al., 1997). The primary mode is attributed to the deflagration of the solid propellant and the secondary associated with a loose coating of cornstarch or talc used on early airbag systems as a form of lubrication to improve release from the airbag module (Chan et al., 1989).

These particles emitted during airbag deployments have been reported as alkali particles emitted as a product of the deflagration of a propellant (Chan et al., 1989). Early studies of sodium azide (NaN_3) inflators identified the presence of alkali particles of sodium hydroxide (NaOH) and sodium carbonate (Na_2CO_3) with a pH of between 9.8 and 10.3 (Chan et al., 1989). Subsequent to this study, standards controlling effluent alkalinity were produced with allowable ranges of 5 to 9 (Audi AG et al., 2001) and 4 to 10.5 (SAE, 2004) defined, with a specific limit placed on NaOH concentration of $5mg/m^3$. However, by the late 1990's highly alkaline effluents were still being identified (Wheatley et al., 1997). Since the mid to late 1990's the use of sodium azide has all but been phased out in favour of perchlorate and nitrates and little information regarding the alkalinity of effluents from these propellants has been presented in the literature.

3.3.1 Human response to effluent

Studies assessing human exposures to the effluent from sodium azide airbags (Gross et al, 1995) investigated the mechanisms of induction of respiratory responses in asthmatics. These hyper-sensitive test subjects have historically been selected by laboratories for effluent exposure studies (Gross et al., 1995 and 1999; Linn and Gong, 2005) as they represent a segment of the populous at a greater risk from exposure to such gaseous and solid particle effluents. Subjects were positioned within a sealed test vehicle during airbag deployment and for a further 20 minutes to assimilate a worst case scenario for a post-crash airbag exposure. The studies defined that for those tested systems, the solid PM and not the gaseous component induced a response (Gross et al., 1995; Caudle et al., 2007). Subsequent assessment of non-azide airbags suggested that the response mechanism may however not be the same (Gross et al., 1999), yet reductions in propellant concentration may still reduce instances of response (Linn and Gong, 2005). There is however considerable evidence in the literature that details exposure to PM and associated health hazards. (WHO, 2013; Davidson et al., 2005; Brunekreef and Holgate, 2002).

Since the PM effluent produced during deployment is associated with a respiratory health hazard, and with substantial opportunities to increase knowledge and understanding in the field by assessment of this output, the focus of this research has been on PM assessment and in particular those factors that are important to assist in defining any respiratory hazard.

Little characterisation of these PM effluents is evident in open literature and available research does not specifically consider the occupational exposure to airbag effluents during ELV neutralisation processes. This exposure to effluents is likely to be significantly greater during the depollution process than for vehicle occupants and further details regarding this exposure are therefore detailed in the following section.

3.4 End of Life Vehicle legislation and neutralisation of occupant restraints

Regulations requiring the neutralisation of occupant restraint system components in the European Union (EU) form part of wider legislation to reduce the environmental impact from ELVs. In the UK the EU end of life vehicle directive has been integrated into legislation by the Department for Environment Food and Rural Affairs (DEFRA) and compliance monitoring and enforcement is conducted by the Environment Agency (EA), who have the legal ability to close vehicle recycling sites and prosecute against non-compliances. The legislation in the UK, (European Commission, 2000) can be considered to comprise of 5 main points (Morris and Crooks, 2007).

- The vehicle producers must pay "all or a significant part" of the cost of take back and treatment of ELVs.
- The vehicle may only be accepted as an ELV at an Authorised Treatment Facility (ATF)
- The ATF must recover or reuse 85% of the vehicle (by mass) as from 1 January 2006, with a target of 80% reuse or recycling (the remainder can be “recovered” for use as a fuel, i.e. burned). This rises to 95% and 85% respectively in 2015.
- The ATF must depollute the vehicle: remove and make safe all hazards from the vehicle, notably removal of all fluids, removal of tyres, removal of battery (lead), removal of wheel weights (lead again) and removal or deployment of all live pyrotechnics, such as airbags.
- The ATF must issue a Certificate Of Destruction (COD) and report the data back to the vehicle licensing authority (effectively declaring the end of that vehicle’s life)

Although enforced through legislation, it was estimated by Morris and Crooks (2007) that in 2008 one third of vehicle dismantlers in the UK would not have gained ATF status and would continue to dismantle and dispose of vehicles illegally, whilst some of those who had gained status were continuing to dismantle vehicles without fully complying with the legislation. It is expected that the proportion of dismantlers not qualified as an ATF will have fallen since the implementation of legislation, as a steady increase in the number of facilities approved by the Environment Agency has been recorded (Environment Agency, 2012)

Although the number of authorised sites has continued to increase, it is estimated that many vehicles still do not pass through the approved disposal channels and have not been depolluted to the required standard, leaving live pyrotechnic components within the vehicle. This worrying fact is illustrated in Figure 3.1, which indicates the presence of a live airbag in the remains of a baled vehicle due for shredding. The leader shows the location of the airbag on the baled vehicle and the ellipse provides a magnified image of the component with identifying labelling visible.

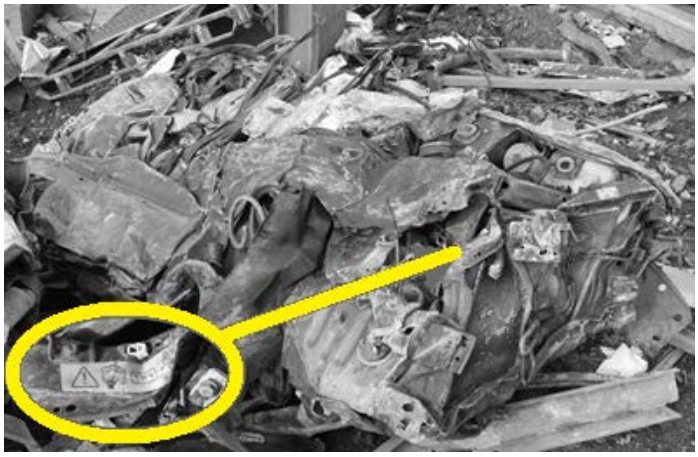

Figure 3.1: Baled vehicle thought to have live airbag inside (Morris and Crooks, 2007)

The issue of compliance and the number of vehicles treated in-line with legislation where all pyrotechnics are neutralised or removed is explored in the following section.

3.5 Scale of exposure

Certificate of Destruction (COD) and deregistration data in the UK suggests that nearly half of all vehicles reaching their EOL do not pass through the approved channel, thus limiting the likelihood of safe pyrotechnic neutralisation as indicated in Table 3.1.

Year	Number of vehicles deregistered and not SORN	Number of CODs issued	Number of vehicles not issued with a COD
2008	1,841,950	924,548	917,402
2009	1,904,661	1,078,734	825,927
2010	1,726,705	967,731	758,974

Table 3.1: Number of CODs issued in the UK (Department for Transport, 2013)

Considering this probable variance in neutralisation and thus exposure, two estimates of the exposure to these systems were considered; the first being the total number of pyrotechnics requiring neutralisation in the UK and the second relating to the total number expected to pass through ATFs and likely to be neutralised. These estimates were calculated by the author through an assessment of the following key elements:

- annual vehicle sales
- pyrotechnic fitment
- vehicle attrition (cause and rate of vehicles reaching their EOL)
- occupant restraint system consumption

Limitations on the availability of robust data regarding pyrotechnic fitment rates for all system types and seating positions prevented the completion of a full assessment and therefore the study was limited to considering the presence and fitment of the following occupant restraints fitted to front seat positions only:

- Driver airbag
- Passenger airbag
- Front seat safety belt pre-tensioners
- Side airbags
- Knee airbag
- Front anti-submarining airbags

Through analysis of vehicle age data (DfT, 2011a), STATS-19 collision information (DfT, 2012b) and other supporting studies (Morris and Crooks, 2007) it has been possible to estimate vehicle attrition and likely pyrotechnic device consumption. This allows an estimate of the number of 'live' devices that have entered and are currently entering the UK ELV waste-stream to be defined, Table 3.2. Comprehensive calculations are presented in Appendix A.

These values have been proportioned for vehicles that will have been depolluted at authorised treatment facilities, where it may be assumed that these pyrotechnic devices will have been neutralised through deployment. It is assumed that the types of vehicles and thus number of pyrotechnics per vehicle, dismantled at authorised facilities do not differ to those treated at unauthorised facilities.

Year	Estimated total of un-deployed automotive pyrotechnics at EOL	Estimated total of un-deployed automotive pyrotechnics at ATFs
2008	4,276,401	2,129,905
2009	5,472,763	2,373,180
2010	5,383,859	2,727,591
2011	6,024,571	3,343,543
2012	6,501,436	3,568,076

Table 3.2: Undeployed automotive pyrotechnics remaining at EOL by year in UK

This data suggests a continuing increase in the number of automotive pyrotechnics reaching the ELV waste stream and requiring neutralisation. The year 2010 was an atypical year and may reflect the substantial reduction in vehicle sales and thus the number of vehicles reaching their EOL that is associated with the global economic downturn.

Calculations are based solely upon the previously identified restraint system components for front seat positions. Therefore, the total number of remaining devices may be expected to be significantly higher when considering inflatable curtain airbags, rear seat occupant restraints (airbags and pre-tensioners) and other actuators (seat adjustment, battery isolation etc.). Morris and Crooks' (2007) projected estimates of remaining pyrotechnics, for 2009, are comparable; yet appear to underestimate by approximately 10%.

Regardless of the exact number of airbags and associated components reaching EOL, the scale of the situation, even using conservative estimates, and the continuing trend to equip vehicles with increasing numbers of pyrotechnically actuated restraints, suggests that exposure to these devices and their hazards is far greater than initial estimates suggested. It is possible however that some equipment and techniques to neutralise these devices may vary the exposure levels and specific hazards that are encountered.

3.6 Exposure characteristics and specific hazards

Whilst it is clear that to comply with legislation a high number of pyrotechnic devices must be deployed each year in the UK, the characteristics of this exposure and the specific hazards to those tasked with their treatment may vary based upon the use of differing techniques, facilities and equipment. However, two general methods for the neutralisation of occupant restraints exist, namely;

- In-vehicle neutralisation
- Removal from vehicles and subsequent neutralisation

The first technique is the most prevalent in the UK and involves the use of an external deployment stimulus to initiate the occupant restraint system in its original position within the vehicle, whilst the second, requires the removal of each system component from the vehicle prior to subsequent neutralisation within the authorised treatment facility or at specialist external facilities. This technique is rarely applied in the UK due to the prohibitive cost associated with removal and it is only ever conducted for airbags and other restraint system that are not initiated with an electrical stimulus. These mechanically initiated restraint systems have now been generally superseded by electrical systems and therefore this technique of removal and subsequent neutralisation has not been considered further and falls outside the immediate scope of this project.

A number of commercially available deployment systems are available to provide in-vehicle neutralisation capabilities and these allow connection to either the restraint system ECU or direct to individual components. Where deployment systems do not provide the functionality to connect directly to the restraint ECU, individual components may be

deployed sequentially by connection to the airbag wiring or alternatively the units may be removed from the vehicle and deployed.

The use of such systems for in-vehicle deployments allow deployment operatives to maintain a position of relative safety, reducing the immediate hazards from airbag deployment. The use of a maintained safety distance limits the risk of injury posed by the rapid inflation and movement of the airbag cushion and is likely to substantially reduce exposure to the deployment noise, as discussed within section 3.2. However a plausible risk to depollution operatives is presented by exposure to the products of deflagration (effluents). During depollution, operatives will enter the vehicle initially to connect deployment equipment to the restraint ECU or an individual component, systems will subsequently be deployed and operatives will return to the vehicle to retrieve their equipment. Both during the deployment and whilst re-entering the vehicle, operatives are likely to come into contact with these effluents.

3.7 Summary

The short durations involved in most vehicle collisions and the requirement to control the high inertial energy of an occupant's body during a collision and prevent ejection from the vehicle, requires the use of solid propellants or compressed gases to rapidly inflate airbags or actuate restraint systems, such as safety belt pre-tensioners. Whilst presenting considerable safety advantages for vehicle occupants in a collision, these safety systems also present hazards to those occupants and those who are tasked with airbag neutralisation at the end of a vehicle's life. Arguably the greatest but also the most comprehensively understood hazard is posed by the movement of the airbag cushion itself. Airbag cushions are released at high speed from the module and can impact occupants, causing injuries which have in some cases resulted in fatalities. These injuries are mostly attributed to occupants who are situated too close to the emerging airbag. The implementation of legislation and substantial work by manufacturers has reduced the prevalence of such injuries and great effort, fuelled by a robust understanding of injury mechanisms continues to drive reductions in the risk to occupants.

Aside from these impact injuries, the generation of inflation gases also produces high temperatures, noise and gaseous and solid particulate effluents which are reported to have resulted in dermal, otological, ocular and respiratory trauma and these are comparatively less well understood and characterised in the literature.

In most cases for vehicle occupants the injury mitigation potential of the system outweighs the risk of injury, yet where there is no direct safety advantage provided by airbags, such as during neutralisation, balancing of the risk is harder to achieve. EU ELV

legislation requires the neutralisation of all of these devices during the depollution process. Whilst neutralising these systems, many of the hazards posed by airbag deployment may be controlled by use of a remote deployment system and safe systems of work which allow the disposal operative to assume a position of safety away from the vehicle. These systems do not however, prevent exposure to the solid particle and gaseous effluents produced on deployment. These effluents will be released to the locale upon ventilation of the vehicle and deployment operatives re-entering the vehicle to retrieve equipment will be subjected to further elevated risks associated with these exposures.

These effluents are capable of initiating clinically significant responses in not only those with pre-existing respiratory conditions but also those with no history of such conditions. The PM element of the effluent has been linked to the initiation of respiratory responses and in other areas PM is known to pose a hazard to health. In comparison to PM, gaseous effluents have been well characterised and appear to fall within tolerable exposure limits and are less commonly described as an injury or response mechanism during airbag deployment.

In addition, assessments of PM effluents have rarely been comprehensive and there is little information regarding their characteristics such as their evolution over time, number concentration, sub-micron size distribution and morphology. For these reasons assessment and evaluation of this effluent was conducted within this research programme to provide an increased knowledge of the PM and enable a more complete study of their characteristics and subsequent risk to human health.

In 2010, of the 1.7 million vehicles reaching their EOL, approximately 1 million vehicles equipped with 2.4 million live pyrotechnic occupant restraints passed through approximately 1,700 ATFs. Consequently, the exposure of deployment operatives to this PM effluent far exceeded that which would be experienced after a collision for individual vehicle occupants. This high frequency exposure has generally not been recognised by those who deploy restraint systems nor has it been characterised within the literature. Therefore the aim of this research programme was to address the gap in knowledge associated with the characterisation of airbag effluents and to focus the analysis on occupational exposures during ELV depollution and airbag neutralisation.

To achieve this aim, the following specific objectives were identified:

- Identify airbag test samples representative of those likely to be encountered at end-of-life vehicle depollution facilities.
- Robustly assess and compare existing test methodologies for airbag effluent characterisation

- Construct suitable test facilities to facilitate comparisons and characterisation of airbag particle effluents.
- Characterise the particulate effluents emitted during airbag deployments.
- Define a test methodology for collecting particle effluents for assessment of morphology and characterise the tested effluents.
- Define new test methodologies for airbag particle effluent testing where required.
- Define the effects of ventilation of a test vehicle after airbag deployment on particle effluent characteristics.

Chapter 4

Focus areas for particle characterisation

4.1 Introduction

It is not the aim of this programme of study to relate any effects of airbag deployment to health exposure but rather to identify the characteristics of the PM effluent which in future research may be related to specific health issues. As such the selection of characteristics detailed within this chapter is based on this premise. This also reflects the focus of work reported in the literature (Chan et al., 1989; Gross, 1994; 1995; 1999; Wheatley et al., 1997) and allows simple comparisons to be drawn.

This assessment of the PM effluents from airbags required testing of a number of key characteristics. These characteristics may include the particle size distribution, number or mass concentration, hygroscopicity, geometry, alkalinity, solubility and composition. To understand these factors and their impact on health risk it is important first to understand the key points of the human respiratory system. This can be simply divided into three regions, as depicted within Figure 4.1; these are the head airways, lung or tracheobronchial and alveolar regions (Vincent, 2007).

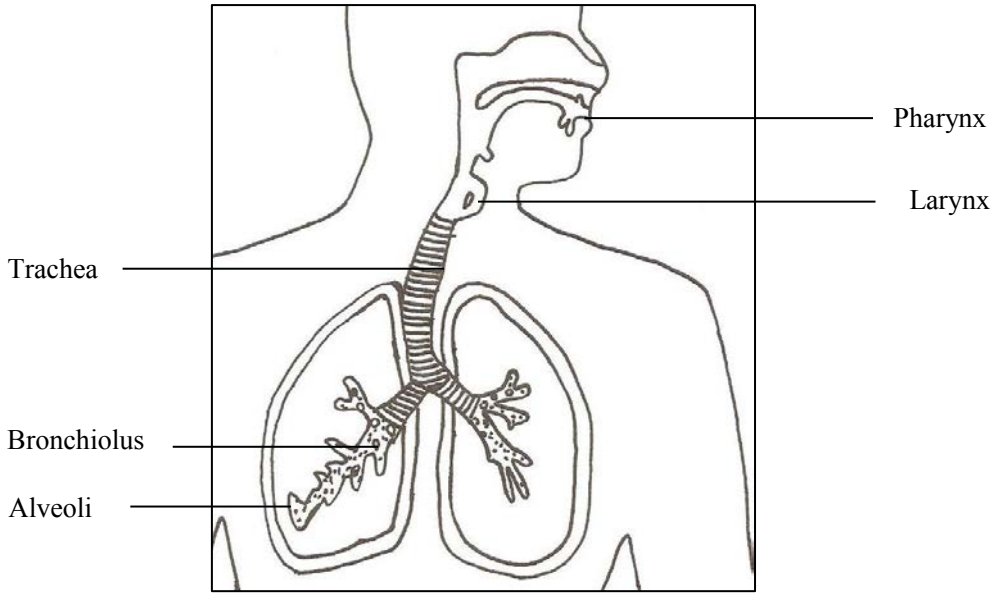

Figure 4.1: Human respiratory system schematic

The head airways region is comprised of the mouth, nose, pharynx and larynx, whilst the lung region covers the airways from the trachea to the terminal bronchioles and the alveolar region is the area below these where gas exchange takes place (Stellman, 1998).

At rest an adult will breathe around 12 times in a minute and inhale and exhale around 0.5l of air (known as the tidal volume) and when heavily exercising these values may increase threefold (Hinds, 1999). The surfaces of the head airways and lungs are covered in mucus that is constantly moved at a slow rate toward the pharynx where it is swallowed into the gastrointestinal tract. This natural clearance mechanism allows particles that have become entrained within this mucus to be transported away from the respiratory system in a number of hours. The alveolar areas of the lungs are however different and are not covered in a mucus as their function is to provide gas exchange which would be prevented by the presence of such mucus (Hinds, 1999).

The deposition and retention of particles in each of these regions of the respiratory system depends on a number of characteristics of both the particle and the respiratory system. These characteristics include the physical and chemical characteristics of the particle, physiological clearance mechanisms and the type and duration of exposure (ICRP, 1994). Whilst each of these factors is important, it is first key to understand the characteristics of the particle and the exposure scenario before considering physiological parameters. The following section therefore discusses the influence that particle characteristics have on human health and their importance, whilst exposure quantification is considered further within chapter 3. Size distribution, mass and number concentration, speciation and alkalinity are among those characteristics considered further.

4.2 Particle size distribution

Particle size is a key factor when determining the type of hazard and specific health risk associated with exposure to PM. The size distribution of an aerosol (solid or liquid particles suspended in gas or air) is especially important as it defines the ability of the particles to penetrate into the different elements of the human body and the likelihood of them being retained. Whilst most emphasis is placed on particles entering the respiratory tract, (ICRP, 1994) it is suggested that smaller particles in the nano-scale (<100nm) are able to transit to the interior of the body, directly through the skin. (Oberdorster et al., 2005)

Particles are either deposited into the respiratory system by impaction, settling or diffusion or they may be exhaled and not retained within the body. Those particles that are deposited into the head and lung airways are able to be naturally cleared from the region within the mucus in which they are deposited (Stellman, 1998).

However, the alveolar region is not protected by a mucus layer and insoluble particles which penetrate to this region can be held within it for a number of months or years. Some particles, however, are able to pass through from the alveolar region and into the bloodstream. Soluble particles dissolve and are able to pass through the alveolar membrane whilst small particles, such as those within the nano-scale may be able to pass straight through whether soluble or not (Ruzer and Harley, 2012). Figure 4.2 shows a model used to calculate respiratory deposition, factored by particle size and type or level of exercise/movement (Hinds, 1999). The 'X' axis defines particle size, whilst the 'Y' axis defines the fraction or proportion of particulate matter respiratory deposition.

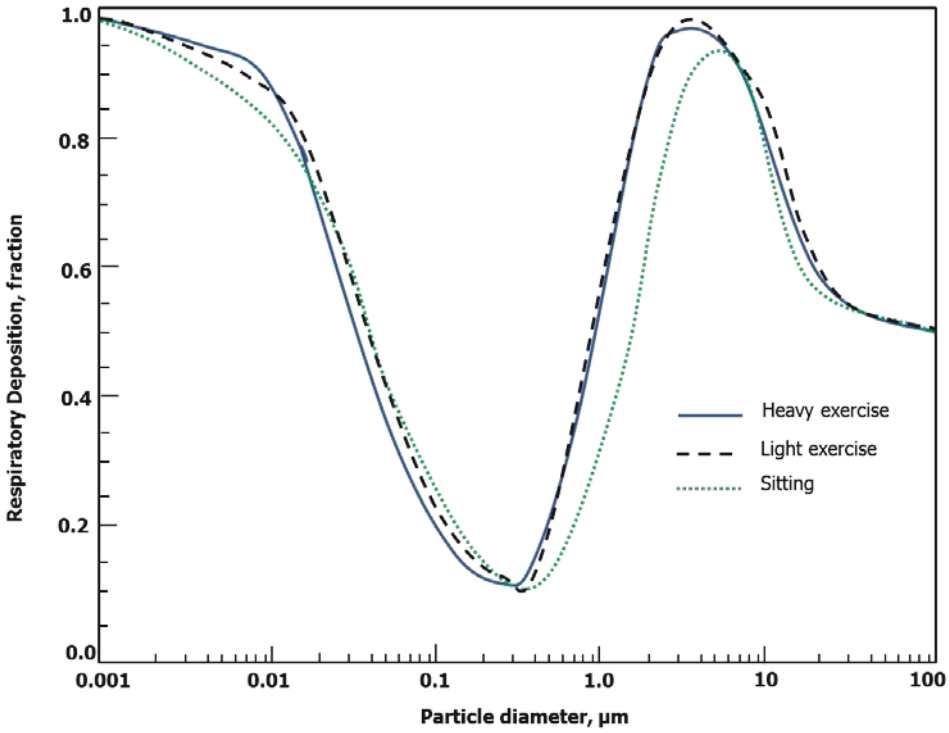

Figure 4.2: Predicted total respiratory deposition at three levels of exercise based on ICRP deposition model. Average data for males and females. Reproduced from Hinds (1999)

These total particle deposition models are based on measuring the concentration of a standardised aerosol (spherical and standard density) that is inhaled and exhaled by a test subject under experimental conditions. The model in Figure 4.2 indicates that the level of exercise has comparatively little effect on the amount of total particle deposition, except some difference can be detected in the 1-5µm range for 'sitting', where lower deposition occurs.

Although total respiratory deposition has been most commonly quantified, the data provides a limited picture within which to understand the specific health risk from exposure. Defining respiratory deposition by the three main regions of interest within the respiratory system provides far greater understanding of the deposition fraction and the point where an injury may be initiated. This regional deposition by particle size has been modelled by the International Commission on Radiological Protection (ICRP) and is detailed within Figure 4.3.

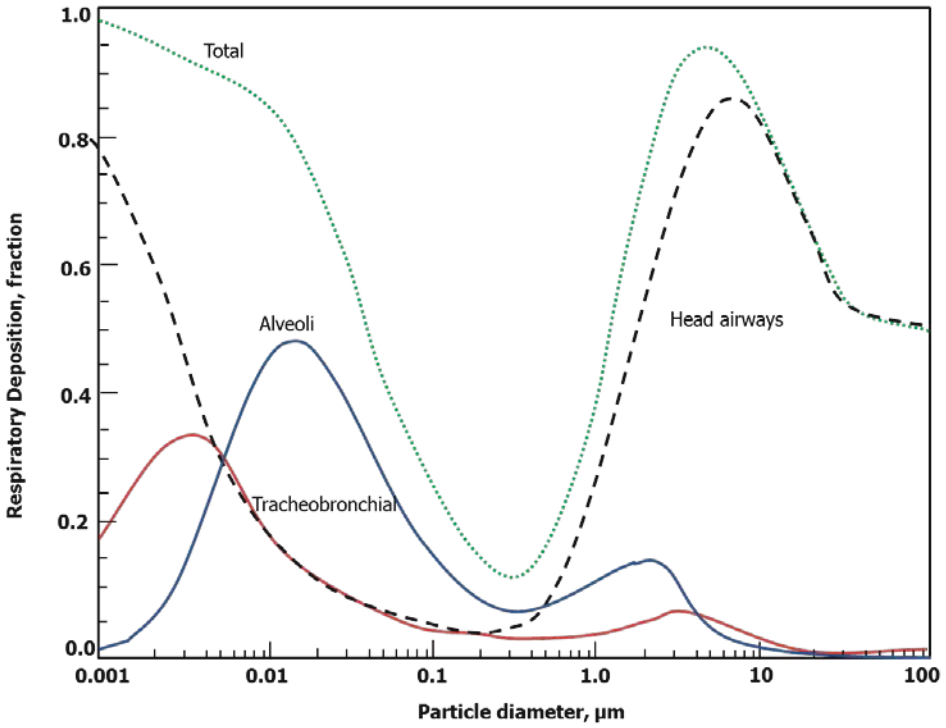

Figure 4.3: Predicted total and regional deposition for light exercise (nose breathing) based on ICRP deposition model. Average data for males and females. Reproduced from Hinds (1999)

As the respiratory system can be considered as a cascading system the amount of deposition within the three elements of the human respiratory system is dependent on that of the preceding region. Therefore a high respiratory deposition fraction in the head airways generally results in low amount of deposition in the following tracheobronchial or alveolar regions. This data is valuable for exposure studies and quantification of injuries arising from regional deposition but may also be used for defining suitable treatment characteristics and doses for drugs that may be administered through the respiratory system.

The knowledge that has been gained regarding deposition in the respiratory system has resulted in the definition and widespread use of a number of terms used to describe a particle's deposition point propensity in relation to particle size. Particles in the range 4-100µm are commonly divided into three size fractions (BSI, 1993); these being the inhalable, thoracic and respirable fraction. The inhalable fraction includes those particles that can be inhaled through the nose or mouth with an aerodynamic diameter of <100 µm, with those particles above 100µm not currently considered inhalable due to a lack of experimental data (Hinds, 1999). Exposure to these particles affects the respiratory tract, eliciting conditions such as rhinitis, nasal cancer and systemic effects, which affect the whole body (Hinds, 1999).

The thoracic fraction is the particle fraction that can penetrate the head airways and pass the larynx, moving in to the lung; with a median particle size of 11.64 μm and a geometric standard deviation (GSD) of 1.5 μm. Up to 50 % of the particles in ambient air, with an aerodynamic diameter of 10μm belong to the thoracic fraction. This fraction is also referred to as the PM_{10} fraction and exposure to PM in this range is an important factor linked to asthma, bronchitis and lung cancer (Vincent, 2007).

The respirable fraction refers to the fraction of particles that are able to reach the alveoli; the median particle size value is 4.25 μm with a GSD of 1.5 μm. Up to 50 % of the particles in air with an aerodynamic diameter of 4μm belong to this fraction. This fraction is also referred to as the PM_4 fraction and is related to the development of chronic diseases such as pneumoconiosis and emphysema (Risto, 2002).

Below the size fractions identified above are those classified as $PM_{2.5}$ (particles with an aerodynamic diameter of <2.5μm), PM_1 (particles with an aerodynamic diameter of <1.0μm) and those in the nano-scale (<0.1 μm /100nm). Particles referred to as $PM_{2.5}$ and PM_1 are classified as fine particles (Hinds, 1999) and those in the nano-scale as ultrafine. The smaller size of these particles facilitates transit in to the deeper reaches of the lungs.

Significant research has now been presented regarding the health risks surrounding $PM_{2.5}$ and PM_1 and particles in these fractions have been linked to increased risk of natural cause, cardiopulmonary and lung cancer mortality (ARB, 2002). Particles in this fraction have also been linked to aggravation of pre-existing conditions; asthmatics have suffered an increase in irritation of the airways, coughing and breathing difficulty (USEPA, n.d.) ; Larson and Koenig, 1994) whilst those with existing coronary artery disease suffered cardio pulmonary symptoms and an adversity to activity (de Hartog et al., 2003).

Those particles in the nano-scale are easily deposited into all areas of the respiratory tract, with their small size facilitating the ability to pass into and across cells and into the blood. Within the blood these particles can transit to sensitive areas of the body, including the heart, spleen, lymph nodes and bone marrow (Oberdorster et al., 2005). Nano-scale particles are reportedly able to access the central nervous system and penetrate directly through the skin, suggesting a new exposure scenario not previously considered.

Aside from transport and deposition in the respiratory system, particle size also influences settling and airborne transport behaviour within exposure environments. Larger particles and those of a higher mass travel with less speed and a shorter distance than their smaller counterparts, whilst also settling quicker. The diagram presented within Figure 4.4 defines particle settling times in still air and illustrates the significant increase in settling time for smaller particles when compared to their larger counterparts.

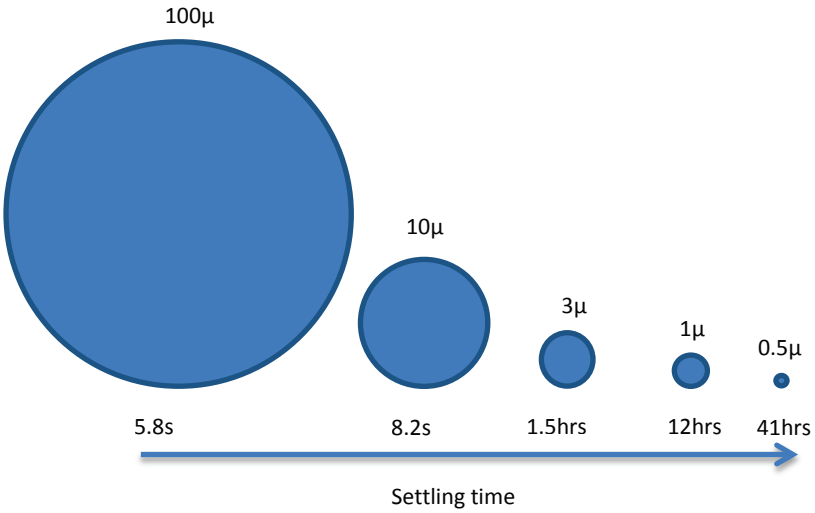

Figure 4.4: Particle settling time in still air defined by size (Baron, n.d.)

This understanding of settling and transport behaviour based upon particle size is valuable when selecting suitable safety precautions and requirements for ventilation within exposure environments.

4.3 Particulate mass and number concentration

Whilst size distribution is a key factor in defining the ability of particles to penetrate to specific areas of the body and be retained, it must be combined in tandem with the concentration of the PM. Particles in lower concentrations may present an acceptable or tolerable health risk, but those same particles in higher concentrations may present an unacceptable risk to health and therefore are to be controlled or avoided completely.

Where values above concentration thresholds for substances have been linked to a quantifiable risk to health, exposure limits have been established. These are ordinarily classified for occupational exposures as either 'short term' for exposures up to 15 minutes in duration or 'long term' for exposures of up to 8 hours (US Dept. of Labour, n.d.). Limit values are classified as parts per million (ppm) for gaseous substances and milligrams per cubic metre (mg/m^3) for particulates. In Great Britain exposure limits are classified as WELs; Workplace Exposure Limits and are categorised as either an 8 hour or 15 minute time weighted average (TWA) within the Health and Safety Executive (HSE) Control of Substances Hazardous to Health (COSHH) regulations (HSE, 2012). These correlate to the permissible exposure limit (PEL) and short term exposure limit (STEL) used in the US for 8 hour and 15 minute TWAs respectively (US Dept. of Labour, n.d.b). In addition to these limits are those that control exposures termed 'immediately dangerous to life or health' (IDLH) as defined by the US National Institute of Safety and Health

(NIOSH). This term is used to describe 'an atmosphere that, poses an immediate threat to life, would cause irreversible adverse health effects, or would impair an individual's ability to escape from a dangerous atmosphere (OSHA, 2011). These IDLH values are defined for specific agents and do not exist for general particulates or those segregated by size as with WELs. Where limits are not specifically defined or aerosols are formed of a combination of different particle components (as is common for many aerosols and dusts), concentration limits are also defined based on particle size fractions. Two particle size fractions for PM are defined within regulations, with these being either inhalable or respirable, as discussed previously. These limit values are defined for long term exposures and differ for each of the applicable regulatory bodies (Appendix B)

Whilst short term (15 min) exposure limits for these particle size fractions are not defined, it is suggested that values three times higher than that of the long term (8 hour) should be used (HSE, 2005). Limits for particles below these size ranges are currently not available due to a limitation in current knowledge (Hinds, 1999).

Whilst concentration limits specified in regulatory texts (Appendix B) focus on particle mass concentrations, measuring particle number concentrations can provide greater understanding of the size distribution of a measured aerosol. This may also be achieved by direct measurement of particles by means of a cascade impactor, although the range of size cut-points ordinarily provides coarse distribution data whilst difficulties during sampling can limit the accuracy and validity of results (Stein, 2005). Where a mass concentration limit exists, this may be composed either from a low concentration of high mass/size particles or a high concentration of lower mass/size particles.

Regardless of the technique employed, the knowledge of an aerosol's concentration allows not only the calculation of safe exposure limits, but also allows control methods to be understood and specified. Higher concentration environments are likely to require increased venting durations or higher efficiency extraction systems to control exposure conditions.

4.4 Speciation and composition

The speciation or composition of a particle is of particular importance to those defining the specific hazard to health that is posed by exposure. Knowledge of the composition not only allows quantification of the risks associated with exposure to substances, but also to identify the hygroscopicity, solubility or alkalinity of a substance. These additional factors associated with specific components allow a definition of the particles tendency to deposit and be retained in the body.

4.5 Alkalinity and acidity

Both alkaline and acidic particles pose a hazard to those exposed and both are capable of causing damage to tissues (Cox, 2013). PM from airbag deployments appear to be predominantly alkaline (Chan et al., 1989; Gross et al., 1994) although both acidic and alkaline effluents are controlled with a range of 5-9 pH, (Audi AG et al., 2001) and 4-10.5 pH (SAE, 2004).

Exposure to alkaline PM has been linked to both dermal burns and ocular injuries during short term post-collision exposures. Arguably the greatest risk of permanent, life-changing injury when exposed to such alkaline agents surrounds damage to eye tissues (Smally et al., 1992; Barnes et al., 2012; White et al., 1995). Alkaline substances continue to cause damage to tissues for far longer than their acidic counterparts and are able to dissolve cell membranes and cause permanent tissue damage. These alkaline agents can penetrate rapidly to the anterior chamber of the eye (the area in front of the iris and behind the cornea) causing damage. Ammonium hydroxide is among the fastest penetrating alkaline agent; with penetration occurring within around 5 seconds (US Army Medical Dept., n.d.) Concentration limits for a number of alkaline agents are defined within occupational exposure regulations (Appendix B) whilst airbag test standards (Audi AG et al., 2001; SAE, 2004; 2011a) define concentration maxima for some alkaline agents alongside an acceptable pH range.

4.6 Hygroscopicity

A particle's hygroscopicity is its ability or tendency to collect water and this influences its deposition behaviour. Those particles that are more hygroscopic can increase in size as they pass through the airways of the respiratory system, which are saturated in water. This expansion in size increases the likelihood of deposition and settling in the distal airways of the lungs (Hinds, 1999). The distal airways are defined as the terminal bronchioles with a diameter <2mm and have a direct connection to the alveolar region (Vogel, 2007).

Therefore, defining the hygroscopicity of the particles will provide greater understanding of their deposition in the respiratory system and the risk to human health. The work of Starner (1998) investigating airbag effluents defined that changes in ambient humidity within the range 25-75%, had little effect on the size or number distribution. However, this study was only limited to defining the influence of variance in test environments.

4.7 Solubility

The solubility of particles is another factor that influences the specific risk associated with such aerosols. Both soluble and insoluble PM is capable of inducing oxidative stress in the human lungs (Zhang and Ding, 2012). Oxidative stress occurs when there is an excess of free radicals over antioxidant defences. This imbalance results in these free radicals attacking and oxidising cell components, such as lipids, proteins and nucleic acids in turn causing tissue injury (Kelly, 2003) It is a key factor in the damaging health effects caused by exposure to PM.

Adamson et al. (1999) suggested that the soluble fraction is the most hazardous portion of PM as it can be more easily absorbed within the human respiratory tract and these soluble fractions are more likely to dissolve and release potentially harmful material to the body (WHO, 2013). The presence of metals within soluble fractions of PM has also been reported, emphasising the importance of reducing exposure to such fractions (Fernandez-Espinosa et al., 2002)

4.8 Particle morphology

The shape and geometry of a particle; its morphology, is less commonly defined than many of the other characteristics previously discussed (McDonald and Biswas, 2004). Some particles such as those formed by condensation or liquid droplets are spherical while most others are non-spherical. These non-spherical particles may have regular geometries, or as with agglomerates, be irregular (Hinds, 1999). The drag force and settling velocity of a particle is affected by its morphology. This in turn affects its transport properties and the point of deposition in the respiratory system.

Indirect measurement techniques and equipment such as the differential mobility analyser (DMA) or differential mobility spectrometer (DMS) define a particle's size based on its aerodynamic diameter, assuming that all particles are spherical and of a fixed density. Whilst in some instances this assumption may be accurate, it is more likely that a measured aerosol is composed of particles of varying morphologies and densities. Where particle morphology differs from that of a spherical particle, a factor known as the dynamic shape factor (Kulkarni et al., 2011) can be applied to Stokes law to define the effect of differences in morphology on particle motion and behaviour. Stokes law is an expression that defines the drag force on spherical objects such as particles. Dynamic shape factor applied to Stokes Law (Shearer and Hudson, n.d.) is shown in Equation 4.

$$F_D = 3\pi\mu V d_v K \qquad \textbf{(Equation 4)}$$

Key:

F_D	=	Drag force
μ	=	Viscosity of fluid
V	=	Velocity of sphere relative to the fluid
d_v	=	Diameter of a sphere with the same volume as the object
K	=	Dynamic shape factor

4.9 Summary

Whilst it is clear that exposure to PM poses a significant risk to health, there are many factors that influence the specific risk posed. The key elements can be generally divided into two main segments concentrating either on (a) PM size distribution and concentration or (b) particle speciation and characterisation. The first segment characterises the transport behaviour of the effluent and its likely deposition point in the human respiratory system whilst the second relates to the chemical hazard posed from exposure to particular substances.

Size distribution, concentration and exposure scenarios were defined by the author as key to classifying the risk from exposure to PM effluents from airbags and have therefore been considered further in the experimental section of this research. Particle morphology was also considered, as shape characteristics for airbag effluents are not evident in open literature and the impact of this attribute on indirectly measured size distribution has not been calculated for this PM source.

The experimental methodologies utilised for testing of the previously defined PM effluent characteristics are defined within Chapter 5 and in addition the scenarios in which exposure occurs have also been considered and characterised.

Chapter 5

Review and Selection of Methods for Particle Characterisation

5.1 Introduction

There are many methods that could be utilised to define the characteristics of airbag effluents, their behaviour and the influence on the risk posed to human health. Technical standards for airbag PM effluent testing are based on mass concentration and chemical composition and are designed for post-collision exposure testing. However, it is not a legal requirement for all manufacturers to even test or comply with the conditions of these test standards. These standards include the Society of Automotive Engineers (SAE) J-1794 (SAE, 2011a), USCAR24 (SAE, 2004) and AKZV-01 produced by a consortium of European vehicle manufacturers (Audi AG et al., 2001), which is primarily based upon the aforementioned documents. These draw on many elements from the early work of Starner (1998) and Chan et al. (1989) who initiated research while working within vehicle manufacturing organisations and little change can be identified between the first iterations of the standards and the most current versions.

This chapter describes standards which, although not completely comprehensive, cover many elements of testing including test environments, environmental conditions, particle mass and number quantification, spectral density and speciation definition. Alongside the techniques presented within these standards, a number of other less common methodologies are discussed. This chapter also identifies the methods used within the research programme.

5.2 Test environments

Effluent assessment and exposure studies may be conducted in either test tank environments or within the interiors of passenger cars, with the latter commonly chosen

for human exposure testing (Gross, 1994; 1995; 1999; Wheatley, 1997; Linn and Gong, 2005). Vehicle environments not only represent the atmospheres in which exposures will occur but allow a comfortable and simplistic situation in which a human test subject may be seated. They do however pose significant challenges in providing a repeatable test environment that can be equipped with varying types and numbers of airbags and other restraint system components. For these technical reasons and a significant reduction in test costs, test tanks are commonly used by vehicle manufacturers and tier one suppliers for assessment of effluents from restraint systems.

There are two common test tanks defined in standards (SAE, 2011a; 2004) that may be employed for effluent testing. The first, a small ballistic tank is predominantly designed to define tank pressure curves for inflators but may be employed for initial effluent tests, Figure 5.1 whilst the second is a larger tank designed specifically for airborne effluent testing, Figure 5.2.

Figure 5.1: Ballistic test tank (NHTSA, 1998)

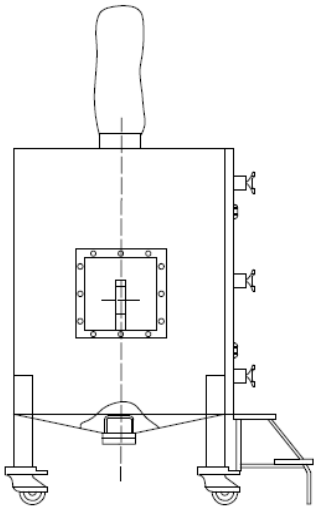

Figure 5.2: Effluent test tank schematic (SAE, 2011a)

The small volume of the ballistic test tank and the lack of similarity to the exposure environment make it unsuitable for use in airborne particle effluent studies. This is supported by the work of Starner (1998) which identified that the ballistic test tank was not a robust method for quantifying effluents. Therefore on this basis, the effluent test tank and a vehicle interior remain the only viable options for use within the research programme and thus were investigated further.

An effluent test tank is intended to represent the interior volume of a car's interior and must be designed to be able to withstand the harsh environment created by repeated airbag deployments. The specified tank volume of 2.83m^3 represents the interior of a North American mid-sized saloon vehicle, although a tank of 2.5m^3 is also an accepted

option when employed with a suitable mathematical correction for the variance in volume.

Whilst a test tank can be of a comparable volume it has discernibly different characteristics to a vehicle interior. These are discussed in sections 5.21-5.2.4.

5.2.1 Effect of geometry

Whilst the use of a simplified (cubic) geometry for the test tank provides advantages within design and manufacture, the resultant structure does not represent that of a vehicle's interior. However, it remains unclear what influence this variation in geometry has upon the effluent test methodology and results that are provided. Whilst the geometry differs, the volume of both environments may be comparable through utilisation of vehicle interiors with internal volumes close to that of the effluent test tank.

5.2.2 Effect of interior fittings and surfaces

In addition to the variation in geometry and potential disparity in volume, variations also exist between the surfaces and fittings present within vehicle and test tank environments. The test vehicle used for both quantification (Audi AG et al., 2001) and human exposure assessments (SAE, 2004) remains in its standard specification, complete with seating, fabrics and all surfaces one can expect from a modern vehicle, whereas a test tank employs a simple metallic, non-corrosive shell with an absence of internal fittings. The presence of these components and variations in surfaces within test vehicles not only may affect the aerodynamic behaviour of the effluent particles but also limits the possibilities of cleaning the surfaces of the environment and removing any residues that may exist from previous testing. If these same particles are deposited upon surfaces and cannot be easily removed, they may be dislodged by the increase of in-tank pressure (from deployment) in subsequent tests, this in turn may result in variances in results.

5.2.3 Effect of airbag mounting and sampling position

Within the test vehicle standards specify that airbags and other restraint system components are to be fitted within the standard positions, whilst within the test tank, standards merely suggest diagrammatically that these same components are to be fitted in the geometric centre of the tank (SAE, 2011a). This variation in mounting position may affect particle dynamics within the environment, yet specific tests of the influence of such variances are yet to have been presented within the literature. However, Starner (1998) suggests that for gravimetric filtration the effects of sampling position variation within a test tank are minimal, suggesting potential homogeneity in the environment and therefore

a limited effect on mounting position. However, further testing to clarify such an assumption is necessary.

5.2.4 Effluent containment capabilities

The test environments exhibit differing characteristics that are likely to affect their capability to contain the effluent within for the duration of the test procedure in a manner representative of the exposure scenario. The environments must be capable of containing the increase in pressure produced by the introduction of inflation gases and be sufficiently strong to enclose the effluent within for the duration of the test procedure. These aspects may be relatively easy to combine within a purpose built environment, however pose more of a challenge when using a vehicle interior.

Although it can be hypothesised that the differences between environments and the associated factors are likely to affect the measured characteristics of the effluent, no data is available in open literature regarding the inter-comparability of the test tank and the vehicle interior that it represents. Therefore it is not currently clear as to which test environment, (interior or effluent test tank) is most suitable for studies of this nature and an initial objective of the research was to quantify this variance to define whether test tanks are suitable for characterising exposures sustained in vehicles, both after collisions or during ELV depollution.

5.3 Effluent characteristics testing

Further to determining the testing environments, suitable methodologies for defining the characteristics of the PM effluents must be selected. These characteristics including size distribution, concentration, morphology and aerosol behaviour and are described within Chapter 4. These characteristics may be defined through direct or indirect measurements and these methods and a number of equipment options are identified within the following sections.

5.3.1 Direct measurement

The direct measurement of PM allows mass concentration to be determined by measuring either particle mass or inertia (Kulkarni et al., 1999). These direct measurements require the means to collect particles and the capability to accurately measure the collected mass, with this commonly conducted through the use of gravimetric filters, cyclones, cascade impactors or one of a number of mass balance systems. These methods and systems are discussed briefly here, whilst further information is defined in the text by Hinds (1999). Direct measurement methods predominantly offer the same capabilities with some providing increased sampling rate resolution and others offering coarse size distribution

measurement. Gravimetric filtration is the simplest and most cost effective of these methods and is a specified option within airbag effluent test standards. This requires a particle mass sample to be collected on filter media and carefully weighted after undergoing sample conditioning.

The same basic concept is employed for assessments using the tapered element oscillating microbalance (TEOM) and quartz crystal microbalance (QCM) which both use an oscillating collection substrate to collect a PM sample, Figure 5.3.

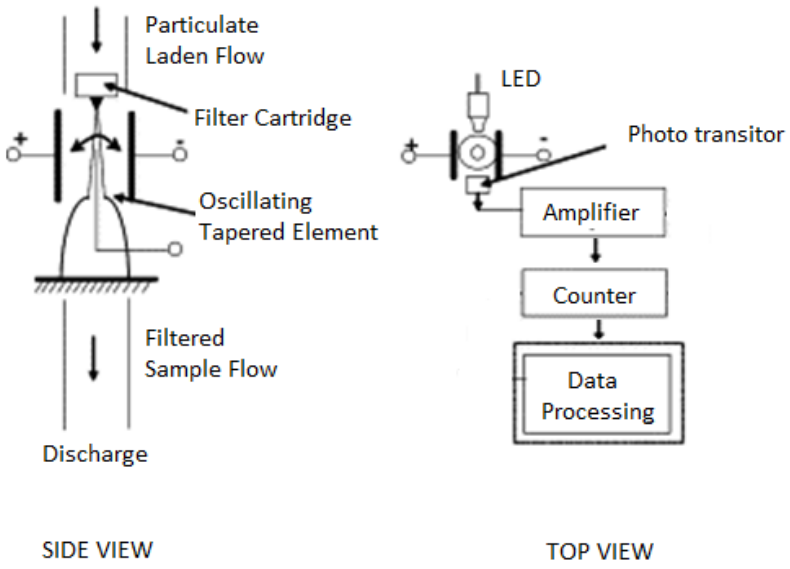

Figure 5.3: Tapered element oscillating microbalance (TEOM) (Vouitsis et al., 2003)

As mass collects on either the QCM's crystal or the TEOM's mass sensor the oscillation frequency changes in response and this change is correlated to particle mass concentration. Neither of these methods nor gravimetric filtration (GF) provide any size distribution measurement capability and are therefore unsuited to the measurement of airbag effluents which are generally both polydisperse (including particles of varying sizes) and non-stable (varies in size and/or concentration over time).

A direct measurement method that does however provide size distribution measurement capability requires the use of a cascade impactor (CI), Figure 5.4 and Figure 5.5. PM drawn into the CI is forced through an orifice and accelerated towards an impaction plate mounted just below the nozzle, Figure 5.5. The impaction plate alters the flow of air and those particles small enough, pass around the plate in the stream of air and onto the next stage or final filter. Those particles that are too large to travel around, impact upon the plate and are collected and subsequently weighted.

Figure 5.4: Eight stage cascade impactor (Envco-Environmental Equipment, n.d.)

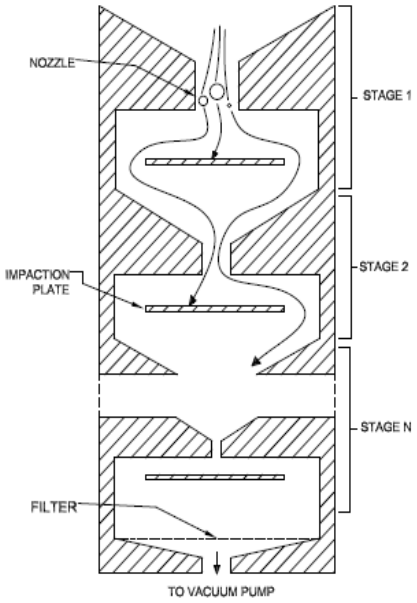

Figure 5.5: Cascade impactor schematic (Hinds, 1999)

Whilst providing size distribution capability the CI is only able to provide a single measurement during an assessment and this limitation on sample resolution time limits the comprehensiveness of testing for robustly defining airbag effluents.

It is therefore clear that whilst direct measurement of particle mass provides compliance with existing test standards and comparison to data presented within the literature, the lack of combined high sampling rates and size resolution in general prevents these measurement methods being used for the testing of airbag effluents, which are known to present both a rapidly changing sample and polydisperse size distribution. Therefore alternative options such as optical and electrical mobility measurement methods have been assessed to define a more suitable solution for the measurement of airbag effluents and are discussed within the proceeding section.

5.3.2 Optical aerosol measurement

Optical PM measurements provide the capability to define the size and number of particles within an aerosol, with these measurements being defined by the way in which light interacts with PM or individual particles; whether through the scattering or absorption of light. The systems used to assess this interaction are able to do so without the need for physical contact and are both sensitive and responsive and generally portable (Hinds, 1999). The most common devices; the light scattering laser photometer (LSLP), condensation particle counter (CPC) and optical particle counter (OPC), (Kulkarni et al., 2011) all measure the amount of light scattered by a PM sample, Figure 5.6.

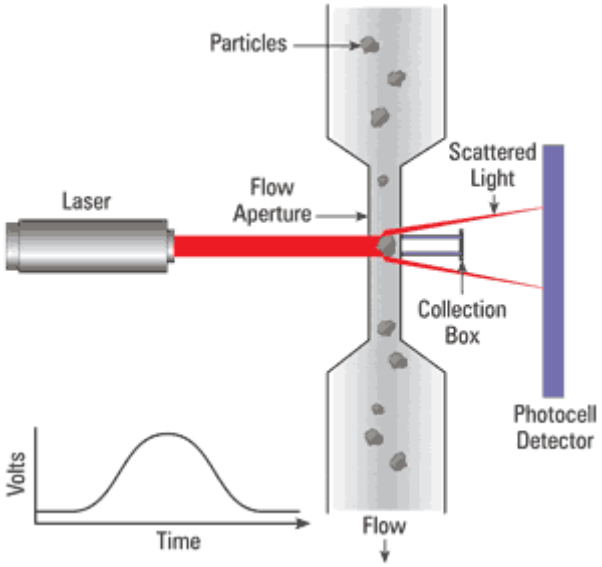

Figure 5.6: Light scattering particle counter schematic (Machinery Lubrication, n.d.)

The amount of light scattered by the aerosol is based upon the particle's size, shape and refractive index. Each of these systems offer varying advantages and disadvantages whilst all are able to provide continuous measurements throughout tests albeit with varying measurement system residence times. The LSLP, although able to measure a broad size range is limited by a minimum particle size measurement threshold of 100nm and a comparatively low maximum concentration measurement capability. A CPC is able to measure far smaller particles than the LSLP (down to approximately 2nm (University of Manchester, n.d.b)) by increasing the size of particles entering the system through condensation; thus allowing easier measurement of smaller particles. Whilst offering increased performance for measurement of smaller particles, CPCs are commonly limited to providing 1 sample per second and in contrast to the LSLP are only able to classify total particle output without size distribution characterisation.

The OPC is similar to the LSLP and CPC yet PM samples are passed in a thin stream through a laser beam, surrounded by a sheath of air, allowing single particles to be illuminated and independently counted (Hinds, 1999). These OPCs are commonly able to count particles within a range of between 0.1µm and 20µm (dependent on the particular equipment used) segregated into a number of size ranges and are able to provide realtime number counts of particles. Whilst providing reasonable size resolution, these instruments are less suitable for studies assessing particles in the nano-scale and are constrained to use in relatively low concentration environments without the use of sample dilution. Further information regarding optical measurement equipment and methodologies is defined in the text by Vincent (2007).

Whilst optical measurement of PM provides many advantages over direct measurements, no single system is able to provide a combination of a fast response time and the capability to define size distribution into the nano-scale whilst operating in high concentration environments such as those experienced during effluent testing. In addition, variations in particle shape and refractive index are able to illicit sizing errors that are not easily corrected if and when identified. For these reasons the measurement of the electrical mobility of particles was considered.

5.3.3 Measurement of electrical mobility

Measuring the electrical mobility of a particle has become an accepted method for measuring PM and significant advances with respect to equipment provision have been made within the field in recent history. The electrical mobility of a particle when considered simply depends on its size and its electric charge (ISO, 2009). Subjecting a charged particle to an electric field results in the motion or migration of the particle at a velocity that is determined by its aerodynamic drag and electrostatic force, (Kulkarni et al., 2011). The particles aerodynamic drag is influenced by the viscosity of the gaseous substance in which the particle is resident and therefore its temperature and pressure, and also the morphology of the particle. For measurement of particle size based on electrical mobility, the morphology of a particle cannot simply be factored and it is assumed that particles are spherical. With particles considered spherical the migration or motion of a charged particle can be determined based on its known charge and knowledge of the electric field, thus allowing its size to be calculated.

A number of options for measurement of the electrical mobility of particles and therefore their size exists and these include the DMA (TSI, n.d.), scanning mobility particle sizer (SMPS) (Sioutas, 1999), DMS and electrical low pressure impactor (ELPI) (Dekati, n.d.a).

The DMA classifies particles based on their electrical mobility to define the concentration of particles of a particular size. Particles entering the system move in an electrical field towards a charged central rod in a manner which is proportional to their electrical mobility. Those particles within a defined measurement size range pass through an outlet at the base of the system and are counted, whilst those outside of this range either collect upon the rod or pass out of the system through an outlet port. The DMA measures particles within a single defined size range and for measurement of a polydisperse aerosol sample varying voltages must be applied to the central rod to collect particles of differing sizes. This voltage change requirement results in a substantial increase in measurement time. This can be avoided by employing the use of a SMPS that is able to measure particles of varying sizes according to their electrical mobility. The SMPS is composed

of a DMA to classify particles based on their electrical mobility and a condensation particle counter (CPC) that defines particle concentration for a given size, but the SMPS is able to scan a wide range of voltages to provide data regarding size distribution. However with an extended residence time in the DMA, a spectrum may only be generated after around 1 minute, with the system therefore still being most suited to measurement of a stable PM sample (University of Manchester, n.d.b)

Whereas a scanning mobility particle sizer uses a DMA to define the electrical mobility of PM by measuring size ranges of particles in turn, a DMS uses multiple detectors operating in parallel to define the size distribution and concentration of PM in realtime, without the need to scan across size ranges independently (Price, 2009). The DMS draws PM samples into the system via a vacuum to a corona discharge charger and on to the classifier column. These charged particles flow in a laminar column of air and are deflected by a central charged electrode to grounded electrometer rings, Figure 5.7. Their landing point is a function of their charge and aerodynamic drag which allows for a representative particle size to be determined.

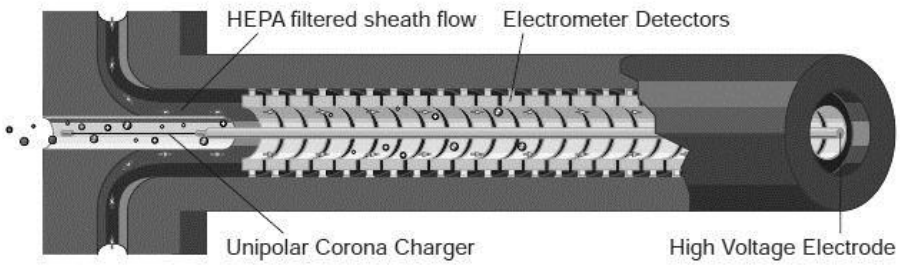

Figure 5.7: DMS Operating principle schematic (Cambustion, n.d.a)

The DMS offered by Cambustion Limited, Cambridge, UK, is able to measure the size spectrum of PM in the range 5nm to 2.5µm and provides real-time measurement with a fast response time (Cambustion, n.d.b); 10Hz data, 300ms $T_{10\text{-}90\%}$ response. An integrated dilution and large particle filtration system allows use in high concentration environments such as those encountered in measurement of combustion products. This high sampling resolution and ability to sample in high concentration environments, makes the DMS an attractive choice for airbag effluent assessments, where changing size distributions and concentrations are likely.

An alternative to the DMS is the electrical low pressure impactor (ELPI) which may be considered a hybrid measurement system, combining a cascade impactor and an electrical charge measurement system. Particles entering the system under a vacuum are electrically charged by a corona charger and subsequently enter the cascade impactor and are impacted upon electrically insulated impaction stages. The particles are collected on

the impactor stages according to their aerodynamic diameter and the electric charge of the particles is measured in realtime by electrometers, to provide size and number concentration data (Dekati, n.d.a). The ELPI is able to operate over a wide particle size spectrum from 10µm to as low as 6nm, but size segregation within this range is limited by the number of impaction plates; with commonly up to 14 in use (Dekati, n.d.b). Consequently with a system incorporating impaction plates, a size segregated sample can be collected and assessed after testing to define chemical characteristics.

The diverse capabilities and limitations presented by direct, optical and electrical mobility measurement methods suggest that suitable equipment and methodologies must be selected based on knowledge of the target aerosol and the characteristic of interest, i.e. size distribution in the sub-micron range. Data presented in the literature states that an airbag effluent is likely to be a high concentration polydisperse aerosol (Gross, 1994; Ziegahn and Nickl, 2002) and other studies (Chan et al., 1989) indicate that combustion product evolve rapidly. It is therefore clear that either the DMS or electrical low pressure impactor would be most suited to the assessment of airbag effluents.

5.3.4 Particle morphology

Whilst there is little evidence of studies investigating the morphology of particle effluents from airbags, an increasing number of studies in other fields have utilised microscopy to define particle morphology (Price, 2009; Marsh, 2011; Wyatt, 2011; Berk, 2009a/b). Information from particle morphology affords a greater understanding of the transport behaviour of the particle and the influence of this on the risk to human health (WHO, 1984; Hinds, 1999; HSE, 2004). Knowledge of particle morphology also allows factors to be applied to the data collected by indirect measurement, such as those from electrical mobility, in instances where non-spherical particles are present.

Selection of a suitable microscopy method is dependent upon both the expected particle size and resolution of the analysis equipment concerned. Data in the literature suggests that a reasonable proportion of the expected particle output may fall outside the resolution range of around 300nm for optical microscopes (Hinds, 1999) and in some cases the typical limits of resolution for Scanning Electron Microscopy of around 20-30nm (University of Utah, n.d.). Therefore Transmission Electron Microscopy (TEM); capable of providing greater resolution beyond this range, below 1nm (Egerton, 2008) was employed as the key method for this morphological study of effluents. Where the measurement range allowed and a further advantage could be gained from its differing capabilities, scanning electron microscopy was also employed.

Transmission electron microscopes operate with the same basic principles as an optical light microscope with electrons being used in place of photons and an electromagnetic

lens used in place of a glass lens (Egerton, 2008). A heated tungsten filament located at the top of the microscope generates electrons through thermionic emission which pass through the main column of the microscope in a vacuum to the electromagnetic lenses, where they are focused into a beam that is transmitted through the sample. The density of the sample affects the amount of transmission of electrons, with high density samples scattering the electrons outside of the beam. Those electrons that are transmitted through the sample and not scattered, hit a viewing screen which results in a shadowed image being generated. The darkness of the image provides an indication of the density of the sample.

Scanning electron microscopes operate in a similar manner to transmission electron microscopes, and again use electrons instead of photons to form an image (Hinds, 1999). An electron source, located at the top of the microscope produces an electron beam that travels within a vacuum through a series of lenses and electromagnetic fields that focus the beam towards the target area. These primary electrons interact with the surface of the sample and secondary electrons are emitted. These are detected by a secondary electron detector and an image is subsequently generated.

For analysis by SEM, samples can be in many different forms and sizes although specimens must fit within the specimen chamber. In contrast to this ease of sample selection, for TEM, test samples are required to be collected on small standardised circular grids of 3.05mm diameter that are able to be inserted in the microscope via a specimen holder. These grids are ordinarily manufactured from copper, gold or molybdenum and vary in thickness from around 10 µm to 100µm depending on the mesh size. The mesh size is determined by the number of holes within one inch, with a higher mesh number resulting in a thicker grid. Samples cannot be imaged when positioned directly on the grids or mesh as the electrons are not able to be transmitted through the material, therefore grids are usually coated with a film that supports the sample and allows imaging, but in some cases where the sample is self-supporting the need for a film is negated. These films are 'electron transparent' (Grid-tech.com, n.d.) and are usually produced from carbon, formvar or a carbon/formvar mix, and are available in varying thicknesses. These films may be deposited on the grid as a solid, yet thin surface or be deposited in a manner that provides a 'holey' or 'lacey' film surface, Figure 5.8 and Figure 5.9.

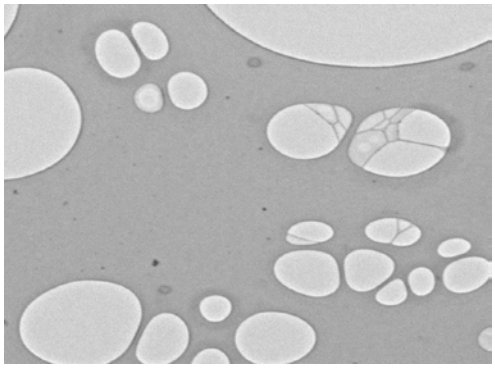

Figure 5.8: Holey carbon support film

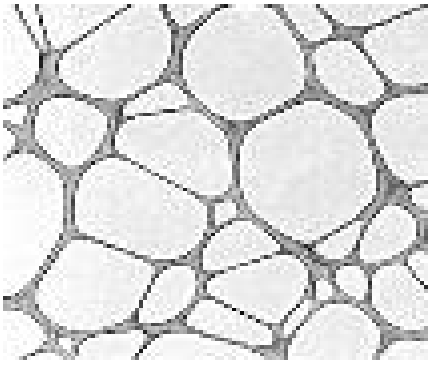

Figure 5.9: Lacey carbon support film

The presence of a thin carbon film can cause absorption and scattering of the electron beam in high resolution assessments, affecting the quality of the resultant image. Holey and lacey films are able to reduce the impact of this 'noise' and allow samples to be collected on areas not obscured by the film, Figure 5.10.

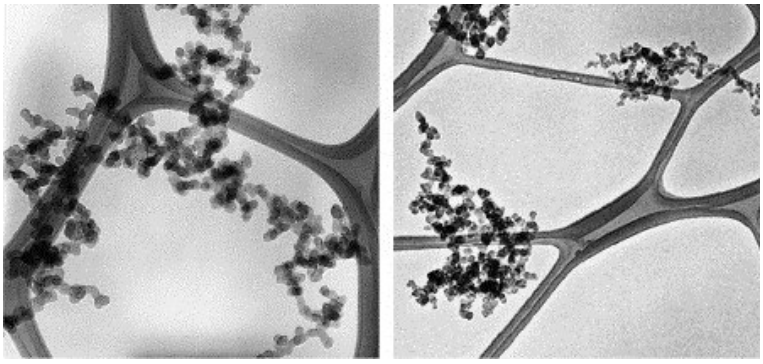

Figure 5.10: Soot particles deposited on lacey grids (Shaddix et al., 2005)

5.4 Summary

There are many options for the testing of effluents from airbags including variations of the test environment and measurement equipment employed.

Testing of effluents is commonly undertaken in either a small ballistic test tank, a larger environmental test tank or a vehicle interior. The literature indicates that the ballistic test tank is not suitable for testing airborne effluents from airbags; however a lack of clarity exists when comparing the larger effluent test tank with a vehicle interior of an equivalent volume. This research programme therefore has sought to identify any variance between these two environments whilst assessing their overall suitability for use in general effluent testing and for exposures sustained by ELV disposal and depollution operatives.

A number of options exist for measurement of effluent and particle characteristics and the choice of equipment employed must be carefully made based on the characteristic to

be defined and the expected output and behaviour. Airbag PM effluent is likely to be high concentration (Wheatley et al., 1997) and polydisperse (Chan et al., 1989), with a number of predominant modes and substantial particle concentrations of less than 1μm in size (Chan et al., 1989; Gross et al., 1994). The effluent will change in concentration and size distribution with respect to time (Chan et al., 1989).

Direct measurement methods such as GF, cascade impaction and the use of the TEOM or QCM generally lack suitable size and/or sampling resolution for airbag deployments. However, whilst not expanding knowledge in the field, GF is a defined method in test standards (Audi AG et al., 2001; SAE 2011a) and is well used in practice. Consequently it was used in this study to show a relation to data in the literature.

Optical measurement systems would likely require calibration based on PM characteristics, such as particle refractive index or morphology that are currently unknown for airbag effluents. These techniques are also generally unsuited to operating in high concentration environments such as those expected for airbag effluent testing.

Use of a DMA which measures the electrical mobility of particles, is limited by the ability to only easily quantify a monodisperse aerosol. Whilst a Scanning Mobility Particle Sizer (SMPS) is able to measure a polydisperse aerosol, it requires a comparably lengthy residence time (up to 1 min) and therefore provides less comprehensive sampling rate resolution than other options.

DMSs and ELPIs do provide the required sampling rate resolution and size distribution capabilities required for the assessment of airbag effluents and are able to operate in high concentration environments. The ELPI offers a larger measurement range capability and the option to collect aerosol samples for subsequent chemical analysis, which cannot easily be offered by the DMS. However, the ELPI only offers 14 size range cut points in the sub-micron size range as opposed to the 22 size segregations offered by the DMS. The ELPI also requires a sample vacuum flow rate of 10 lpm (Dekati, n.d.a) higher than that of the DMS which, when sampling from a contained environment with a relatively long test duration, will result in a higher than acceptable sample removal (SAE, 2011a).

Assessing these relative factors, it was decided that the DMS technique would be utilised to measure particle size distribution and concentration and facilitate the characterisation of PM behaviour in a more comprehensive manner than GF alone.

The only available method for characterising particle morphology requires the use of suitable microscopy equipment and methodologies. With an aim to characterise sub-micron and nano-scale particles, a high resolution Transmission Electron Microscope (TEM) was selected for the analysis as it provides the required measurement range

resolution; allowing measurement and morphological characterisation of particles of 1nm and below.

Further details regarding the specification of the equipment and the methodology used for sample collection and analysis are presented in the following chapter.

Chapter 6

Sample selection, apparatus and methodology

6.1 Introduction

The testing of PM effluents generated by automotive restraint systems during their operation provides the capability to better understand the effluents composition, characteristics and behaviour. Data provided by these assessments may be used to define the impact of these effluents on humans and the environment, the need for any control requirements and the efficacy of the airbag itself.

Whilst the testing and assessment of PM arising from ambient pollution and vehicle emissions is well used and defined in the literature, the same cannot be said for particle effluents arising from occupant restraint systems such as airbags. There are however a number of methodologies that have been utilised by manufacturers as guidance during the development of such systems and where possible these have been evaluated within this research programme; where standards or methodologies are lacking, test options are proposed and subsequently appraised.

Aside from the assessment of existing procedures, the experimental methodologies described in this Chapter have been used to define many elements and features of the tested airbags, their deployment characteristics and in particular the generated PM effluents. The majority of the tests undertaken concentrate upon measuring effluents by means of an assessment of particle electrical mobility. Gravimetric measurement has also been used to assess particle mass and to allow a link to the existing literature. High speed film and environmental pressure testing have been employed to assess inter-test consistency and evaluate existing methodologies and test environments. In addition, initial methodologies for particle morphology assessments and optical measurement of particle size have been presented and employed to provide further information on these effluents.

Initially airbags assessed within the programme were selected and their characteristics outlined prior to the definition of an experimental test hierarchy and associated matrices. The methodology for each test identified within the experimental test hierarchy is subsequently presented.

6.2 Test airbag selection and characteristics

The selection of test airbags was based upon a number of factors; including vehicle fitment rates, expected attrition and proliferation within the ELV waste-stream and propellant mass. Considering these factors, driver frontal impact airbags mounted within steering wheels were selected as the focus for this study. These became commonplace in vehicles on sale in the UK in the early 1990's and by 1993, 65% of all new vehicles were being fitted with a driver's airbag, by 1999 this had risen to ~95% (Appendix A). This early fitment to even vehicles in the highest volume sales segments has resulted in large numbers of devices already reaching the ELV waste-stream (Chapter 3). When compared to other inflatable restraints, driver airbags will continue to be the most prolific within the ELV waste-stream for a number of years, until the passenger airbag becomes nearly as common, from 2016 onwards (Chapter 3). Currently, seatbelt retention devices are more prolific than driver airbags at EOL, as in most cases they were fitted when the seating position was equipped with an airbag (IDIS, n.d.). Although more prolific in absolute number, these were not selected for the focus of this research study due to their ordinarily lower propellant load and comparative reduction in effluent output.

6.2.1 Inflator type selection

The selection of inflator types for testing required consideration of two main factors, namely:

1. Inflator type i.e. hybrid or solid propellant
2. Inflator staging i.e. single or dual

The difference in utilisation rates between hybrid and solid propellant driver airbag inflators remains unclear in the literature, therefore, an assessment of inflators (sample size = 30) from 12 of the top selling vehicles in the UK between 1996 and 2006 was conducted. This identified that 17% (n=5) of these operated a hybrid inflator, comprised of a stored gas and solid propellant. Of these five inflators only one was fitted to a vehicle produced before 2002. Although not statistically robust, the assessment concurs with the expectation that as development of hybrid systems intensified in the mid to late 1990's their uptake increased.

Based on the initial information regarding fitment rates, the selected test airbags chosen included driver airbags utilising a combination of solid propellant and hybrid inflators, with a bias toward the former, and included the following:

- A solid propellant inflator which has only reached the ELV waste-stream in the last 3 years
- A solid propellant inflator currently reaching the ELV waste-stream in large numbers
- A hybrid inflator currently reaching the ELV waste-stream in large numbers
- A contemporary solid propellant inflator from the late 2000s:

To define indicative inflator staging, a further assessment of 'staging data' (IDIS, n.d.) from six vehicle manufacturers (sample size =169) was conducted. This identified that since 1988, 91.4% of inflators have used a single stage inflator and prior to 1998 no vehicles used a dual stage inflator. Since 1998, dual staging of inflation has become more prevalent, yet currently remains considerably less common than single stage inflation, Figure 2.19. Therefore driver airbags using a single stage inflator were selected as test samples.

6.2.2 Propellant types

Most studies regarding particulate effluent have focused on airbag systems that use Sodium azide based solid propellants (Chan et al., 1989; Gross, 1994; 1995). Sodium azide is water soluble and when in contact with moisture produces hydrazoic acid; capable of causing substantial environmental and health impacts (Lewis University, 1999). Concern associated with these hazards is likely to have been responsible for the reduction of its use as a propellant in the 1990's in vehicles available in both Western Europe and the USA.

The author's assessment of a number of driver airbags from vehicles available in the UK since the mid 1990's has only identified a small proportion (~6%) of vehicles fitted with an inflator operating a Sodium azide propellant compared with a larger proportion of seatbelt retention devices (~16%). Whilst data regarding specific utilisation of propellant compounds remain scarce in the literature, it is thought that the proportional split between azide and non-azide, identified by the author, is broadly accurate for vehicles sold within the UK. A number of the largest pyrotechnic restraint manufacturers began developing non-azide alternatives in the early 1990s (Automotive Systems Laboratory, 2005; Henry and Solverson, 1995; Poole, 1991) and it is thought that their uptake rapidly overhauled the use of azide propellants by the early 2000's. With over 80% of vehicles purchased new in the mid 1990's already scrapped, it is likely that the majority of vehicles continuing to reach the EOL waste-stream will be equipped with non-azide inflators.

With this marked reduction in the use of azide since the mid 1990's, and the associated expectancy of ever dwindling numbers at EOL, non-azide propellants were selected for testing.

The selected inflator types were identified upon the highest selling vehicle types and each of the inflators utilised a different propellant composition and are all derived from the same mid-size vehicle class. All inflators were of the 'single stage' variety and airbag types A-C utilised a solid propellant whilst airbag D was equipped with a hybrid inflator using a solid propellant and compressed gas.

6.2.3 Airbag shape and volume:

With airbag volume varying appreciably by purpose (passenger/driver/side) and vehicle interior geometric size, airbags were selected from comparable vehicles within the mid-size class; the largest selling segments in the UK. These cushions were similar in volume, being less than 40 litres and representative of the median cushion size likely to require treatment at ATFs. Whilst airbag shape is generally circular (when viewed face on), some vehicles utilise fixed inflator modules (Citroen C4), which allow a shaped airbag to be used. This shaped airbag can be larger and provide greater coverage of the outer extents of the vehicle interior, such as the A-pillar. Those selected for testing were all circular in geometry and utilised a module design that rotates with the steering wheel when turned.

Cushion volumes were measured by water displacement. Tested cushions were provided with an airtight waterproof lining and inflated to a low static pressure before being used to displace water. Such a technique did not consider any stretch in the cushion fabric created by a higher pressure as with airbag deployment and any non-sphericity caused by the inability to tightly match the lining to the contours of the airbag. Measurements from displacement tests were subsequently compared to those derived from high speed film analysis (Chapter 12). Sizes and estimated volumes of each tested airbag are shown within Table 6.1 and

Figure 6.1 to Figure 6.4

Sample	Diameter	Volume (litres)
A	620	32
B	565	30
C	700	40
D	695	37

Table 6.1: Airbag cushion volumes

Figure 6.1: Airbag cushion A: Rear image

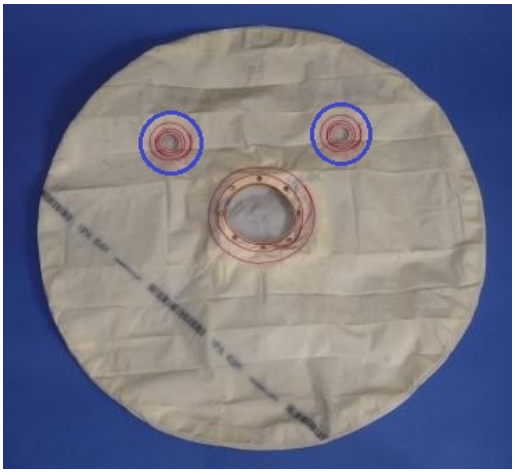

Figure 6.2: Airbag cushion B: Rear image

Figure 6.3: Airbag cushion C: Rear image

Figure 6.4: Airbag cushion D: Rear image

6.2.4 Control of airbag shape and volume

Whilst all test airbags utilised passive venting, all bar one (airbag B) used an internal cushion tether to control cushion shape, forward displacement and volume. This control can limit the risks to occupants situated in close proximity or OOP, from the cushion's forward motion. A tether made of fabric, (Figure 6.5 and Figure 2.22) is attached to a secondary panel stitched to the front and rear of the airbag close to the inflator.

Figure 6.5: Airbag Cushion B: Tether connection to front panel (internal view)

6.2.5 Airbag venting

Vent voids positioned to the rear of airbags are used to allow controlled deflation of an airbag when impacted by a vehicle occupant during a collision; the ride-down phase. In some cases these have been replaced by the use of a permeable airbag fabric, which upon impact (by an occupant) releases pressure within the airbag and controls occupant 'ride-down'.

The test airbags all used vents positioned to the rear of the airbag and did not use active or variable venting, discussed further in Chapter 2. Examples of the vents in the test airbags are shown within Figure 6.6 and Figure 2.24.

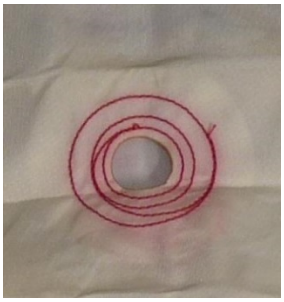

Figure 6.6: Airbag cushion B: Rear vent

Table 6.2 details the number, size and position of vents upon each tested airbag.

Airbag	No. of vents	Vent diameter (mm)	Radial distance from cushion centre (mm)
A	1	20	260
B	2	27	165
C	1	23	245
D	2	36	235

Table 6.2: Test airbag venting characteristics

6.2.6 Airbag materials, permeability and coatings

All test airbags used a polyamide 6, 6 (PA6.6) materials, representative of the great majority, if not all airbags, since the 1970's (CITA, 2002). Coatings are used on the inner and outer surfaces of airbag fabrics to aid smooth release from the module and provide protection against the heat generated in certain areas of the airbag.

Examination of the test airbags showed that all airbags were coated and although not characterised by material type, test samples were thought to have a neoprene or silicone coating. These adhered coatings are likely to affect the ability of the fabric to allow permeation of gas and therefore a release in pressure.

However, as all tested airbags appeared to use a comparable adhered coating and similar venting configurations and cushion volumes, the influence of cushion permeability was not considered relevant for a comparative assessment.

6.2.7 Inflator filter media assessment

The inflator filter media, although expected to provide limited filtration of sub-micron particulate, was subjected to basic analysis of filter pore dimensions and type, by means of optical microscopy equipped with a digital camera. Filter samples were removed from both deployed and un-deployed airbag modules and where multi-layer filters were employed, dismantled before examination. This assessment sought to define approximate pore size dimensions and the likely particle capture efficiency and therefore the effect on effluent entering and leaving the airbag cushion. All the assessed airbags used filter media with pore sizes greater than 20µm and commonly filter pores were far larger at around 500µm, as shown in Figure 6.7 and Figure 6.8

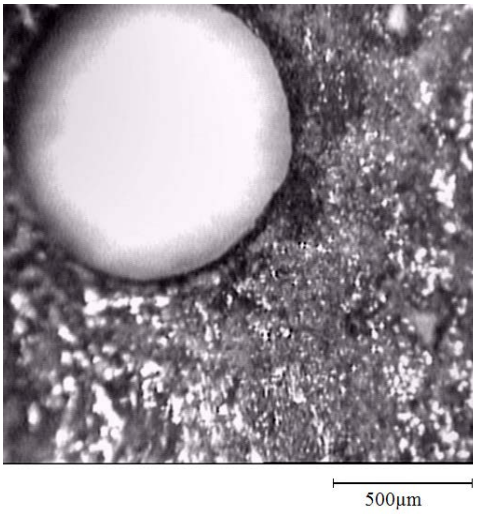

Figure 6.7: Airbag A filter media

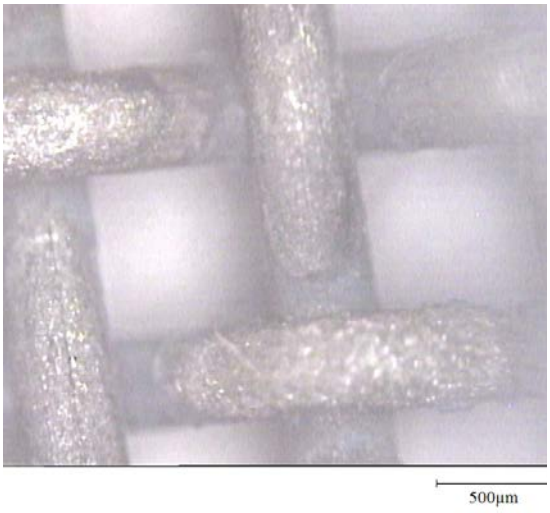

Figure 6.8: Airbag C filter media

This large filter pore characteristic is to be expected since the filter media is designed to capture heated particles large enough to potentially damage an airbag. It is therefore expected that filter media is unlikely to capture any particles within the size range assessed with the DMS and may only influence total particle mass concentrations measured with GF.

6.2.8 Test airbags selection summary

The four selected airbag types that were comprehensively tested during the research programme are as follows:

A. A solid propellant, non-azide, driver airbag from a class B/C vehicle, that has started to reach EOL in the last 3 years
B. A solid propellant non-azide, driver airbag from a class B/C vehicle currently reaching EOL in large numbers
C. A contemporary solid propellant non-azide, driver airbag from a class B/C vehicle from the late 2000s
D. A non-azide, driver airbag utilising a hybrid inflator, from a class B/C vehicle currently reaching EOL in large number

Whilst these airbags are not likely to represent the full range of airbag or inflator variants found on the UK market, or those currently reaching EOL, it is likely that these do represent the most common types of airbags.

6.3 Definition and matrix of testing

The assessments detailed as phases 3, 4 and 5, originally in the research programme structure in Chapter 1, are shown below.

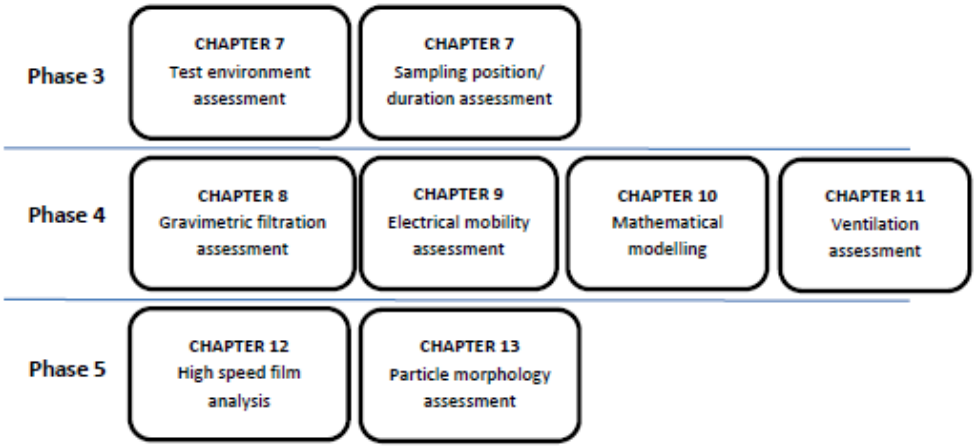

Figure 6.9: Testing research structure

These phases were expanded into a test matrix, Table 6.3, to define each of the tests undertaken. Each test was identified with a number within the test matrices and three repeated tests of this type were conducted to provide a robust assessment.

The assessment of particle morphology, Phase 5, has been omitted from the test matrix as in this stage an iterative test process was employed to define optimum particle sample collection. All tests were undertaken in the effluent test tank and any variables and the iterative test process are discussed in section 6.9 and Chapter 13. Section 6.4 that follows presents the experimental procedures used in each of the experimental phases.

Research Phase	Thesis Chapter	Test Numbers (x3 for each)	Test type			Test Environment			Sample Position						Venting	Test airbag			
									Vertical			Horizontal							
			GF	DMS	HSF	Vehicle	Tank	External	A	B	C	A	B	C		A	B	C	D
3	7 / 9 / 11	1		X			X			X		X				X			
		2		X			X			X			X			X			
		3		X			X			X				X		X			
		4		X			X		X				X			X			
		5		X			X			X			X			X			
		6		X			X				X		X			X			
		7		X			X			X			X				X		
		8		X			X			X			X					X	
		9		X			X			X			X						X
		10		X		X				X		X				X			
		11		X		X				X			X		X	X			
		12		X		X				X				X		X			
		13		X		X				X		X							X
		14		X		X				X			X		X				X
		15		X		X				X				X					X
		16		X		X				X			X		X		X		
		17		X		X				X			X		X			X	
		18		X		X				X			X			X			
4	8	19	X				X			X			X			X			
		20	X				X			X			X				X		
		21	X				X			X			X					X	
		22	X				X			X			X						X
5	12	23			X			X								X			
		24			X			X									X		
		25			X			X										X	
		26			X			X											X

Table 6.3: Experimental test matrix

*GF = Gravimetric Filtration DMS = Differential Mobility Spectrometry HSF = High Speed Film

6.4 Test environments

In this study airbag deployment was performed in an airborne effluent test tank and the interior of a vehicle with a comparable volume ($2.83m^3/100ft^3$). Further information regarding test environments and their selection is detailed within Chapter 5.

The test tank was used not only to allow assessment and characterisation of airbag effluents and their behaviour but also to compare both test environments and to allow the effect of ventilation of the test environment to be defined.

To perform these tests a suitable standardised test tank was manufactured by the author and a comparable test vehicle was purchased and modified.

6.4.1 Test tank design and construction

The test tank provides a uniform method of testing airborne effluents from airbags and is specified within existing test standards. To ensure full compliance with existing standards, a tank of $2.83m^3$ was developed and utilised as shown in Figure 6.10 (SAE, 2011a; Audi AG et al., 2001).

Figure 6.10: Test tank and workstation

The test tank, designed solely by the author, drawing upon core information from standards (SAE, 2011a; Audi AG et al., 2001) and constructed by DGL Fabrications (Daventry, UK), with the authors comprehensive support and assistance.

The main test tank body was constructed from plate steel, strengthened by a latticework structure and lined internally with stainless steel, to limit the build-up of contaminants and corrosion and allow repeated cleaning of internal surface.

Post-construction measurement of tolerances identified that the volume of the test environment constructed fell well within the tolerance (+/-5%) specified (SAE 2011a; 2004) and therefore it did not require the use of a correction factor, as with smaller tanks (Ziegahn and Nickl, 2002).

An access point, Figure 6.10, sealed by a distributed pressure compression gasket, provided access to the test environment for installation of test modules and general maintenance, whilst preventing un-intended sample dilution. An adjustable pressure relief valve (BES, UK), Figure 6.11, allowed for over-pressure levels to be adjusted depending upon the expected pressure output, and multiple sampling ports allowed connection to sampling equipment; Figure 6.11. A Local Exhaust Ventilation (LEV) was also provided which consisted of a compressed air source and vacuum extraction system capable of evacuating the test environment prior to re-entry.

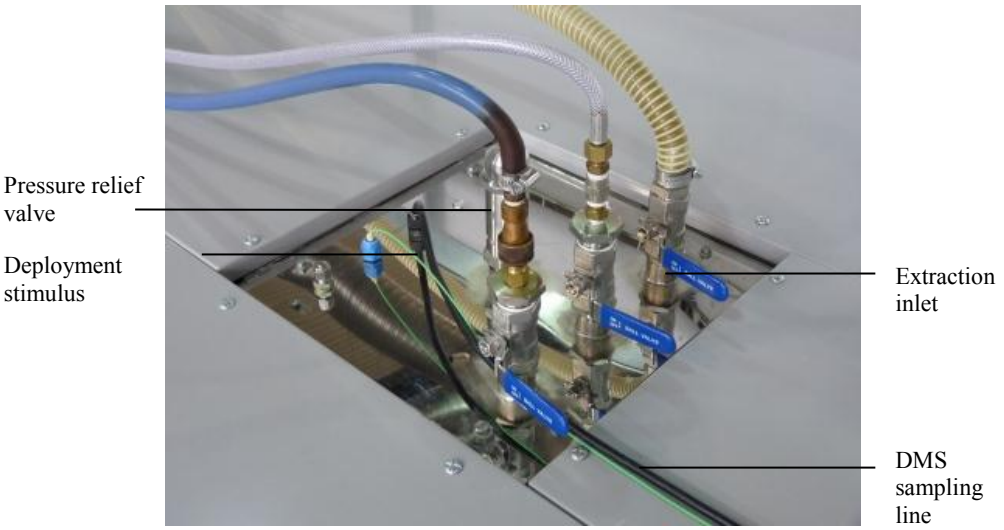

Figure 6.11: Test tank instrument panel and pressure relief valve

An electrical deployment system was designed and manufactured to allow both simultaneous and sequential activation of test airbags, whilst an interlock system prevented inadvertent deployments during test setup and preparation. Fixtures were designed to allow fitment of various airbag modules in a number of positions and orientations, allowing comparisons between test setups to be drawn and recorded, Figure 6.12.

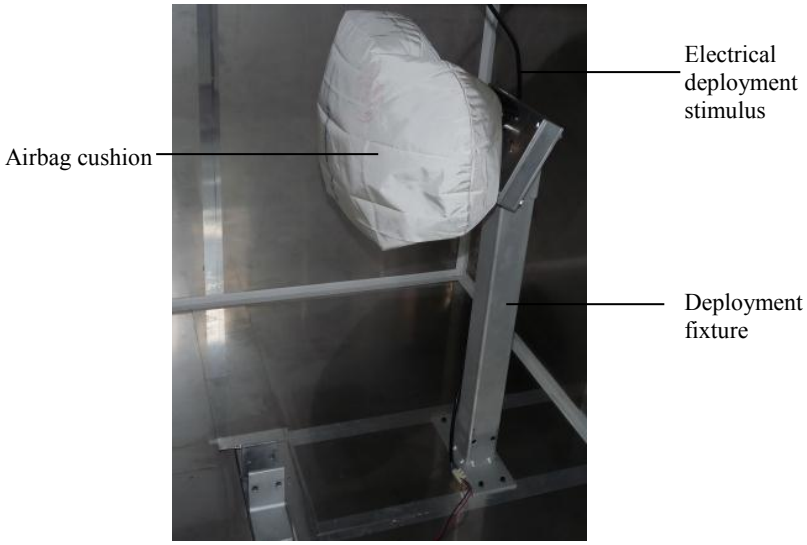

Figure 6.12: Test tank mounting positions

6.4.2 Test vehicle selection and modification

A vehicle with an interior volume comparable to that of the standardised test environment was selected for testing effluents and a comparative assessment of test facilities (Figure 6.13). Analysis of vehicle characteristics information (US Dept. of Energy, 2010), showed that a 1994 Saab 9000 hatchback would provide an interior volume of 2.8m^3; comparable to within 2% of the volume of the effluent test tank, Figure 6.13.

Figure 6.13: Saab 9000 test vehicle

Although in general unchanged from that of a standard vehicle, modifications were made to the vehicle interior to allow fitment of test airbags (other than those fitted to the vehicle originally) in driver and passenger front airbag and front belt pre-tensioner positions.

To reduce in-vehicle deployment pressure capable of damaging door seals (Chan et al., 1989), and changing the pre-venting behaviour and concentration of the effluent, two pressure relief valves capable of resealing when pressure was reduced, were fitted to the front doors, Figure 6.14. The same deployment system utilised for the effluent test tank

was employed for vehicle based tests and sealed ports were provided to introduce cabling and sample lines, Figure 6.15.

Figure 6.14: Pressure relief valve outlet

Figure 6.15: Sampling and deployment ports

The methodologies for the two test environments are considered in the following sections. General methodologies that were applied during tests in both environments to ensure consistency and safety are also defined within section 6.4.3.

6.4.3 Test environment general usage methodology

Initial setup of both test environments was comparable for most tests and neither vehicle nor tank was occupied, for example by crash test dummies as per a number of previous studies (Chan et al., 1989; Linn and Gong, 2005). During ELV exposures (and the focus of the research programme) vehicle occupants would not be present within the vehicle. The earlier studies that utilised human forms, focused on post-collision exposure to effluents and used test dummies to account for any effect that a vehicle occupant compressing an airbag during a collision may have on PM and gas dynamics, Figure 6.16.

Figure 6.16: Frontal collision, driver airbag 'ride-down' (Hynd et al., 2011)

During all vehicle tests ventilation/circulation ducts were shut, seat track position and recline was set in the mid/mid position and all windows and doors were closed securely. For tank tests no interior fittings were present except those required for fitment of test airbags and equipment. The design also provided a simple, sealed entry door area that was closed securely prior to deployment, Figure 6.10.

Prior to each test the surfaces of the environment were cleaned with a mild soap, rinsed with a clean water spray and air dried with a portable, circulating fan in compliance with relevant standards (SAE, 2004; 2011a). This process was simple in a test tank with few internal fittings and a corrosion resistant, level surface lining, yet was rather more complicated in the test vehicle where many surfaces, such as seating and carpeting could not be effectively cleaned in this manner. Those surfaces unable to be cleaned in the standard manner were however cleaned at regular intervals with a water vacuum cleaner.

The basic process for undertaking measurements within both test environments is detailed below.

- Check vehicle/tank and pressure relief systems for signs of deterioration or damage
- Ensure test environment is clean and free of debris or equipment
- Locate sampling equipment in the required sample position
- Locate test airbag in required position
- Connect electrical deployment stimulus and ensure adequate safe clearances
- Seal test environment by closing all doors and windows for the test vehicle and ensure any unused sampling ports are sealed
- Sample for the required test duration (see note below)

- Ventilate test environment for specified duration in accordance with ventilation test requirements or to allow safe re-entry
    - For GF, sampling media is removed prior to test environment ventilation with adequate safety precautions.

Sampling durations were defined by the test type and for GF this information can be found in section 6.6, for testing using the DMS section 6.7 and for morphological assessment in Chapter 13. Durations of tests to assess the effect of test tank environment ventilation on PM behaviour are defined in Chapter 11.

6.4.4 Test environment sampling positions

The influence of sampling position on PM measurement and exposure characteristics has been initially investigated and reported in the literature. Gross et al. (1995) reported that exposure to airbag effluents would be the same for occupants in the front and rear of a vehicle, and Starner (1998) reported that so long as samples were not taken at the lower extents of an effluent test tank then little variance would be detected. However as these findings were not comprehensively reported and to allow inter-comparability between test environments, samples were drawn at multiple locations in both the test tank and vehicle. These sample measurement points were decided to either;

(a) assist in understanding variability in the test environment, or,

(b) replicate the likely vehicle entry position for EOL, Figure 6.17, and post-crash exposures, Figure 6.18.

Samples were not taken to the rear of the airbag as this would not replicate likely exposure scenarios.

Figure 6.17: End-of-life vehicle depollution re-entry

Figure 6.18: Indicative seated position for post-crash exposures

6.4.4.1 Test tank sampling positions

A number of sampling positions in the test tank were assessed to determine whether any variance in this position would influence the measured effluent. Three vertical and three horizontal positions were assessed. The three vertical positions, Figure 6.19, were required to be offset from the centre of the tank to prevent interaction with the inflating airbag cushion.

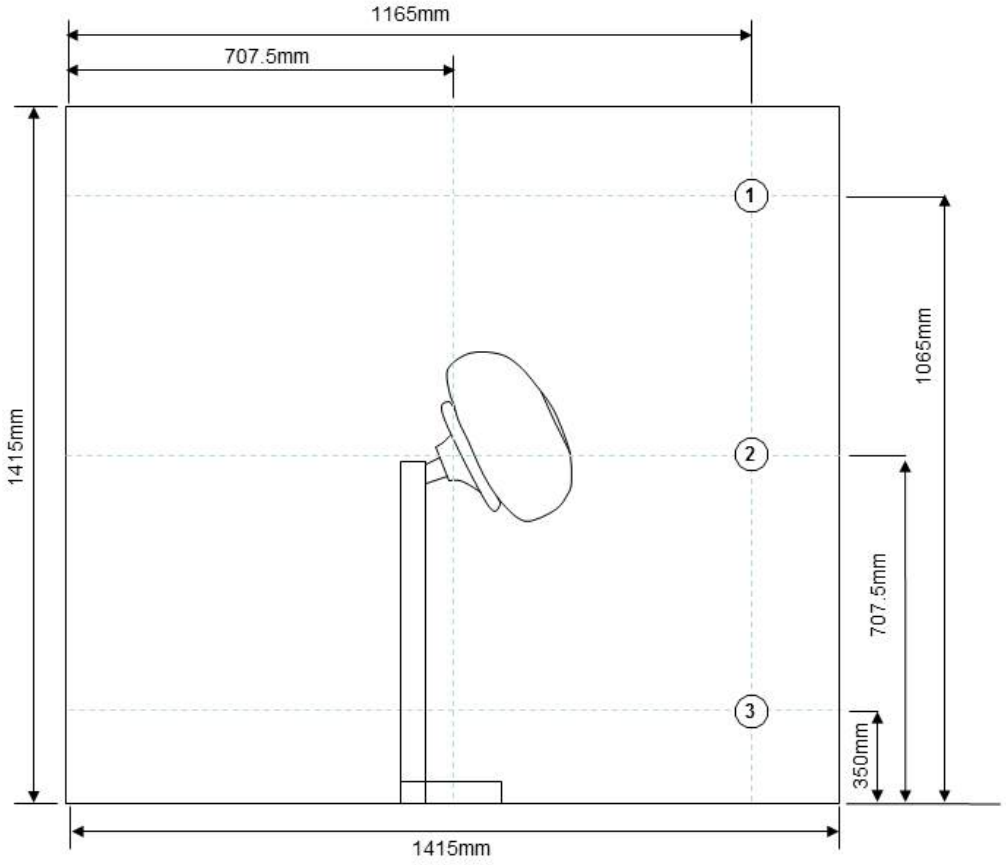

Figure 6.19: Schematic of test tank showing vertical sampling positions (not to scale)

The author decided that the three equidistant sampling positions should be located where occupants and ELV depollution operatives are always positioned, i.e. in front of or alongside the airbag cushion, not at the rear of the airbag assembly.

Horizontal sampling positions were spaced equidistantly, as shown in Figure 6.20.

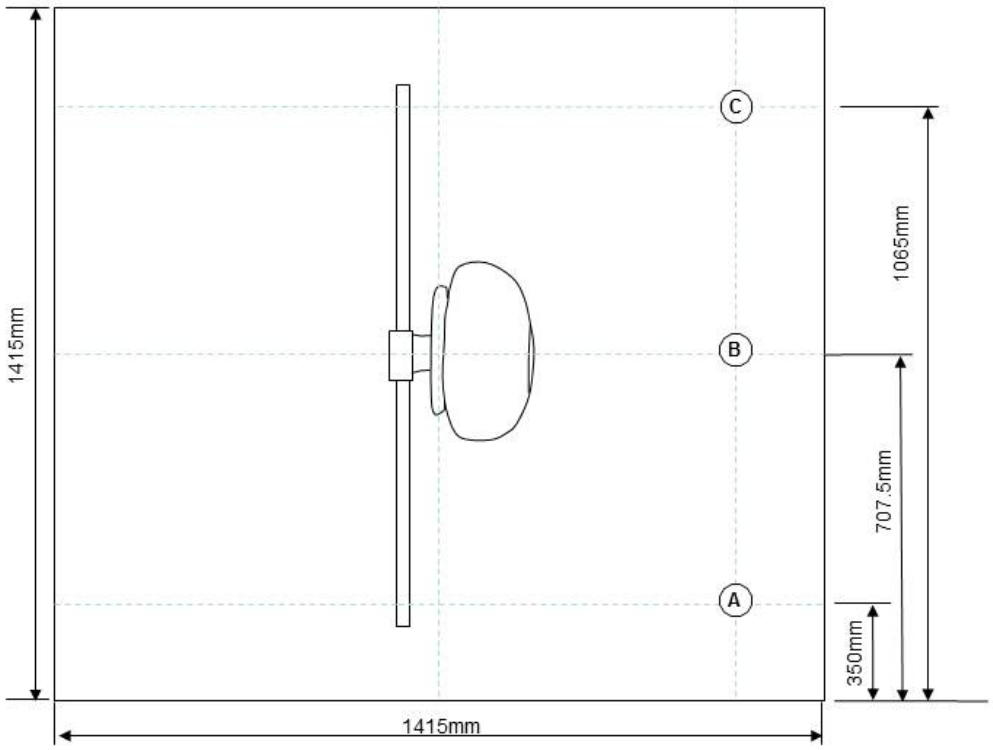

Figure 6.20: Schematic of test tank showing horizontal sampling positions (not to scale)

The sampling positions defined within (Figure 6.19 and Figure 6.20) do not directly replicate the seated position of a vehicle occupant or that of an operative entering a vehicle during the ELV depollution process. However, these positions are likely to provide similar data and be representative of the exposure conditions whilst providing comprehensive data regarding sampling variables that are not available in open literature.

A rigid mounting position was provided to ensure that sampling equipment could be positioned consistently and not move during the increase in pressure encountered during airbag deployment or within the post deployment sampling period, Figure 6.21.

Figure 6.21: Test tank horizontal sampling positions

6.4.4.2 Test vehicle sampling positions

As with the test tank a number of sampling positions were assessed within the test vehicle to determine whether a variance in this position affected the measured effluent. All sampling positions were in the front of the vehicle, thereby replicating the common exposure scenario and as initial measurements in previous studies suggested there was little variation between measurements in the front or rear of a vehicle (Gross et al., 1994). A single vertical position was used, since exposures in the vehicle are likely to occur at the approximate seated height of an occupant. Therefore samples were drawn at three equidistant spacings at the approximate seated height of a 50^{th} percentile male, as shown in Figure 6.22 and Figure 6.23.

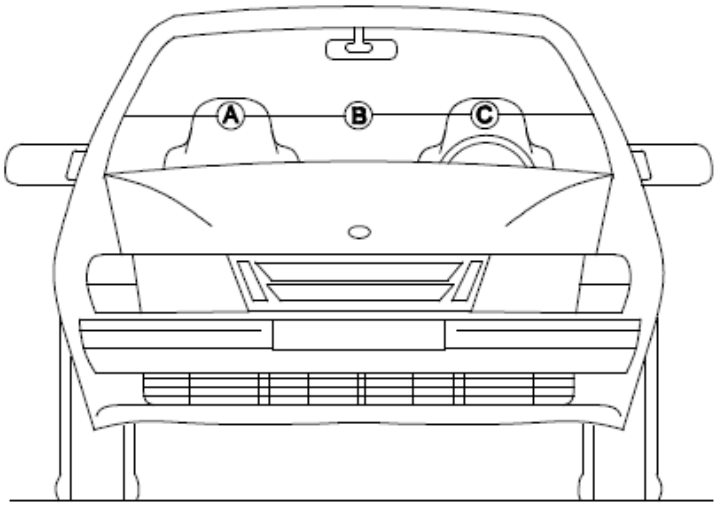

Figure 6.22: Test vehicle sampling position - Front view

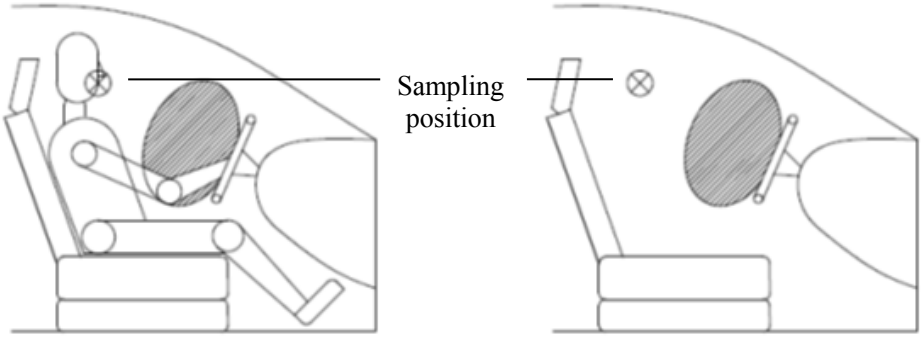

Figure 6.23: Test vehicle sampling position - Side view

As per the test tank, a rigid mounting position was provided to allow consistent positioning and limit movement during airbag deployment. Further controls were applied to the test environments to ensure consistency of testing and the methodology is explained in section 6.4.3.

6.4.5 Environmental control

Temperature and humidity are both factors known to influence the behaviour of effluents, (Starner, 1998), therefore the control of environmental variables and provision of a repeatable environment is important to robustly characterise the tested effluents. Technical standards state acceptable humidity ranges of 40-60% (SAE, 2011a; Audi AG et al., 2001) and 25-75% (SAE, 2011a) and test temperatures in the range 23°C ±5°C (SAE, 2011a; Audi AG et al., 2001) and 22°C ±3°C (SAE, 2011a).

Although indications are that aside from extremes in humidity, a wider range of humidity (i.e. 25-75%) would provide limited effects on particle effluent (Starner, 1998); little information regarding the influence of temperature has been reported in the literature. Nonetheless, the tighter tolerances for both humidity and temperature were selected for all testing, both to ensure compliance with all relevant standards and to reduce the likelihood of inter-test variance.

Control of these environmental variables in both the test tank and vehicle interior was only conducted prior to testing to ensure pre-test consistency. These variables were controlled by means of a portable dehumidifier and humidifier and temperature conditioning unit (Jack Sealey Ltd., Bury St. Edmunds, UK). Tests were conducted within a controlled laboratory environment and generally both tank and vehicle interior required minimal conditioning.

Environmental data measurements were taken each second with a calibrated HOBO U12 datalogger (Onset, MA, USA). Pressure measurements within the test environments were taken and logged each second with an Extech RHT50 pressure datalogger (Extech, MA, USA).

6.5 Ventilation of test environments

Ventilation of the test environments was assessed to define the effect on effluent characteristics such as concentration, size distribution and behaviour. Ventilation of vehicles may be conducted during ELV airbag neutralisation operations to reduce the concentration of the effluent prior to re-entry to the vehicle interior by EOL depollution operatives, as most organisations choose to deploy airbags within sealed environments, to reduce the risk of injury from projectiles that may be present in damaged ELVs. This ventilation may be ‘natural’ where doors or windows of the vehicle are opened, (Figure 6.24) or ‘stimulated’ through use of an extraction system designed to remove the effluent (Figure 6.25).

Figure 6.24: Natural ventilation with a single vehicle door opened (Jackson, 2012)

Figure 6.25: Stimulated ventilation with local exhaust ventilation highlighted in amber (Re-source Engineering Solutions, n.d.)

In practice, and as observed by the author, operatives re-enter the vehicle after naturally ventilating vehicle interiors for several minutes, by opening one or more of the vehicle doors and not by means of an extraction system. Whilst there is little information in the literature that considers ventilation subsequent to airbag deployment, a single 'recommended practice document' (SAE, 2010) specifies the use of a

ventilation/extraction system for use after deployment to reduce in-vehicle effluent levels. The text provides limited information and simply recommends the use of 'extraction' for several minutes after deployment and before re-entry to the vehicle (SAE, 2010). Since there is little data regarding ventilation of vehicle interiors, it was decided that testing would focus on 'natural' ventilation to assimilate the practice observed by the author. Tests to assess ventilation behaviour would be conducted using the general process previously specified, with ventilation conducted after 60 seconds, for a maximum of 600 seconds; replicating the process used in practice. Although actual ventilation practices are likely to vary, for initial tests it was decided that only a single front passenger side door would be opened. These ventilation tests were assessed with the DMS and only conducted in the test vehicle. The use of the DMS allowed the author to capitalise on the rapid response time of the equipment to allow changes in PM characteristics to be assessed.

Sampling was conducted at measurement point 'B', Figure 6.22, during deployment and ventilation and all tests were conducted in a laboratory with a stable temperature and relative humidity of 20°C +/-3°C and 50% +/-10%, with limited air movement.

6.6 Particle mass measurements

Gravimetric filtration as a method for total particulate mass measurement is well documented and understood for ambient particulate assessment, and, more importantly, for the quantification of particulate effluents from automotive pyrotechnics (Gross et al., 1994, 1995, 1999; Chan et al., 1989, Starner, 1998). These measurements are taken by using a vacuum to draw a sample through a filter. Total particulate mass measurement within the test tank and vehicle was achieved with a grounded, stainless steel, open face particle filter (Millipore, USA) with a 9.6cm^2 filtration area and 47mm pure quartz, T60A20, filters (Pall, Port Washington, NY, USA) rated at >99% efficient for 0.5 μm at 15 litres per minute (lpm) flow rate (SAE, 2011a). Vacuum flow rates of 3.0 and 5.0 lpm +/-10% were used (SAE, 2011; 2004) and achieved by use of a 'Flite 2' air sampling pump, (SKC, PA, USA) and flow limiting orifices (Millipore, Billerica, MA, USA). Flow was routinely checked by means of a calibrated, direct volume bubble flowmeter. The gravimetric sampling positions in the tank are shown schematically, Figure 6.26.

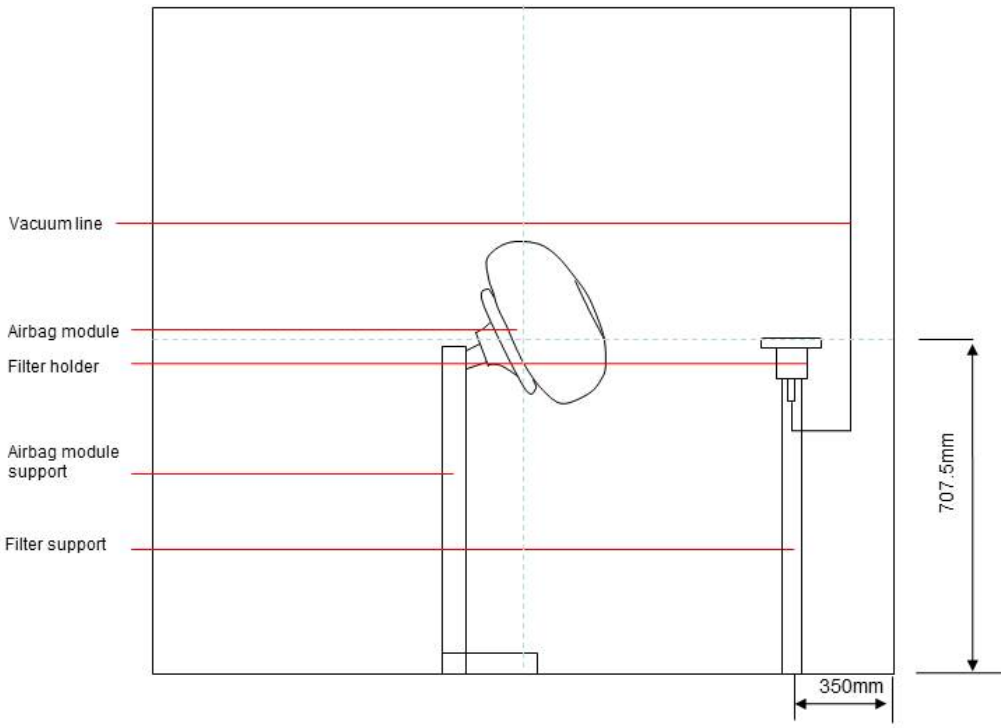

Figure 6.26: Gravimetric filtration sampling setup and positions

Single total particulate mass samples were drawn within the tank to replicate exposure conditions as closely as possible, and prevent any losses or agglomeration through or within sample tubing. Sampling equipment was positioned in varying locations depending on the test to be conducted. Background particle mass was measured in the test environments prior to any testing to determine the effect on measurements from airbag deployments. These values were consistently below $0.3mg/m^3$ in both environments, and were therefore not considered sufficiently high or variable to be taken into account; therefore replicates the method and findings of Starner (1998).

Sample durations of 20 minutes at a steady flow rate of 5 lpm were employed as specified within standards (SAE, 2004; SAE, 2011a; Audi AG et al., 2001). If recorded sample flow rate varied by more than 10% during testing the data was rejected (SAE, 2011a). The process for data collection with GF is as follows:

- Condition filter media
- Measure filter media pre-test mass
- Install filter media in filter holder
- Position filter holder to desired sampling position
- Seal test environment
- Start pressure sensor, temperature and humidity recording apparatus
- Start sample vacuum and ensure compliance with flow requirements

- Connect sample line to filter media and begin sample extraction
- Deploy airbags after 1 minute
- Sample for desired test duration and stop sample vacuum
- Retrieve filter media
- Ventilate test environment
- Re-condition filter media
- Measure filter media mass
- Assess pressure sensor data

Test environment pressure, temperature and relative humidity (RH) were recorded as specified within section 6.4.5. These factors were measured to ensure compliance with test requirements and ensure consistency and to also accurately define particle mass concentration, as required by Equation 5 from SAE test standard J1794 (SAE, 2011a).

$$TPC = \frac{TPM}{AF * t\left[\frac{P}{101{,}325\ (Pa)}\right]\left[\frac{295\ (°K)}{T}\right]\left[\frac{1(m^3)}{1000\ (L)}\right]} \qquad \textbf{(Equation 5)}$$

TPC = Total Particulate Concentration (mg/m^3)

TPM = Total Particulate Mass (mg)

AF = Average Flow (l/min)

t = Sampling Time (min)

P = Atmospheric Pressure (Pa)

T = Temperature (°K)

Subsequent to testing, filter media were retrieved without ventilation of the test environment to prevent any unintended sample deposition or contamination likely to occur during this process. As a precaution the author utilised breathing apparatus and dermal and ocular protective equipment to re-enter the test environment.

Filter media were conditioned to 50% RH and 21°C for 48 hours, prior to and post testing. Pre and post-test filter masses were measured with a routinely calibrated analytical balance (A200S Model, Sartorius, Germany). Efforts were made to ensure minimal sample contamination during testing and analysis by utilising 'clean' environments where possible.

PM mass concentration values were recorded in milligrams (mg) to a resolution of 0.1mg and concentrations calculated as mg/m^3, by recording total drawn sample volume and PM mass and correcting for pressure and temperature. Calculation of the total particle concentration (in mg/m^3) was achieved using the following process:

a) Measure pre-conditioned filter mass
b) Condition at 50% RH (+/- 5%) and 21°C (+/- 1°C) within 'clean' environment for 48hrs
c) Measure pre-test, conditioned filter mass
d) Test vacuum source and calibrate if required
e) Deploy components
f) Remove filter and condition for 48hrs (as above)
g) Subtract initial tare mass from post-deployment mass. Record this value as Total Particulate Mass (in mg)
h) Apply values to Equation 5 and define total PM (mass) concentration as mg/m^3.

6.7 Particle electrical mobility measurement

The DMS used for the research programme was a Cambustion DMS500 (Cambustion, Cambridge, UK), as shown in Figure 6.27, connected directly to a PC operating control and output software. The DMS500 is able to measure particle size distribution and number concentration at a high sampling rate and can operate in one of two size ranges depending on setup and the type of in-built cyclone filter. For this research study, the finer measurement range of 5nm – 1000nm (1µm) was selected to provide high resolution and fulfil the requirements and key objectives of the study (Chapter 3).

Figure 6.27: Cambustion DMS500 Differential Mobility Spectrometer

The system draws a sample by means of an external vacuum pump at a rate of 8 lpm through a flow limiting orifice and is monitored through integral flow sensors. Initial

tests conducted by the author identified that the flow limiting orifice became susceptible to build-up of particle deposits and a subsequent reduction/variation in flow was recorded, although this variation allowed flow to remain within 10% of the set-point and therefore complied with standards for similar tests (SAE, 2011a). Although remaining within acceptable flow parameters, the orifice was removed and cleaned subsequent to each test to prevent any risk of sample inaccuracy. Total sample volume removal from the tank is unlikely to rise above 164 litres or approximately 5.7%. This level of sample removal is commensurate with the value of 5% defined in standards (SAE, 2011a; 2004).

Prior to testing, the DMS and all peripheral equipment had been calibrated by the manufacturer with a known aerosol.

The DMS is capable of providing an output of size segregated number concentration for particles within the measured range. The integral software provides conditioned data that takes into account the effect of sample dilution and other factors.

Data provided by the DMS software can also be outputted and manipulated using alternatives such as Matlab, Microsoft Excel or SPSS. The software also has the capability to record sample flow rate which allows more precise calculation of total sample removal and compliance with test requirements.

Since the DMS was not specified for use in airbag effluent sampling studies, the test process was developed from that for GF, with a corresponding sampling duration of 20 minutes, with sampling positions defined within section 6.4. Prior to sample collection the system was 'zeroed' to take into account any background particle concentration and allow quantification of only PM emitted during airbag deployment. Samples were drawn through short lengths of black silicone sampling line to reduce agglomeration (Cambustion, 2008).

In contrast to measurements of particle mass by GF, the test environment could be ventilated without immediate post-test re-entry being required, as sample media did not require removal.

The process used for measurement with the DMS is defined below:

a) Locate sampling line at desired sampling position
b) Seal test environment
c) Start sample vacuum and verify flow is within allowable tolerances and connectivity requirements are met
d) Deploy test airbag(s) 30 seconds after vacuum started
e) Sample for desired test duration and stop DMS
f) Ventilate test environment
g) Extract data and copy to secondary location

h) Remove sample line

i) Clean all sampling equipment and undertake standard operational checks.

The DMS was utilised in both the test tank and vehicle. Details of the tests conducted with this apparatus are provided within the experimental structure and the experimental test matrix, Table 6.3.

6.8 High speed digital video analysis of airbag deployments

The use of high speed digital video for analysis of airbag deployments is defined in test standards (SAE, 2011b) for measuring deployment performance and repeatability yet is rarely documented in the literature. This form of measurement and analysis has been utilised within effluent testing programmes for measurement of fabric speed (Schreck et al., 1995) and is also commonly used for calculating airbag volume by means of software based image tracking (Image Systems, 2012). For the purposes of this research programme, video analysis has been used to define fabric speeds and inflation rates.

With airbag deployments commonly being completed within 30ms (CITA, 2002), a camera able to operate at a high 'frame rate' (the number of images or frames per period of time) is required to provide resolution capable of delivering sufficient information regarding the deployment. A Photron SA1 high speed colour digital video camera, Figure 6.28, provided by the Engineering and Physical Sciences Research Council, operating at a frame rate of 4,000 per second was chosen for testing. At the selected frame rate the system is capable of providing a resolution of 1024 x 1024 (20μ) pixels. At high frame rates these cameras rely on high power lighting to provide sufficient illumination for imaging. Light Emitting Diode (LED) light sources were employed to reduce the likelihood of flicker ordinarily found when using standard filament lighting during high speed photography (Sutphen and Varner, 2003).

Figure 6.28: Photron SA1 High Speed Film Camera (EPSRC, n.d.)

A two sided enclosure allowing sufficient light to enter the scene was manufactured and a dark material backing selected for the enclosure; this provided a contrast between the light coloured inflating airbag and visible effluents and the backdrop; the test setup is shown schematically in Figure 6.29.

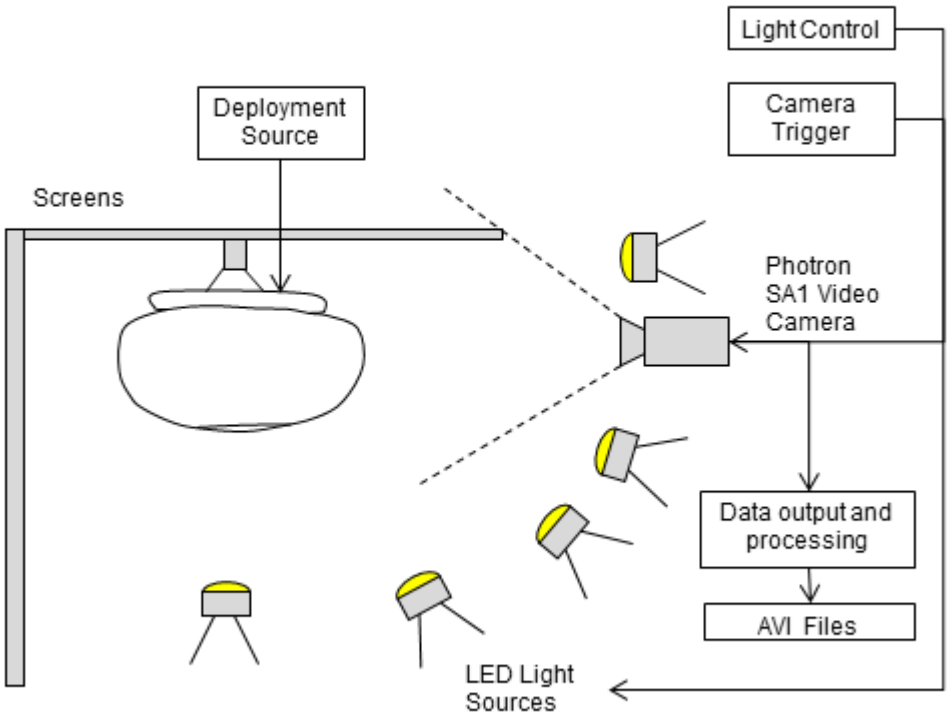

Figure 6.29: High speed film equipment setup schematic (SAE, 2011b)

When operated at 4,000 frames per second (fps) the available memory constrained the collection of data to a maximum of 2 seconds (or 8,000 frames) of video. Each frame was output as an individual image file and edited to produce .AVI video files where required. The display of a grid upon the resulting image, Figure 6.30, allowed for fabric speed, maximum inflation dimensions and volume displacement to be calculated. The grid spacing (scaled from a known distance upon the image) was used to define accurate dimensions.

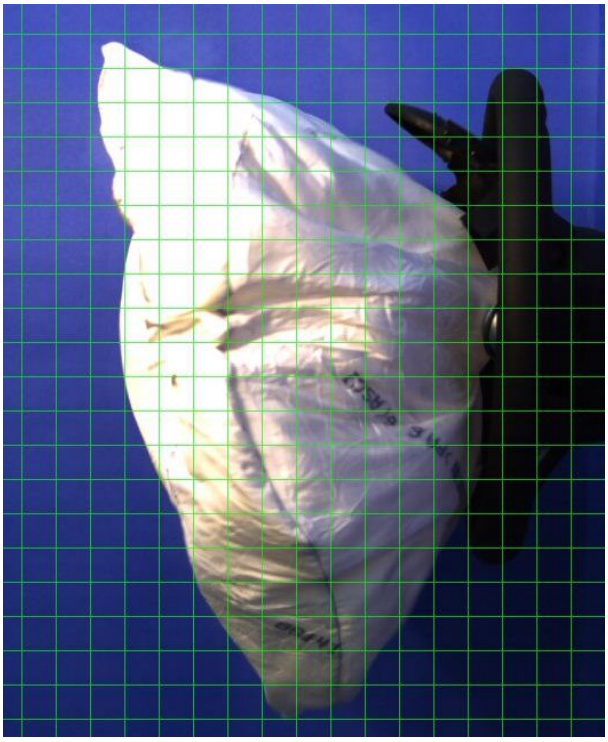

Figure 6.30: Post-processed high speed film image of airbag deployment

The camera operated by Photron software was used on the 'continuous centre' setting, which results in the camera continuously recording and overwriting every two seconds. The camera was triggered manually at the same time as the deployment. When the camera record trigger was activated via a manually operated trigger button, the software captured one second of data on each side of the trigger point, utilising data stored in a buffer prior to the trigger.

For the quantitative assessment of airbag cushion volume and displacement, images output from the camera system were assessed by employing image analysis software. From the known distance on the deployment enclosure it was possible to derive a scale for accurate measurement. For change in volume measurements, the image (and therefore the frame) with the greatest airbag side profile area was identified. For the purpose of this research, the 'greatest side profile area' measurement was considered as the maximum airbag cushion volume. This assumption was likely to be accurate although some variability was likely to exist for partial inflation points as the profile area may not directly correspond to overall cushion volumes during deployment.

The volume of the airbag cushion was calculated by pixel counting via image analysis software. This provided an area in pixels^2 (px^2), this value (183,351px^2 in Figure 6.31), was then divided by the known inflation volume (40 litres) to provide the scale (1 litre = 4584px^2), allowing other measurements of derived airbag volume to be calculated. The process of image analysis occasionally resulted in poor edge fitting or the inability to

select elements of the airbag cushion, as shown in Figure 6.32, therefore care was be taken to ensure these were minimised so that robust values were calculated.

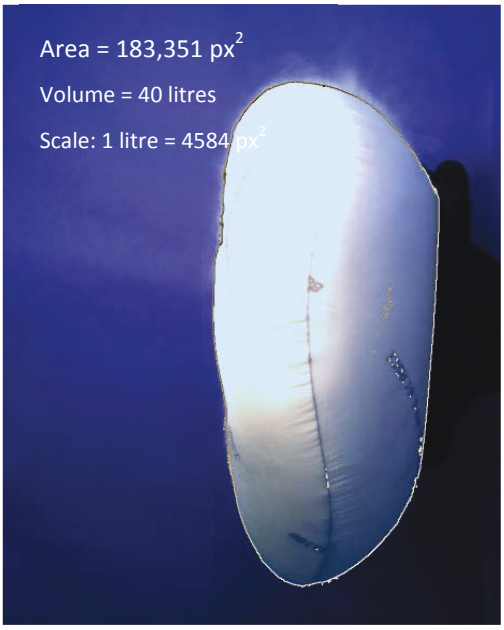

Figure 6.31: Deriving airbag cushion volume from high speed photography using image analysis

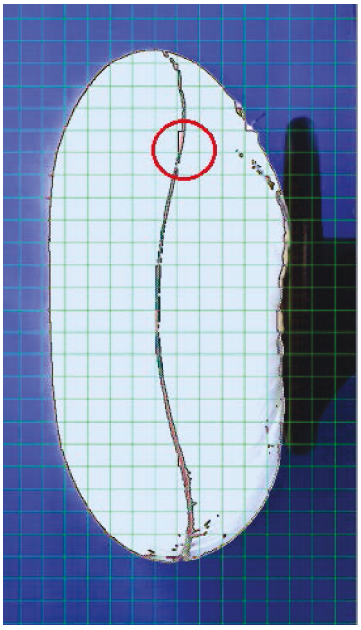

Figure 6.32: Airbag cushion volume image analysis errors

Average and peak fabric speed measurements similar to those presented by Schreck et al., (1995) were calculated by tracking the horizontal or vertical motion of the airbag cushion and measuring the pixel distance travelled. These values were calculated as averages over the duration taken to reach maximum forward and vertical displacement, as shown by the horizontal (forward) and vertical lines within Figure 6.33 and over each millisecond to provide a peak value.

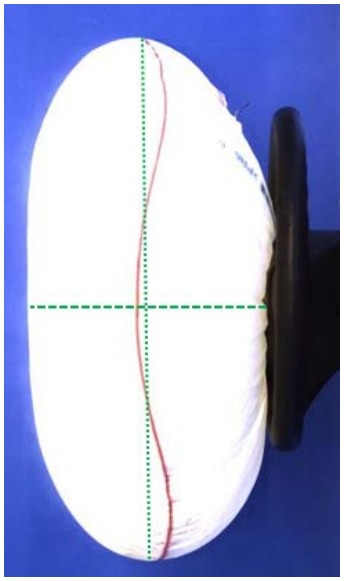

Figure 6.33: Airbag cushion maximum forward and vertical inflation dimensions

Use of image analysis software allows inflation distance to be calculated with some degree of accuracy and as such this analysis method was considered by the author as suitably robust for the comparative analysis of airbag variability and behaviour as required by this research.

It should be noted that this analysis does not account for any time duration required to process the signal from the deployment stimulus to the initiator or the time taken for the initiator to commence the deflagration of the propellant (commonly 3ms) and therefore the 'T' or 'trigger time' for these assessments is considered as the point at which movement of the module cover can be first detected.

6.9 Particle Morphology Assessment by Electron Microscopy

Transmission electron microscopy (TEM) was selected as the most suitable method for morphological assessment mainly due to the expected size of particles emitted when an airbag is deployed (Chapter 3) and because the technique does not appear to have been used for assessment of airbag effluents. Whilst TEM was the primary method employed, where particles were identified (with TEM) as being large enough, scanning electron microscopy (SEM) was also employed. The use of SEM can provide further information regarding particle morphology, which cannot be achieved with TEM, such as the sample's surface topography and to identify if particles are 'resting' upon one another or agglomerating.

For TEM assessment, particles were collected directly onto pre-manufactured grids, Figure 6.34, which could also be used for SEM examination.

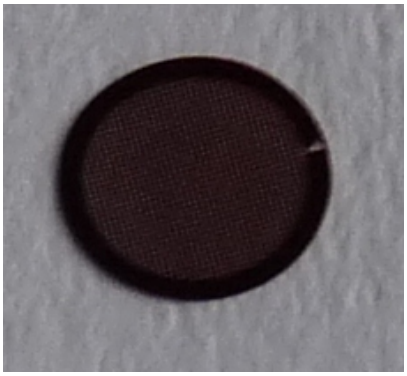

Figure 6.34: Lacey Carbon filmed TEM grid

Alternative methodologies have been presented in the literature for collection of airbag particle samples for SEM including use of a collection stub covered with an adhesive (Matney-Wyatt, 2011 and Berk, 2009a; 2009b) or an acetate tape (Marsh, 2011). These techniques required the sample to deposit on the stub or tape as particles were forced out of the airbag. Alternatives to deposition include interception where a vacuum line draws a sample onto or through a suitable sampling surface. This technique has been employed for TEM assessments, by collecting particles from within the sample flow of a cascade impactor (Wentzel et al., 2003) and within a DMS (Price, 2009).

The interception method was selected in this study and samples were drawn by a vacuum line onto and through a TEM grid. The sample vacuum flow rate and sampling duration were identified as variables that would influence the concentration of sample collected and the suitability for assessment. It was decided in this case that a constant low sample vacuum of 3 lpm was employed and the sampling duration was varied. In the same manner as for GF measurements, vacuum flow rates were achieved by use of a 'Flite 2' air sampling pump, (SKC, PA, USA) and flow limiting orifices (Millipore, Billerica, MA, USA). Flow was routinely checked by means of a calibrated, direct volume bubble flowmeter and if recorded sample flow rate varied by more than 10% during testing the data was rejected (SAE, 2011a).

Although it was clear that sample concentration would vary between the airbags being tested it was decided that a suitable compromise of sample duration would be employed. An iterative testing process was used to define sampling durations with samples initially drawn for 3 minutes and then sampling times reduced or increased until an optimum was identified.

A grid holder etched from a copper-nickel alloy, Figure 6.35, was produced to support the grids within a vacuum line, allowing particle samples to be drawn across and through the surface of the grid.

Figure 6.35: TEM Grid holder

The grids selected were 300 lines/inch mesh variants, consisting of a copper substrate overlaid with an amorphous carbon film. A high grid mesh was used as it provided increased stability for the film when under pressure from the sampling vacuum and airbag deployment. A carbon film overlay was used as samples cannot be imaged when positioned directly on the grids or mesh as the electrons are not able to be transmitted through the material during TEM.

Analysis was conducted with a Hitachi A-7650 tomographic Transmission Electron Microscope, Figure 6.36, and in some instances with a Hitachi S-3400N Scanning electron microscope operated by the author and Dr. Louise Hughes from the Oxford Brookes University Department of Life Sciences.

Figure 6.36: Hitachi H-7650 Transmission electron microscope

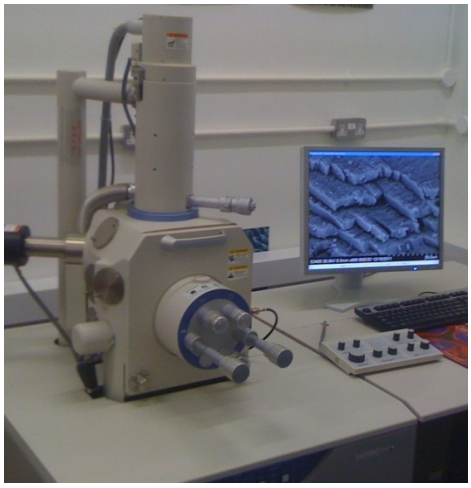

Figure 6.37: Hitachi S-3400N Scanning electron microscope

The process utilised for particle sample collection and assessment by electron microscopy is defined below:

a) Test apparatus setup
b) Test environment sealed
c) Stabilise sample vacuum flow at set-point and attach to sample collection tubing
d) Airbag deployed and vacuum operated for specified test duration
e) Sample removed from test apparatus and stored for subsequent analysis
f) Test environment thoroughly ventilated
g) Test specimen transferred to TEM or SEM platform
h) Electron beam energy set to 100.0kV and sample assessed

Chapter 7

Evaluation of Test Environments and Methodologies

7.1 Introduction

The main airbag effluent tests use the effluent test tank and vehicle interiors. However, it is not clear how they perform and compare to one another. The effluent test tank is designed to replicate a vehicle interior, being of a comparable volume (SAE, 2011a; 2004); however this is the extent of similarities, with shape, interior fittings and materials differing discernibly. Therefore, this element of the research programme measured the performance of both the effluent test tank and the vehicle interior and their ability to provide repeatable data to characterise PM effluents. Two control airbags (B and D) were deployed in the two test environments to determine any variance in terms of measured environmental conditions. These measurements were not associated with measurements of effluent characteristics until later in the research programme (see Chapters 8-13).

The comparison of the effluent test tank and vehicle interior performance consisted of;

a) A qualitative evaluation of factors likely to influence the choice of a test facility

b) Measurement of humidity and temperature to define environmental performance

c) An assessment of variation in airbag effluent particle number concentration and size between the two methodologies and environments.

Further tests and analyses were also conducted to establish the effect that a variation in sampling position could have on measurements of particle number concentration and size.

Finally the test duration was evaluated to help assess existing test requirements and their effect on measurement consistency.

7.2 Qualitative evaluation of test environment performance

When considering the test environments suitable for this research, several factors such as cost, availability and ease of use were also determined by the author prior to testing and during early stages of assessment.

The design of the test environments and subsequent effluent tests showed that whilst initial construction of a test tank is at the outset more costly and time consuming than modifying a vehicle's interior, its use for repeated testing is more cost effective and efficient. With a specifically designed structure, it has proven significantly easier to install and remove airbag modules within the test tank than within the interior of the test vehicle. The tank's deployment mounting positions were designed to fit as many airbag configurations as possible, as opposed to a standard vehicle interior which is designed to accommodate generally specific airbag components. The custom built test tank was designed to seal efficiently to contain repeated airbag deployments and its modular design was able to accommodate effective pressure relief mechanisms with ease. These design features were able to reduce post deployment sample loss to a minimum.

It was rather more complex to seal the test vehicle than the test tank, as there were many more sealing areas (doors, windows, vents etc.) to consider and with repeated use the door seals were likely to be damaged by the increase in pressure in the test environment when the airbag was deployed (Chan et al., 1989). The use of pressure relief valves on the test vehicle did prevent such instances of damage.

The vehicle interior used within the test programme was complete with all internal fixtures and fittings. This proved challenging to clean and remove any PM residue from repeated deployments. This issue was not encountered during use of the test tank as the lack of interior fixings and utilisation of a flat, metallic surface allowed easy cleaning. It may have been expected that the presence of this PM from previous tests would result in higher concentration measurements being encountered in each subsequent test within the test vehicle; however such an increase was not identified during testing.

7.3 Environmental conditions and performance

Whilst both the test tank and vehicle differ appreciably to one another in terms of their appearance, their performance in regard to providing consistent environmental conditions, which is the basis of repeatable testing, is yet to be defined in the literature.

Figure details the results of an assessment of the environmental characteristics of both the test tank and test vehicle. These measurements were taken over 20 non-consecutive days to understand how well each of the environments was able to maintain temperature and relative humidity set-points within the specifications of applicable test standards (Audi AG et al., 2001; SAE 2004; 2011a). Both test environments were located within a single laboratory that provided generally consistent environmental conditions with automated adjustment of ambient temperature.

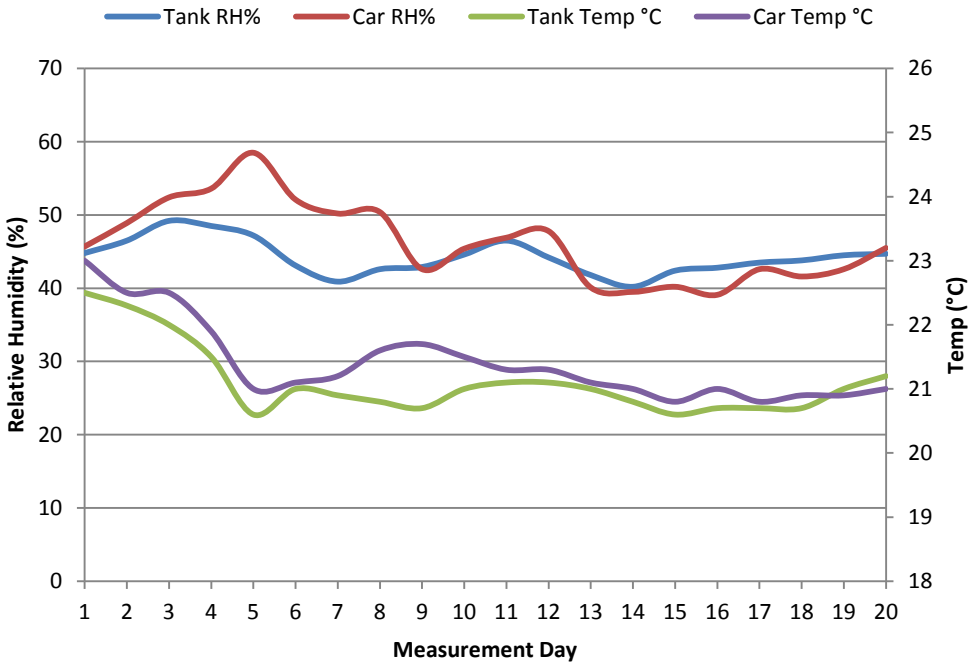

Figure 7.1: Test environment temperature and relative humidity comparison

This data suggests that both the test tank and vehicle interior were able to provide generally consistent test environments which were generally comparable. In general the test vehicle maintained a slightly higher level of relative humidity and temperature than the test tank. This increased humidity may be attributed to the presence of moisture in the test vehicle whilst the temperature differential may be associated with increased heat transfer through the window glass in comparison to the insulated metallic test tank.

Understanding variations in these environmental factors prior to airbag deployment allowed for testing of effluents in a manner commensurate with the requirements of the test standards. Initial deployment tests showed that temperature and relative humidity measured in the test environments appeared to change in response to the release of inflation gases and solid particle effluents. Consequently, to understand how this affected the consistency and comparability of both test environments, a series of tests were undertaken.

Figure 7.2 shows temperature and relative humidity measurements taken in both the test tank and vehicle for (airbag B) which was known to produce a higher temperature effluent from the deflagration of a solid propellant.

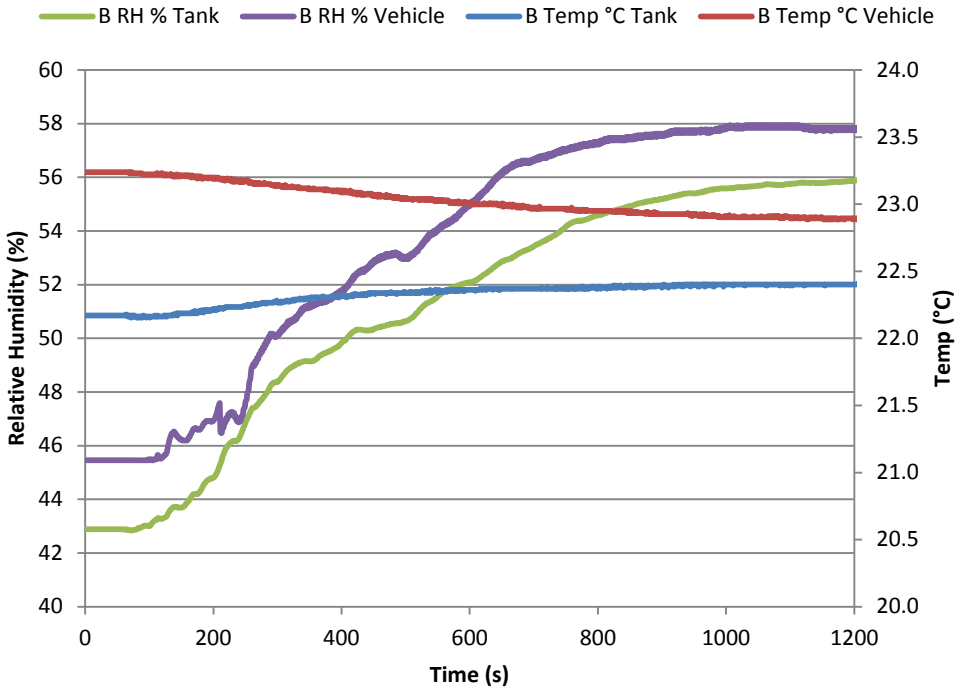

Figure 7.2: Test airbag B tank and vehicle interior environmental performance

This data shows that RH increased substantially after deployment in both test environments, whilst temperature remained generally consistent and comparable in both the test tank and vehicle. The RH level in the test vehicle started higher than in the test tank but overall RH increased by a similar magnitude in both environments.

A second series of environmental measurements were taken from airbag D, as this airbag utilised a hybrid inflator that was known to produce lower temperature inflation gases and this data is shown in Figure 7.3.

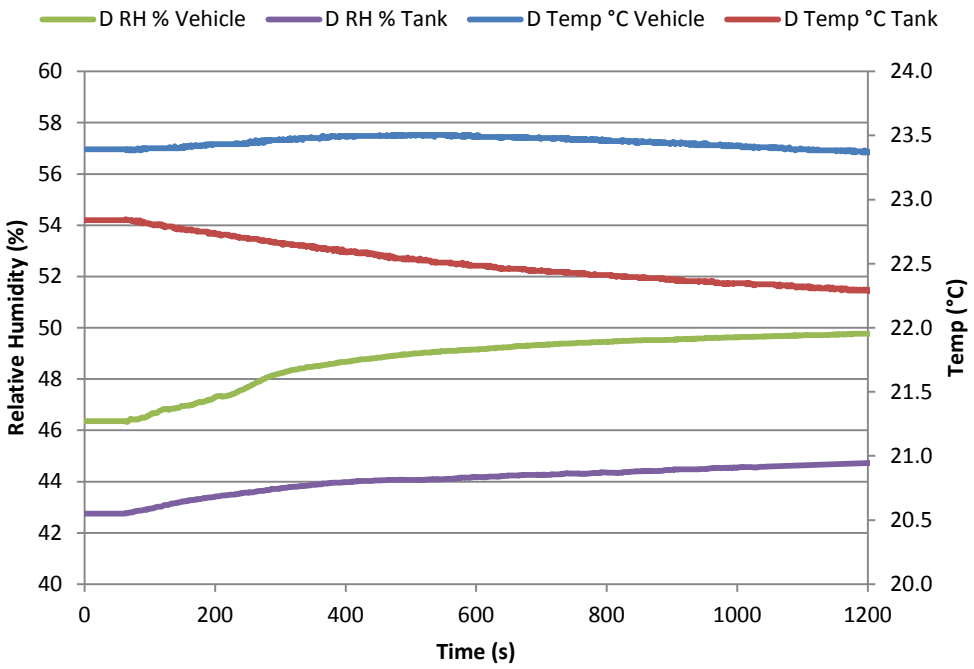

Figure 7.3: Test airbag D, tank and vehicle interior environmental performance

These measurements again show that both vehicle temperatures and RH were initially higher in the test vehicle than in the tank and that after deployment RH increased by a similar magnitude in both environments. Measured temperatures reduced in both environments albeit by a greater degree in the test tank than in the vehicle.

Whilst it is clear that changes in environmental conditions identified during the tests could be attributed to the deployment of the airbag, and that each tested airbag produced notably different effects on humidity and temperature, these are not directly considered here and will be discussed more comprehensively in Chapter 9. This data does however suggest that aside from pre-deployment variations in temperature and RH, little variation between each environment could be detected, with temperature and RH increasing or decreasing in a similar manner.

7.4 Particle number concentration and size variance

To identify any variability in PM size spectral density, measurements were conducted within both environments by means of the DMS. A series of tests of three airbags of types 'B' and 'D' were completed within both the test tank and vehicle and total particle number count and size was determined over a 20 minute test duration. The data presented within this chapter details the results of test numbers 1-18 in the test matrix, Chapter 6.

Initially mean particle number concentrations and sizes were calculated over the full test duration of 20 minutes and measurement range of 5-1000nm to identify both inter-test

variability and whether or not a statistical difference could be detected between both test environments.

When considering particle size under the same conditions within the measured range, no statistically significant difference ($p>0.05$) could be identified between results in each of the test environments could be identified. However, inter-test variability (the variability between tests) was defined as 1.92% in the test tank and 12.94% in the test vehicle.

Similar results were identified for particle number concentration with no statistically significant difference detected between results in the two test environments ($p>0.05$). Again, inter-test variability was lower in the test tank, at 5.16% and 14.14% in the test vehicle.

It was identified that the particular airbag utilised for assessment of the test environments produced a considerable proportion of particles below 200nm and therefore variability and variance within a more finite range of 5-200nm was defined. This secondary assessment detected no statistical difference between either test environment in terms of particle aerodynamic diameter and number concentration ($p>0.05$). The level of variability for each test environment and condition were comparable at 2.36% and 12.73% in the test tank and test vehicle respectively for particle size and 5.11% and 14.48% for number concentration.

Whilst these values indicate comparability between the effluent test tank and the interior of the test vehicle, albeit with greater variability in the test vehicle than the tank, they do not take into account variability in relation to time. Therefore further analysis of data measured with the DMS was conducted to define the variability in measured particle size and concentration between tests in both the test tank and vehicle interior, in relation to time.

Figure 7.4, defines inter-test variance, presented as a co-efficient of variation (CoV) in each of the two test environments in relation to time for both particle size and number concentration (N/cc) for the single particle size range of 5-1000nm.

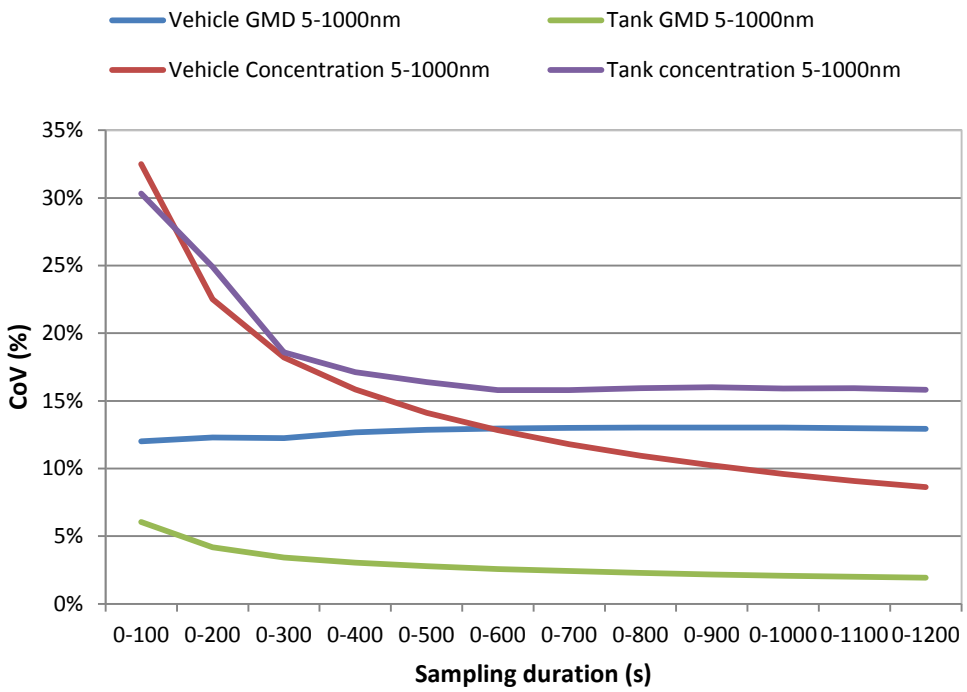

Figure 7.4: Test environment measured number concentration and geometric mean diameter inter-test variance: 5-1000nm range

This data indicates that in the measured size range of 5-1000nm, particle concentration and size varies between tests by a considerably greater degree in the test vehicle than it does in the environmental test tank. This suggests that under the tested condition the test tank is a more controlled environment for airbag particulate effluent testing.

Assessments of particle size, suggest that a considerable proportion of the effluent emitted from the tested airbag is below 200nm in size. Therefore the data was assessed in this more finite range to provide greater understanding of variability between tests in each of the environments. Figure 7.5 details this variability for particle number concentration.

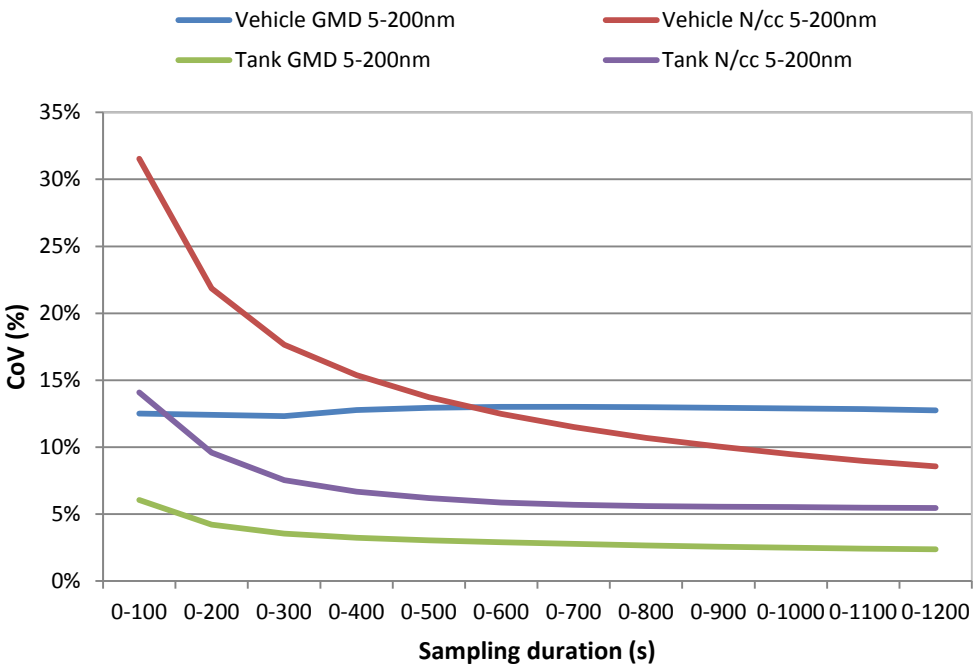

Figure 7.5: Test environment measured number concentration and geometric mean diameter inter-test variance: 5-200nm range

This data again suggests that greater inter-test variability exists in the test vehicle than in the effluent test tank in relation to particle number concentration. Use of the smaller measurement range has shown that in the dominant size range (5-200nm) a greater reduction in variability in the test vehicle could be seen. This indicates that the test vehicle is capable of providing relatively consistent and repeatable measurement datasets albeit with greater variability than tests undertaken in the test tank.

With the test tank appearing more favourable for repeated testing, a further assessment of its performance with regard to variability in relation to time was conducted, in 50nm segments. Figure 7.6 details this variability for particle number concentration only, as particle size variability remained lower and more consistent.

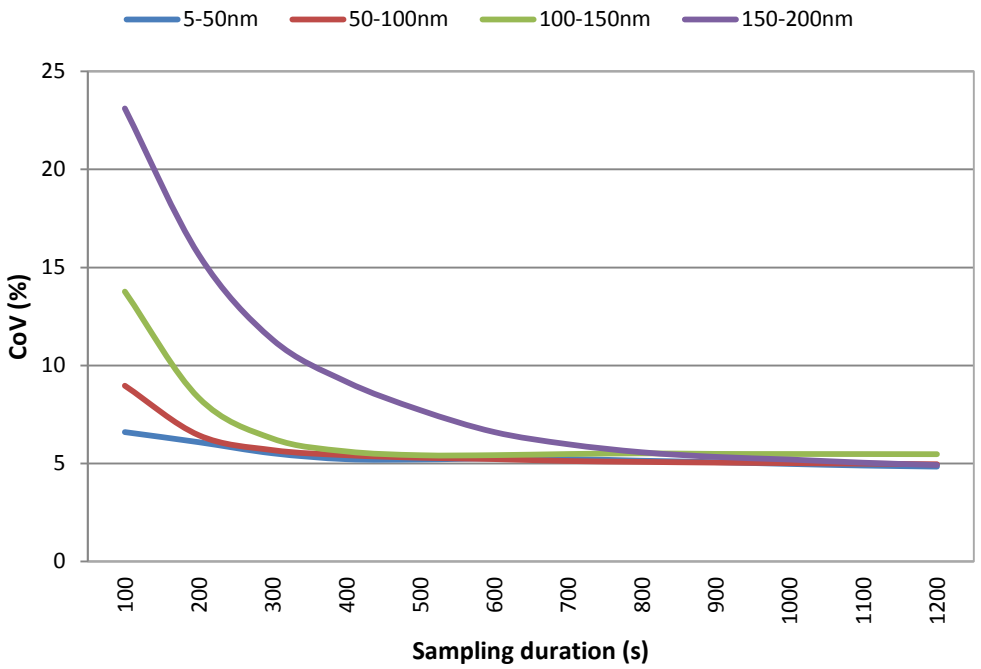

Figure 7.6: Effluent test tank measured number concentration inter-test variance: 5-200nm range, 50nm segments

This data shows that inter-test variability is initially higher for larger particles, with variability reducing rapidly in the 5-150nm size range. Variability reduces at a lower rate for particles in the 150-200nm size range until the four size ranges are closely comparable after 900 seconds, with variability of 5-6%.

In summary, whilst no statistical difference could be detected between the two test environments, when only mean values were evaluated, a difference could still be seen between these values, with the test tank able to provide substantially less variable results than the test vehicle. This variation became clearer when assessing inter-test variability in relation to time. Variability was substantially higher in the test vehicle than in the test tank throughout the test duration.

7.5 Test duration

The previously presented data that has been used to define inter-test variability in relation to time provides sufficient information to assess existing test durations and define suitable durations. Existing test standards for the assessment of effluents produced by airbag deployment employ a 1200 second test duration, with the rationale being associated with the maximum length of time in which an occupant may be contained in a vehicle where an airbag has deployed without it being ventilated after a collision (SAE, 2011a; Audi AG et al., 2001). Secondary assessment of this data indicates that for the test tank a test

duration of at least 900 seconds after deployment is required to reduce measurement variability to a consistent level of between 4.5% and 6%,

For the test vehicle the position is less clear and it appears that inter-test variability is still reducing after 1200 seconds, Figure 7.5.

This work has indicated that existing test standards (SAE, 2004; 2011a; Audi AG et al., 2001), with test durations of 1200 seconds are sufficiently robust, in terms of test duration, to measure airbag particle effluents with a DMS in the effluent test tank.

7.6 Sampling position assessment

Once the test tank was defined as the preferred option for repeatable testing of automotive airbags, the influence of variation of the sampling position in the tank was considered. The previously reported data is defined from measurements taken from a single centralised position in the test tank and test vehicle and therefore does not take into account the effect of any variation in sampling position. Earlier research assessing the influence of varying this sampling position by Starner (1998), suggested that in a test tank environment, provided the samples were not drawn in the lower 25% of the environment, there was little identified effect on particle concentration. However, Starner's (1998) study only considered a mean particle mass concentration calculated over a test duration of 20 minutes. The present study evaluated particle number concentrations per second over a 20 minute duration using the DMS, with a measurement range of 5-1000nm.

A series of measurements were taken at horizontal and vertical positions, as defined in chapter 6, with the airbag positioned centrally in the test environment. In total five sampling positions were assessed with a central sampling position being shared by the horizontal and vertical arrays, Figure 6.19 and Figure 6.20. Sampling positions 1, 2 and 3 refer to vertical positions from the top to the bottom of the test tank and sampling positions A and C refer to horizontal positions with C being closest to the tank entry door. Sampling point 2 is also positioned at the mid-point between positions A and C, negating the need for additional horizontal sampling point measurements to be taken. The assessment of sampling position was conducted with the control airbags used in the assessment of test environments using the same methodology and data evaluation procedures.

Initially mean particle number concentrations were calculated over the full test duration of 1200 seconds and measurement range of 5-1000nm to identify both inter-test variability and whether a statistical difference can be detected between any of the sampling positions.

Within the particle size range 5-1000nm, no statistically significant difference ($p>0.05$) could be detected between each of the vertical or horizontal sampling positions, with inter-test variability of 8.1% for vertical and 5.9% for horizontal positions.

Again, as it was known that a considerable proportion of particles were below 200nm in diameter, a secondary assessment of variability was conducted in the range 5-200nm. As in the wider size range, no statistically significant difference ($p>0.05$) could be detected between each of the vertical or horizontal sampling positions and inter-test variability was reduced to 2.0% for vertical and 5.1% for horizontal positions.

This data suggests that of the 5 sampling positions no statistical difference in particle number concentration could be detected. However, this initial assessment of mean values did not take into account variability in relation to time; therefore the data was assessed to define any variance and is shown in Figure and Figure for particle size ranges of 5-1000nm and 5-200nm respectively.

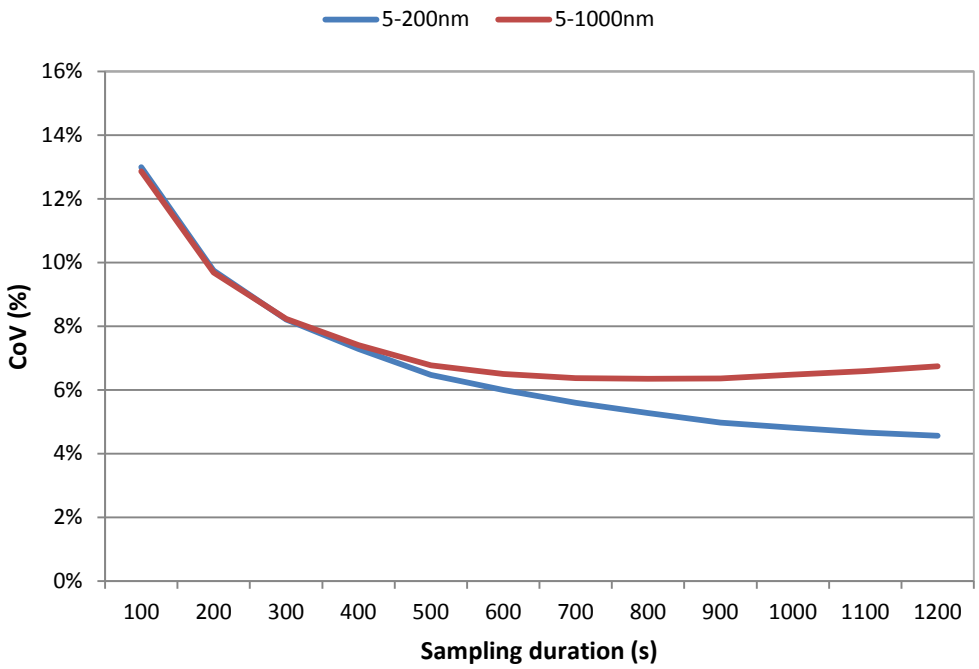

Figure 7.7: Vertical sampling positions number concentration measurement inter-test variability

Figure shows the variability in particle number concentration in relation to time for the three vertical sampling positions. Variability between sampling positions is between 15% and 13% and reduces to a consistent level of around 6% and 4.5% for 5-1000nm and 5-200nm measurement ranges respectively.

The variability in particle number concentration in relation to time for the horizontal sampling positions is shown in Figure 7.8.

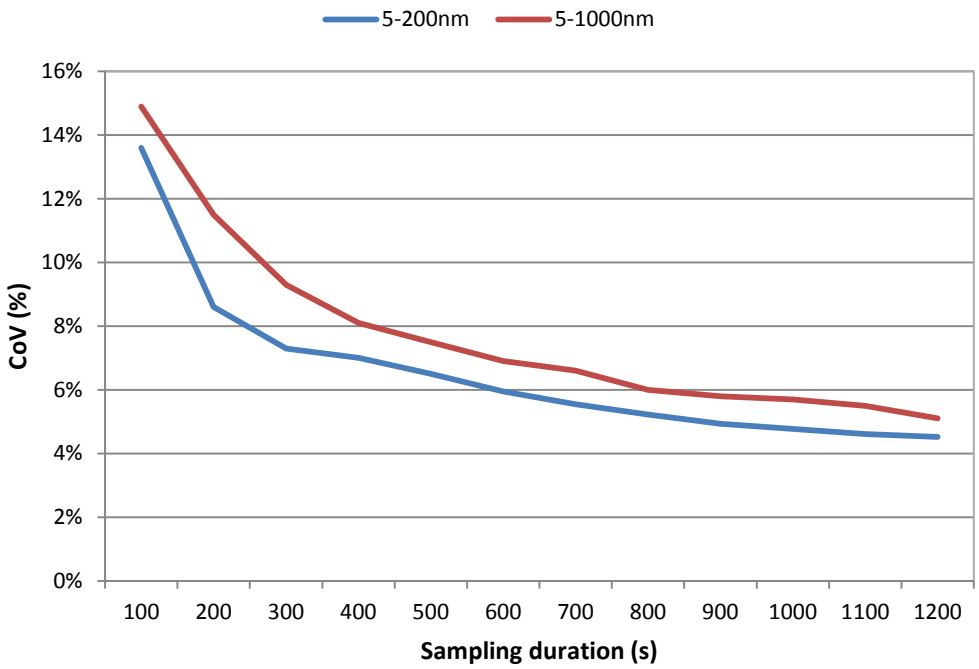

Figure 7.8: Horizontal sampling positions number concentration measurement inter-test variability

A similar trend and level of variability to the vertical sampling positions can be seen. Variability between sampling positions is initially higher at around 15% but reduces to a consistent lower level of around 5% for both 5-200nm and 5-1000nm measurement ranges.

This data indicates that varying the sampling position horizontally or vertically within the test tank appears to have little effect on measured particle number concentration.

7.7 Summary

Environmental test tanks are commonly used for effluent testing as they are cost-effective and easy to use. However, based on the literature review, no data has been identified that compares the environmental test tank and the vehicle interior.

Initially this work assessed the abilities of the test tank and vehicle to maintain a repeatable environment with respect to environmental temperature and humidity. The data gained indicated that the vehicle environment was slightly less consistent than the test tank and suggests that the test vehicle was more susceptible to fluctuations in temperature and that a higher level of moisture in the vehicle may exist when compared to the test tank. However, this is not a particular problem, but shows the possible need for conditioning of the test environments under some conditions.

After the deployment of airbags, changes in environmental conditions were observed and each airbag tested produced notably different effects on humidity and temperature. It is important to note that relative humidities and temperatures changed by a similar magnitude in both environments. This therefore indicates that, aside from pre-deployment variations in temperature and RH, little variation between each environment could be detected.

A comparative study of the test environments measured particle number concentration and size of the effluent produced during airbag deployment. This assessment showed that for the tested airbags, mean particle size and number concentration, calculated over the 1200 second test duration, were comparable with no statistically significant variation (p >0.05) identified. However, a difference in the level of variability between tests was identified. This inter-test variability was considerably higher for measurements conducted in the test vehicle when viewed as a mean value over the full test duration of 1200 seconds, as compared to measurements taken each second. When considering this variability progressively over the 1200 second test duration, it was observed that the variability reduced at a faster rate and to a lower level in the test tank than in the vehicle.

The presented data therefore supports and verifies the methodology options within existing test standards which allow the use of an environmental test tank in place of a vehicle's interior. The data in fact suggests that the test tank is able to provide a more repeatable test environment than the vehicle for effluent tests with the DMS.

As the test environments used were of comparable volumes, and based on the data in this work, it was decided that all further characterisation tests would be conducted in the environmental test tank.

The tests on sampling locations suggested that changing sampling position had little effect on particle concentration measurements and that no statistical difference between each sampling position could be detected. This supports the findings of Starner et al. (1998) using GF measurements. Further assessment of variance in relation to time showed that variance between sampling positions reduced over time to as little as 4.5% for horizontal and vertical sampling positions, thus indicating that the particle effluent emitted during airbag deployment and contained within the test tank created a homogeneous measurement environment.

Currently test durations specified in test standards are only based on the maximum length of time in which an occupant may be contained in a vehicle after an airbag has deployed without ventilation after a collision (SAE, 2011a; Audi AG et al., 2001). This work assessed test repeatability and the comparability and consistency of measurements with the DMS and suggested that a test duration of at least 900 seconds after deployment is required to reduce measurement variability between tests to a consistent level of between

4.5% and 6%. This indicated that existing test standards, (SAE, 2011a; Audi AG et al., 2001) with test durations of 20 minutes are sufficient to measure airbag particle effluents with a DMS.

In summary, the data and analysis presented within this chapter provide a firm evidence basis for definition of a suitable methodology for testing of the airbags defined in section 6.2. All further testing conducted within this research programme has been undertaken within the environmental test tank, for 1200 seconds with a common sampling position in most cases.

Chapter 8

Effluent Characterisation: Mass Concentration Test Data

8.1 Introduction

The data presented and assessed within this chapter details the results gained from the evaluation of effluent particle mass concentration from the four previously identified test airbags using GF and as defined in the test matrix. Whilst measurement of particle mass was not the focus of the research programme, definition of this characteristic allows alignment with current test standards (SAE, 2011a; Audi AG et al., 2001) that are yet to incorporate the definition of particle number by measurement of either optical or electrical mobility characteristics and for the subject airbags to be viewed in context with other data previously presented in the literature for particle mass concentrations from airbag deployments.

8.2 Gravimetric filtration analysis data

Measurements of particle mass concentration by GF were conducted within the environmental test tank only and the data presented within this chapter details the results of tests 19-22 in the test matrix.

The data defines particle mass concentrations calculated from three tests of each subject airbag, conducted in-line with the methodology defined within section 6.6.

Temperature, environmental pressure and RH were recorded within the test tank for the duration of tests with pre-deployment values required to comply with the parameters specified within test standards (SAE, 2011a; Audi AG et al., 2001) and mean temperature and pressure values were used to allow volume corrections to be made (SAE, 2011a). In addition to these measurements, sampling flow rate and duration were recorded and

utilised to define total particle concentration as a value in mg/m^3 by means of Equation 5 in Chapter 6.

Tables 8.1 – 8.4 define the results from tests of each subject airbag. Data from assessment of subject airbag 'A', an airbag using a solid propellant inflator is detailed in Table 8.1. Three tests were conducted to allow test characteristics and ultimately particle mass concentration to be robustly defined and error reduced.

Test parameters	**Test A1**	**Test A2**	**Test A3**
Total particle mass (mg)	7.2	8.2	7.4
Mean temperature (°C)	19.5	19.8	19.3
Mean RH (%)	45	47	44
Pressure (kPa)	102,500	102,600	102,300
Mean flow (lpm)	4.8	4.6	4.5
Total particle concentration (mg/m^3)	73.6	87.4	80.7

Table 8.1: Gravimetric filtration test series - airbag A

Although temperature and relative humidity measurements were recorded each second for the full test duration, only mean values are presented within this chapter and used for volume corrections. These environmental characteristics are however considered in more detail within Chapter 9.

Recorded mean temperatures and relative humidities in the tank were consistent between tests and varied by only 0.5°C and 3% for relative humidity, whilst mean flows also remained closely comparable. Calculated particle mass values remained relatively consistent to one another (within 19%) with a maximum particle concentration of 87.4 mg/m^3 recorded during test A2.

Data for subject airbag 'B', also utilising a solid propellant inflator is defined within Table 8.2 and this shows broadly comparable results to those of airbag 'A'.

Test parameters	**Test B1**	**Test B2**	**Test B3**
Total particle mass (mg)	7.6	6.9	7.1
Mean temperature (°C)	22.0	22.4	22.8
Mean RH (%)	55.6	57.2	54.5
Pressure (kPa)	100,500	100,800	100,700
Mean flow (lpm)	5.2	5.4	5.1
Total particle concentration (mg/m^3)	73.7	64.3	70.3

Table 8.2: Gravimetric filtration test series - airbag B

Again, tank pressure, temperature and relative humidity remained relatively consistent during each test. A maximum particle mass concentration of 73.7 mg/m^3 was recorded during tests and concentration values again appeared reasonably consistent varying by up to 15% between tests, a similar value to that recorded during tests of airbag A. Total particle concentration values appeared comparable to that of subject airbag 'A' with no statistical difference ($p>0.05$) able to be detected between the effluent measurements of the two airbag types.

Table 8.3 details the results of the analysis of airbag 'C'. This airbag is a more modern system than airbags A and B but still uses a solid propellant.

Test parameters	**Test C1**	**Test C2**	**Test C3**
Total particle mass (mg)	4.5	3.2	4.9
Mean temperature (°C)	22.3	22.6	22.0
Mean RH (%)	52.5	54.5	48.0
Pressure (kPa)	101,000	100,750	101,250
Mean flow (lpm)	5.2	4.8	5.1
Total particle concentration (mg/m^3)	43.9	33.6	48.1

Table 8.3: Gravimetric filtration test series - airbag C

Measured environmental characteristics such as temperature, relative humidity and pressure again appeared comparable not only between tests C1-C3, but also to those measured during tests of airbags A and B. Total particle mass concentration values were substantially lower than the previously tested airbags with a maximum of 43.9 mg/m^3 recorded; a value nearly 40% lower than that recorded for airbag B and 50% lower than airbag A. Consequently, values recorded for airbag C were statistically different to both A and C ($p<0.05$). Inter-test variance was calculated as greater than previously recorded at 23%.

The results of the measurement of particle mass concentration arising from deployments of airbag D are detailed in Table 8.4. This airbag was different to those previously assessed as it utilised a hybrid inflator that produced inflation gases. This inflator used a substantially lower propellant mass than that used in the full solid propellant inflators such as those utilised by airbags A, B and C.

Test parameters	Test D1	Test D2	Test D3
Total particle mass (mg)	0.58	0.6	0.72
Mean temperature (°C)	22	21	21.5
Mean RH (%)	52	48	51
Pressure (kPa)	100,850	101,000	101,300
Mean flow (lpm)	4.60	4.90	4.70
Total particle concentration (mg/m^3)	6.3	6.1	7.7

Table 8.4: Gravimetric filtration test series - airbag D

It is immediately clear that particle mass concentrations recorded for airbag D were significantly lower than those for airbags A, B or C with a maximum total particle concentration of $7.7mg/m^3$ recorded and therefore a statistical difference was detected ($p<0.05$) between this airbag and all others tested. Inter-test variance was higher than that recorded during tests of other airbags at approx. 26%, however such a variance should be viewed in context to the emitted particle mass in this case as it reflects an increase of 1.6 mg/m^3.

With particle mass concentrations for each of the four subject airbags defined, summary Table 8.5 allows each airbag type to be easily compared.

Test parameters	Airbag A	Airbag B	Airbag C	Airbag D
Mean concentration (mg/m^3)	80.6	69.4	41.9	6.7
Concentration range (mg/m^3)	+ 6.8 / - 7.0	+ 4.3 / - 5.1	+ 6.2 / - 8.3	+ 1.0 / - 0.6
Standard deviation	6.9	4.8	7.5	0.9
Co-efficient of Variance (%)	8.6	6.9	17.8	13.0

Table 8.5: Gravimetric filtration test series summary

The data identified that variation in total particle mass concentration existed between airbag types in all cases, although no statistically significant difference could be detected between subject airbags A and B ($p>0.05$), whilst all other airbags remained statistically different to one another ($p<0.05$). The three solid propellant airbags (airbags A, B and C) provided mass concentration values significantly higher than hybrid airbag (airbag D), who's recorded mass concentration (mean) was only 8 percent of that recorded for the highest emitter; airbag A.

8.3 Summary

The concentration values obtained from these tests ranged from 6.7 mg/m^3 to 80.6 mg/m^3 with the three subject airbags utilising a solid propellant inflator providing broadly comparable concentration values. These solid propellant airbags ('A, B and C') provided markedly different results to those for airbag D which used a hybrid inflator to provide inflation gases. Measurement of effluents from airbags A, B and C defined mean particle mass concentrations of 80.6, 69.4 and 41.9 mg/m^3 respectively, whilst airbag D provided a mean concentration of 6.7 mg/m^3. This data identified that airbag A could not be statistically differentiated from airbag B ($p>0.05$), but airbags C and D differed statistically to all other tested airbags ($p<0.05$). Neither calculated mean concentration values nor those from individual tests exceeded the maximum specified limit of 125mg/m^3 (SAE 2004; 2011a; Audi AG et al., 2001). However, values may exceed apportioned values (SAE 2004) when measuring particle mass concentrations for multiple airbags.

This data appeared to provide a robust assessment of particle mass concentrations for each of the evaluated airbags with the co-efficient of variance being in the range 8.6-17.8 %. Similar variance of 6.4-25.7% was reported by Gross et al., (1999) for non-azide airbags and of in excess of 20% by Ziegahn and Nickl (2002).

Chapter 9

Electrical Mobility Evaluation

9.1 Introduction

While measurement of particle mass concentration provides information regarding particle effluents emitted during deployment of an airbag, the use of electrical mobility measurement provides far greater information regarding the effluent's characteristics and how these vary with respect to time and represents a novel approach to airbag particle effluent assessment. The results of an assessment of particle effluents by these methods by means of a DMS are presented within this chapter. This assessment was composed of 10 elements that are defined in Table 9.1

Analysis type	Specific analysis type	Section presented in
Particle size	Geometric mean diameter	9.2
	Transient geometric mean diameter	9.2
	Geometric mean diameter with respect to time and in relation to environmental factors	9.9
Particle number concentration	Mean particle number concentration	9.3
	Transient particle number concentration	9.4
Combined particle number concentration and size	Particle size spectral density	9.5
	Number concentration size proportions	9.6
	Particle size spectral density in relation to time	9.7
	Size segregated number concentration with respect to time	9.8
	Size segregated particle number concentration with respect to time and in relation to environmental factors	9.10

Table 9.1: PM Effluent Electrical Mobility Evaluation Results Structure

9.2 Particle size definition

Initially particle geometric mean diameter (GMD) was calculated over the full test duration of 1200 seconds and these values may be compared to particle size values presented in the literature and gained predominantly through cascade impaction tests.

Table 9.2 summarises these GMDs as mean values for particles within the specified size resolution capabilities of the DMS; namely 5-1000nm. All mean values were recorded within a range of between 79.64nm and 135.02nm.

Analysis of this data identified a maximum inter-test variance of 4.13% and this low and consistent level of variability evident in all tests indicates the repeatability of the method.

Airbag	Particle size			
	Geometric mean diameter	Standard deviation	CoV (%)	No. of tests
A	135.02	5.57	4.13	3
B	134.58	5.46	4.06	3
C	109.62	1.90	1.74	3
D	79.64	1.53	1.92	3

Table 9.2: Particle size calculated as mean values for airbags A-D

Airbags A and B, both use a solid propellant inflator and provide comparable results, with a larger GMD of around 135nm than solid propellant airbag 'C' (109nm) and the hybrid airbag, 'D' (80nm).

Whilst this data provides core information regarding GMD that is comparable with studies in the literature using cascade impactors (Gross et al., 1994; 1995; Schreck et al., 1995), it provided no information to assist in understanding any change in particle size over the duration of the test and therefore further analysis was undertaken.

Transient GMD data calculated each second over the 1200s test duration is defined within Figures 9.1 to 9.4, with deployment of airbags initiated 60 seconds after commencing collection of data with the DMS.

Figure 9.1 shows GMD with respect to time for the three tests of airbag A. This data shows that GMD increases quickly after deployment and within approximately 500 seconds has reached the maximum value of ~190nm. After approximately 900 seconds GMD subsequently decreases to a minimum level of ~160nm. The three tests (A1-A3) were closely grouped and showed comparable general trends, therefore indicating a repeatable test.

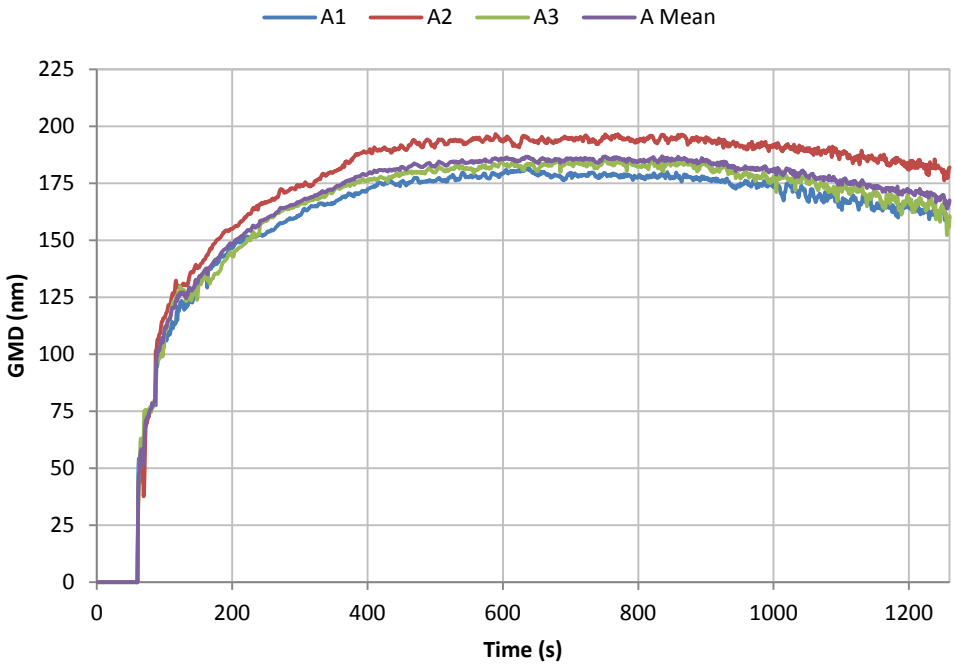

Figure 9.1: Particle GMD with respect to time: Airbag A

Figure 9.2 shows the transient particle GMD data for airbag 'B'. Whilst the initial GMD increase appears broadly comparable to that of airbag 'A' the reduction in GMD observed during testing of airbag 'A' is not evident, with GMD continuing to increase over the test duration. This increase is greatest again in the first quarter of the test (360s) with an increase to between 167nm and 172nm, with GMD increasing to a maximum of 200nm over the remainder of the test. As with airbag 'A' GMD measured between tests is closely comparable, again suggesting that a repeatable test has been employed.

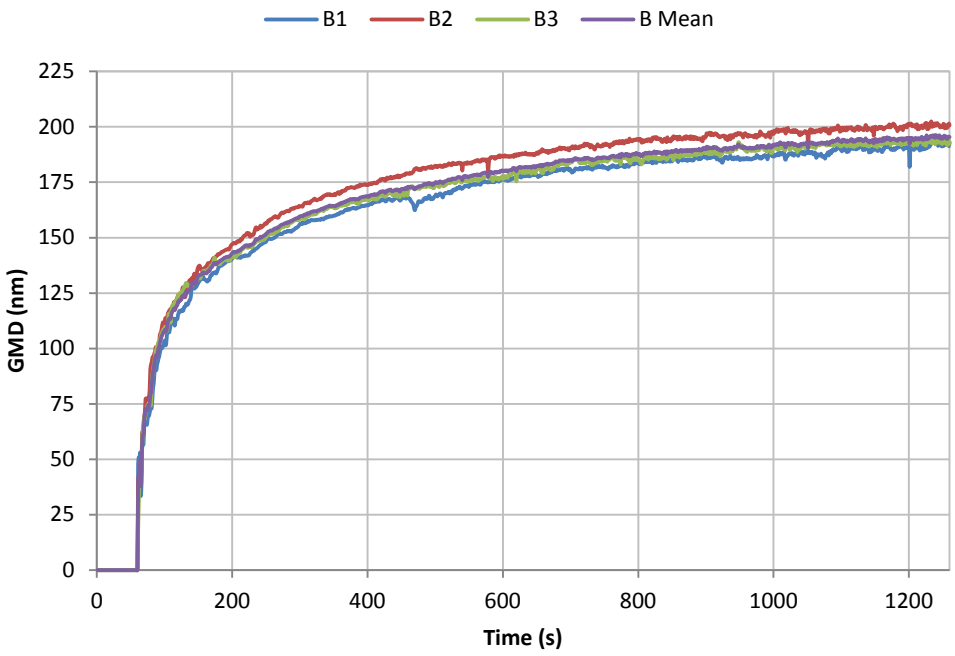

Figure 9.2: Particle GMD with respect to time: Airbag B

Particle GMD measured for airbag C with respect to time is shown in Figure 9.3 and shows similar characteristics to that for airbag B with particle GMD increasing at a greater rate, approximately during the first 360 seconds than over the remaining 900 seconds. Whilst the trend of increasing GMD is comparable between airbags B and C, GMD calculated for airbag C only reaches a maximum of 155nm at the end of the test and therefore is lower than the maximum attained by airbags A and B. It can be seen that in general the tests are highly repeatable.

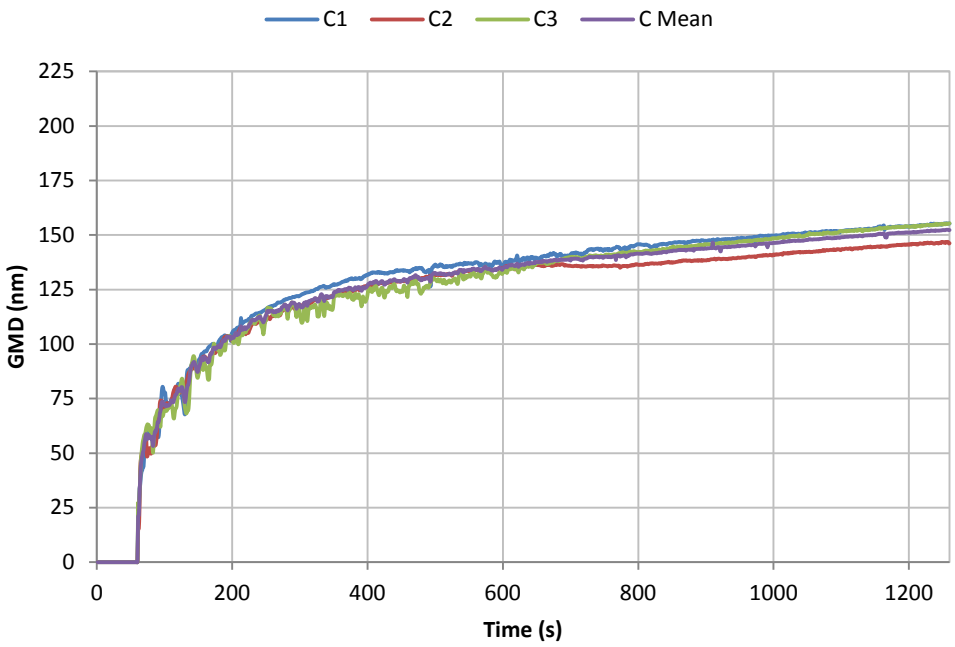

Figure 9.3: Particle GMD with respect to time: Airbag C

The data shown within Figure 9.4 was calculated from measurements of airbag 'D', which utilises a hybrid inflator to produce inflation gases. This data shows that particle GMD increases in a more uniform manner over the 1200 second test duration when compared to the effluents from the airbags utilising a solid propellant to provide inflation gases (A-C). This increase is almost linear after the initial deployment and GMD increases to a maximum of 128nm at the end of testing. This more linear increase in GMD will result in lower GMD means as defined in Table 9.2.

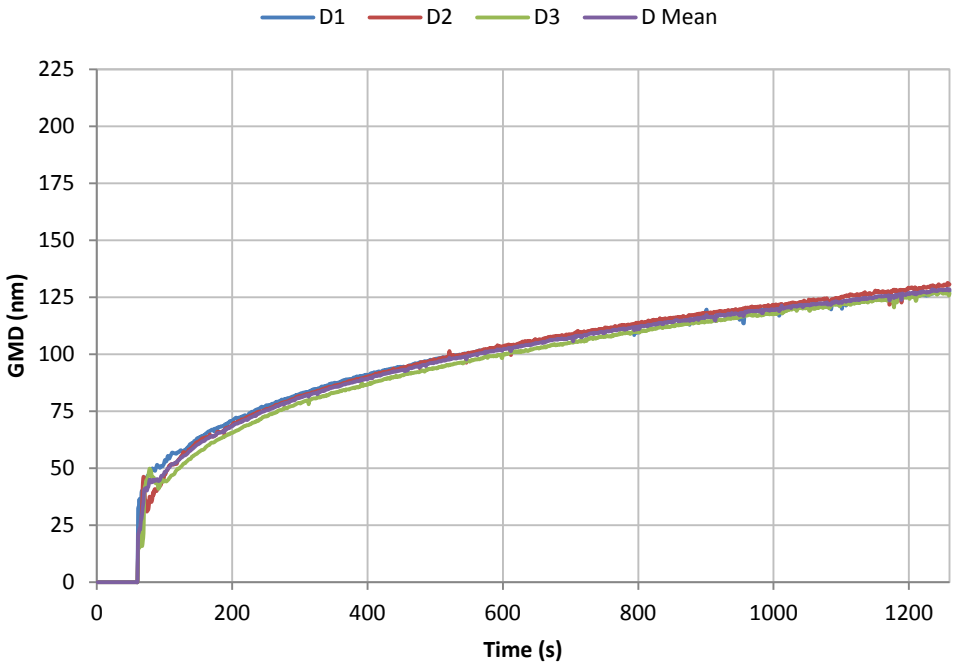

Figure 9.4: Particle GMD with respect to time: Airbag D

Comparing the transient particle GMD data for each of the tested airbags, Figure 9.5, it is clear that each airbag type differs discernibly, allowing airbags to potentially be identified from such data. Airbags B, C and D all demonstrated broadly comparable trends, with GMD increasing throughout the test. The rate of change of GMD and magnitude of the increase did however differ between the airbags. The effluent from airbag B differed to all others tested and whilst GMD initially increased in a comparable manner, it subsequently reduced after around 900 seconds.

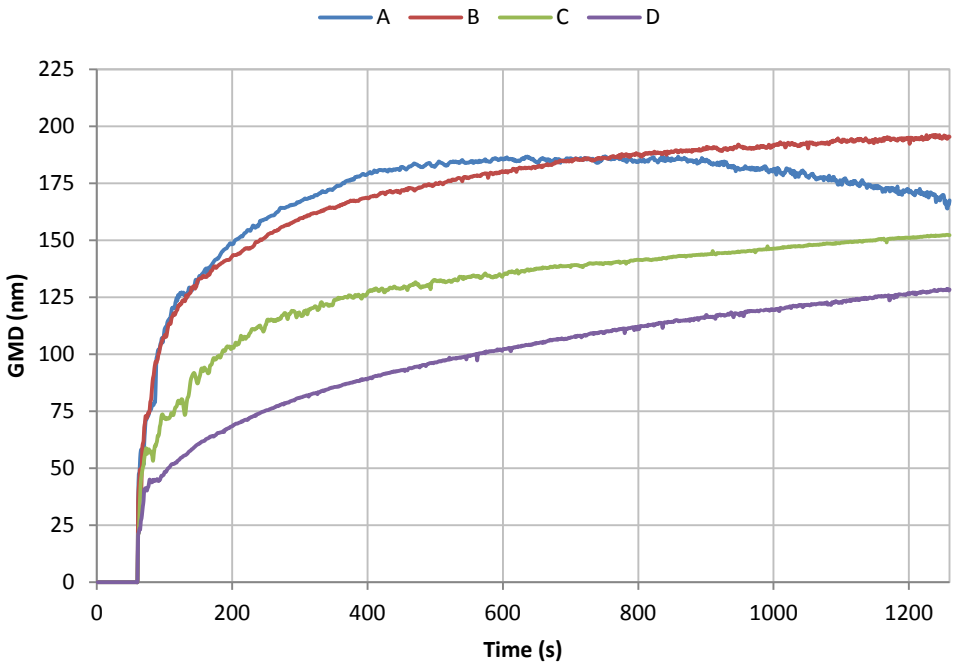

Figure 9.5: Particle GMD with respect to time: Airbags A-D means

9.3 Particle number concentration

Aside from particle size data, the use of a DMS for particle effluent assessment has also allowed considerable investigation of particle number concentration and represents a novel approach to airbag particle effluent analysis. As with particle size, number concentration was initially calculated as a mean value over the full test duration and this data is presented within Table 9.3. This assessment considered the specified full measurement range of the DMS of 5-1000nm diameter. This data shows that particle number concentrations (means) of between 2.05E+06 and 2.85E+06 were recorded, suggesting a substantial particle output upon deployment of airbags.

Airbag	Total particle count (N/cc)			
	Mean	Standard deviation	CoV (%)	No. of tests
A	2.07E+06	6.03 E+04	2.92	3
B	2.18E+06	6.66 E+04	3.05	3
C	2.85E+06	3.54 E+05	12.45	3
D	2.05E+06	1.06 E+05	5.16	3

Table 9.3: Particle number concentration and variability summary

Inter-test variability presented as a co-efficient of variation (CoV) appears to fluctuate depending on the airbag tested with the airbag emitting the greatest particle number (Airbag C) presenting a considerably greater level of variability (12.45%) than the others (min. of 2.92%).

This particle number concentration data and associated indication of inter-test variability has been calculated over the full measurement range of 5-1000nm. However, the assessment of particle sizes as mean values and with respect to time indicated that a considerable proportion of particles were likely to be smaller than the upper particle measurement size limit. An assessment of particles in the range 5-300nm was therefore conducted to determine any effect on measured concentration and inter-test variability. The range of 5-300nm was selected as all mean particle sizes were below 200nm and it was presumed that a high proportion of the emission would be below 300nm. This assessment was possible because the DMS was capable of measuring size segregated number concentration.

The assessment in this more finite range, Table 9.4, showed data that was generally similar to that presented in Table 9.3 for particles in the range 5-1000nm. A large proportion of particles emitted during airbag deployment were below 300nm in size, for instance the total particle count in the range 5-1000nm for airbag A is 2.07E+06 (N/cc) with 1.98E+06 falling below 300nm. Inter-test variability is closely comparable, reflecting the high proportion of particles being within the more finite measurement range.

Airbag	Total particle count (N/cc): 5-300nm size range			
	Mean	Standard deviation	CoV (%)	No. of tests
A	1.98E+06	7.57E+04	3.82%	3
B	2.09E+06	6.66E+04	3.19%	3
C	2.84E+06	3.51E+05	12.35%	3
D	2.04E+06	1.10E+05	5.37%	3

Table 9.4: Particle number concentration and variability summary, 5-300nm size range

9.4 Number concentration with respect to time

To this point number concentration has been considered as a mean value over the test duration of 1200 seconds in the same manner as Starner (1998). However, as with the definition of particle size, number concentration can also be defined with respect to time, with much greater resolution than the 5 minute sequential filter measurements commonly

used and reported in the literature (Wheatley et al. 1997; Gross et al., 1994; 1995; 1999; Schreck et al., 1995). Such data provides a greater understanding of the way in which particle concentration varies in relation to time and this can be used to define particle exposure concentrations where scenarios differ to that defined in the test. Such cases are likely to include post-collision exposures and those experienced when neutralising airbags during ELV treatment and recycling. In these scenarios exposure durations are commonly likely to be less than 20 minutes and, the use of a mean value based on the 20 minute tests may provide erroneous information.

Particle number concentration data defined with respect to time for airbag A, Figure 9.6 indicated that particle concentration increased substantially almost immediately after airbag deployment, and in the case of airbag 'A', a peak concentration value of 2.37E+07 N/cc was reached 25 seconds after deployment. However, after 1200 seconds particle concentration had reduced to a minimum value of 1.89E+05 N/cc. It can be seen that the number concentrations in relation to time for airbag A were closely comparable, with low variability between tests.

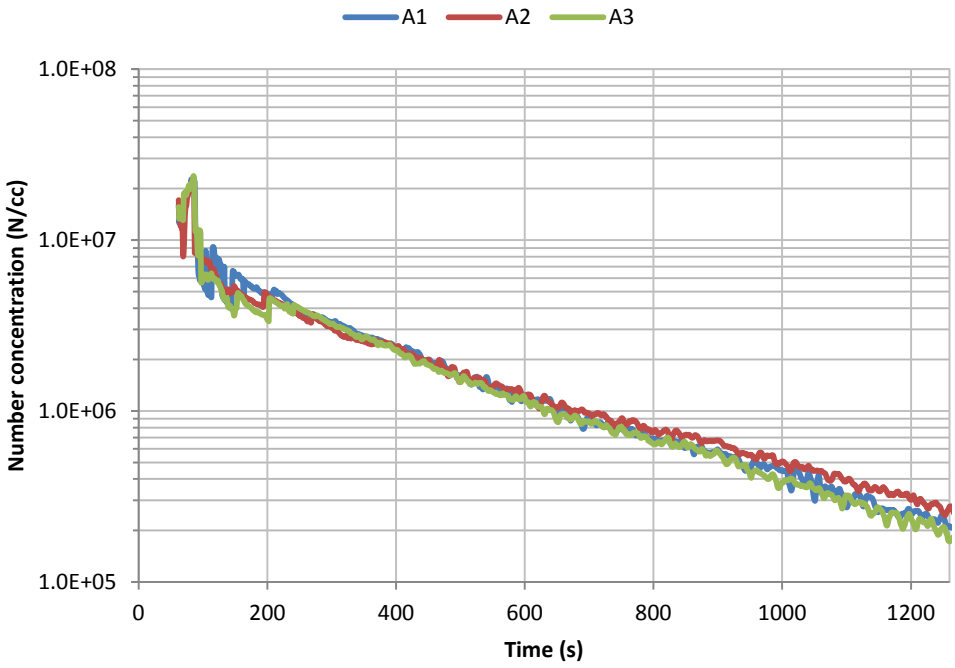

Figure 9.6: Number concentration (N/cc) with respect to time, 5-1000nm range: Airbag A

In the case of airbag 'B', Figure 9.7 the number concentration appeared closely comparable to that of airbag 'A' in a number of ways. Maximum particle concentration of 2.18E+07 N/cc was reached after only 18 seconds and reduced to a minimum of 4.67E+05 N/cc after 1200 seconds. Again inter-test variability was generally low over the great majority of the test durations.

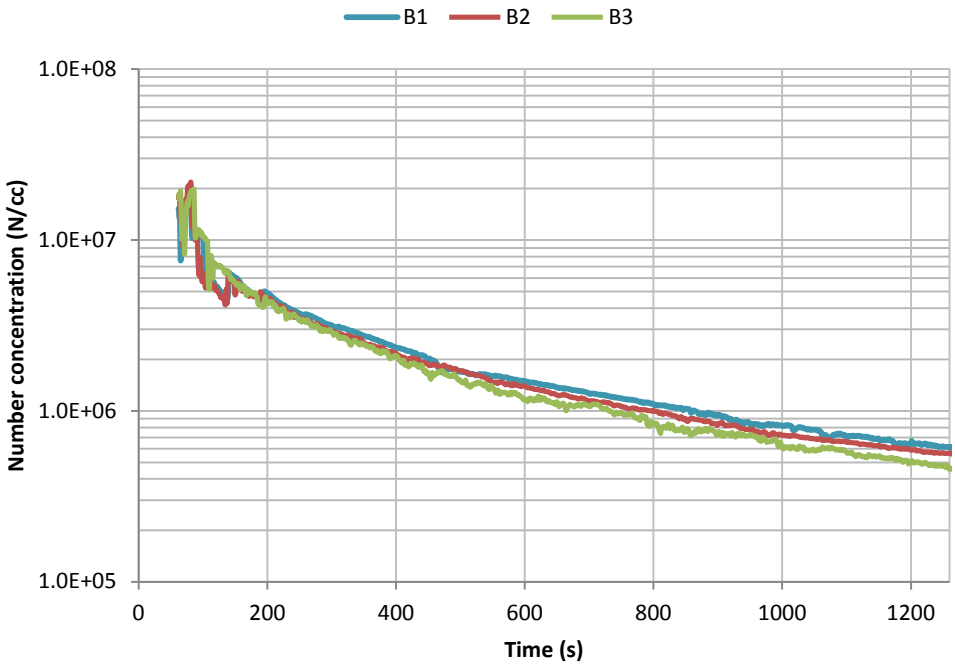

Figure 9.7: Number concentration (N/cc) with respect to time, 5-1000nm range: Airbag B

Figure 9.8 shows number concentration in relation to time for the three repeated tests of airbag 'C'. This data differs to that found for airbags 'A' and 'B' where maximum concentration was higher at 6.04E+07 N/cc and this was reached only two seconds after deployment. However, the concentration appeared to reduce in the same manner as for airbags 'A' and 'B' albeit at a lower rate of change. After 1200 seconds concentration reduced to a minimum of 1.46E+06 N/cc. Inter-test variance was more noticeable than during testing of airbags 'A' and 'B' with maximum concentration varying from 2.35E+07 N/cc (test C3) to 6.04E+07 N/cc (test C1). Tests C1 and C2 appeared to be comparable over the full test duration, whilst test C3 presented greater variability in the first 600 seconds.

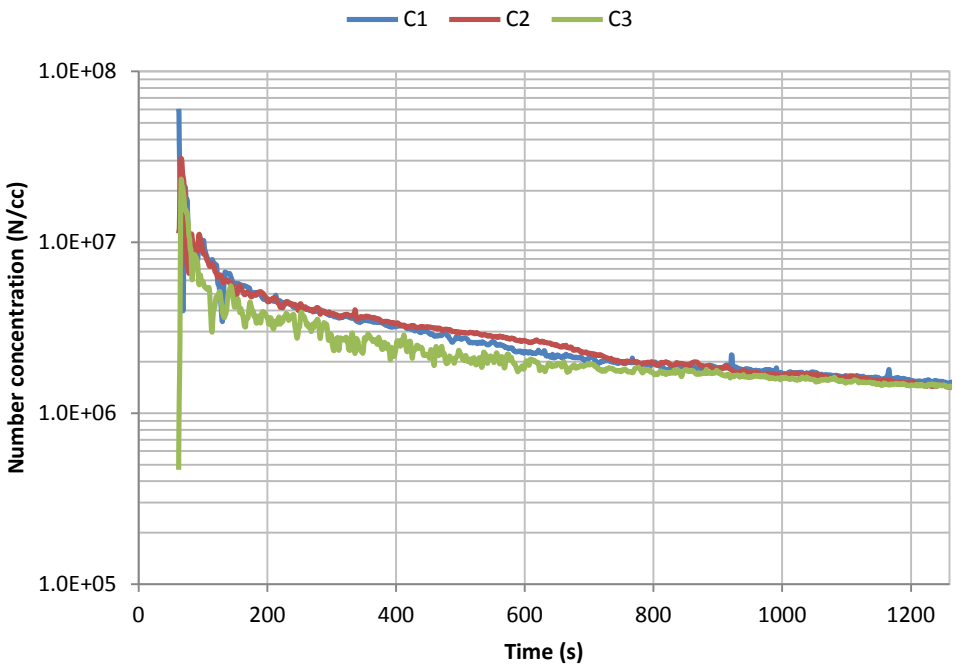

Figure 9.8: Number concentration (N/cc) with respect to time, 5-1000nm range: Airbag C

The data defining number concentration with respect to time for airbag 'D', Figure 9.9, again showed the same general trend presented by the other airbag types, with a high particle number concentration being measured soon after deployment and a generally steady reduction in particle concentration over time. Maximum particle concentration of 1.95E+07 N/cc was reached 6 seconds after deployment and after 1200 seconds had reduced to 9.21E+05 N/cc. Inter-test variance appeared to be low with all datasets tightly grouped.

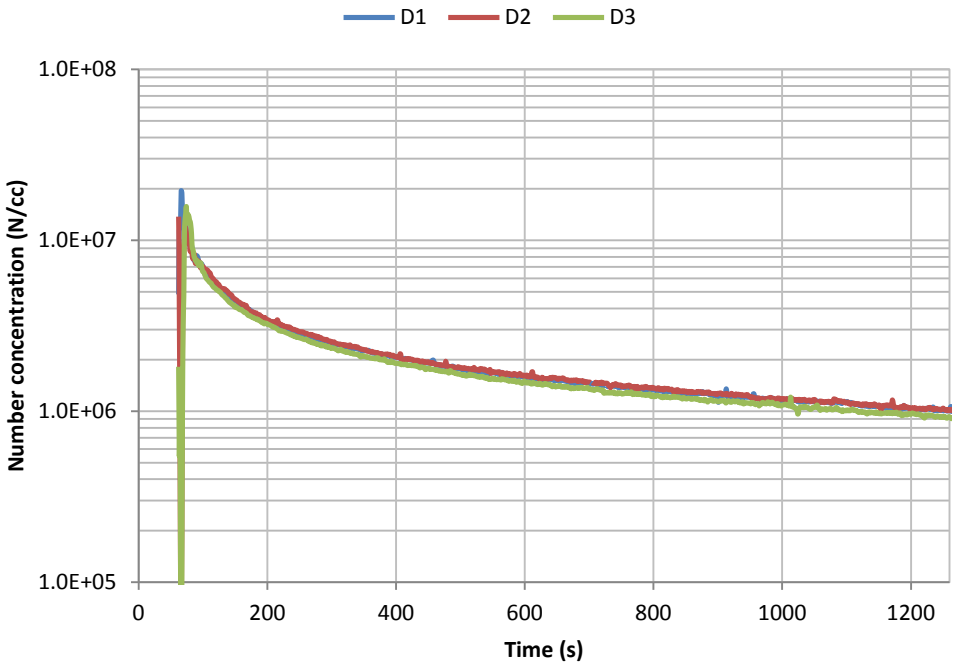

Figure 9.9: Number concentration (N/cc) with respect to time, 5-1000nm range: Airbag D

A summary plot which presents the mean number concentration data for the four airbag types, Figure 9.10, shows that the same basic characteristic of a high number concentration emission occurring shortly after deployment was evident for all airbag types. The variation in maximum number concentration, the elapsed time from deployment at which this occurs, and the manner in which number concentration reduced did provide differentiation between airbag types. Airbag 'C' which used a solid propellant inflator to provide inflation gases maintained a higher number concentration than the other tested airbags with the rate of reduction being considerably lower than for airbag types A, B and D.

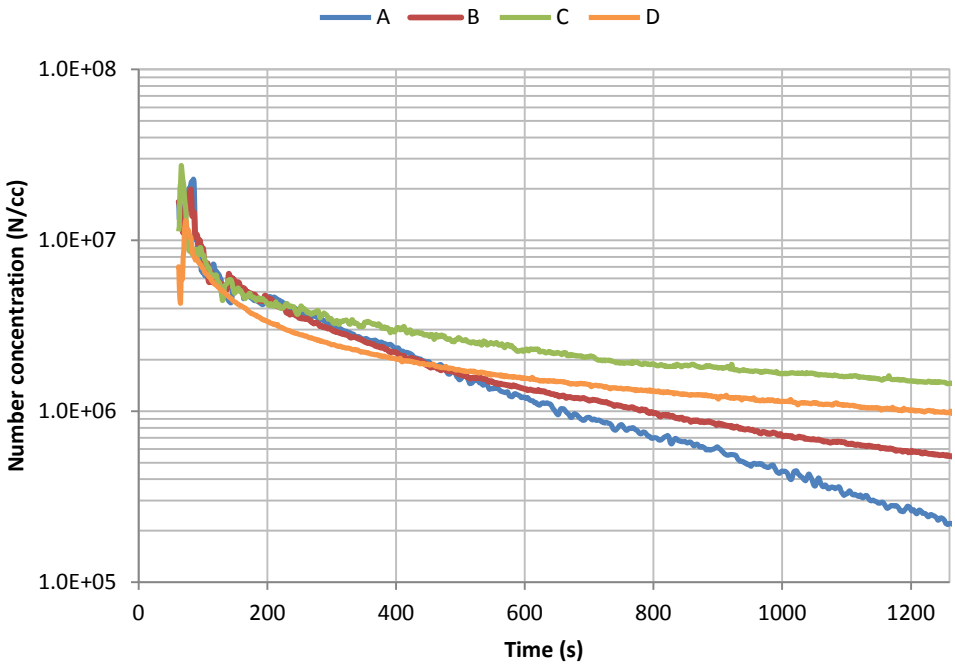

Figure 9.10: Number concentration (N/cc) with respect to time, 5-1000nm range: Airbags A-D

9.5 Particle size spectral density

Figure 9.11 shows the size spectral density plot for airbag 'A', which defines the concentration of particles in relation to particle size for the full test duration of 1200 seconds. Data is plotted using normalised concentration (TSI, 2010). The number concentration is normalised by the size range particles and shown as a size distribution function.

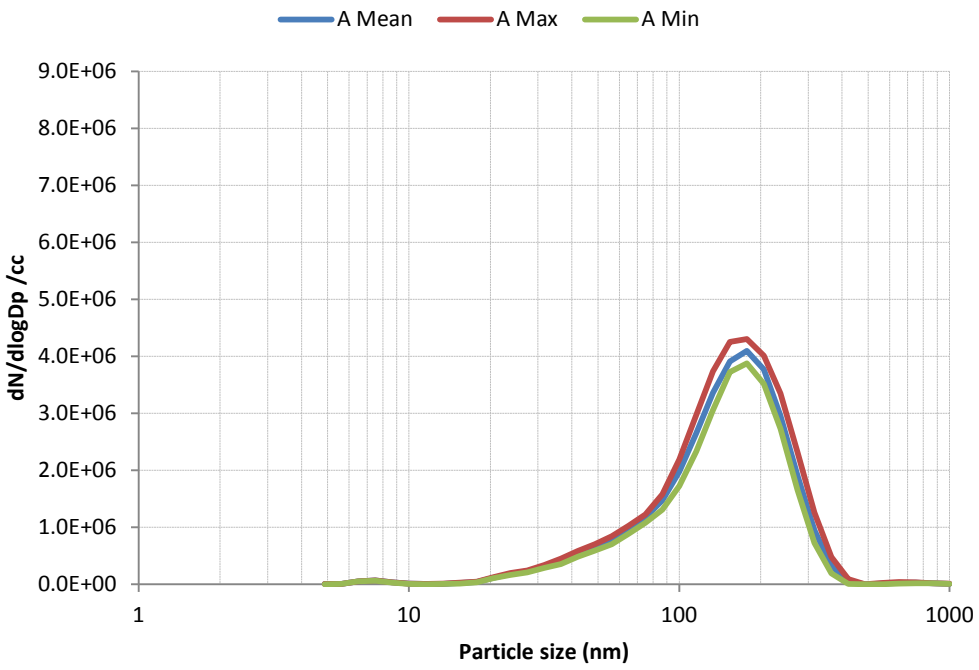

Figure 9.11: Size spectral density: Airbag A

This shows a predominantly unimodal size distribution between approximately 150nm and 180nm. With a mean particle size of 135nm (Table 9.2) it is clear that the particle size and number distribution would be skewed toward a higher proportion of the particles being smaller than the dominant mode and this is shown in Figure 9.11. Concentration values for each of the tests are generally tightly distributed although some variability in concentration can be seen around the dominant mode.

A similar trend is again seen for airbag 'B' with a unimodal size distribution between 150nm and 180nm. Maximum concentration in this size range is closely comparable at around 4.5E+06 N/cc to airbag A as is the overall distribution shape and therefore concentration in relation to particle size. Inter-test variability levels again appear similar with a greater degree of variability existing in the dominant size range for higher particle number concentrations.

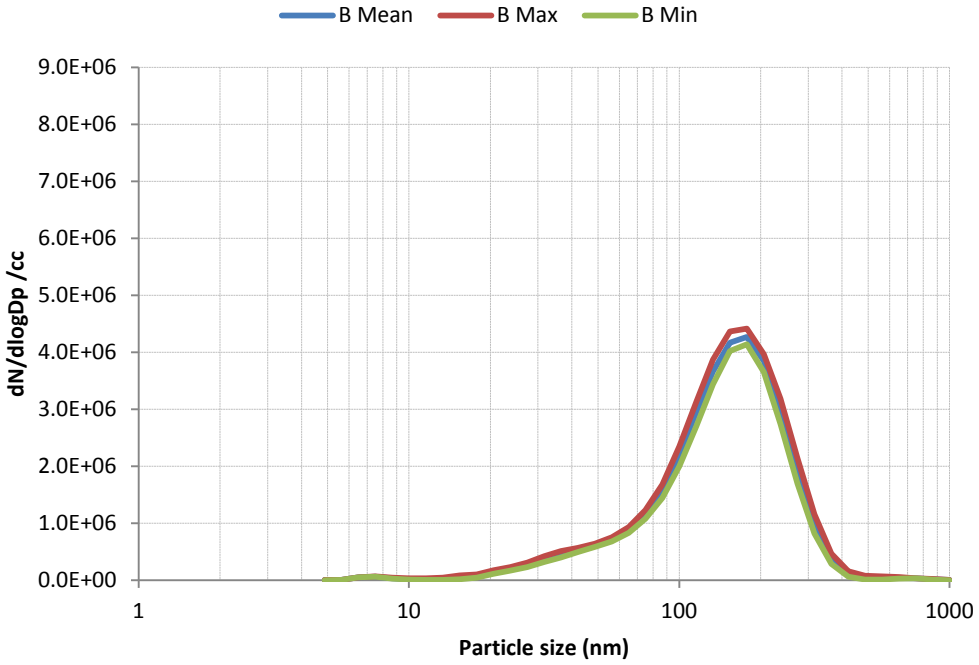

Figure 9.12: Size spectral density: Airbag B

The size spectral density data from airbag 'C' defined within Figure 9.13 shows a more apparent bimodal size distribution (highlighted in figure 19.3) than for airbags A and B with a higher total concentration of particles being emitted and a comparably higher concentration of smaller particles than generated by airbags A and B. The dominant mode occurs at around 135nm where a maximum concentration of 8.39E+06 N/cc was measured and the secondary mode occurs at 40-50nm. Greater variability could be seen between tests than for airbags A and B, with most being associated with a variation in concentration of the dominant particle size.

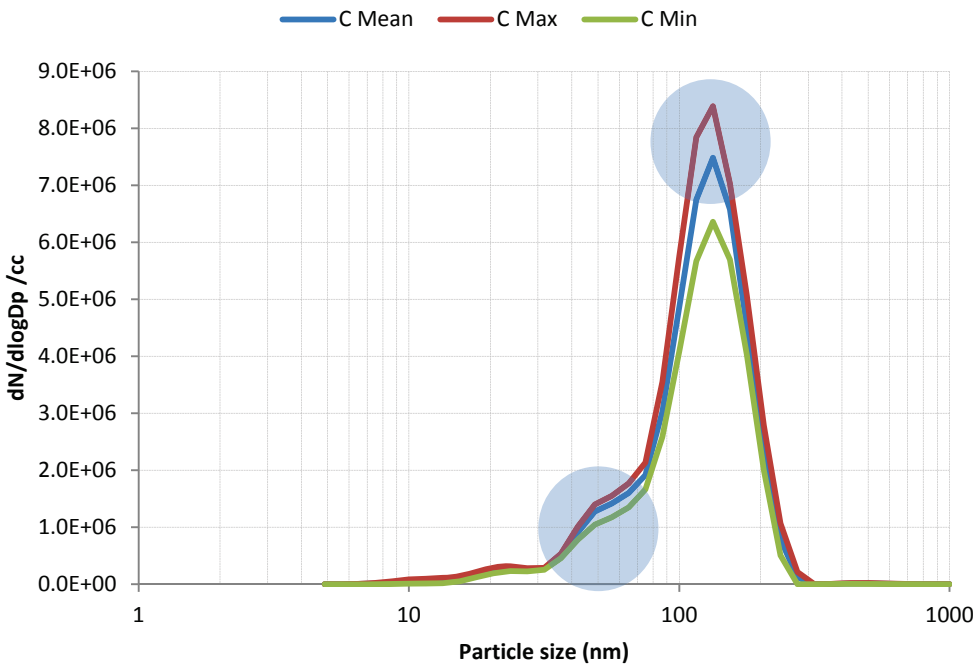

Figure 9.13: Size spectral density: Airbag C

The size spectral density data for airbag D, Figure 9.14, shows a different general distribution to airbags A, B and C. This airbag produced a bimodal particle size distribution with a primary mode at less than 100nm and a secondary mode of a far lower magnitude at around 20nm. The concentration of particles at this secondary mode was 4.10E+05 and approximately 4.5E+06 at the primary mode which is comparable to peak values recorded for effluents from airbags A and B. Inter-test variability appeared similar to that for airbags A and B and appeared considerably lower than for airbag C.

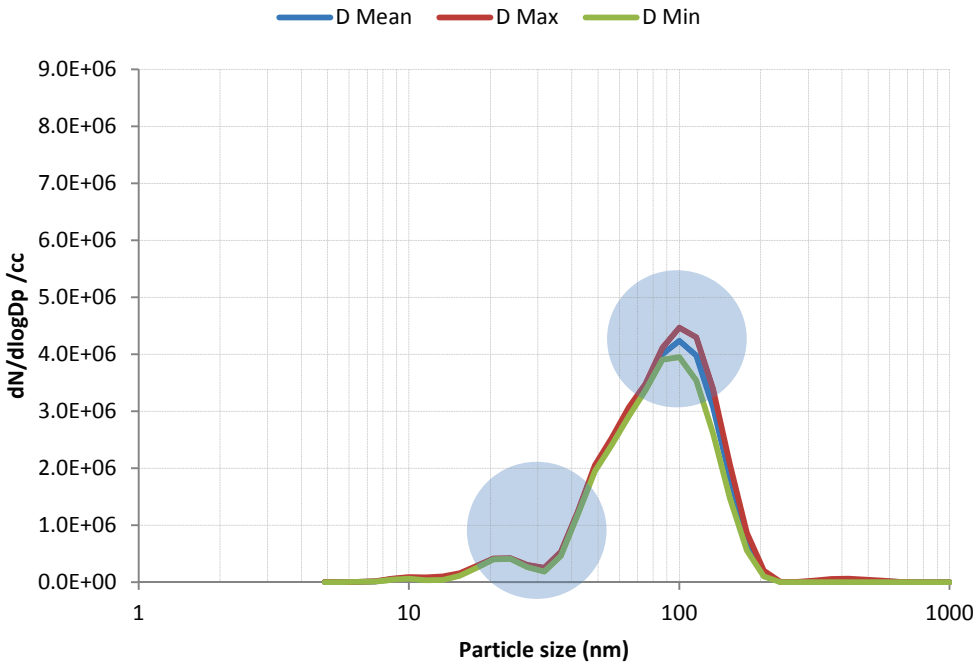

Figure 9.14: Size spectral density: Airbag D

It is clear from these initial analyses that there are differences in particle concentration and size between the tested airbags and these can be more easily identified in a comparative size spectral density plot as shown in Figure 9.15. This data shows a particular characteristic of each airbag, albeit with airbags A and B appearing similar. Number concentration is comparable for airbags A, B and D and is considerably higher for airbag C. Tested airbags A and B demonstrated a unimodal size distribution, whilst a bimodal size distribution was identified for airbags C and D. The primary, dominant mode was between ~95nm and 180nm depending on the airbag tested, with the lowest value being measured during testing of airbag D, the only airbag to utilise a hybrid inflator.

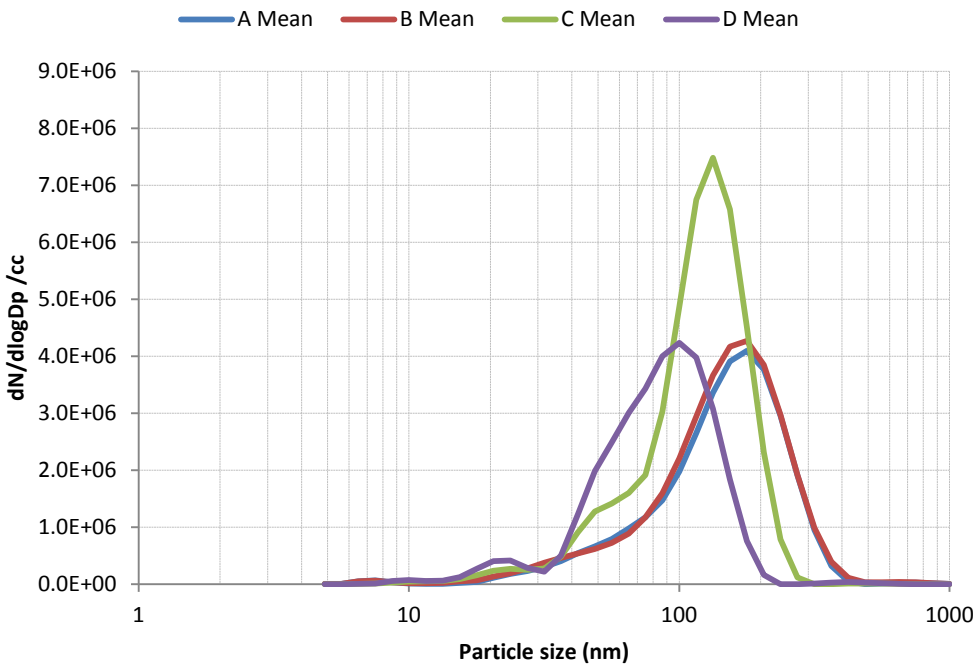

Figure 9.15: Size spectral density: Airbags A-D

9.6 Number concentration size proportions

Analysis of particle size in relation to test duration and size spectral density indicated that a substantial proportion of particles emitted during airbag deployment are below 300nm in diameter. An assessment of the size proportion of total particle number concentration was therefore conducted to define a more finite measurement range within which further analysis should be focused.

Figure 9.16 shows the size proportion of total particle number concentration for emissions from airbag A. This data showed that nearly all particles (>99.5%) emitted during airbag deployment are below 400nm in size and over 96% of particle emitted are below 300nm in size. Approximately 22% of all particles were emitted in the nano-scale and are therefore below 100nm.

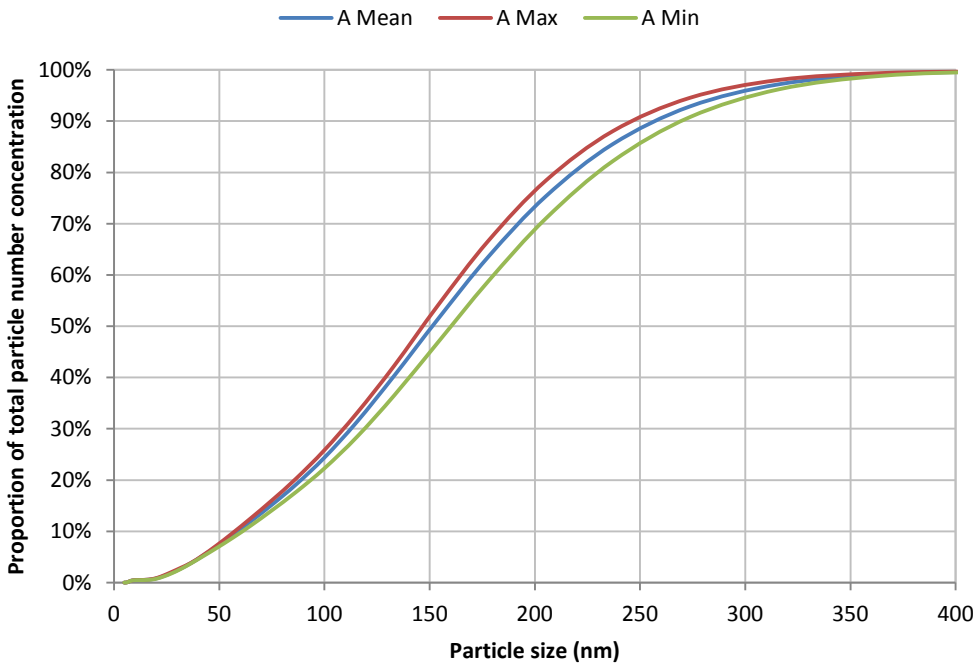

Figure 9.16: Size proportion of total number concentration, 5-400nm: Airbag A

Analysis of the data for airbag B, Figure 9.17, showed a closely comparable particle size proportion characteristic to that identified for airbag A. Again over 99% of particles emitted were smaller than 400nm, over 96% were smaller than 300nm and at least 22% of particles were less than 100nm in size.

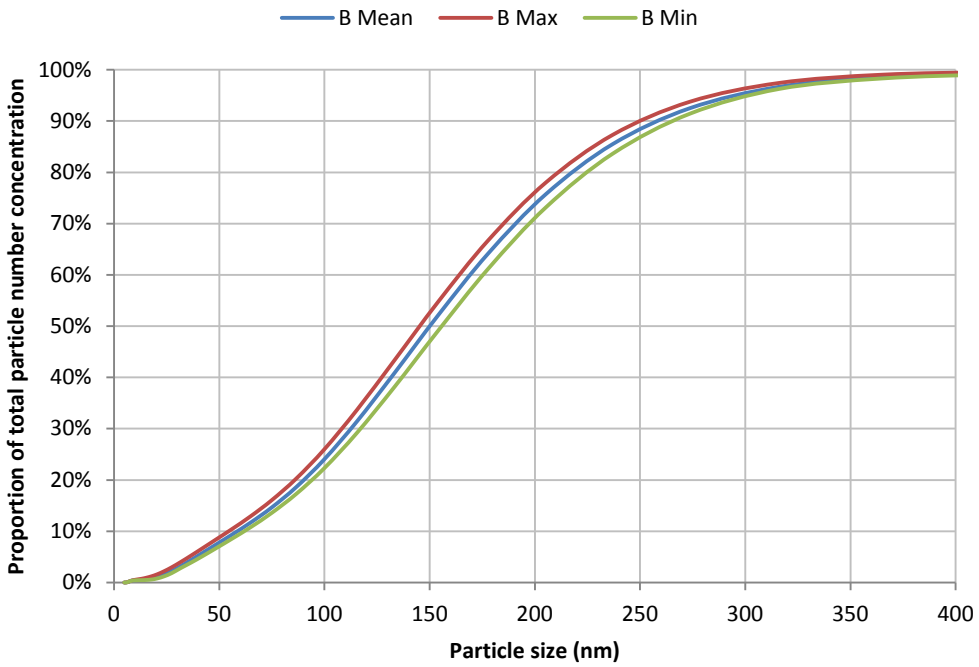

Figure 9.17: Size proportion of total number concentration, 5-400nm: Airbag B

The size proportion trend identified for airbag C, Figure 9.18, differed to airbags A and B with a higher proportion of smaller particles than previously identified. Over 99.8% of all emitted particles were below 300nm in size and over 94% of particles were below 200nm. An increased number of particles below 100nm (31%) were also emitted. This data supports the size spectral density and mean size data previously presented, which suggested that airbag C emitted a smaller mean particle size than airbag A or B.

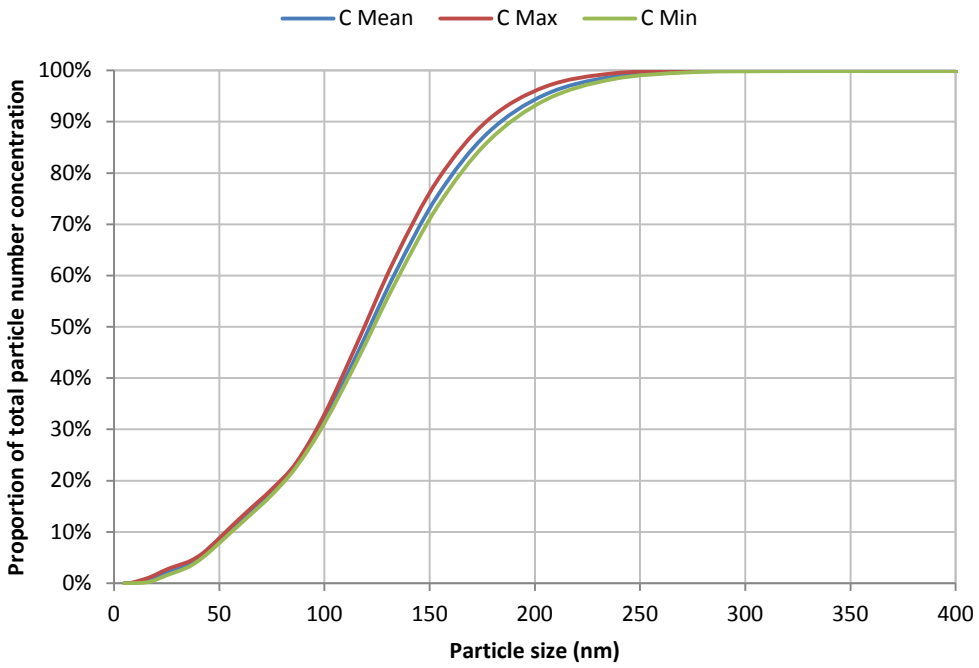

Figure 9.18: Size proportion of total number concentration, 5-300nm: Airbag C

Figure 9.19 shows the particle size proportion data for airbag D. This data appears to be more comparable to airbag C than A or B however a greater proportion of smaller particles were measured. In this instance over 93% of emitted particles were below 150nm in size and over 62% of emitted particles were below 100nm. The proportion of particles in this range was far greater for airbag D than for any other.

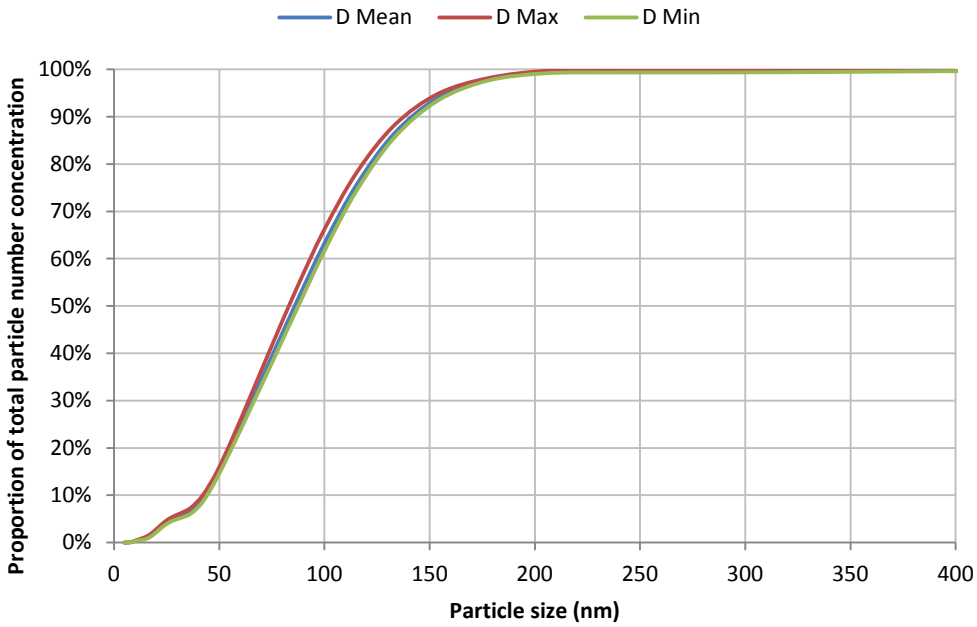

Figure 9.19: Size proportion of total number concentration, 5-400nm: Airbag D

Assessing this size proportion data comparatively for all tested airbags (Figure 9.20) shows three clear distributions for the four tested airbags.

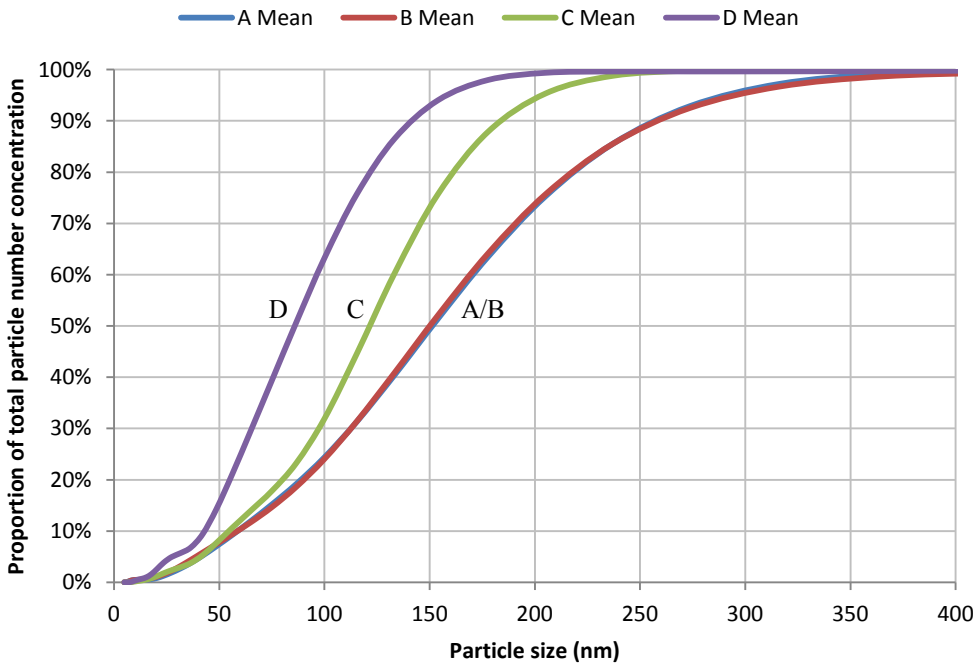

Figure 9.20: Size proportion of total number concentration: Airbags A, B, C and D

Whilst not assessed statistically, it appears that the size proportion data generated from assessments of airbags A and B cannot be differentiated from one another whilst the

emission from airbags C and D were markedly different. Although there are significant differences in the size proportions of emitted particles depending on the particular airbag tested it is important to note that nearly all particles (>99%) generated during airbag deployment were lower than 400nm in size. This analysis of test data from airbags A-D, also identified that high concentrations of particles in the nano-scale (<100nm) were produced during deployment.

9.7 Particle size spectral density in relation to time

To this point particle emissions from airbags have been defined most comprehensively either by measuring concentration in relation to time or particle size, but no analysis has considered particle concentration in relation to both size and time. There are two primary ways of presenting this data;

1. Size spectral density plots in relation to time
2. Number concentration in relation to time segregated by particle size

Figure 9.21 to Figure 9.24 define particle size spectral density in relation to time. Data is presented in relation to time and segregated into 120 second segments. Figure 9.21 which shows this analysis for the emission from airbag A.

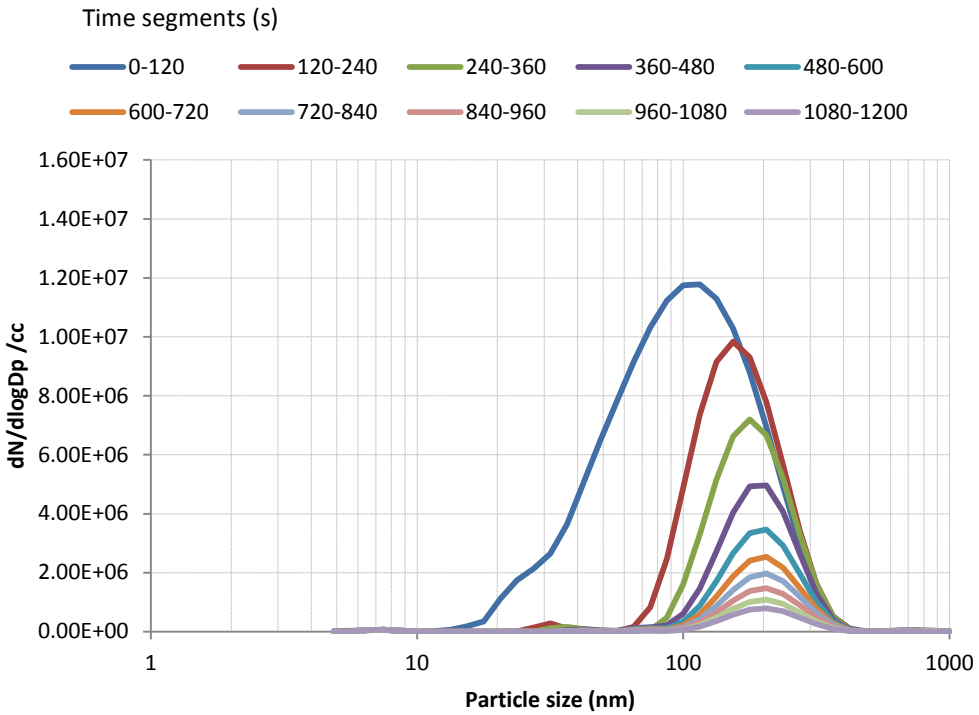

Figure 9.21: Size spectral density detailed in 120s segments: Airbag A

This data shows in a single plot that particle number concentration (N/cc) reduces over the test duration whilst size increases. This data verifies the findings presented in this Chapter for particle size and concentration. The data also showed that when assessing particle size distribution the range of particles emitted during the early stages of the test was wider than in the later stages, with the distribution curve becoming comparably tighter as the test time lengthened. This shows that the smaller particles measured in the early stages of testing become less numerous as time elapses.

A similar distribution to that presented by airbag A can be seen when assessing the emission from airbag B, Figure 9.22. The initial high particle number concentration of smaller particles (up to 100nm) reduced as test duration elapsed and therefore the distribution begins to tighten. Again concentration reduces throughout the test and particle size increases.

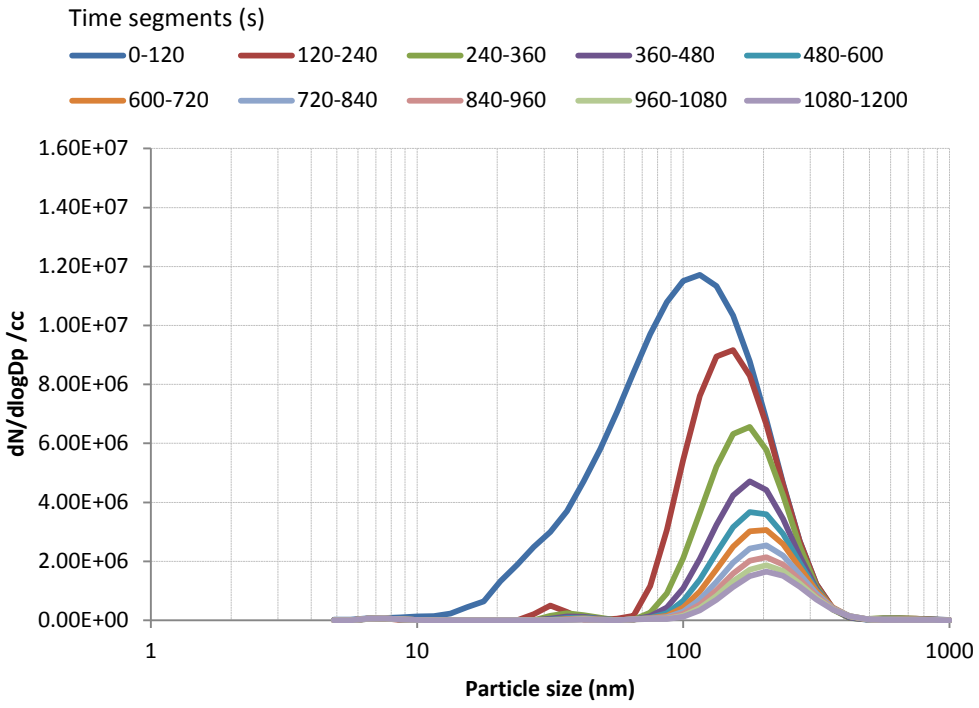

Figure 9.22: Size spectral density detailed in 120s segments: Airbag B

A different distribution trend was identified for the emission from airbag C as shown in Figure 9.23. Whilst an increase in particle size and reduction in concentration can be seen over the 1200 second test, after the first 120 seconds this increase in size and reduction in concentration appears to occur at a comparably lower rate. Over the first 120 seconds a marked bimodal size distribution can be seen, with a primary mode at approximately 65nm and a secondary lower magnitude mode at approximately 25nm. Over the next 120 seconds this primary mode increases in size to around 115nm and the secondary mode

reduces substantially. Over the remaining 960 seconds the changes in particle size and number concentration appear to be less apparent.

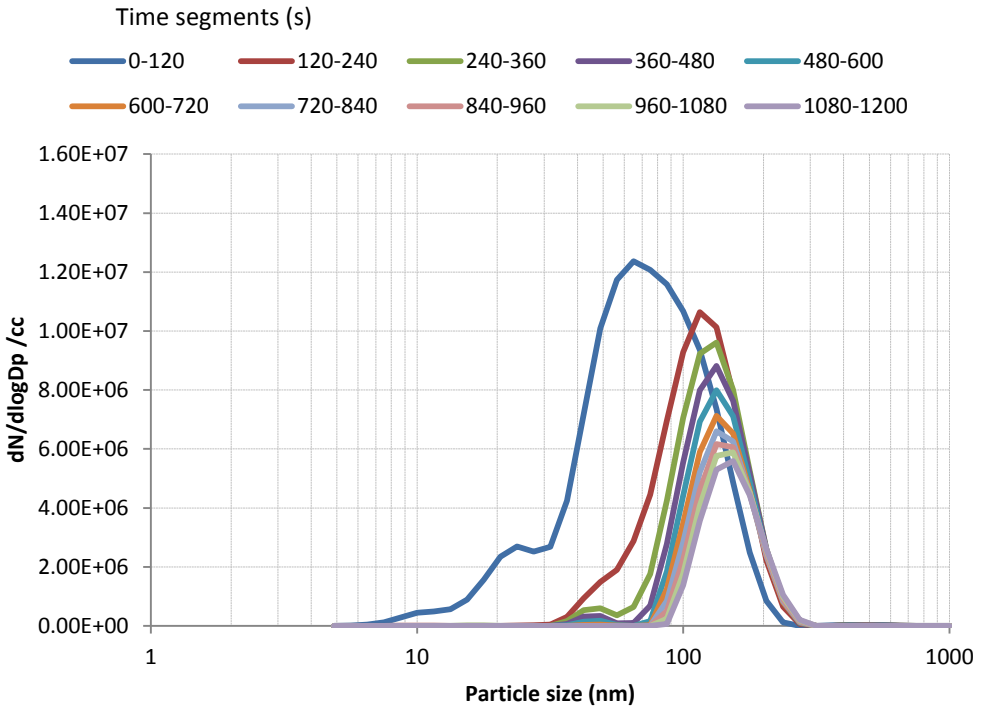

Figure 9.23: Size spectral density detailed in 120s segments: Airbag C

Some similarities can again be seen between the distribution data defined for airbag D, Figure 9.24 and that from airbag C, Figure 9.23. In the first 120 seconds particle concentration was substantially higher than throughout the rest of the test and a bimodal distribution was evident with a primary mode at 55nm and a secondary mode at 21nm. As the test time elapsed the secondary mode appeared to recede and the primary mode increased in size and reduced in concentration. The rate of change in respect to particle size and concentration also appeared substantially lower after the first 120 seconds.

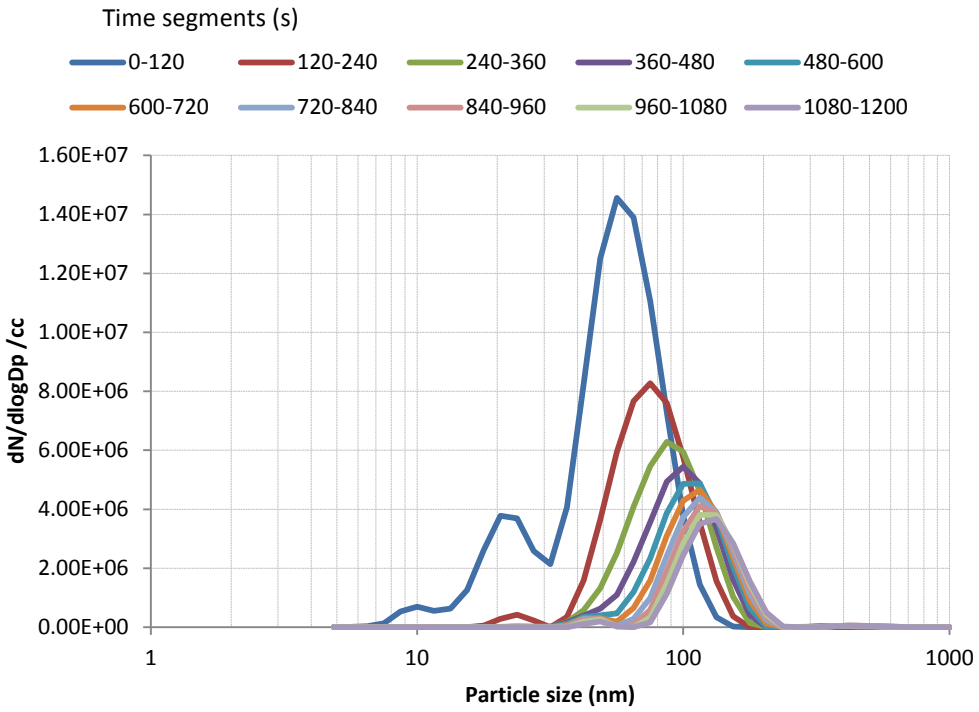

Figure 9.24: Size spectral density detailed in 120s segments: Airbag D

9.8 Size segregated number concentration with respect to time

The following analysis allowed size segregated particle number concentration with respect to time to be defined, with measurements taken each second throughout the test as opposed to being in 120 second segments as previously presented.

Figure 9.25 shows the data from tests of airbag A and represents mean values generated from the three repeated tests. This data showed that particle concentration in the smallest size ranges of 5-50nm and 50-100nm, whilst initially dominant, reduced at a faster rate than in other size ranges. In particular particle concentration in the range 5-50nm decayed at a high rate and within 100 seconds concentration was lower than for all other measured size ranges. Whilst a reduction in concentration could be seen almost immediately for particles in the range 5-150nm a reduction in concentration could only be seen for particles in the range 150nm-1000nm after around 360 seconds with values staying generally stable until this point.

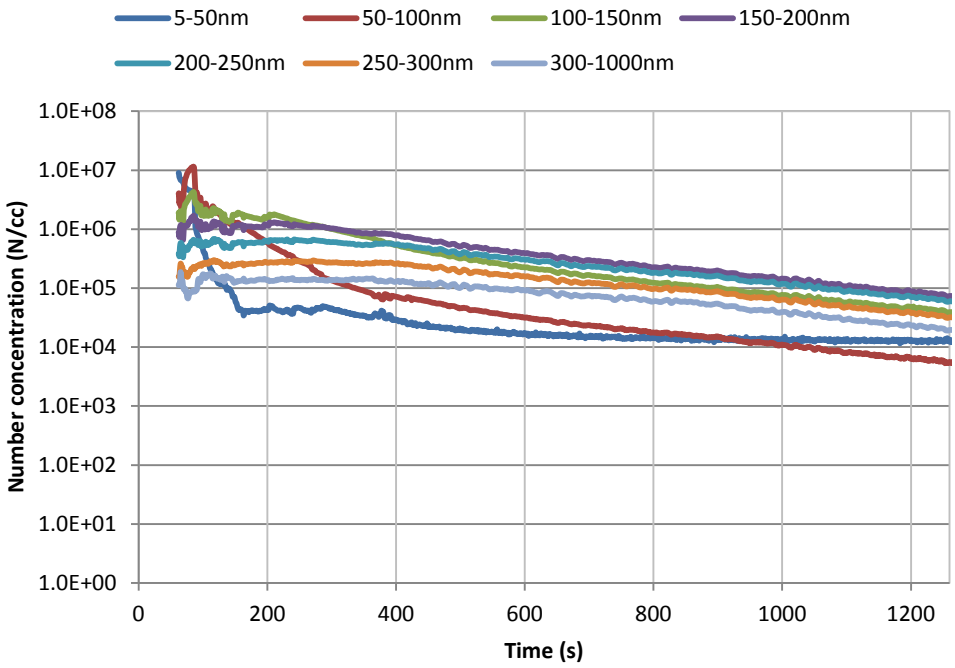

Figure 9.25: Number concentration (N/cc) with respect to time, shown in 50nm segments: Airbag A

Assessment of data defined from the emissions of airbag B, Figure 9.26, showed a very similar trend to that established for emission from airbag A. Particles in the range 5-150nm were again dominant with concentration reducing rapidly for smaller particle ranges during the test. A slight increase in concentration of particles in the ranges 150nm-1000nm could be seen after the initial deployment of the airbag with smaller particles in the range 150nm-300nm being of a greater magnitude than those in the range 300nm-1000nm.

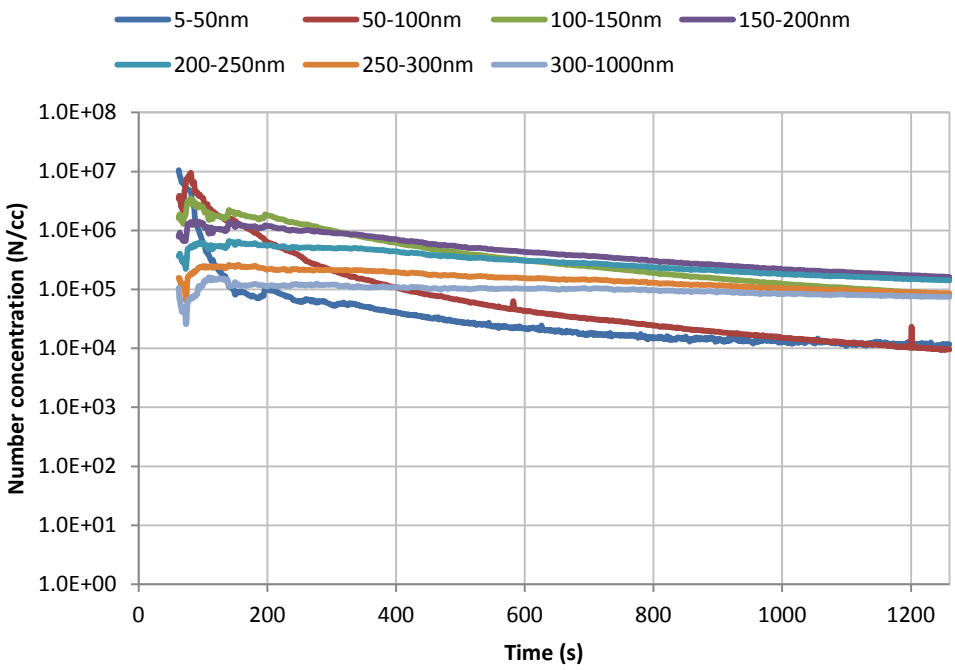

Figure 9.26: Number concentration (N/cc) with respect to time, shown in 50nm segments: Airbag B

The emission from airbag C, Figure 9.27, provides a rather different characteristic than for airbags A and B. Similarities are however identifiable with particles in the range 5-150nm initially dominant. The rate of reduction in concentration for particles in these size ranges is far lower than previously seen for airbags A and B and little reduction in concentration can be seen for particles in the range 100nm-150nm over the test duration. An increase in particle concentration in the size range 150nm – 300nm can be seen during the first 300 seconds of the test.

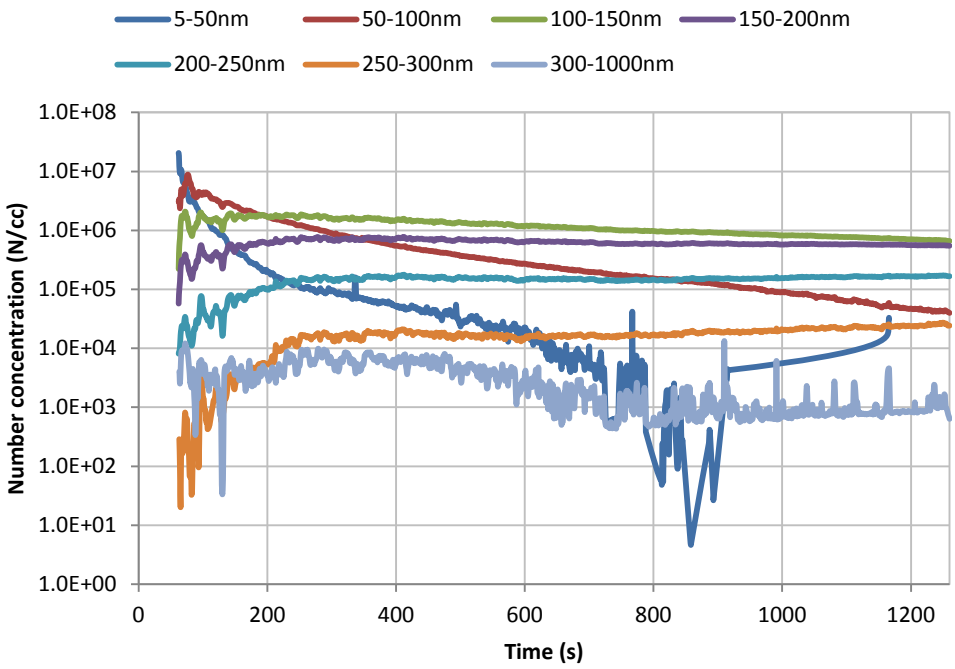

Figure 9.27: Number concentration (N/cc) with respect to time, shown in 50nm segments: Airbag C

The data generated from assessments of airbag D, Figure 9.28, bears some resemblance to that of airbag C. Particles in the range 5-100nm dominate the emission immediately after deployment and reduce in concentration at a lower rate than for any of the previously assessed airbags. Whilst there is a comparably lower emission of particles in the range 150-1000nm upon deployment of the airbag, there is a substantial increase in concentration in these larger ranges during the test. For particles in the range 100-200nm this increase occurs mainly in the first 600 seconds and continues to rise throughout the test. Particles in the range 200-250nm also appear to continue to increase substantially throughout the test. The concentration of particles >250nm appeared to increase over the first 360 seconds before generally stabilising.

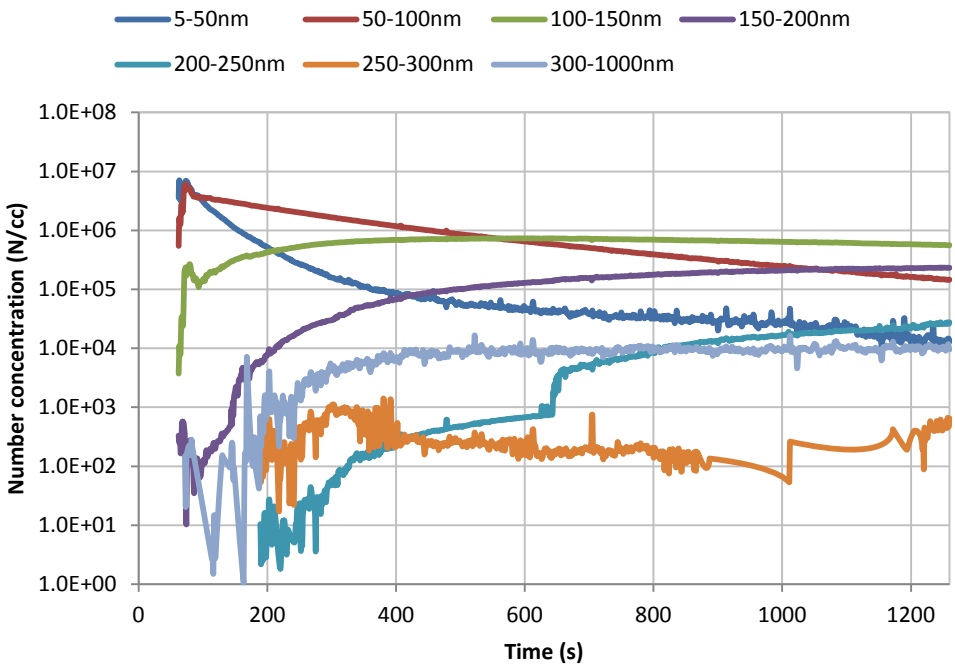

Figure 9.28: Number concentration (N/cc) with respect to time, shown in 50nm segments: Airbag D

9.9 Particle GMD with respect to time and in relation to environmental factors

This assessment was carried out to identify whether any correlation between humidity and temperature and particle size and concentration could be observed. Figure 9.29 therefore shows particle GMD in relation to time for each of the three tests of airbag 'A' and shows mean relative humidity and temperature measurements. After deployment the RH in the test tank increased substantially from 43% to 53% by the end of the test, whilst temperature appears stable throughout the test with little change identified. This increase in relative humidity occurs only after deployment and as particle GMD increases. The increase in humidity appears relatively linear over the first 800-900 seconds of the test and as GMD subsequently decreases relative humidity appears to stabilise.

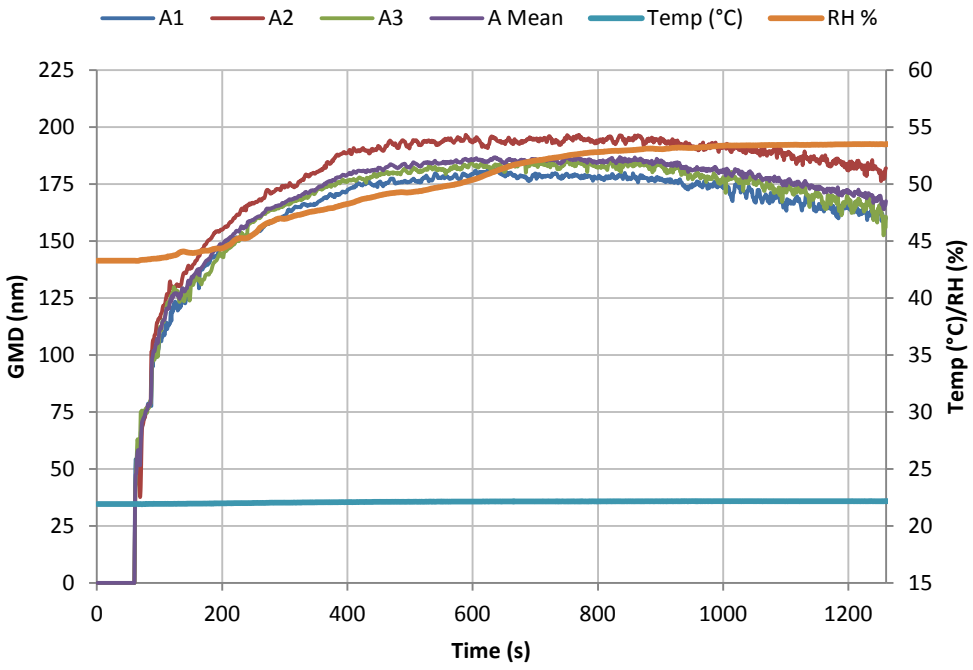

Figure 9.29: GMD with respect to time and in relation to environmental factors: Airbag A

The increase in relative humidity in the test tank after deployment and relatively stable temperature seen during tests of airbag A are comparable for tests of airbag B, as presented in Figure 9.30. Whilst temperature remains stable throughout the test, RH increases after deployment of the airbag from 43% to 56%. This increase in RH appears to be associated with an increase in GMD.

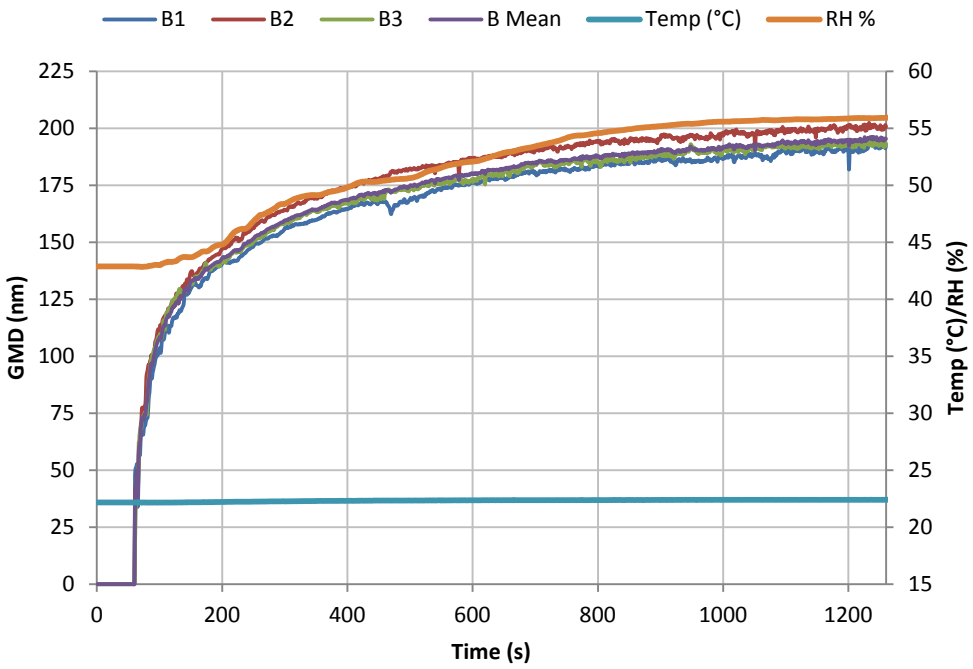

Figure 9.30: GMD with respect to time and in relation to environmental factors: Airbag B

The change in environmental conditions measured in the test tank and its association with an increase in GMD is again replicated during testing of airbag C, as shown in Figure 9.31. Temperature measured within the test tank remained stable throughout the test and RH increased from 41% to 54%; a change of a comparable magnitude to that seen during tests of airbag A and B.

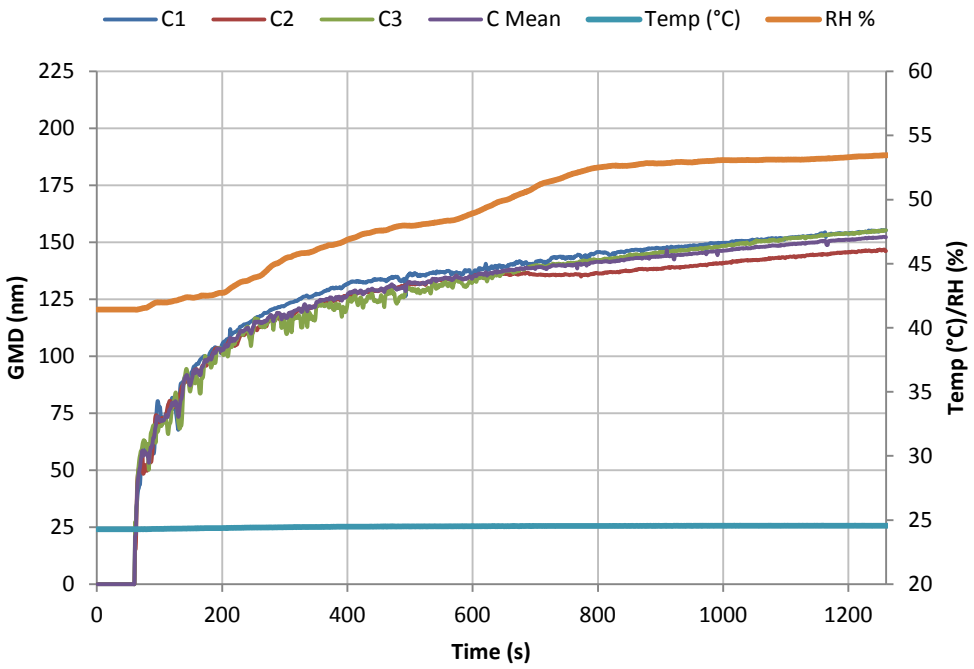

Figure 9.31: GMD with respect to time and in relation to environmental factors: Airbag C

The increase in GMD of particles emitted during deployments of airbags A, B and C appear to be associated with an increase in relative humidity measured within the test tank whilst temperature appears to stay relative stable throughout the test. This general trend does not appear to be replicated during tests of the emission from airbag D, as presented in Figure 9.32. Whilst again there is little change in measured temperature, there is only a comparatively small increase in relative humidity which occurs in the first 240 seconds after airbag deployment. Over the full test duration RH only increases by 4% from 46% to 50%.

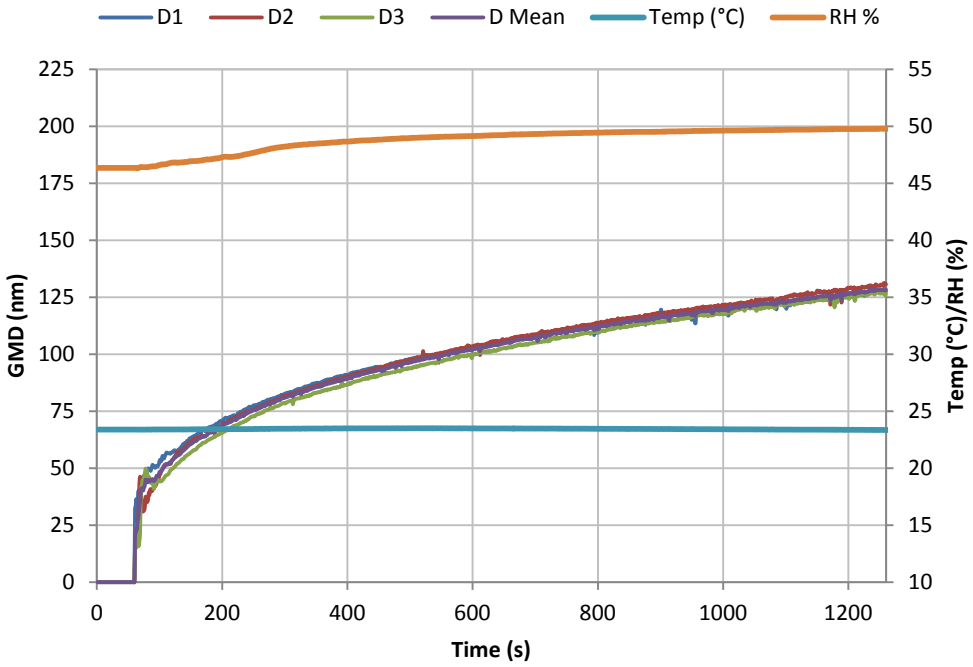

Figure 9.32: GMD with respect to time and in relation to environmental factors: Airbag D

This assessment of environmental conditions has suggested that temperature within the test environment did not notably change during and after airbag deployment. This lack of change can not only be attributed to the resultant, consistent test environment conditions but may have been attributed to the relatively poor resolution of the measurement equipment. If the change in temperature is highly transient then this would not have been detected by the equipment employed. For this reason, further analyses did not consider changes in temperature.

9.10 Size segregated particle number concentration with respect to time and in relation to environmental factors

The data presented previously assessed the change in GMD in relation to the temperature and relative humidity levels measured in the test environment and appeared to show some weak correlation between GMD and relative humidity levels in most cases. This analysis does not however take into account particle number concentration and any possible association with these environmental measurements. The following section therefore defines particle number concentration with respect to time and in relation to humidity levels in the test tank for a number of particle size ranges. As no clear change in test tank environmental temperature could be identified during testing, no further consideration has been given to this factor.

For Airbag A, Figure 9.33, this data showed that after the initial deployment and high output of particles into the test environment, particle number concentration generally reduced with only a small increase in particle concentration being seen for particles >150nm. After airbag deployment relative humidity increased from 43% to 54% in the test tank and therefore it appears that there is some correlation between the overall reduction in number concentration and increase in particle size and an increase in RH.

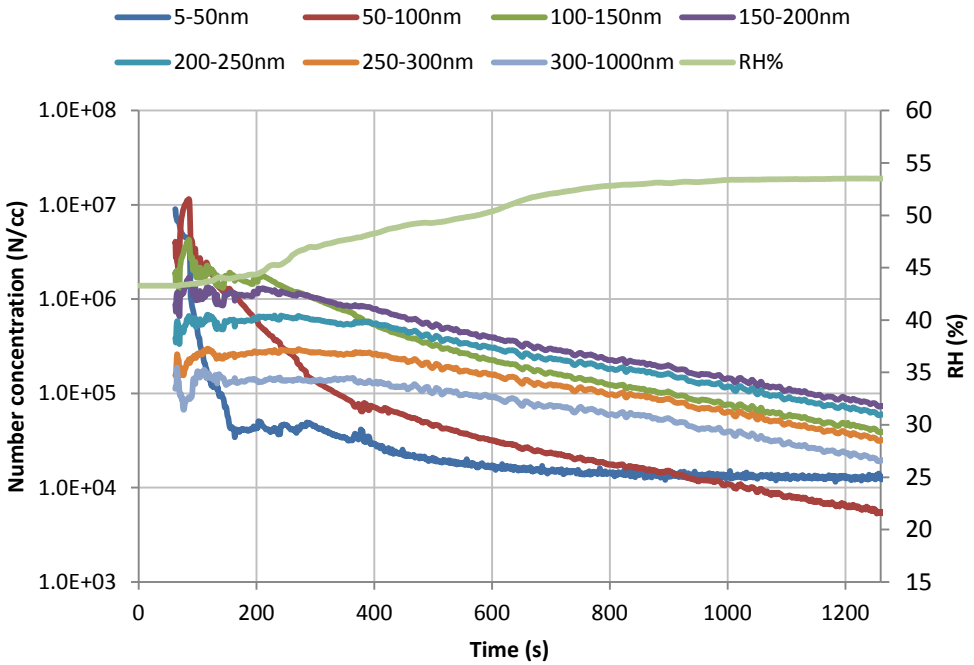

Figure 9.33: Size segregated concentration with respect to time and humidity - Airbag A

The general concentration behaviour established for airbag A appeared comparable to that of airbag B, Figure 9.34, with the concentration of particles in the lower size ranges (5-150nm) reducing rapidly whilst an initial small increase and stabilisation can be seen for larger particles in the range 150nm-1000nm diameter. Relative humidity again increased during the test from 43% to 56% and the same link between overall reduction in number concentration, increase in particle size and increase in RH was observed.

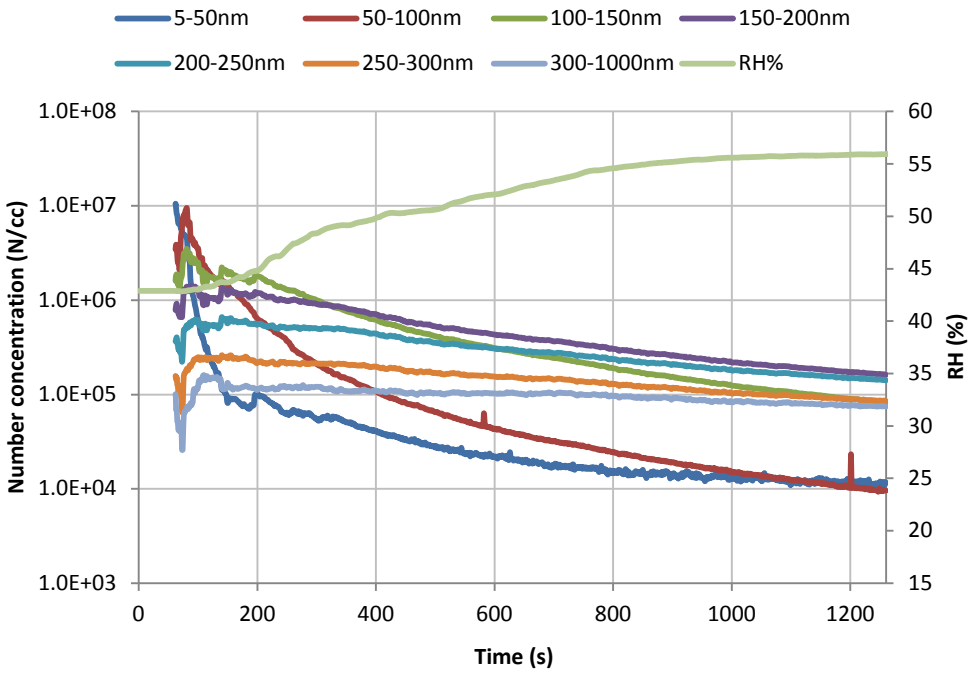

Figure 9.34: Size segregated concentration with respect to time, humidity and temperature - Airbag B

The emission from airbag C, Figure 9.35, differs to that from airbags A and B, Figure 9.35, but again after deployment and the initial output of high particle concentrations; there is a reduction in concentration of the smallest particles and an increase in the number of particles greater than 150nm in diameter. Relative humidity was again seen to increase from 41% to 54% during the test and may be associated with this reduction in particles in the lower size ranges (5-150nm) and increase in larger particles greater than 150nm in diameter. Although a greater increase in particle concentration in these lower size ranges can be seen, the magnitude of increase in RH remains similar to that during testing of airbags A and B.

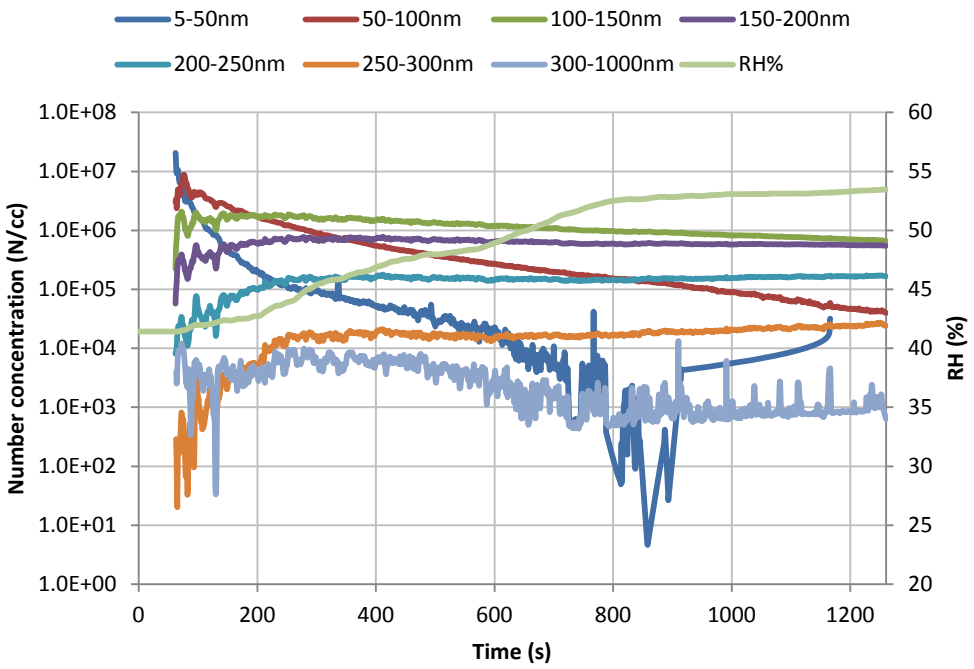

Figure 9.35: Size segregated concentration with respect to time and humidity - Airbag C

The association between relative humidity and particle number concentration in particular size ranges is less clear when assessing the emission from airbag D. The data presented in Figure 9.36 showed that after the initial dominance of particles in the range 5-100nm, concentration reduced at a slower rate than previously seen for airbags A, B and C whilst substantial increases in particle concentration in the size range 100nm-1000nm were seen. Whilst this general trend is comparable in some respects between the airbag types, albeit with differing magnitudes, only a small increase in RH from 46% to 50% was identified for airbag D.

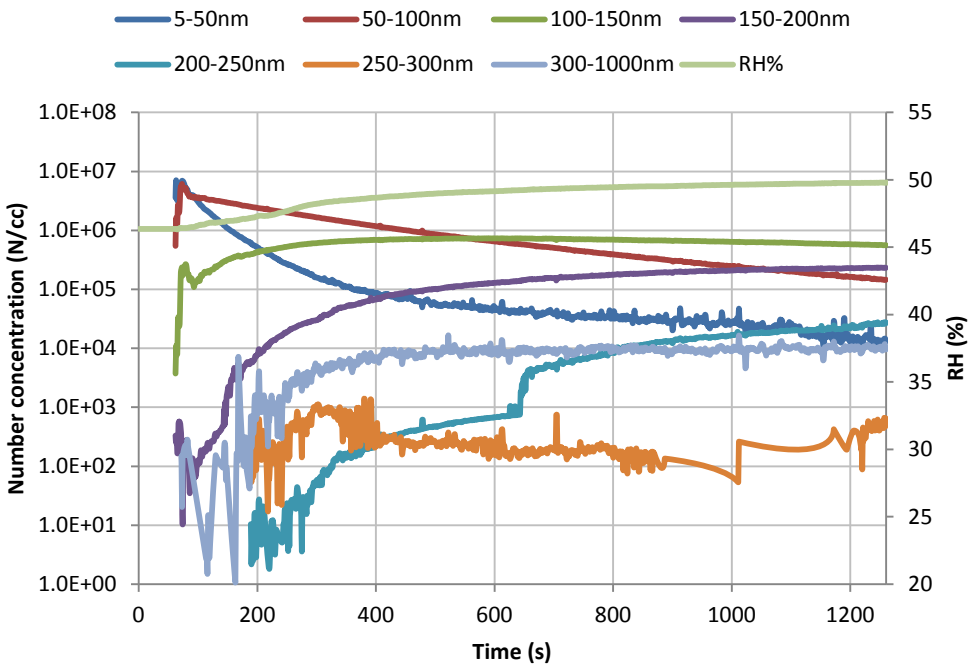

Figure 9.36: Size segregated concentration with respect to time and humidity - Airbag D

9.11 Summary

The use of a DMS allowed for considerably more insight to be gained regarding airbag effluents than has previously been presented in the literature. The DMS classifies particles based on their electrical mobility, assuming that they are of a defined shape and density. The DMS' capability to measure particle size and number concentration over three times per second with a measurement range of 5-1000nm allowed the sub-micron, and in particular nano-scale, particle size range to be investigated which formed the focus of this airbag effluents assessment. This assessment has demonstrated a new approach in the field and the analysis indicated the following:

Particle size data:

- Particle GMD calculated over the 1200s test duration ranged from 79nm to 135nm, depending on the airbag tested, with those using a solid propellant inflator, producing effluents with a mean size substantially higher than those produced by airbags using a hybrid inflator.
- Particle GMDs were lower than those previously presented in the literature (Chan et al., 1989; Gross et al., 1994; 1995; Ziegahn and Nickl 2002) with >99% of particles emitted by tested airbags being smaller than 400nm diameter.

- Time resolved GMD data produced during this study showed that for all airbag types particle size increased considerably in the early stages after initial deployment (commonly after 60-360s) and then generally continued to increase throughout the test, albeit at a reduced rate. The smallest increases in GMD were identified for the airbag using a hybrid inflator, airbag D.
- A unimodal size distribution was apparent for solid propellant airbags A and B with the dominant mode arising between 150nm and 180nm diameter. Solid propellant airbag C and hybrid airbag D demonstrated a bimodal distribution. For airbag C the primary mode occurred at around 135nm diameter and the secondary mode at 40-50nm. For airbag D the primary mode occurred at less than 100nm diameter and the secondary mode at 20nm-25nm.
- The increase in size of particles emitted during deployments of airbags A, B and C appeared to be associated with an increase in relative humidity measured within the test tank, whilst temperature appeared to stay relatively stable throughout the test. This general trend was not replicated during tests of the emission from the hybrid airbag.

Particle concentration data:

- Mean particle number concentrations of between 2.05E+06 and 2.85E+06 were recorded. However, little data from comparable PM sources was evident in the literature in terms of number concentration and therefore simple associations are not easily drawn.
- Airbags utilising a solid propellant inflator produced higher PM concentrations than airbags using hybrid inflators.
- The length of time after deployment at which maximum particle concentration occurred varied from 2-21 seconds, with no clear difference found between the airbags using hybrid and solid propellant inflators.
- After the maximum concentration was attained, the concentration reduced over the remaining test duration at different rates depending on the airbag being tested. This reduction in concentration may well be associated with particle agglomeration.

Combined particle size and concentration:

- Concentrations of smaller particles, in the nano-scale (<100nm) were initially greater than those in the higher size range of greater than 100nm. Over time the concentration of these smaller particles reduced whilst conversely the larger particles increased in concentration.
- This suggests that smaller particles agglomerated, which resulted in an increase in concentration of larger particles over time and a reduction in smaller particles.

Chapter 10

Modelling airbag particle effluent size proportions

10.1 Introduction

The ability to mathematically model the characteristics and behaviours of the particle effluents produced during airbag deployment, allows greater application of the presented data and other linked analyses, such as exposure quantification and identification of airbag types from their characteristics.

Mathematical models, defined in literature, have been used to good effect during assessments of solid particle characteristics and behaviours. Other complex models have been used to model particle deposition and retention in the human lung for medical applications (ICRP, 1994), to increase the efficiency of airborne drug delivery. More simplistic models have also been developed for measurement of characteristics such as particle settling (Baron, n.d.; Adetunji et al., 2009). However, models defining airbag effluent characteristics, including those in the sub-micron and nano-scale size ranges, appear not to have been presented in the literature. Therefore the data from electrical mobility measurements made with the DMS, (Chapter 9) was assessed to define a mathematical model that could be used to increase knowledge in the field of airbag effluent assessment.

10.2 Modelling airbag PM effluents

It was determined that a mathematical model could be utilised to identify the proportion of the total particle number concentration emitted during airbag deployment within a

defined particle size range, by assessment of particle size distribution and number concentration data, as detailed in Chapter 9.

The data used for modelling originated from a minimum of three directly comparable tests of each airbag. Little variance was identified between each test with regards to size proportion of total number concentration and consequently a mathematical model was developed using mean data. The size proportion of total number concentration curves are shown in Figure 10.1 for each tested airbag. Three distinct curves are evident, with airbag A not able to be differentiated from airbag B.

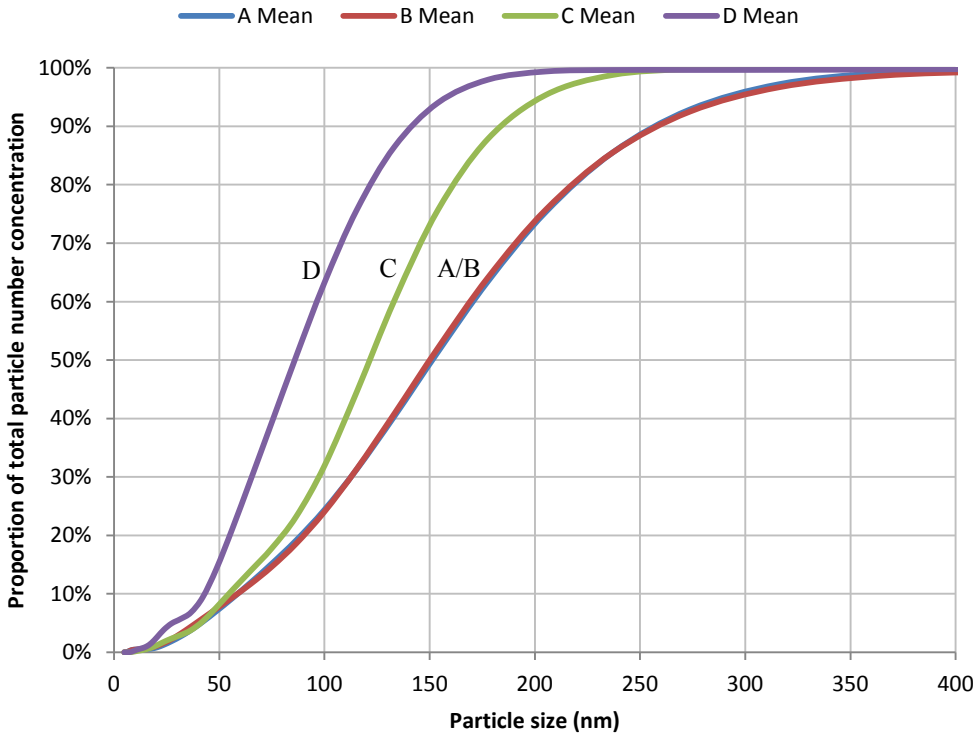

Figure 10.1: Size proportion of total number concentration: Airbags A, B, C and D

The relationship between particle size and number concentration shown in Figure 10.1 has shown an exponential curve which is described by the exponential function in Equation 6. This was derived for each of the three curves (1) A/B, (2) C and (3) D. Each of these curves appeared to have some comparability in shape and trend although with gradients that differed substantially from one another. The curves appeared exponential in nature and the following function was identified as suitable for a mathematical model albeit with varying constants depending on the airbag type to be modelled.

$$P = 1 - EXP\left(\frac{(F \times S_1 - X)}{(F - S_2{}^G)}\right) \qquad \textbf{(Equation 6)}$$

P = Size proportion	F = Constant	G = Constant
S_1 = Measurement range minimum	S_2 = Measurement range maximum	X = Subject measurement range

Table 10.1 shows the values of constants 'F' and 'G' defined using Equation 6, for the four airbag types and Figures 10.2-10.4 indicate the resultant curves and comparison with experimental data.

Airbag	Constant 'F'	Constant 'G'
A/B	3.6	2.1
C	9.6	2.7
D	12.0	2.3

Table 10.1: Exponential mathematical model constants

The theoretical data derived for airbags A/B, Figure 10.2, is closely comparable to the measured data with little variance throughout the range, although there is some variability evident in the size range of 25-175nm.

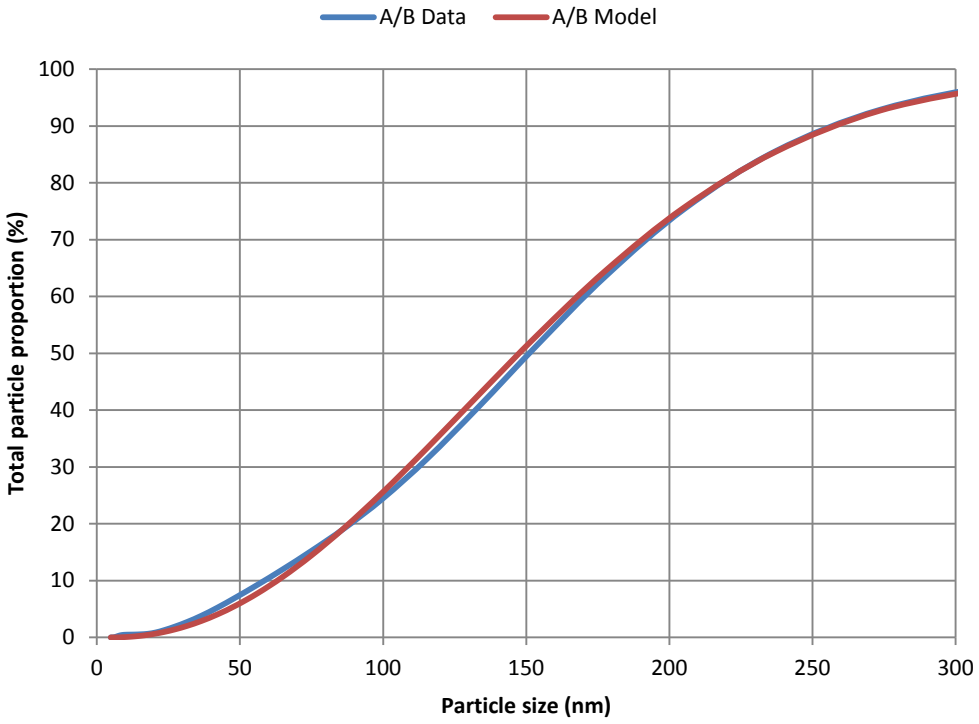

Figure 10.2: Size proportion of total number concentration mathematical model and measured data: Airbags A and B

This close comparability to measured data seen for the model of airbags A and B is also observed for the model of effluents for airbag C, although there is a slight variance in the range 20-75nm, Figure 10.3.

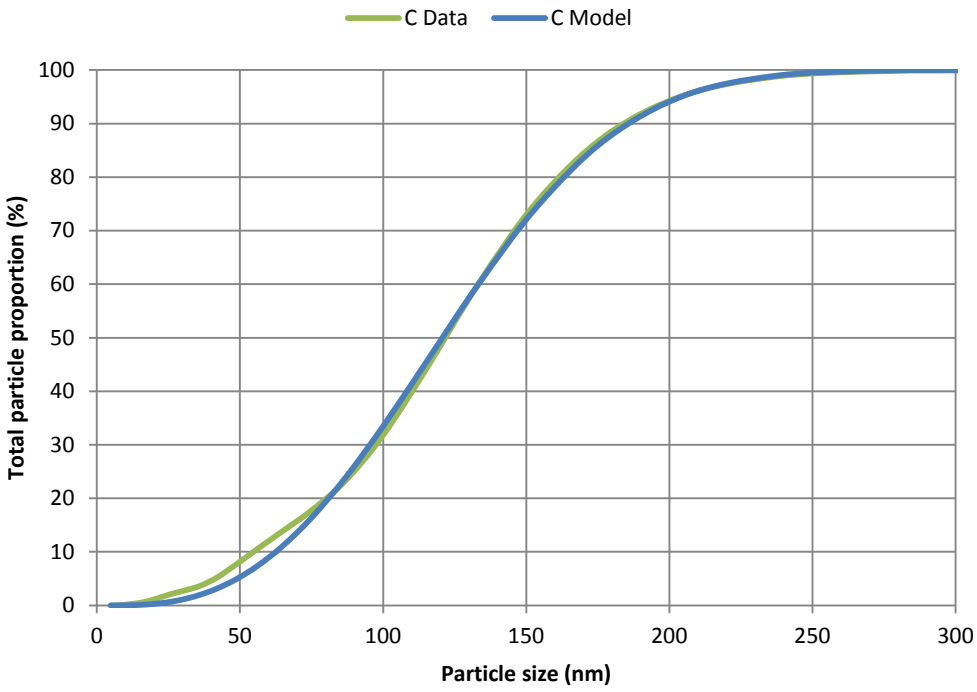

Figure 10.3: Size proportion of total number concentration mathematical model and measured data: Airbag C

Figure 10.4 derived for airbag 'D' is again closely comparable to the measured data, as for airbags A/B and C, with only slight variance able to be seen in the lower range of 20-45nm.

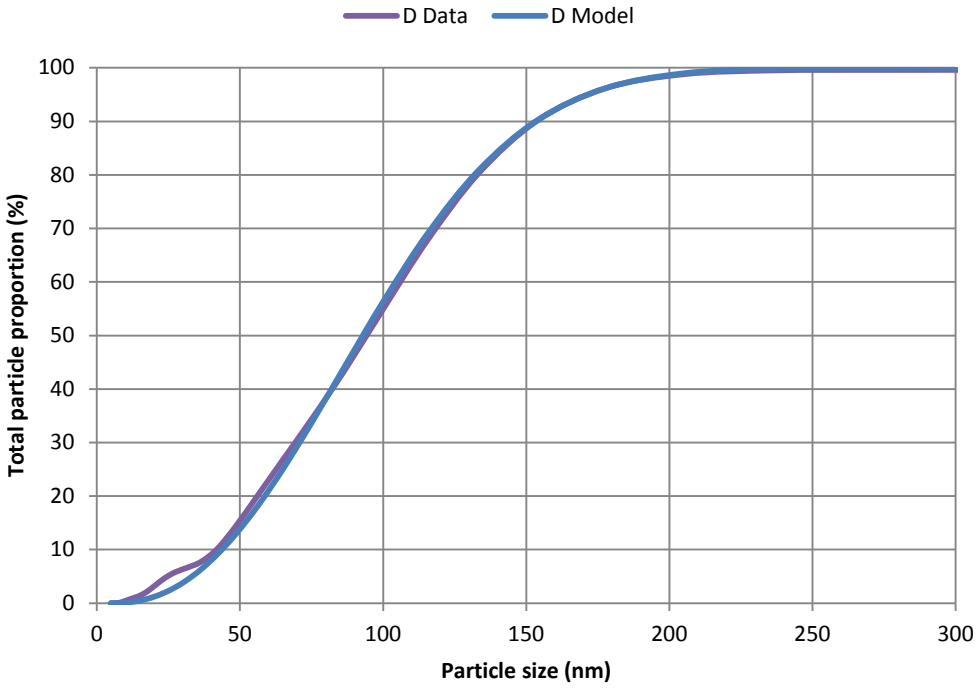

Figure 10.4: Size proportion of total number concentration mathematical model and measured data: Airbag D

Figures 10.2 – 10.4 indicate that the mathematical model is capable of modelling the characteristics of airbag effluents, and with little variation between the model and the measured data, variance was not assessed statistically. A mathematical evaluation that defined the 'co-efficient of determination' provided a measure of how well 'observed outcomes' were replicated by the model (Steel and Torrie, 1960) and this was represented as an R^2 value. This analysis showed that the mathematical models applied to the size proportion data, for each of the tested airbags, were closely comparable to the actual data with R^2, values in excess of 0.97.

The three mathematical models defined for the four airbag types provided a distinct 'signature', based on the size proportion of total number concentration data that can be used to identify airbags or propellants of these types during further analyses. This data again indicated that the effluents from airbags A and B are similar to one another and whilst the airbags are in fact different, it is possible that the propellants used are comparable.

This mathematical model data may be used to define airbag propellant types when such data is not available from manufacturers, by matching the models or proportional curves defined in testing to already characterised signatures from airbags and propellants.

10.3 Summary

A mathematical model has been defined, which when applied to the airbag number and size concentration data calculated the proportion of particles emitted within a particular size range. The model was based on an exponential function with varying constants and defined the effluents from the four tested airbags. The model was applied with varying constant values to describe three size proportion curves. No discernible difference could be determined between the effluents from both airbags A and B.

Mathematical assessment of how well the models represented actual observed data was conducted and an R^2 value of greater than 97% was calculated for each of the models. An R^2 value of this magnitude indicates that 97% of values are represented by the model and only 3% of the total variation in the size proportion value remains unexplained.

The mathematical model presented in this research for airbag PM effluent modelling provides a number of functions which include:

- A distinct 'signature', defined for each of the tested airbags that can be used to identify airbags of a particular type during further analyses.
- Model data that may be applied to total number concentration values to define the likely concentration of particles of a particular size.
- An identification of the likely exposure to particles of particular sizes for vehicle occupants after a collision and for dismantling operatives who are involved in the process of end-of-life-vehicle (ELV) neutralisation.

This model therefore provides an easy assessment tool to identify the proportion of total particle number emitted in a particular size range for differing airbag types. This represents a novel approach for assessment of PM effluents created during airbag deployment.

Chapter 11

Test Environment Ventilation

11.1 Introduction

At an ATF, dismantlers must by law neutralise all the airbags and other pyrotechnic devices in a vehicle before the vehicle is recycled. End-of-life vehicle depollution operatives commonly undertake airbag deployments remotely whilst situated outside of a vehicle, before re-entering the vehicle to retrieve deployment equipment. In some cases operatives may use extraction (SAE, 2011b; Re-Source Engineering Solutions, n.d.) prior to re-entering the vehicle, but most commonly operatives allow the effluent to ventilate from the vehicle naturally for a varying duration or simply re-enter immediately after deployment to reduce depollution processing times. To assist in understanding these exposures, an investigation was carried out to define the effect of ventilation of a vehicle on particle concentration after deployment.

11.2 Venting behaviour methodology and variables

To measure the influence of ventilation after airbag deployment on particle number concentration, the DMS was again utilised. The test vehicle was used for the ventilation tests as the environmental test tank was only equipped with a single access point that did not represent the apertures of a vehicle and was therefore unlikely to be representative in this type of study. Aside from the test environment type and measurement equipment used, there were many possible variables that could affect measurements of particle number concentration after airbag deployment and during ventilation of a test environment. These included the type, number and position of airbags deployed, sampling position, duration between deployment and initial ventilation, length of ventilation, whether extraction was used, and the number of doors/windows opened either prior to or after deployment.

With consideration to the scope of this research programme, and within the constraints of the test programme, many of the above variables were investigated and therefore an initial selection of variables was made with justification as follows;

- Four driver airbag types were tested and mounted in the driver front airbag position
    - The four test airbags utilised were those defined in Chapter 6. The mounting position represented the 'in-service' position for a driver airbag and therefore replicated exposure scenarios.
- A single central sampling position was employed
    - Although in confined environments (without ventilation), the influence of sampling position had little effect on concentration values, it was expected that during ventilation a variance in particle concentration was more likely. As there were many possible variants of sample position, a single sampling position was used to reduce the test matrix size.
- A duration of 60 seconds between deployment and test vehicle ventilation was employed
    - Observations conducted at ELV depollution facilities in the UK, conducted by the author, identified a minimum deployment to ventilation period of 60 seconds, thus representing a worst case scenario.
- A maximum ventilation duration of 600 seconds was utilised
    - This was based on the maximum observed duration employed by operatives undertaking airbag neutralisation during ELV depollution.
- Extraction not utilised
    - During visits by the author to ELV depollution facilities in the UK, extraction systems were not used and therefore were not assessed during the research programme.
- Test vehicle was sealed during deployment and ventilated by completely opening the passenger front door
    - The opening of a single door for ventilation was again observed during visits to ELV depollution facilities in the UK. This was likely to represent a worst case scenario when compared to opening more doors and windows of the vehicle.

With the core methodology defined, a series of three tests of each airbag type were conducted and the data analysed and the results are reported in the following section.

11.3 Venting behaviour definition

Particle concentrations gained during ventilation showed significant variability. To account for this large degree of variability, the data is presented as a moving average. The core data and the moving average are shown for mean datasets of the four tested airbag types, in Figures 11.1-11.4. These mean values were calculated from a series of three tests of each airbag and define particle concentration in relation to time as a proportion of the total particle concentration measured within the test environment immediately prior to ventilation.

Figure 11.1 shows the raw data from tests of airbag A and also data presented as a moving average. A marked reduction in the proportion of pre-venting particle number concentration and therefore actual particle number concentration was observed over the first 300 seconds after venting. During this time particle concentration reduced to only 20% of the pre-ventilation value. After this initial 300 second period, the concentration continued to reduce, albeit at a reduced rate, with concentration values as low as 5-6% of pre-ventilation values. During the 600s ventilation period, particle concentration varied significantly, with the greatest variability occurring in the first 300 seconds.

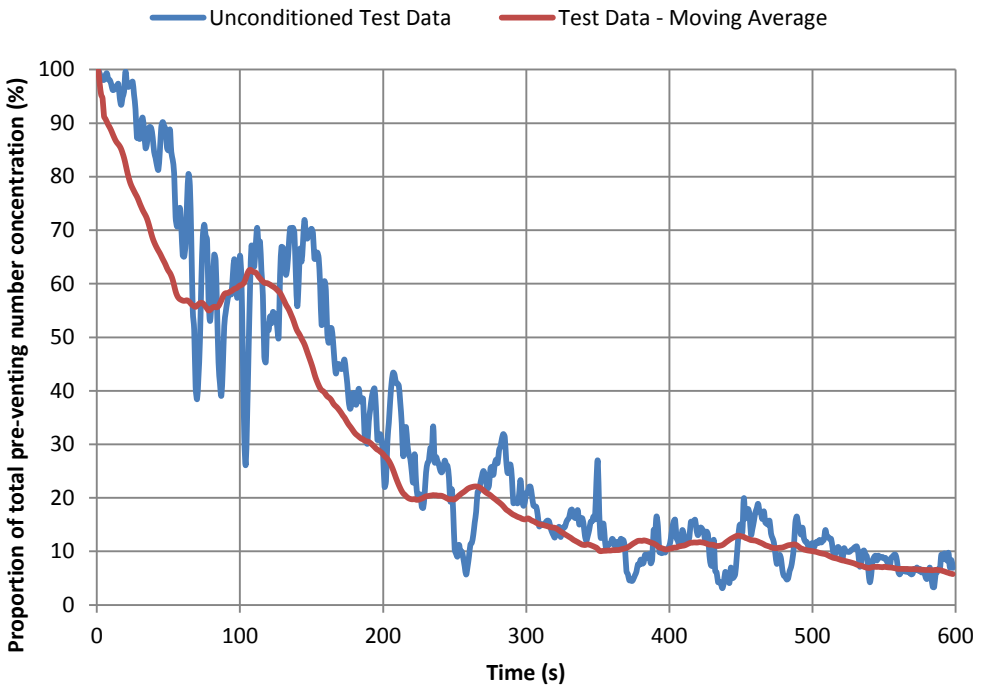

Figure 11.1: Test airbag A mean venting behaviour

A relative increase in the proportion of particle concentration remaining in the vehicle interior was observed after around 75 seconds and continued for a further 75 seconds. Although concentration was unlikely to be truly increasing, an increase in concentration

at the measurement location was identified. Assessment of particle concentration data (Chapter 9) showed that after the initial output of PM during deployment, particle concentration did not increase. This therefore suggested that the PM ventilated from the test vehicle in an inconsistent manner. This may have been associated with the movement of air within the laboratory.

In general the dataset shows a comparable trend to aerosol particle settling models and analyses presented in the literature (Adetunji et al., 2009).

The proportion of total particle number concentration present after ventilation of the test environment is shown in Figure 11.2 for airbag B. A similar trend can be seen to that of airbag A with significant variation in number concentration occurring in the early stage of ventilation, with variability reducing considerably after the first 300 seconds. The proportion continued to vary with relation to time with a general downward trend being observed over the full 600 seconds of ventilation and after the first 300 seconds variability dropped to around 10% of the pre-venting number concentration. After 600 seconds only 15% of the total particle concentration remained in the test vehicle.

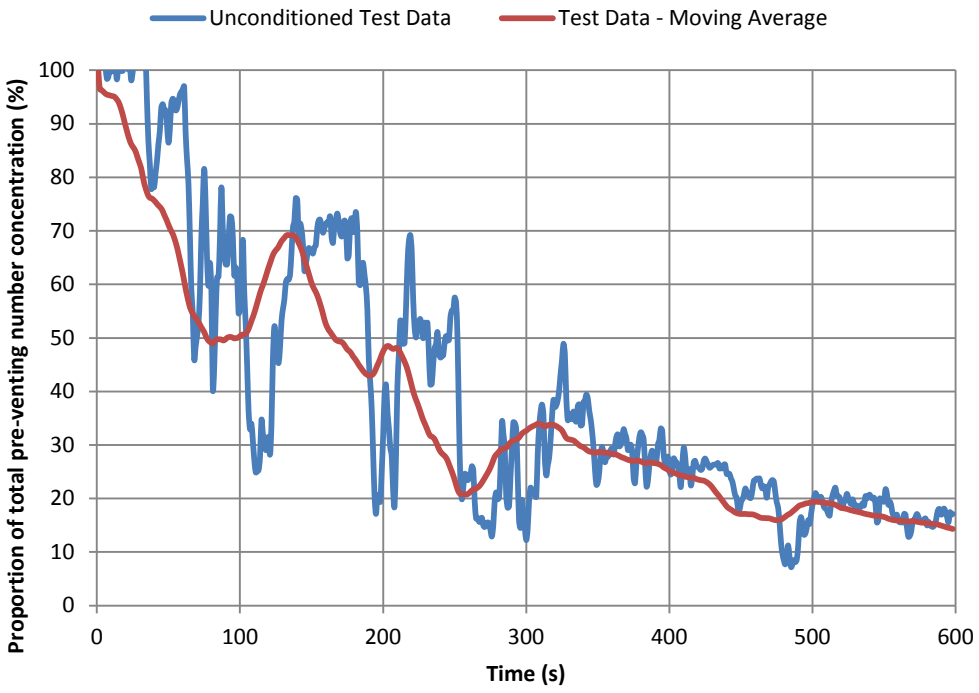

Figure 11.2: Test airbag B mean venting behaviour

The data for airbag C after ventilation of the test environment, (shown in Figure 11.3) appears to differ to that of Airbags A and B. The reduction in remaining particle proportion in relation to time appears more marked during the first 200 seconds. After this time the concentration reduced to around 5% with considerable variability over time. This variability was greater than that seen during tests of airbags A and B, yet no specific changes in gas dynamics within the laboratory were identified as being responsible.

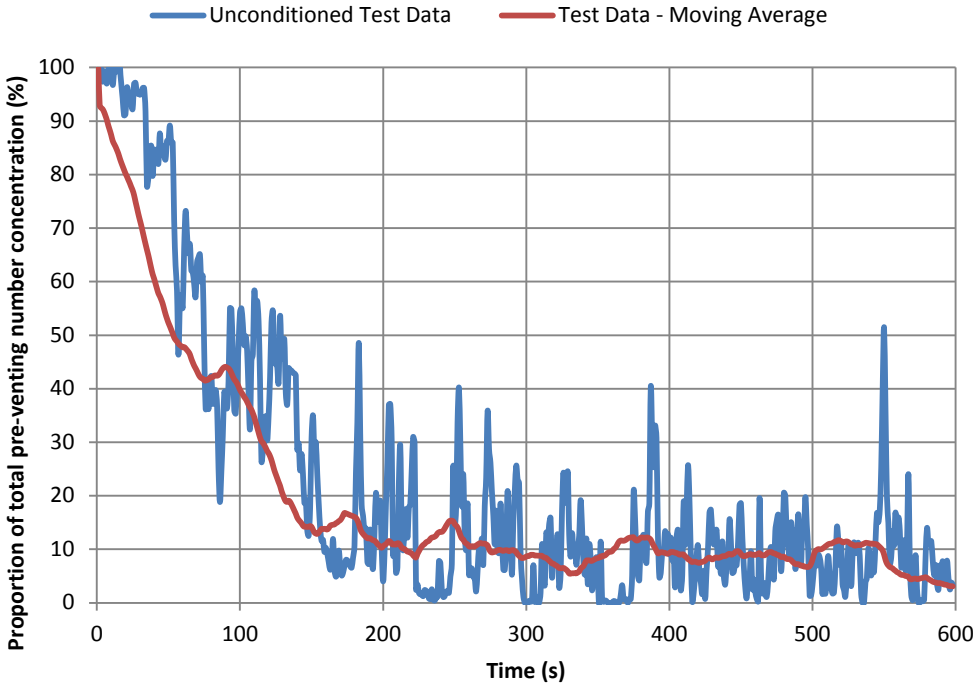

Figure 11.3: Test airbag C mean venting behaviour

Figure 11.4 shows the particle number concentration proportions for Airbag D. The reduction in concentration measured over time was similar to that of Airbags A and B with concentration reducing to between 10% and 20% in the first 250 seconds, again with considerable variability. The initial variability observed in the first 250 seconds is comparable to that seen during tests of airbags A and B. After this initial reduction, the concentration appeared to stabilise at around 10% of the pre-venting concentration value for a further 300-325 seconds with a further reduction to 5% after 600 seconds. Variability during this period of the test appeared less variable than for airbags A, B and C.

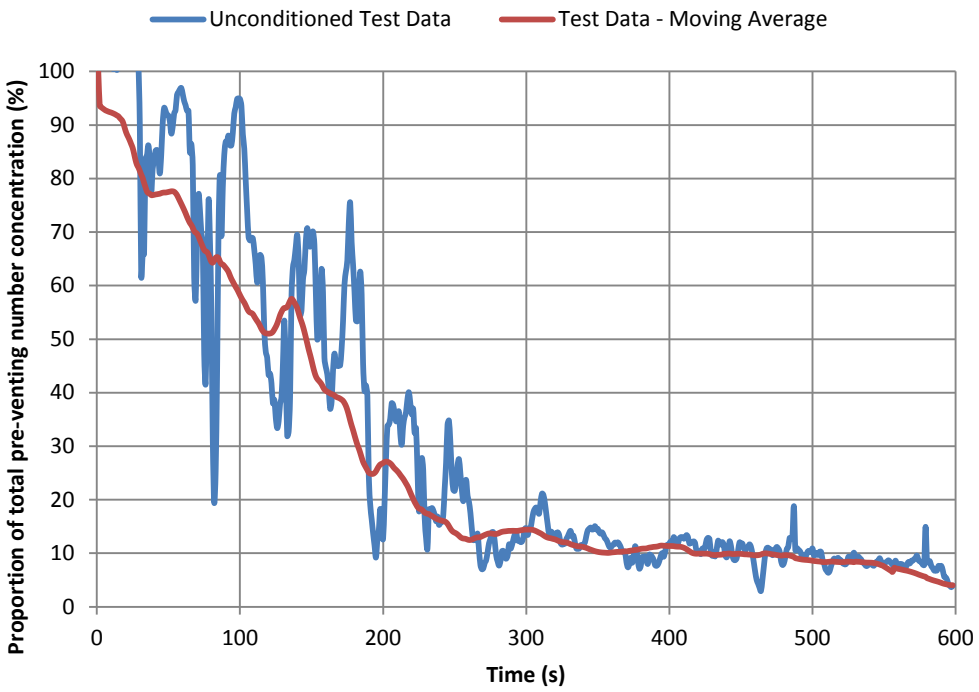

Figure 11.4: Test airbag D mean venting behaviour

Figure 11.5 shows the moving average values for concentration during test environment ventilation for the four airbag types and allows simple comparisons to be made. It can be seen that for all tested airbags particle number concentration reduced relatively quickly over the first 300 seconds of ventilation of the vehicle, to between 33% and 8% of the pre-ventilation values. After this 300 second period, concentration continued to reduce, albeit at a reduced rate, until 600 seconds after the beginning of ventilation, particle concentration had reduced to between 15% and 8% of the respective pre-ventilation values. A similar trend can be seen for all airbags with effluents from airbag C appearing to reduce at a faster rate in the first 300 seconds than airbags A, B and D.

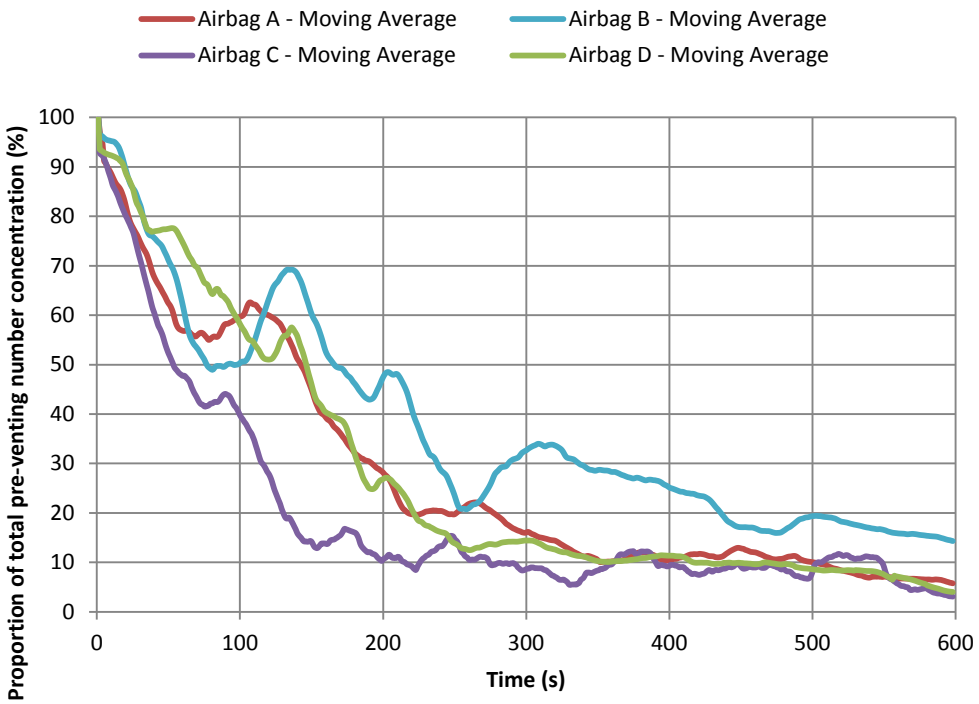

Figure 11.5: Test airbags mean venting behaviour - moving average

The mean concentration proportion values remaining after 600 seconds for the four tested airbags was derived from data within Figure 11.5 and is shown in Table 11.1 alongside the range which provided an indication of inter-test variability.

Airbag	Mean proportion remaining	Range
A: Solid Propellant	5.8	+6.40 -3.71
B: Solid Propellant	14.3	+1.31 -2.12
C: Solid Propellant	3.1	+0.46 -0.25
D: Hybrid	4.0	+2.18 -1.46

Table 11.1: Remaining number concentration (N/cc) proportion after 600s

After 300 seconds there is little differentiation between the datasets for airbags A, C and D whilst tests of airbag B appeared to result in higher particle concentrations being measured. However, these values must be considered with caution as significant variability has been observed over the 600 seconds of ventilation and between tests, especially for airbags A and D.

Absolute concentration values can be defined by applying the proportional number concentration data to mean, pre-ventilation, number concentration data for each test

airbag. These concentrations for each airbag and their variation in relation to time are shown in Figure 11.6.

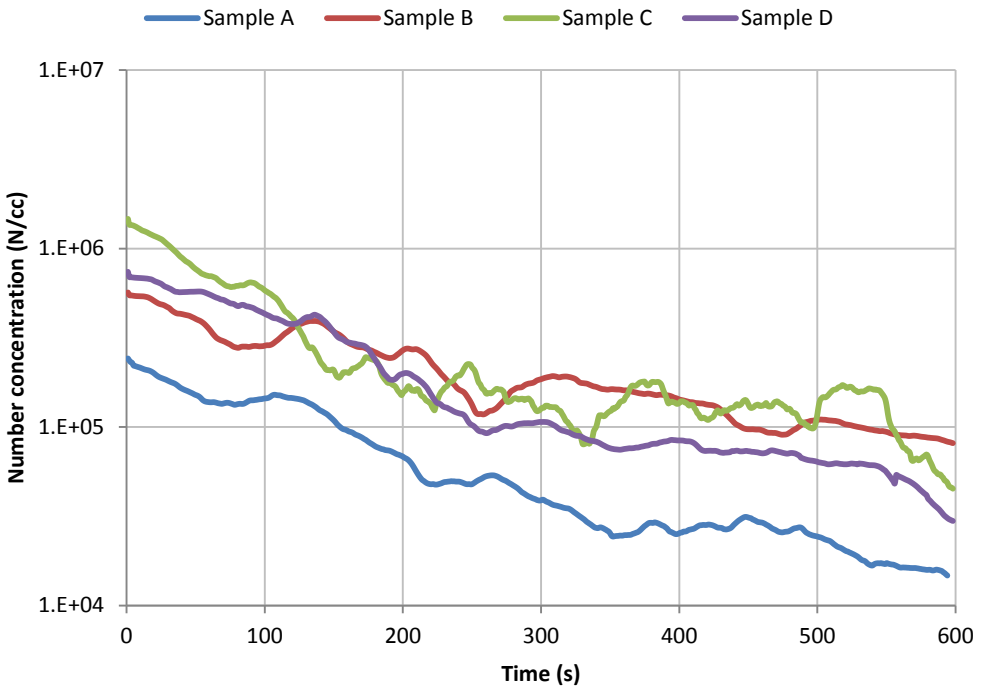

Figure 11.6: Particle number concentration during post-test ventilation

Substantial reductions in particle concentration over the 600s test resulted in mean particle number concentration levels of between 8.48E+04 and 1.57E+04. Although some variability can still be seen in relation to time, the lowest concentration values were measured at the last measurement point; 600 seconds after the vehicle interior was initially ventilated. The highest pre-ventilation number concentration value was recorded for airbag C, however, after 600 seconds of ventilation, the number concentration had reduced to below that of airbag B, the airbag which produced the second lowest pre-ventilation concentration value.

11.4 Summary

The analysis provided an initial indication of the likely changes in particle number concentration in a vehicle after airbag deployment and subsequent ventilation. Understanding the effect of ventilation provides important information to help quantify exposure experienced by ELV depollution operatives. These operatives are commonly required to re-enter a vehicle interior after deploying airbags and other automotive pyrotechnic systems and little guidance has been provided regarding this practice. The testing conducted within this research programme, focusing on ventilation, has not been

found in the literature and therefore demonstrates a novel assessment and approach in the sector of automotive airbag testing and analysis. However, this work does not intend to result in the provision of guidance on any process for depollution operatives at the current time.

The data showed that, in general, particle concentration in the range of 5-1000nm dropped markedly in the first 300 seconds after ventilation of the test vehicle, to between 8% and 33% of the pre-ventilation concentration level. After a further 300 seconds concentration had dropped to, on average, between 3% and 14%. In general there was significant variability in concentration values during each of the tests, although on a clear downward trend, fluctuating, sometimes on a second by second basis. Significant variability also existed between tests for each of the airbags but in general variability reduced as the test progressed and as particle number concentration reduced. After 600 seconds the particle number concentration dropped to values in the same order of magnitude, being between 8.48E+04 and 1.57E+04, depending on the airbag type and therefore to values significantly lower than those measured in the vehicle interior prior to ventilation. This suggests that ventilation of a vehicle, even by opening a single door is an effective way of reducing exposure for those tasked with airbag deployment. The highest pre-ventilation number concentration value was recorded for airbag C. However, after 600 seconds of ventilation, the number concentration had reduced to below that of airbag B, the airbag which produced the second lowest pre-ventilation concentration value. This indicates that there are other over-riding factors that influence the effect of ventilation on remaining particle number concentration, than the pre-ventilation number concentration, and these may also account for some of the observed variability. This variability and the observed variation in resulting number concentration may be associated with a number of factors, such as variations in the air exchange rate from the vehicle to the laboratory environment, and the high sampling resolution of the DMS.

Although considerable variability was observed, the presented data may be used as a basis to quantify the effectiveness of ventilation after airbag deployment to reduce the exposure of operatives to particle effluent from airbag deployments.

Chapter 12

High Speed Film Deployment Analysis

12.1 Introduction

This chapter details the results gained from high speed film analysis of the four tested airbags, types A-D. Tests were conducted externally from the two test environments, as detailed within Chapter 6, and the data obtained was used to define the following airbag deployment characteristics:

- Peak cushion fabric speeds: the maximum speed at which the airbag cushion travels in any plane.
- Mean cushion fabric speeds; the mean speed of travel of the airbag cushion calculated across the 'x-plane', Figure 12.1.
- The duration to maximum cushion inflation: the time taken for the airbag cushion to reach its maximum volume.

Measurement of these characteristics allowed deployment consistency and variability to be defined.

12.2 Airbag cushion fabric speeds

Establishing airbag cushion fabric speeds was achieved by measuring the movement of the fabric of each airbag cushion across the 'x-plane, Figure 12.1. The 'x-plane', Figure 12.1 was utilised as it formed the predominant plane or direction in which the airbag cushion travels toward an occupant in a collision. Both peak and mean fabric speeds were calculated from this movement by tracking the leading edge of the airbag until the airbag reached its maximum volume and inflation.

Measured peak fabric speeds for the four subject airbags, Table 12.1, ranged from 178 kph (111 mph) to 278 kph (174 mph), with a co-efficient of variance broadly comparable between tests of each airbag type, at 5.5-8.1%.

Airbag	Peak fabric speed (kph)					
	Test I	Test II	Test III	Mean	SD	CoV %
A	235	208	222	222 (+13/-14)	13.5	6.2
B	211	229	248	229 (+19/-18)	18.5	8.1
C	241	254	280	259 (+21/-18)	19.9	7.6
D	190	179	200	190 (+10/-11)	10.5	5.5

Table 12.1: Airbag cushion peak fabric speeds

In all cases these peak fabric speeds were recorded in the initial stages of deployment of the cushion and generally within the first 5 milliseconds (ms), as the cushion moved along the x-plane, as shown in Figure 12.1and Figure 12.2.

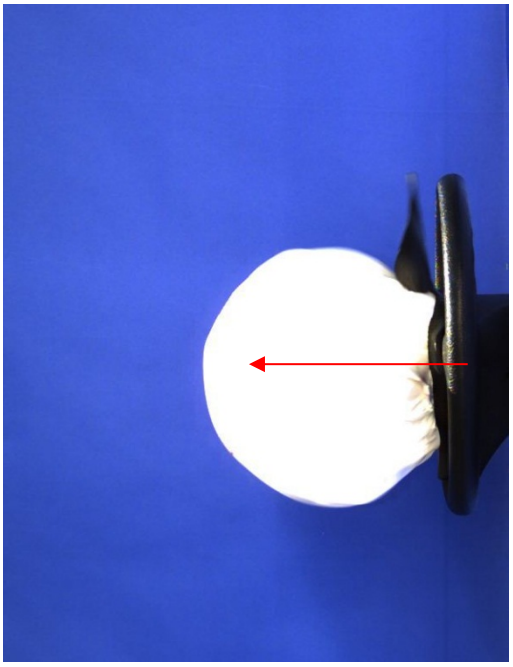

Figure 12.1: Airbag D forward inflation motion

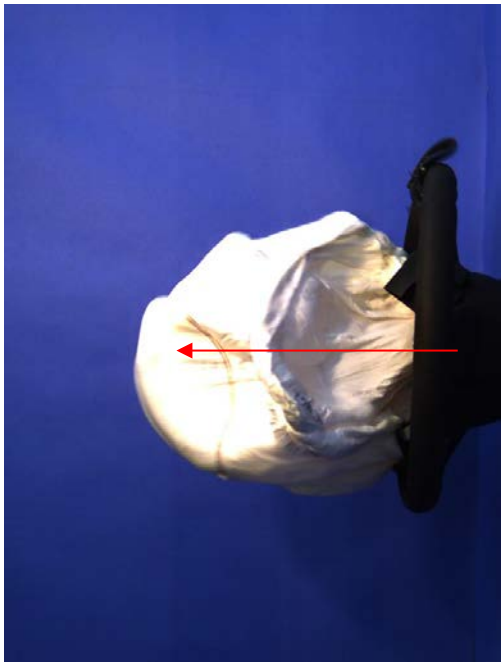

Figure 12.2: Airbag C forward inflation motion

This initial forward motion continued until the cushion reached its maximum forward displacement as dictated by the internal cushion tethers, as discussed within Chapter 6.

Airbags using a solid propellant inflator (airbags A-C) showed higher peak fabric speeds than the airbag using a hybrid inflator (airbag D). This type was up to 27% slower than the fastest; airbag C. Airbags A, B and C appeared comparable and a statistical test (t-test) of the data identified that no statistically significant difference in their peak fabric

speeds was detected ($p>0.05$). However, a statistical difference was detected between airbag D and all other airbags ($p<0.05$), although consideration should be given to the relatively small datasets used for the analysis.

As with peak fabric speeds, mean fabric speeds were calculated by assessing the maximum forward displacement of the airbag cushion travel in the 'x-plane' and the duration over which this movement occurs.

These mean fabric speeds are presented in Table 12.2 for all tested airbags with an accompanying calculation of variance.

Airbag	Mean fabric speed (kph)					
	Test I	Test II	Test III	Mean	SD	CoV %
A	175	156	167	166 (+10/-10)	9.7	5.8
B	174	180	188	180 (+8/-6)	7.2	4.0
C	195	220	243	219 (+26/-24)	24.1	11.0
D	132	137	151	140 (+11/-8)	9.9	7.2

Table 12.2: Airbag cushion mean fabric speeds

Fabric speeds for all subject airbags were in the range 131kph (82 mph) to 242kph (151 mph) with similar trends to that for peak fabric speed but with a greater range. As with peak fabric speeds, airbag 'D', (hybrid inflator), presented the lowest fabric speeds and airbag 'C' the highest, whilst airbags 'A' and 'B' appeared comparable.

When assessed statistically the mean fabric speeds of airbags A and B were again not statistically different from one another ($p>0.05$), whilst all other airbags remained statistically different ($p<0.05$).

12.3 Airbag cushion inflation timing

In addition to the assessment of airbag cushion fabric speeds, measurements of the time taken for the airbag to reach its maximum inflated volume were determined to provide a greater understanding of inflation behaviour and to act as an indicator for comparative over-pressure values. The increase in volume of the airbag and its effect of displacement of air within the test environment or interior of a vehicle creates this over-pressure (Hickling, 1976; 2002). Over-pressure is likely to be linked to inflator pressure output and this in turn has been linked to airbag PM effluent concentrations. Figure 12.3 shows a number of example images depicting this inflation process, with the final image depicting the maximum inflated volume of subject airbag 'D'.

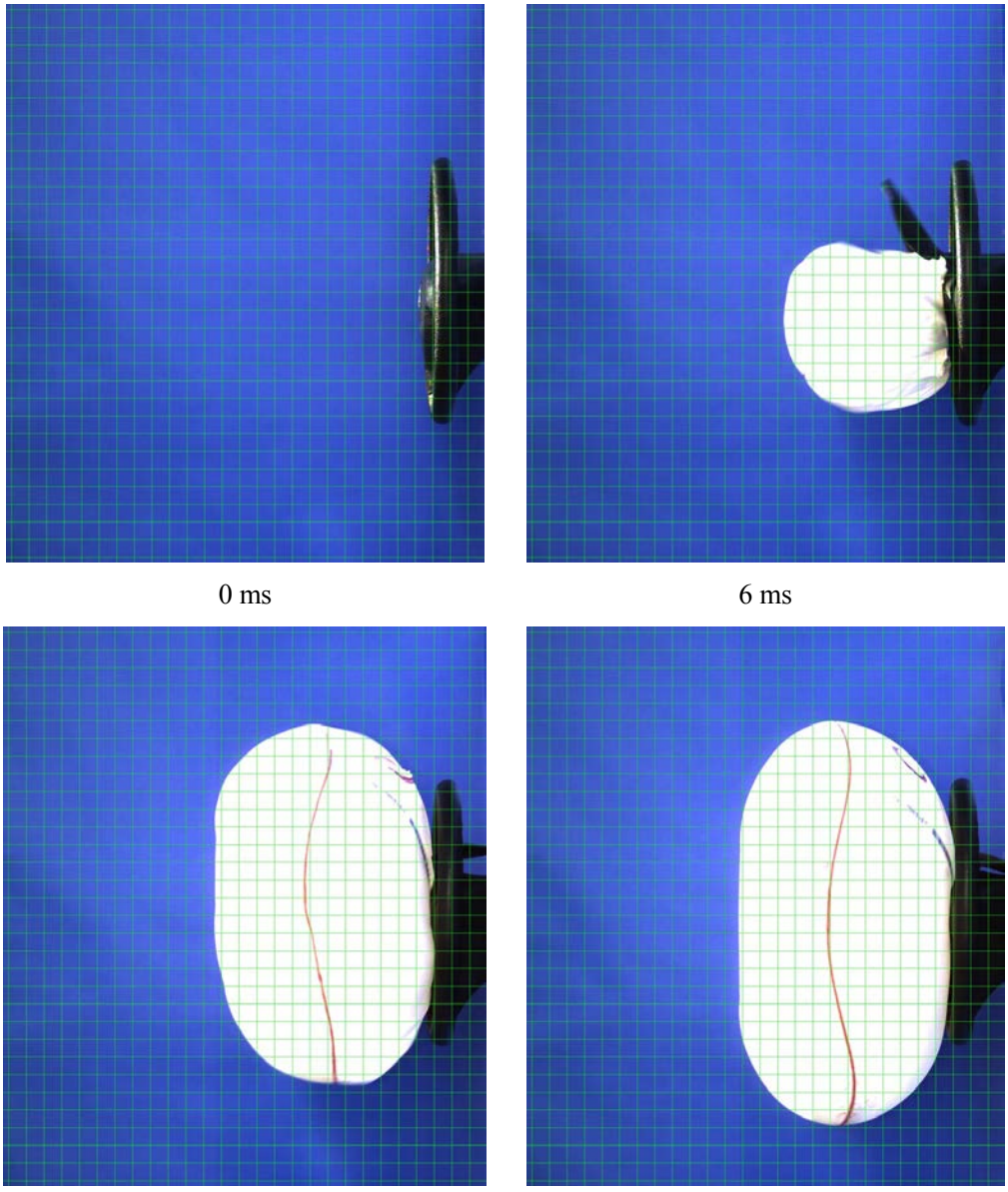

Figure 12.3: Images from high speed photography showing Airbag D duration to maximum inflation

Using images such as those shown in Figure 12.3 and the methodology detailed in Chapter 6, cushion inflation curves for each of the subject airbags have been defined and are shown within the following section. In addition comparisons between each airbag and basic indications of consistency have been presented.

Figure 12.4 shows the inflation duration curves for the three tests conducted of subject airbag 'A', an airbag utilising a solid propellant inflator. This data presented broadly comparable cushion inflation curves and therefore behaviours during each of the three tests. Values expressed as a proportion of the maximum inflation volume were consistent within the first 5ms for all airbags before diverging and then converging again after

approximately 20ms. The convergence of the curves after the initial 20ms of the test indicated that the cushion volume increased at a slower rate and represents the beginning of cushion 'stabilisation'. Stabilisation of the cushion occurred after its full release from the airbag module and is considered as the period of time in which the cushion movement, created by the deployment from the module, decreases and the cushion stabilises. This appears to reflect the inflation characteristics and timings reported in the literature (NHTSA, 2001; CITA, 2002).

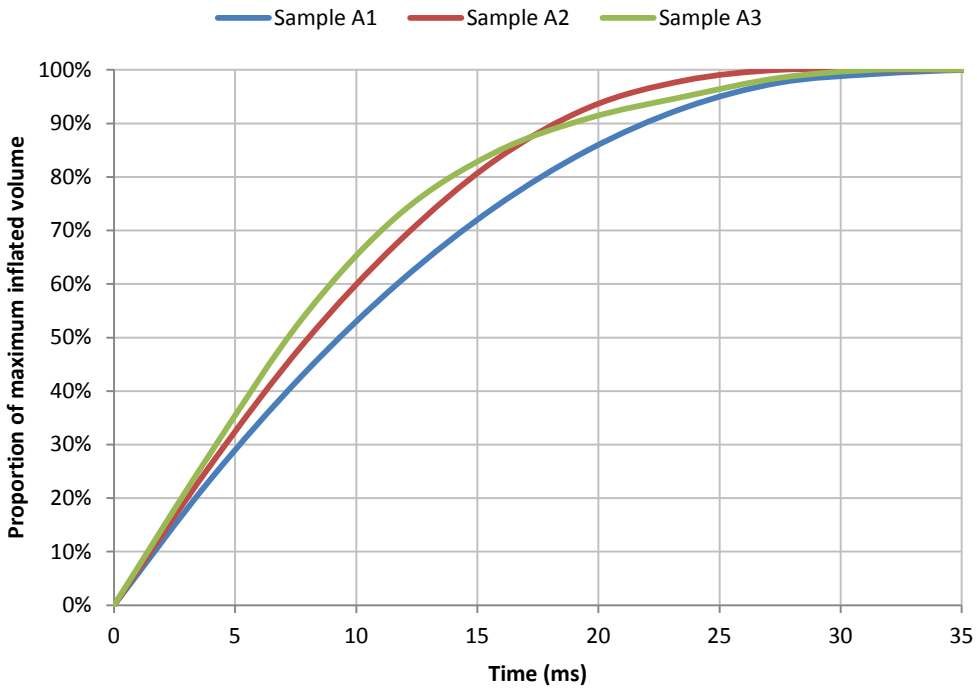

Figure 12.4: Airbag A inflation duration curves

Cushion inflation curves for airbag 'B', shown within Figure 12.5, appear comparable to those for airbag 'A', Figure 12.4, with the cushion volume in relation to time appearing to first diverge before subsequently converging, as inflation volume reached maximum values.

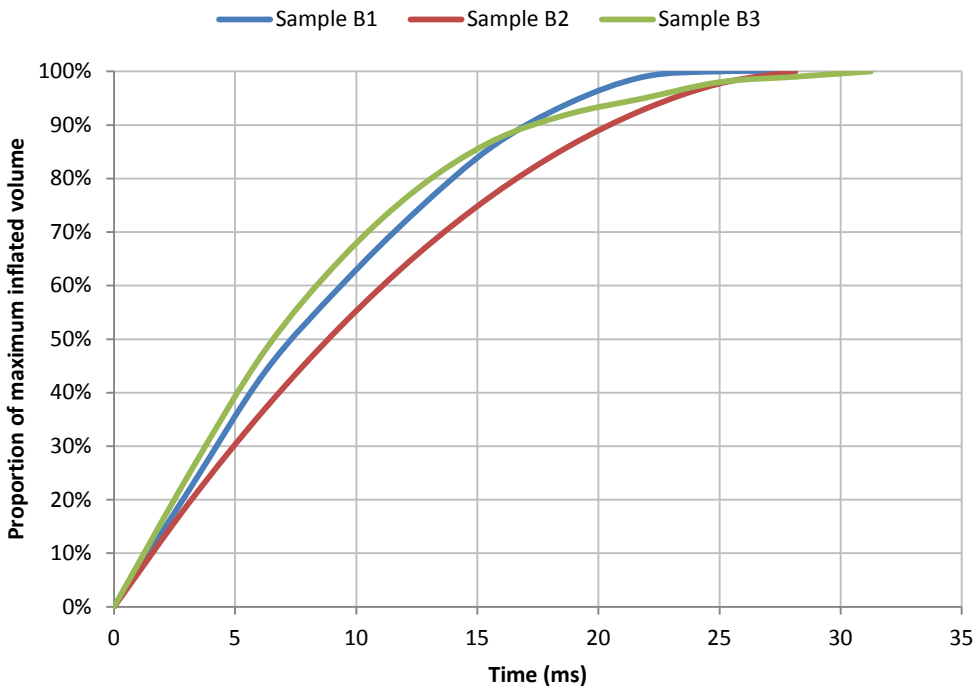

Figure 12.5: Airbag B inflation duration curves

Although these curves again appear to be similar to subject airbag 'A', the inflation duration or time to reach maximum cushion volume appears to be lower for airbag 'B'.

Figure 12.6 shows the cushion inflation curves for airbag 'C', a solid propellant airbag. These show a steeper gradient than those presented for airbags A and B and therefore an increased inflation rate. Low variability between tests can also be identified as inflation curves do not diverge to such a degree, when compared to Figure 12.4 and Figure 12.5.

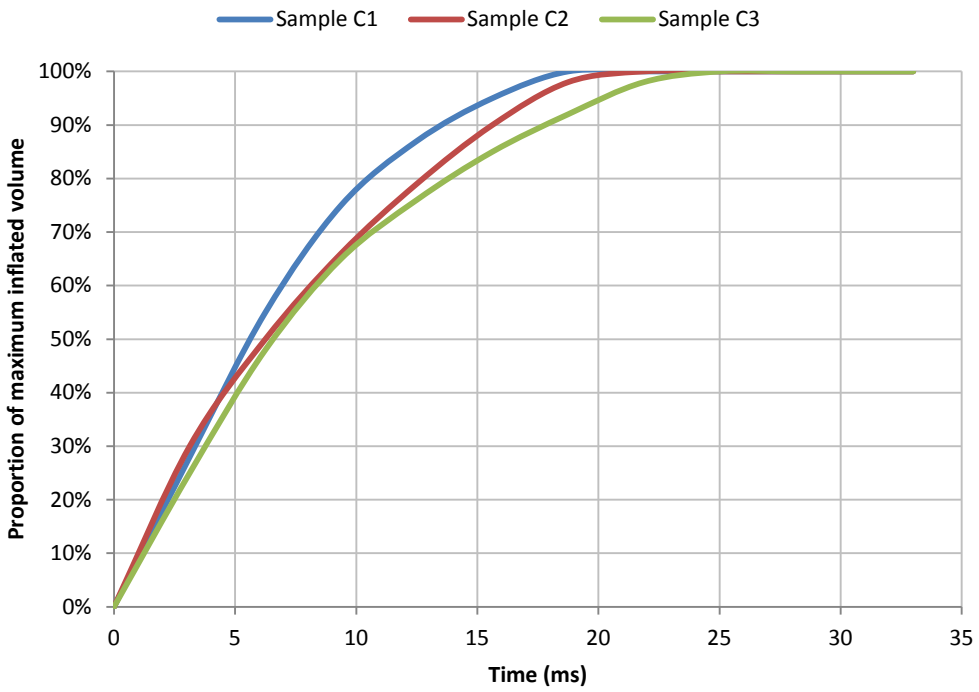

Figure 12.6: Airbag C inflation duration curves

Figure 12.7 presents the cushion inflation curves from deployments of airbag D which appear to differ substantially to those for airbags A, B and C, with a comparably reduced gradient to each of the curves, therefore defining a reduced cushion inflation rate and total inflation time of 36-39ms. This appears to result in more consistency between the airbags initially before a divergence of values. After the divergence, once again, the values converged as the cushion reached its maximum inflation volume and began to stabilise.

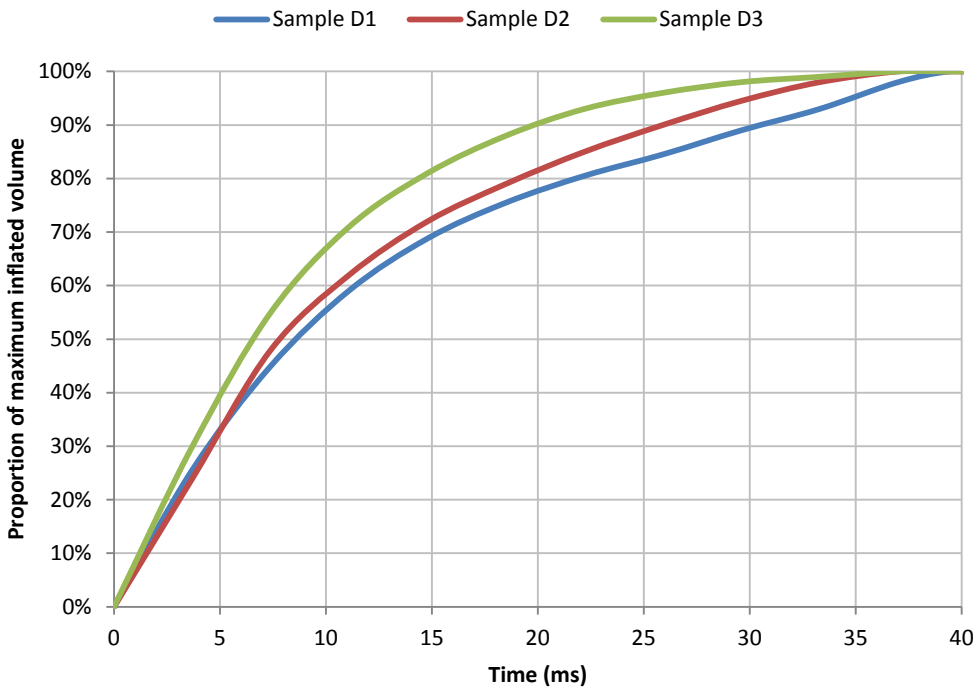

Figure 12.7: Airbag D inflation duration curves

Mean durations to reach the point of maximum inflation are shown in Table 12.3. These mean durations ranged from 20.9 to 37.4ms with a maximum duration of 39.4ms, for an individual test of airbag D. The minimum duration of 18.8ms was recorded for a single test of airbag C.

Airbag	Mean duration to max. inflation (ms)					
	Test I	Test II	Test III	Mean	SD	CoV
A	31.3	27.4	31.0	29.2	2.5	8.7 %
B	25.0	27.8	30.4	27.7	2.7	9.7 %
C	18.8	21.9	22.2	20.9	1.9	9.0%
D	39.4	37.0	35.9	37.4	1.8	4.8 %

Table 12.3: Mean durations to maximum inflation

Mean values for inflation duration were similar for airbags A and B yet markedly different for airbags C and D. A statistical assessment of these durations identified that airbags A and B were not statistically different from one another ($p>0.05$), however statistically significant differences were present between all other airbag types ($p<0.05$). Variance between airbag tests were closely comparable for all three airbags using a solid propellant inflator at 9-10% and substantially lower for hybrid inflator airbag D. This lower variability in deployment characteristics for the hybrid airbag is consistent with lower variability in other areas such as particle concentration.

Figure 12.8 shows the rate of inflation (defined by the line gradient) for the mean values of each of airbag types. The mean rate of inflation, calculated as a percentage of total inflation per millisecond was calculated and varied from 2.7%/ms, for airbag D to 4.8%/ms for airbag C. The rate of inflation for all airbags (A-D) remained relatively consistent to approximately 12.5ms after release from the airbag module. Within 20ms all the airbags had reached in excess of 80% of their maximum inflated volume. This data supports the inflation data presented in the literature, which cites mean deployment times of 33ms (NHTSA, 2001), fulfilling a requirement for inflation of a driver airbag in 35ms (CITA, 2002) to ensure the bag is fully inflated in a collision prior to impact by a vehicle occupant.

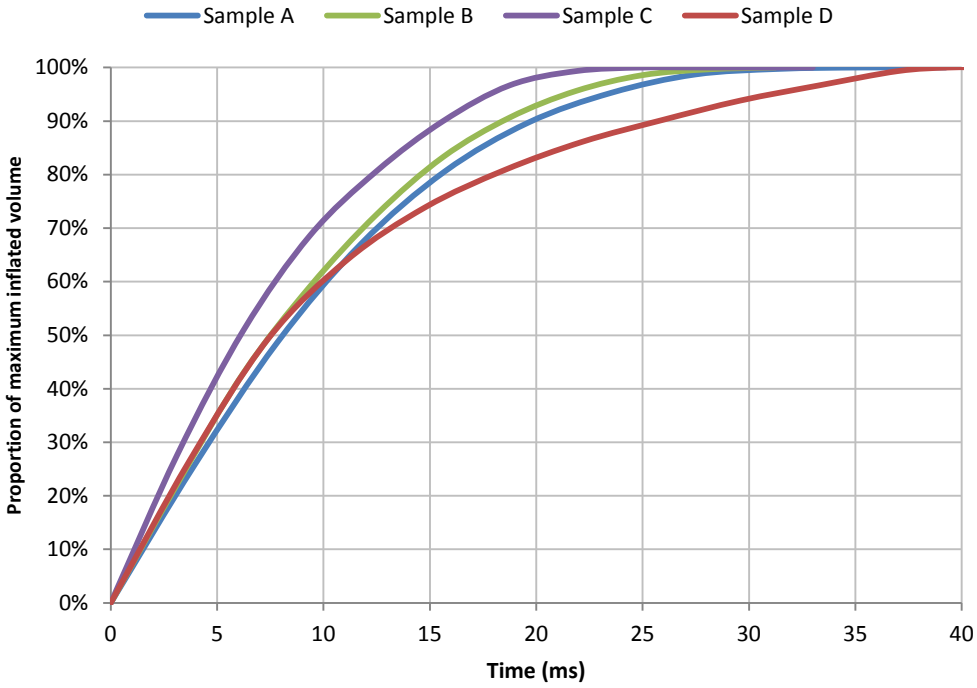

Figure 12.8: Mean inflation duration curves

12.4 Summary

Peak fabric speeds of between 190kph (118mph) and 259kph (161mph) were recorded during assessment of the four subject airbags, with mean fabric speeds of between 139 kph (87mph) and 218 kph (136mph) being measured.

Higher peak and mean fabric speeds were recorded for the airbags utilising a solid propellant inflator (airbags A-C) than the airbag using a hybrid inflator (airbag D), with this type being up to 27% slower than the fastest; airbag C. Although differences were observed between each tested airbag, the peak fabric speed of airbags B and C and the peak and mean fabric speeds of 'A' and 'B' could not be differentiated statistically from

one another ($p>0.05$). In general these speeds varied by up to 8.l% (CoV) for peak fabric speeds and 11.0% (CoV) for mean speeds. Variability was broadly comparable between all of the tested airbags and no particular trend could be identified.

For the airbags tested, mean inflation durations ranged from 21 - 37ms. The airbag using a hybrid inflator, 'D', presented a slower inflation rate than the other three airbag types tested utilising solid propellant inflators. These durations matched the lower fabric speeds measured and therefore suggests that solid propellant airbags may be quicker to inflate than their hybrid counterparts.

Whilst there is limited comparable data presented within the literature, mean and peak fabric speeds are comparable to those measured by Schreck et al., (1995) and inflation rates appear to reflect the inflation characteristics and timings reported in the literature (NHTSA, 2001; CITA, 2002).

Whilst the majority of data presented from this research will assist in developing understanding within the sector, in the context of the project objectives the assessment of airbag inflation and fabric speed is arguably the least likely to develop knowledge regarding airbag PM effluents. The assessment and results provided allow comparison to that in the literature, but provide little novelty in terms of method or the data provided. However, where the data is valuable to this assessment is in providing a basic assumption that higher inflator pressures, inferred from inflation rate and fabric speed data result in higher effluent PM number and mass concentration. This assumption supports a more controlled evaluation with varied inflator pressures conducted by Starner (1998) who measured higher PM mass concentrations with higher inflator pressures.

Chapter 13

Particle Morphology and Microstructure

13.1 Introduction

Particle effluents so far, in this work have been characterised in terms of their mass, by means of GF and, more comprehensively, on representative particle size, using the DMS. The DMS classifies particles based on equivalent diameters derived from their electrical mobility; presuming that all particles are spherical and are of an assumed mass and density. However, in many cases particles are not spherical and may collect in groups as aggregates, and for this reason an initial assessment using microscopy was undertaken and the results presented within this chapter. In addition, little data has been presented in the literature regarding morphology of particles emitted during airbag deployment, with the research being restricted to only a small number of studies focusing on the forensic value of such knowledge to specific automotive crimes (Berk 2009a; 2009b; Wyatt, 2011; Marsh, 2011). It is suggested that in a collision where the driver cannot be conclusively identified by other means or flees the scene, the knowledge of airbag 'residues' and their transfer to human subjects and their clothing may allow for suspects to be associated with a vehicle. These studies appear to focus on particles larger than those identified by the DMS in this project and therefore an assessment of smaller particles using TEM will provide novel data regarding the particles emitted during the deployment of automotive airbags.

13.2 Sampling methodology and grid loading

The basic experimental method defined in Chapter 6, for providing samples for electron microscopy resulted in 'high grid/film loading', where significant particle mass and

number were present upon the films and grids themselves. This produced images that provided limited value in defining particle morphology. The high loading, lack of support from the grids and in some cases a varying vacuum pressure resulted in damage to some films upon grids, Figure 13.1 and 13.2.

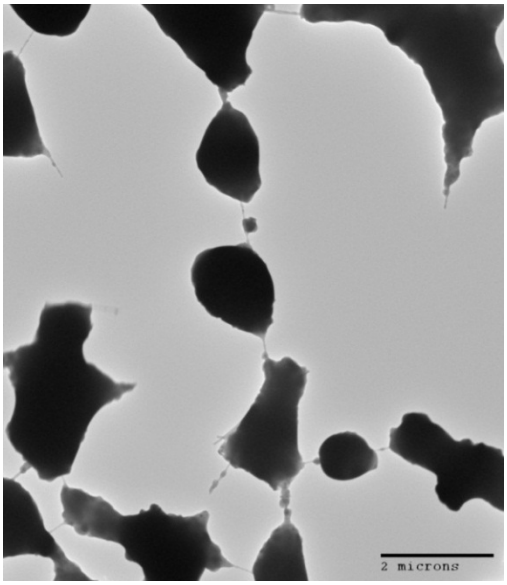

Figure 13.1: High grid loading and film damage example

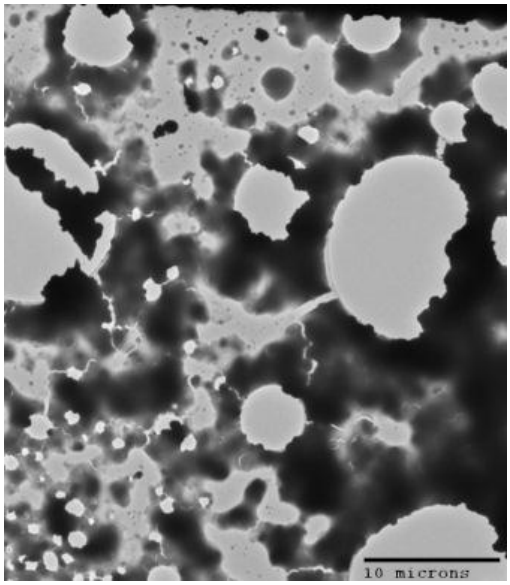

Figure 13.2: Lower grid loading and film damage example

It was surmised that high grid loading occurred during initial tests because of a combination of excessive sampling durations and sample vacuum pressures and flows. As there was little comparable literature available to define sampling parameters, two options were considered to define sample vacuum flow and sample duration:

(a) Undertake an iterative test process with vacuum flow rate and sampling duration to optimise grid loading, for each of the subject airbags, or,
(b) Calculate expected grid loading by using number concentration data from the DMS.

As option (a), would be time consuming and costly, and require each micrograph to be checked prior to defining test parameters for subsequent airbag deployments, it was initially decided that option (b) would be performed.

However, calculations (detailed in Appendix C) used many assumptions regarding how particles would theoretically be collected upon grids and films. This suggested that at a low flow rate of 1-3 lpm, with particle concentrations as measured by the DMS that the grid would be close to full loading in less than 2 seconds. However when comparing these parameters and expected results with micrographs from initial tests of loading, with substantially higher vacuum flows and sample durations, the results suggested that such a

simplistic calculation was an unsuitable option for calculating the sampling parameters. Therefore option (a) was subsequently undertaken with the highest emitting airbag (airbag C) to define sampling duration and vacuum flow rate. As a higher flow rate resulted in high grid loading, a low vacuum flow of 3 lpm was utilised and sample duration varied. A sample duration of less than 1 minute was identified and provided a sample of a suitable concentration onto the grid film to allow analysis of morphological characteristics of individual particles. As all other airbags emitted lower number concentrations it was expected that no further high grid loading would be experienced.

13.3 Airbag assessment by TEM

The PM collected from deployments of the four subject airbags was assessed by transmission electron microscopy. Micrographs defining representative particle distributions and morphologies were obtained from effluents of the four subject airbags and these were assessed to define morphology and basic particle size distribution and concentration. In addition, any association with data from the DMS was identified.

13.3.1 Test airbag A

The micrographs shown in Figure 13.3 to Figure 13.5 represent particle size distributions and morphologies identified during repeated tests of subject airbag 'A'. Particle size distribution and morphology remained consistent throughout testing, although some variation in particle loading and concentration was identified.

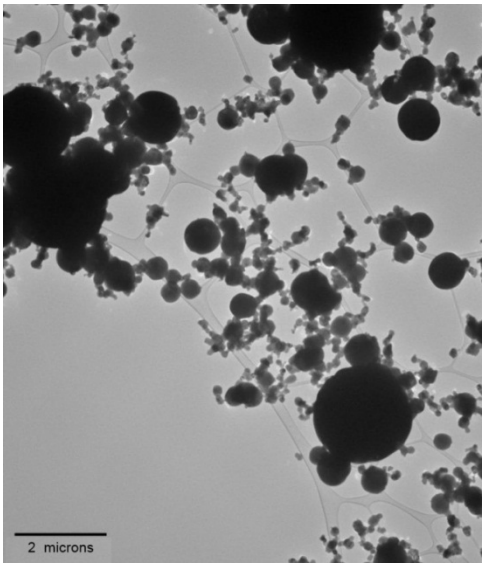

Figure 13.3: Low magnification micrograph of airbag A particle characteristics

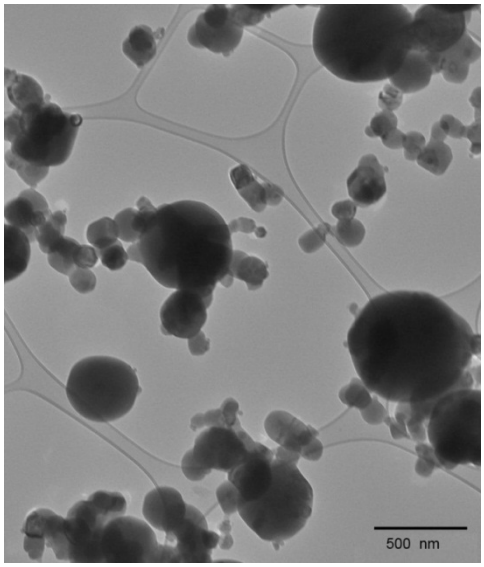

Figure 13.4: High magnification micrograph of airbag A particle characteristics

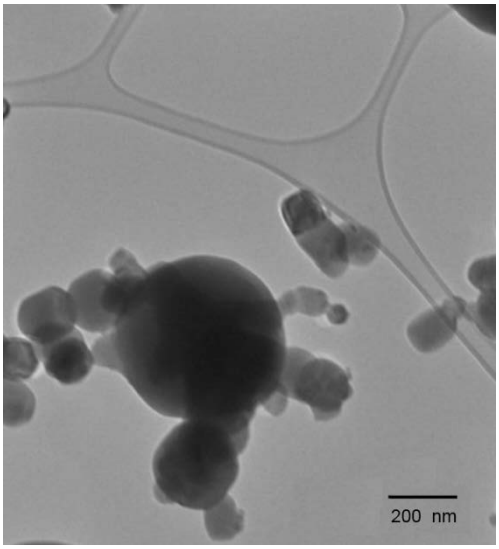

Figure 13.5: High magnification micrograph of airbag A particle characteristics

Figure 13.3, a lower resolution micrograph, illustrates overall distribution of particles on the grid film, whilst Figure 13.4 and Figure 13.5 are of a higher resolution and provide greater understanding of particle morphology.

Assessment of these micrographs allowed identification of particle characteristics including size; with particles classified generally into three main diametric groups; (a) 30-150nm, (b) 300-600nm and (c) those of approximately 2 microns in diameter. Very few particles were identified outside of these three particle classifications.

Whilst the larger particles of approximately 2 microns dominate the grid films and therefore samples in terms of area coverage, the smaller particles of between 30nm and 150nm are dominant in terms of number concentration and are thus referred to as the 'dominant particle'. The larger particles of approximately 2 microns diameter fall above the upper measurement range of the DMS and therefore were not defined within the data presented based on electrical mobility. These particles are far less common than the dominant particle sizes of 30-150nm but appear in similar concentrations to those in the 300-600nm range.

The particle types classified into three general groups by size all appear spherical in shape with larger particles having greater sphericity than their smaller counterparts.

Particles in the dominant size range (30-150nm) commonly appear as chain-like agglomerates/aggregates; whilst those in the larger size ranges (300-600nm and ~2 microns) appear to exist predominantly in isolation or as agglomerates of particles of varying sizes. It is not clear whether this aggregation of particles originates as the particles are generated, when in the test environment or as particles are deposited/collected upon the grid film.

The larger identified particles (300-600nm and 2 micron) appear with greater image contrast than those in the dominant size range (30-150nm). Greater image contrast exists when the particle or substance being analysed does not allow as effective transmission of electrons compared to others and is associated with higher density or variations in composition.

A comparison of the data from microscopy with the particle size data from electrical mobility measurements made with the DMS, showed strong comparability. Particle size measured by the DMS ranged from 35-125nm during an equivalent test duration and therefore compared well to the dominant particle size of 30-150nm defined through microscopy.

13.3.2 Test airbag B

Figures 13.6-13.8 illustrate representative micrographs of particles emitted during deployments of subject airbag 'B' and allow grid loading, basic particle size distributions and also morphologies to be defined. Figures 13.6 and 13.7 illustrate particle collection and grid loading; when these figures are compared with Figures 13.3-13.5 for airbag 'A', it appears that a considerably lower concentration of particles have been captured upon the grid film.

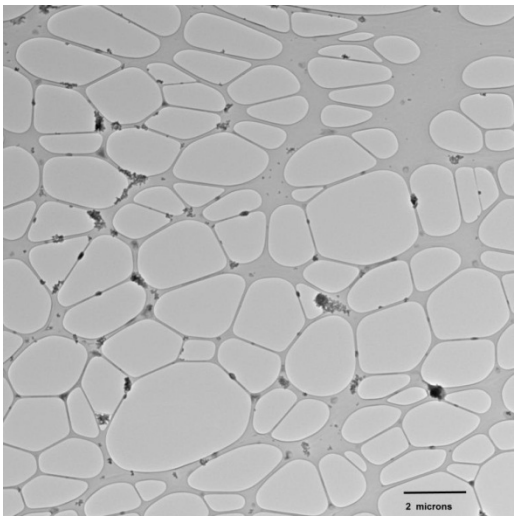

Figure 13.6: Low magnification micrograph of airbag B particle characteristics

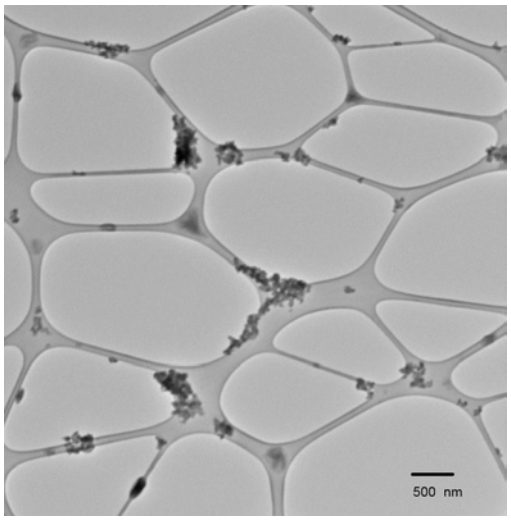

Figure 13.7: High magnification micrograph of airbag B particle characteristics

Figure 13.8 illustrates a representative element of particle accumulations shown within Figure 13.7 with the high resolution of the TEM allowing particle size and morphology to be more easily characterised.

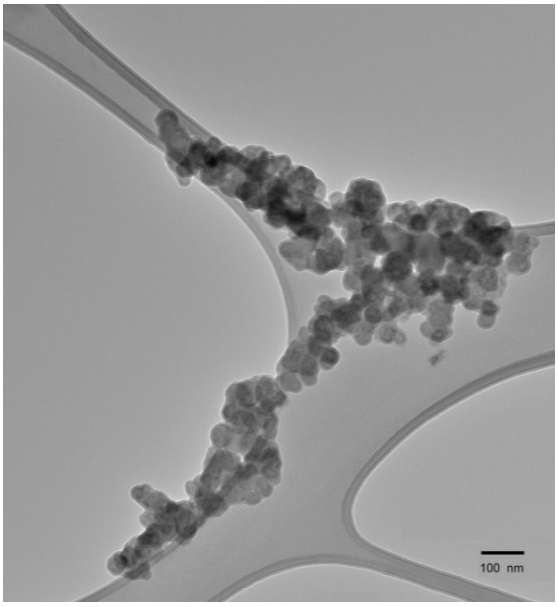

Figure 13.8: Higher magnification micrograph of airbag B particle characteristics

In contrast to PM emitted from deployment of airbag 'A', particles of one predominant size range of 20nm to 80nm were identified. These individual particles appeared generally spherical in nature and similar to those identified during analyses of particles from airbag 'A'.

Particles appeared to accumulate as chain-like agglomerates in groups of varying size and number and very few isolated particles were observed. The aggregates of these particles ranged in size from a few hundred nanometres to over one micron.

Comparing this size distribution data with that collected by the DMS showed general comparability. The particle geometric mean diameter of 35-120nm recorded with the DMS being comparable to individual particles of 20nm-80nm identified in micrographs.

Micrographs of the identified particles showed some variations in image contrasts. This variation may suggest differences in particle density or composition, indicating that although particles can be classified in one general size range there may be some differences unrelated to size.

13.3.3 Test airbag C

Figures 13.9 - 13.12 illustrate representative micrographs of particles emitted during deployments of airbag 'C'; these have been used to identify grid loading, basic particle size distributions and also morphologies. In Figures 13.9 and 13.10 the concentration of particles captured on the grid film appears similar to that of airbag A but is considerably higher than that from airbag B.

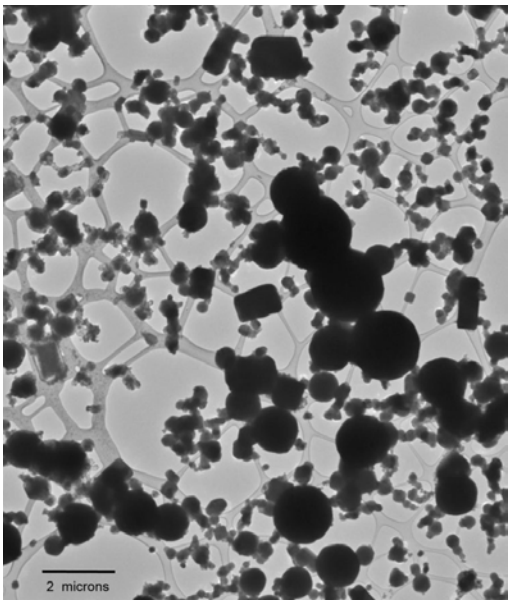

Figure 13.9: Low magnification micrograph of airbag C particle characteristics

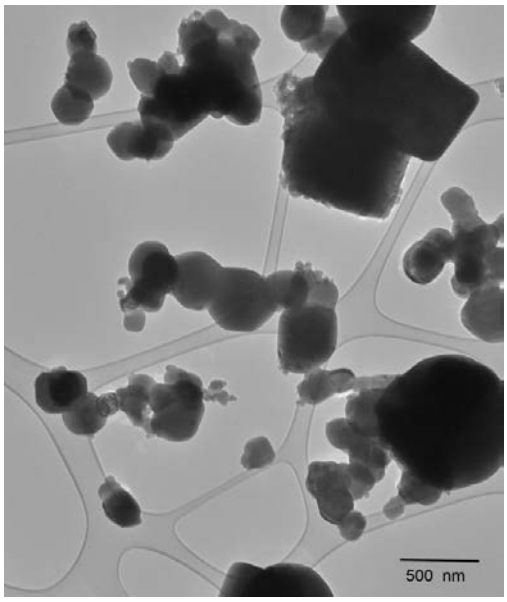

Figure 13.10: High magnification micrograph of airbag C particle characteristics

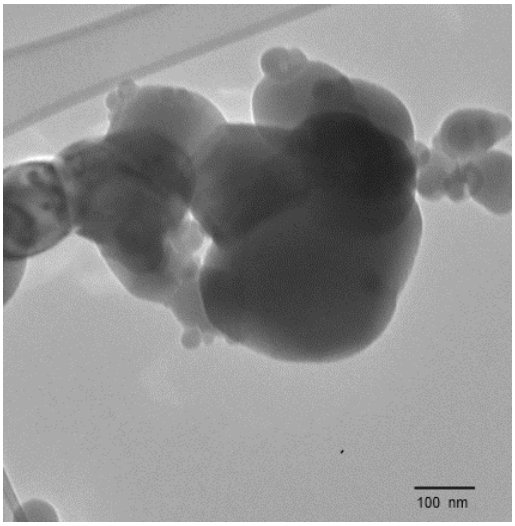

Figure 13.11: Higher magnification micrograph of airbag C spherical particle characteristics

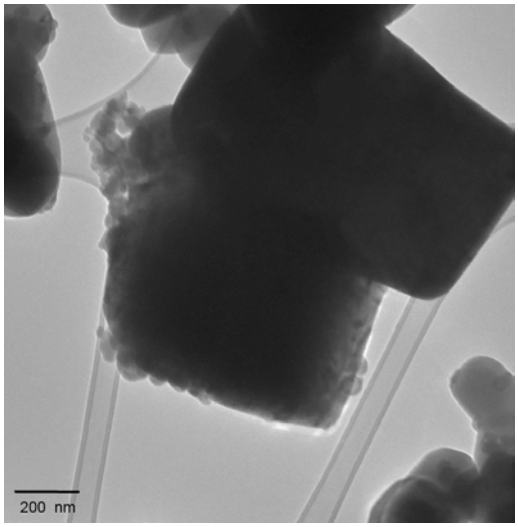

Figure 13.12: Higher magnification micrograph of airbag C rectangular particle characteristics

Individual particles could be classified into a number of different groups based on both size and geometry. Spherical particles were identified in two distinct ranges of 15-150nm and 500nm – 1500nm, Figure 13.10, and in addition, a low concentration of apparently rectangular particles with no dimension greater than ~750nm were also identified, Figure 13.12. The spherical particles appeared similar to those emitted by airbags A and B, whilst the rectangular forms had not been identified before.

The dominant particle in terms of number concentration was the spherical particle in the range 15-150nm which appeared in far greater concentrations than the larger spherical or rectangular particles.

Aggregates composed of spherical particles were commonly identified and in addition some smaller spherical particles appeared to be appended to the larger rectangular particles, Figure 13.12.

Again some comparability was evident in size distribution data defined from microscopy with that collected by the DMS. The microscopy analysis identified dominant particle sizes of 15-150nm diameter compared to the geometric mean diameter of 25-90nm recorded with the DMS.

In general the larger spherical and rectangular particles appeared with greater contrast than most of the smaller spherical particles of 15-150nm. This association between size and contrast is comparable to that found during tests of effluents from all other subject airbags, where in general larger particles had greater image contrast than smaller particles.

13.3.4 Test airbag D

Micrographs representative of particles emitted during deployments of airbag subject 'D' are shown in Figure 13.13 – 13.15. Grid loading appeared similar to that of micrographs from airbag 'B' but lower than from airbags 'A' and 'C'. Figure 13.14 and 13.15 provide higher resolution images of an area of the main particle accumulation shown in Figure 13.13, and illustrate that the number concentrations of smaller particles in this area of accumulation are higher than those for particles generated by airbags 'A, B and C'.

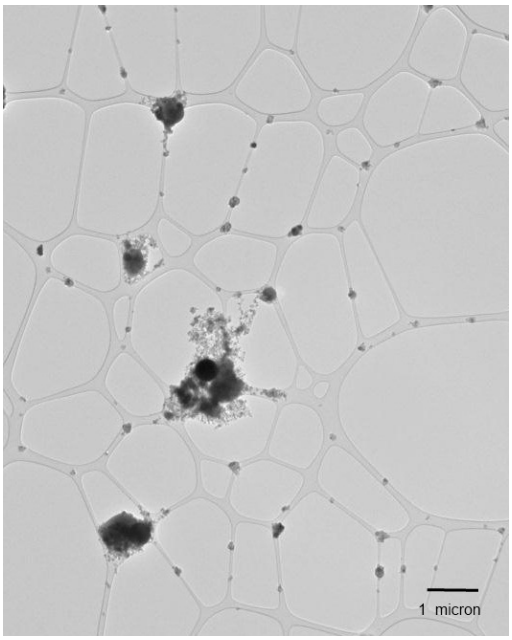

Figure 13.13: Low magnification micrograph of airbag D particle characteristics

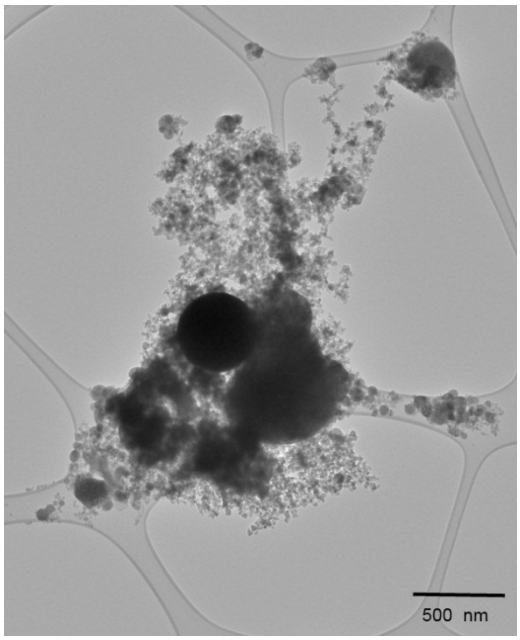

Figure 13.14: Higher magnification micrograph of airbag D particle characteristics

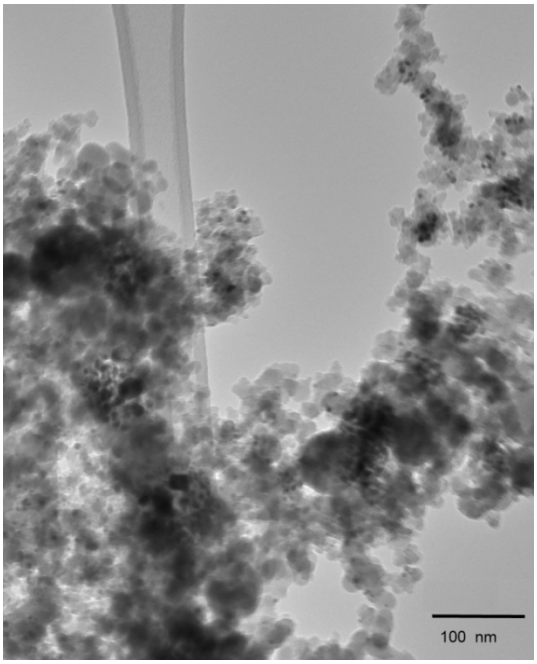

Figure 13.15: Highest magnification micrograph of airbag D particle characteristics

Individual particles varied in size from 2-500nm diameter, with no particles larger than 500nm observed during any tests. Particles in the range 2nm to 500nm could be classified into three main groups; those of (a) 2nm-40nm, (b) 50nm-80nm and (c) 200nm-500nm.

Particles in the dominant size range of 2nm to 40nm, (a), were far more numerous than those in the two larger particle size groups of up to 500nm; (b) and (c). Particles more commonly appeared as agglomerates in the smallest size range (2nm-40nm) but this was also evident with the larger particles.

The size distribution data defined from electron microscopy appeared in general to correlate well with size distribution data from the DMS, with a particle geometric mean diameter of 20-50nm measured during an equivalent test duration and juncture. Whilst this data generally correlated well, it is important to note the presence of an apparent large concentration of individual particles below the lower measurement capabilities of the DMS i.e. those <5nm diameter.

All collected particles from airbag type 'D' appeared spherical in nature, with the larger particles appearing to have greater sphericity than those in the lower size ranges. This is comparable to particle effluents from airbags 'A' and 'B', but is generally different to those from airbag 'C'.

Assessment of the micrographs from airbag D indicated that the larger particles appeared in general to have a higher image contrast than the smaller particles; however some smaller particles in the range 2nm-80nm also presented a high image contrast. This again

suggests that although particles may be classified by size it is likely that some differences between particles in a particular size range are likely.

13.4 Scanning Electron Microscopy

In addition to TEM, scanning electron microscopy (SEM) was employed to determine if the technique could provide further information about the particle accumulations previously observed by TEM. Subject airbag A was assessed and the generated images showed that high concentrations of particles accumulated on the surface of the metallic grid (Figure 13.16) which was not visible or identified during TEM analysis.

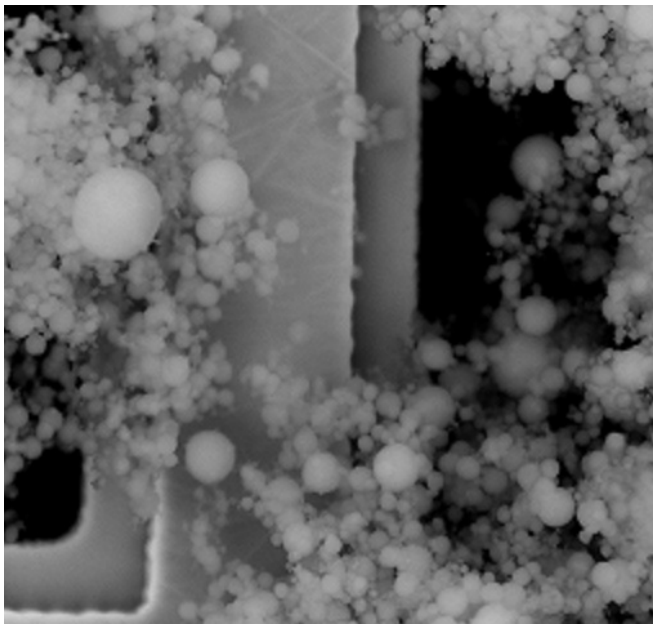

Figure 13.16: SEM image showing particle accumulations on grid surface

The TEM does not allow imaging of the metallic surfaces as it relies on transmission of electrons through the material being assessed. Analysis of these previously unseen particles did not identify any additional particle types and therefore did not provide any additional information relating to particle morphology characteristics. The use of SEM does however indicate that the TEM may not provide suitable micrographs to allow particle concentrations to be quantified. The micrographs provided by SEM, such as Figure 13.16, also identified clearly the way in which particles append and layer upon one another. It is possible therefore that with TEM, particles residing upon other particles may not be identified and Figure 13.17 and Figure 13.18 from testing of subject airbag A illustrate this. Figure 13.17 shows an apparently large spherical particle which has the appearance of being appended by smaller particles around its circumference, yet it is difficult to identify the quantity or type of these appending particles. By using SEM it is possible to identify these additional particles around the perimeter of the large spherical

particle, but the technique also shows that there are other particles within its circumference that could not be seen when using TEM.

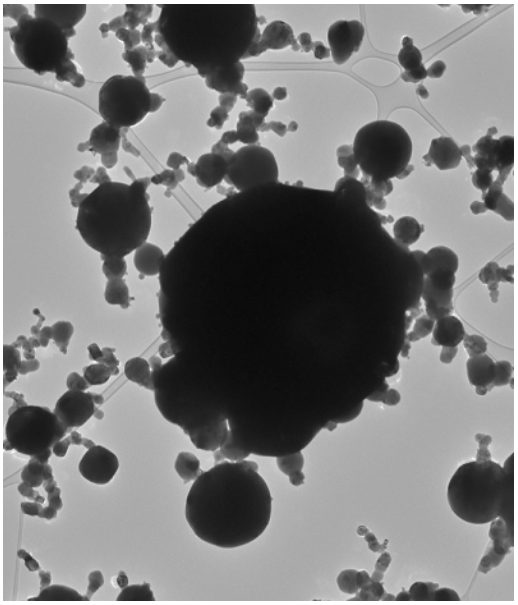

Figure 13.17: Example particle accumulations imaged by TEM

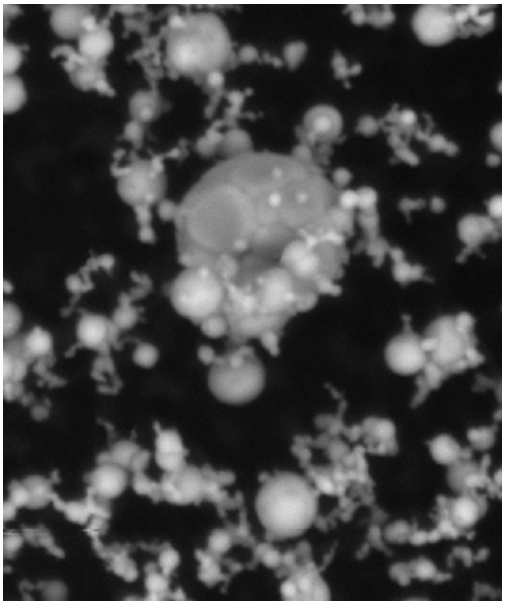

Figure 13.18: Equivalent example particle accumulations imaged by SEM

This comparative analysis has shown that the use of SEM in combination with TEM provides information likely to be beneficial to a comprehensive assessment of particles generated during automotive airbag deployment. However, the SEM data provided little additional information regarding particle morphologies that could not be gained by using TEM, which was the main focus of the assessment. The methodology did however provide information that would be valuable for any assessment of particle concentration by means of microscopy.

13.5 Summary

There is little data or analysis of the morphologies of PM emitted during airbag deployments in current literature, with what is present being limited to a small number of studies of larger particles as part of forensic studies (Berk, 2009a; 2009b; Wyatt, 2011; Marsh, 2011). These studies are all similar in nature and output and have focused on the collection of particles for analysis using scanning electron microscopy and have commonly used energy dispersive spectroscopy (EDS) for compositional analysis. Whilst these studies provide interesting data, they provide little information about particle morphology and fail to assess smaller particles (generally <1 micron) such as those identified during assessments of electrical mobility. The use of TEM within this study therefore demonstrated a novel approach to characterising the morphologies of particles

arising from airbag deployments and allowed for far greater size resolution than previously presented. The analysis using TEM not only allowed characterisation of particles in the range 5-1000nm but also allowed the identification of particles both below and above the measurement range of the DMS, namely those <5nm and >1000nm.

This analysis has shown that the use of TEM is a suitable method for defining the morphology of particles generated during airbag deployments. In addition scanning electron microscopy (SEM) has been utilised to provide greater understanding of the data generated using TEM.

Airbag deployments generally produce high particle number concentration outputs which can result in high grid/film loading during air vacuum sample collection for morphological assessment. This loading hinders or prevents image analysis and therefore to reduce loading, sampling vacuum pressure and/or sampling duration must be varied and an iterative testing procedure was used to define the most appropriate sampling parameters. This iterative process allowed suitable micrographs of the particles generated during airbag deployment to be assessed. These micrographs provide novel information regarding particle morphology and collection behaviour that is yet to be presented comprehensively in the literature.

With the methodology verified, the assessment identified that, in general, there were similarities between the morphologies of particles emitted from each of the four subject airbags with the great majority of particles appearing generally spherical in nature. The dominant (primary) particle size varied from approximately 150nm to as low as 2nm and these commonly appeared as agglomerates in each airbag effluent being assessed. In addition to the dominant particles, other less numerous particles of varying sizes were identified, including those up to a few microns in size that appeared in isolation or with smaller particles appended. Whilst each of the particle effluents assessed showed some similarities, the analysis allowed the identification of effluents from each airbag type based on a combination of the sizes of particles, their morphologies and collection concentration characteristics.

A comparison of particle sizes identified through morphological assessment with the size distribution data gained from the use of the DMS showed close comparability for all samples. The dominant particle size range identified by microscopy for each of the subject airbags was also identified with the DMS albeit with differing minimum and maximum size range boundaries. This assessment therefore verifies the data provided by the DMS, which classifies particle sizes by their electrical mobility, with some assumptions made regarding their characteristics including the assumption that particles are spherical. However, whilst the DMS utilised for particle assessment in the majority of this work has excellent size resolution capabilities, it is not able to measure particles less

than 5nm or greater than 1 micron. High concentrations of particles smaller than 5nm were identified during tests of subject airbag D, the airbag utilising a hybrid inflator. These particles were therefore not identified or characterised previously and the data presented from testing using the DMS shows a larger particle size characteristic than was actually emitted. Although in comparison to the sub 5nm particles, the particles of 1 micron and above identified during tests of airbag A and C, were far less numerous, again they were not characterised by DMS analysis. Whilst there are many options for measuring particles larger than 1000nm there are few options for the measurement of those below 5nm, especially when high sample rate resolution is required. This suggests that the use of TEM is a valuable tool for particle effluent characterisation in conjunction with other measurement methods such as the DMS.

The use of SEM also allowed further assessment of collected particle samples and identified that large numbers of particles were collected on the grid itself and as such were not identified during TEM analysis. TEM does not allow imaging of grid surfaces as it relies on transmission of electrons through the material being assessed. Assessment of the particles collecting on these grids did not result in the identification of any alternate or additional particle types to those collected on the grid films and assessed with TEM. However the identification of significant concentrations of particles collected on the grids is beneficial for those who attempt to define size distribution and concentration using TEM. This therefore ensures that accurate quantitative analysis is conducted on all particles and not only those collected on grid films.

Chapter 14

Discussion

14.1 Introduction

Occupant restraints such as airbags and safety belts have been proven as effective mitigation against injuries to vehicle occupants in collisions and now even for pedestrians who may be involved in a collision with a vehicle (Volvo, 2013). Whilst the first airbag systems were originally conceived in the 1950's, their uptake into the vehicle fleet remained slow until the 1990's when changes to legislation required the use and therefore development of airbags (NHTSA, 1998) prestige and luxury vehicles were generally fitted with airbags and other restraint systems first but changes to legislation in the US required fitment of airbags for the front seats. Rapid increases in restraint system fitment rates were therefore observed, not only in the US but across Europe and in the UK by 2005 nearly 100% of all new vehicles produced contained a driver and passenger front airbag and front safety belt pre-tensioners. The rapid development of restraint system technologies and the associated increase in fitment rate in Europe in particular cannot only be attributed to legislation but also a number of other factors including; consumer testing programmes such as EuroNCAP, (EuroNCAP, n.d.) the drive of manufacturers and the increased mindfulness of the consumer. The awareness of these stakeholders to the effectiveness of restraint systems at preventing fatalities and injuries in vehicle collisions has not only driven their uptake but continues to fuel the development of innovative systems and the fine tuning of those that already exist.

Most current advances in the field surround airbags and pyrotechnic actuators that form parts of safety systems such as 'anti-whiplash' pyrotechnic head restraints (BMW, 2013). Airbags are now fitted in many positions in vehicles to protect particular elements of the human body from injury and in some instances to prevent ejection from the vehicle. Current advances include the use of centre airbags, designed to prevent interaction

between occupants in side and rollover collisions and those that protect pedestrians from impact on a vehicle's structure. The use of airbags and other occupant restraints is likely to continue until the widespread use of fully autonomous vehicles that are able to prevent collisions, therefore removing the need to mitigate their effects.

Whilst the wide variety of occupant restraint systems that are currently available for collision injury mitigation are extremely effective at reducing injury risk, they can pose hazards, during and directly after their deployment, to vehicle occupants and those tasked with airbag neutralisation during ELV disposal.

Exposure to these hazards during ELV airbag neutralisation, as required by EU legislation (European Commission, 2000), is far more frequent than for vehicle occupants and represents an area yet to be thoroughly investigated and presented in the open literature. In 2010, in the UK alone, of the 1.7 million vehicles that reached their end of life, approximately 1 million vehicles equipped with 2.4 million live pyrotechnic occupant restraints passed through ATFs and should have been deployed by ELV depollution operatives. The exposure of operatives to many of the hazards during neutralisation is generally limited by use of remote deployment equipment and safe systems of work, however, exposure to the airborne effluent emitted during deployment is likely to pose the most frequent and uncontrolled risk to the health of those undertaking such tasks.

More specifically the exposure to the PM element of the effluent in the nanoscale arguably poses the greatest risk of harm.

Methodologies documented in the literature for the assessment of airbag PM effluents are generally simplistic and are focused purely on post-collision exposures for vehicle occupants, with limited detail and mostly in the micron size range (SAE, 2011a; Audi AG et al., 2001). They require either the quantification of particle mass concentration and speciation or assess the respiratory response of human subjects when exposed to airbag PM effluents. A test tank or a vehicle may be used for assessments and there is yet to be any assessment of the acceptability and comparability of these two environments in open literature.

The most common findings from the literature suggests that deployment of airbags produces a PM effluent with a bimodal size distribution and a primary mode of between 0.4µm and 1µm (Chan et al., 1989; Gross et al., 1994; 1995; Schreck et al., 1995), attributed to deflagration of the solid propellant. The secondary mode occurring at 3-10 micron is reportedly associated with the loose coating of talc or cornstarch employed on earlier un-coated airbag cushions to aid deployment (Chan et al., 1989; Gross et al., 1994; 1995; Schreck et al., 1995). Particle concentration measured exclusively in terms of particle mass in studies reported in the literature has varied substantially from 12mg/m^3 to 684mg/m^3 (Chan et al., 1989; Gross et al., 1994), with airbags using an inflator with a

non-azide propellant producing concentrations in the lower extent of this range (Gross et al., 1999 & Linn et al., 2005). Whilst providing some characterisation of particulate matter effluent characteristics, these methodologies and the associated data presented within the literature, offer little detail regarding the evolution of the effluent over time, its size distribution in the nanoscale and the morphology of particles in the sub-micron size range.

To increase knowledge regarding effluent and particle characterisation and to assess test environments, all in particular context to EoL exposures, a number of airbags were tested, and characterised, and the test environments assessed comparatively. The effluent test tank was designed and constructed by the author and a test vehicle was modified suitably for the assessment. Airbags selected for evaluation originated from end-of-life vehicles and represented those most likely to be encountered by operatives in large volumes at the current time and in the near future, during neutralisation activities. These airbags were a combination of systems utilising dual and single stage, solid propellant and hybrid inflators and used propellants known not to contain sodium azide.

14.2 Overview of test programme

To allow analysis of the four subject airbags an evaluation of test environment performance and comparability was conducted to assist in providing a consistent and coherent methodology. The methodology employed and specific tests conducted are detailed in Chapter 6, with comprehensive results shown in Chapter 7.

14.2.1 Test environment and methodology evaluation

Two test environments used for the assessment of effluents from automotive airbags were constructed for use within this research programme:

1) Airborne effluent test tank of 2.83m^3, constructed in compliance with test standards (SAE 2011a; Audi AG et al., 2001)
2) Modified test vehicle with an interior of an equivalent volume to the effluent test tank.

A quantitative evaluation of the two test environments using direct, gravimetric filtration measurements and particle size distribution and concentration measurements with a differential mobility spectrometer (DMS) was conducted. This identified that the effluent test tank, although initially more costly and time intensive to manufacture, allowed quicker and easier mounting of test samples, provided better seal integrity when subject to airbag over-pressure, (Hickling 1976 and 2002) and can also be cleaned subsequent to deployments with ease. This is in contrast to the test vehicle, which has a lower initial

cost and manufacturing requirement, but offers generally poor seal integrity and is comparably more difficult to clean. These are likely reasons that the majority of quantification testing is conducted in effluent test tanks and the method is documented more comprehensively in test standards (SAE, 2004; 2011a; Audi AG et al., 2001). Over-pressure which has previously been documented as being attributed to seal damage and ultimately sample loss (Chan et al., 1989) has been overcome during this study, by employing a series of pressure relief valves to reduce this pressure from deployment. It is therefore recommended that when a vehicle is used for repeated airbag exposure tests that additional pressure relief is provided.

Aside from the qualitative basis for the selection of test environments this research more importantly, quantitatively assessed the performance of both test environments and identified the comparability and performance of the two environments.

This testing and analysis has shown that the effluent test tank is capable of providing airbag PM effluent characterisation comparable to that measured in a vehicle interior and in most instances replicates exposure in an enclosed vehicle, as intended as the focus in test standards.

To this point no studies have been reported in open literature that have compared the two test environments. However, many studies have used one or other of the environments with no consideration of how the tests relate to each other. This assessment showed that the test tank was not only comparable, but in fact provided less variable results than during tests conducted in an equivalent vehicle.

When viewed as a mean, over the full test duration, no statistical difference could be observed between the test tank and vehicle in terms of particle number concentration and size.

However, when viewed in relation to number concentration over time, greater variability was observed. In all cases, the inter-test variability reduced as the test duration increased, but measurements remained more variable in the test vehicle than the test tank. After 900s, variability in the effluent test tank was reduced to a consistent level of 4.5-6%, whilst in the test vehicle; this variability remained higher throughout the test and reduced at a slower rate. Whilst rarely reported, this variability of 4.5-6% in the test tank, compares favourably to inter-test variability of in excess of 20% reported in the literature for comparable assessments of effluents from airbags and other occupant restraints (Ziegahn and Nickl., 2002). When considering the disparity in inter-test variability between this study and that reported by Ziegahn and Nickl (2002), it is not possible to conclusively identify any defining factors for the difference, due to a lack of data in the

literature, but it may be associated with the measurement methodology, airbags tested or other unknown variance.

Studies such as those by Ziegahn and Nickl (2002) and Gross (1994; 1995; 1999) employ test durations specified in test methodologies (SAE 2004; 2011a; Audi AG et al., 2001) which are based on the defined worst-case exposure scenario for vehicle occupants, where a vehicle occupant remains in an un-ventilated vehicle for 20 minutes. Whilst this duration may be justified, there is a lack of any evidence that this is able to provide a representative sample with little variability between tests. This analysis has shown however that a minimum of 15 minutes is required to reduce variability to an acceptable level of 4.5-6%.

This data confirms that the existing test durations specified in standards are sufficient to reduce inter-test variability to an acceptable level. However, where only short durations are employed for testing (Chan et al., 1989 and Schreck et al., 1995) an unacceptably high level of sample variability may be experienced. These short durations have been used to reduce sample removal from the test environment and to comply with sample removal maxima specified in test standards (SAE 2004; 2011a). Therefore to reduce variability and provide representative data it is recommended that not only should a minimum sampling duration of 15 minutes be employed, but equipment with a flow rate of below 10 lpm, to reduce sample removal and comply with test standards (SAE, 2011a). Equipment such as the ELPI, with a vacuum flow rate of 10 lpm (Dekati, n.d.b) or the DMS, at 8 lpm are recommended to be utilised in place of higher vacuum flow rate alternatives, such as many cascade impactors which can remove as much as 30-40 lpm (New Star Environmental, 2004).

In addition to defining test duration and environment comparability, the influence of varying the position at which samples were drawn was also assessed during the research programme. Previous studies have suggested that as long as samples are not drawn from the very bottom of the effluent test tank, little variation would exist between sampling positions, (Starner, 1998). This was surmised from a single, granular, total particle mass concentration measurement, and provided little understanding of any variability over the duration of the test. The assessment of variability between sampling positions conducted in the test tank, supported the findings of Starner (1998) and showed that little variability was detected in the test tank in relation to sampling position. After 500-600 seconds from the point of deployment, variability between the sampling positions reduced to a consistent level of 5-7% and no statistically significant level of variability, ($p>0.05$), was observed. This indicated homogeneity within the test environment, which was likely a product of ‘stirring’ of the environment from the deployment pressure, rapid movement of

the airbag (Chapter 12) and the high concentrations of particles in size ranges with high mobility, such as those of 100nm, and therefore the mean free path of the ambient air in the test environment (Giordano, 2012). These particles did not settle out during the 1200s test (Baron, n.d.) but may have been deposited upon the surface of the test environment by impaction, caused by the over-pressure created on deployment.

The measured low variability between sampling positions, allows a comparison of testing conducted in the literature with varying or unspecified sampling locations. This indicates that no amendment to existing methodologies (SAE 2004; 2011a; Audi AG et al., 2001) is required, and the use of a single, representative sampling location, as specified, shall provide suitable results.

In summary, this assessment of methodologies has shown that an effluent test tank of a comparable volume to the vehicle interior that it represents is not only a suitable environment for airbag effluent testing but is comparable to a vehicle interior. The test tank in fact provides substantially less variable results than those gained in an equivalent test vehicle. To reduce this variability to a consistent level of 4.5-6% a sampling duration of in excess of 900s should be employed for tests in the test tank. This research therefore provided detailed and evidenced data of the robustness of existing test techniques and provides a framework for any future methodologies, such as those using the DMS, as employed in this research programme.

14.3 Test airbag assessment

Four driver frontal airbags representative of those likely to be encountered in large volumes currently, and in the near future, during treatment of ELVs, were identified and selected for assessment. These airbags all utilised a single stage inflator and a non-azide propellant and originated from mid-sized vehicles in the largest selling vehicle class. Three of the assessed airbags used solid propellant inflators, whilst the fourth used a hybrid inflator.

The four airbags and the PM effluents that originated from them were characterised with a number of methodologies to assess the PM effluents arising with respect to particle size distribution, mass and number concentration and morphology. The methodologies are defined in Chapter 6 and reported on in Chapters 8 to 13. A summary of the results from each of the tests for the four tested airbags are shown in Tables 14.1-14.5.

14.3.1 Particle size characteristics

Table 14.1 shows summary data detailing mean particle size, size distribution and particle concentration size proportions with an indication of variability between tests.

Airbag Type	GMD (nm)	Size distribution (nm)	Concentration, size proportion
A: Solid Propellant	135 CoV: 4.1%	Unimodal Primary mode: 150-180	99% <400 96% <300 22% <100
B: Solid Propellant	135 CoV: 4.0%	Unimodal Primary mode: 150-180	99% <400 96% <300 22% <100
C: Solid Propellant	109 CoV: 1.7%	Bimodal Primary mode: 135 Secondary mode: 40-50	99% <300 94% <200 31% <100
D: Hybrid	80 CoV: 1.92%	Bimodal Primary mode: <100 Secondary mode: 20	93% <150 62% <100

Table 14.1: Particle size characteristics summary data

Measurements made with the DMS over the full test duration of 20 minutes identified mean particle size of 80-135nm, with the airbag using a hybrid inflator generating the lowest mean. Tested airbags produced both unimodal and bimodal size distributions, with the primary mode being in the range <100nm – 180nm diameter.

Airbags 'A' and 'B', which both utilised a comparable solid propellant produced a unimodal size distribution with closely comparable mean particle sizes of 135nm, suggesting that other variable factors between the airbags, such as the number of cushion vents, had little effect on measured particle size. However, airbag 'C' that again utilised a solid propellant inflator and airbag 'D', using a hybrid inflator, both produced a bimodal size distribution with the primary mode occurring at 135nm for airbag 'C' and 100nm for airbag 'D'. A secondary mode was also identified at 40-50nm for airbag 'C' and 20nm for airbag 'D'. Whilst these two airbags used substantially different inflators to generate inflation gases they produced similar size distributions, albeit with modes and mean particle sizes smaller for airbag D.

For all airbag types the distributions show a primary mode of lower size than previously presented in the literature, where particles of 0.4 –1 micron were found to be dominant (Chan et al., 1989 and Gross et al., 1994). This apparent reduction in size may be associated with the measurement method employed, as cascade impactors, which were employed in most studies in the literature, provide varying size resolutions, with some offering lower cutpoints of only 0.4 microns (New Star Environmental, 2004). However,

it is difficult to conclusively determine this theory without supporting information regarding these studies in the literature.

Most studies in the open literature reported a clear bimodal size distribution, with the first mode being attributed to the PM emitted during deflagration of the propellant and the second, larger particle mode of 3-10 microns, being attributed to a loose coating on the airbag cushion used to aid its release from the module housing. This study however did not focus on the identification of the larger particle mode but centred on an assessment of the sub-micron element of the effluent. This focus indicated that the DMS employed for the great majority of the analysis, with a measurement resolution of 5-1000nm, was the most suitable measurement apparatus, for this study, with high sampling rate and size resolution capabilities.

However, although the larger particles (>1 micron) were not the focus of the research programme, the use of TEM and SEM allowed the identification of these particles, including those that may represent the second, larger particle mode reported in the literature. This analysis identified the presence of particles between 1-2 micron in size being emitted during deployment of airbags 'A' and 'C', both using a solid propellant inflator. However, basic assessment suggested that these particles were low in concentration and therefore unlikely to produce a notable secondary mode, unless measured by mass as opposed to number concentration.

The general absence of this larger secondary mode was likely to be attributed to the use of adhered cushion coatings on the airbags tested in this study, and therefore a lack of a loose coating. In some cases however, a secondary smaller particle size mode was identified, in the range 7-25nm. A similar mode was identified by Gross et al. (1994) whose assessment showed a less prominent mode of smaller particles of around 50nm. This study by Gross et al. (1994), however, only measured particle mass with an impactor and did not provide any transient concentration measurements.

It is likely that the increased size resolution and particle number measurement capabilities offered by the DMS, especially in the sub-micron and nano-scale size range, allowed these small particle secondary modes to be identified with greater clarity than previously presented by Gross et al., (1994). The DMS offered 38 size cutpoints in 5-1000nm range whilst the ELPI, which offers good size resolution capabilities, offers only 10, within the same size range (Dekati, n.d.a) and the impactor used by Gross et al., (1994), only provided 8.

Further assessment of particle size and number concentration for all the airbags showed that of the particles emitted in the range 5-1000nm, over 99% were below 400nm in size

and in the case of the hybrid airbag, 93% were below 150nm. A mathematical model based on an exponential function was defined to describe this size proportion distribution, with differing constants used for each airbag tested. This model provided closely comparable results when compared to measured data and can be used to quantify exposure to particles of a particular size, without the requirement to undertake further testing.

In addition to direct measurements by gravimetric filtration and indirect measurement by means of the DMS, the assessment of particle size and morphology by means of EM, allowed the verification of particle size measurements recorded by the DMS in the same manner as Price (2009), who measured PM from engine exhaust emissions. In addition to verifying the size measurement capabilities of the DMS, the technique allowed measurement and characterisation of particles not only in the 5-1000nm range of the DMS but also in a wider size range. This assessment identified particle sizes both below and above the measurement range of the DMS in a number of cases. In most instances these particles were larger than 1 micron, but in the case of the airbag using a hybrid inflator, a large concentration of particles were identified below the lower size resolution of the DMS and therefore less than 5nm in size. The identification of these particles would not have been possible with either the DMS or the other measurement methods commonly employed for airbag effluent particle assessment and would only be identified by the use of EM or a condensation particle counter (The University of Manchester, n.d.a) and therefore demonstrates the value of complimentary measurement techniques as endorsed by Ziegahn and Nickl (2002).

The identification of particles in the nano-scale size range is of particular interest due to their ability to translocate within the body (Oberdorster et al., 2005) and a lack of characterisation in the literature of these particles originating from airbags. Whilst the aim of this study was not to determine the effect of exposure to these effluents on human health, the propensity of these effluents to pose harm to human health is closely linked to many of the key characteristics defined in this study, such as particle size, concentration and morphology.

14.3.2 Particle mass and number concentration

Table 14.2 shows summary data detailing mean particle mass and number concentration and associated variability between tests.

Airbag Type	Mean mass concentration (mg/m^3)	Mean number concentration (N/cc)
A: Solid Propellant	80.6 CoV: 8.6%	2.07E+06 CoV: 2.92%
B: Solid Propellant	69.4 CoV: 6.9%	2.09E+06 CoV: 3.19%
C: Solid Propellant	41.9 CoV: 17.8%	2.84E+06 CoV: 12.35%
D: Hybrid	6.7 CoV: 13%	2.04E+06 CoV: 5.37%

Table 14.2: Particle concentration summary data

Particle mass concentration measured by gravimetric filtration, showed that PM effluents from airbags remained below maximum concentration values, of $125mg/m^3$ specified in test standards (SAE 2011a; Audi AG et al., 2001). However, values may exceed apportioned values (SAE, 2004) when measuring particle mass concentrations for multiple airbags. Tested airbags using a solid propellant inflator produced higher outputs than airbags using a hybrid inflator, with concentrations being as low as 7% of the highest concentration value. However, whilst effluent PM mass from solid propellant airbags was higher, measured values remained lower than for airbags using a sodium azide solid propellant (Chan et al., 1989) and compared well to other mass concentrations defined in the literature for effluents from non-azide, solid propellant airbags (Gross et al., 1999). Analysis of airbags using a hybrid inflator are yet to be reported in open literature and therefore comparisons cannot easily be made, but lower propellant masses, as commonplace in hybrid airbags, is reported as resulting in lower effluents (ARC, 2009).

Test and analysis showed that the airbag from the more modern vehicle (airbag C) produced lower PM mass concentration than the more aged systems (airbags A and B). This may have been expected as theoretically PM mass concentration from airbags should have reduced over time as systems have developed.

The direct measurement of PM mass, although a defined method in airbag effluent test standards, has provided limited information regarding smaller particles, especially those in the nano-scale, due to the need for extreme levels of accuracy in mass measurement, and therefore the measurement of particle number concentration is rapidly becoming the favoured method for smaller particle measurement (Cambustion, 2008; Oberdorster et al., 2005; Zheng et al., 2011).

As with mass concentration, one may have also expected that the more contemporary airbag (airbag C) would have produced a lower PM effluent number concentration, but this airbag produced a higher number concentration than the more aged airbag systems. This indicated that the particles emitted by airbag C were not only smaller but likely of a lower mass than those emitted by airbags A and B.

The airbag using a hybrid inflator produced lower particle number concentrations than all other solid propellant airbags. However, unlike mass concentration, this was not substantially lower, and was in fact comparable to other airbags (A and B) using a solid propellant inflator. This indicated that as PM mass concentration was significantly lower, and particle number concentration comparable, that mean particle size and mass were substantially lower from the airbag using a hybrid inflator than those airbags using a solid propellant inflator, yet number concentration remained comparable.

As an airbag utilising a hybrid inflator uses a substantially lower mass of propellant than those that use a solid propellant exclusively, this analysis indicates that propellant mass is not necessarily an indicator of PM number concentration, but appears to correlate more with PM mass measurements. These findings cannot be verified by other studies in the open literature and this lack of data prevents any contextual evaluation of the findings from this study.

The accurate quantification of particle number concentration using the DMS negated the requirement to undertake any accurate concentration quantification as part of the morphological assessment of particles by electron microscopy conducted within this study. Whilst not being used for accurate quantification, EM was used to simply estimate the proportion of total particle concentration attributed to particles larger and smaller than the measurement limits of the DMS.

14.3.3 Particle number concentration and size evolution with time

This analysis of airbag PM effluents has shown that the evolution of particle size and concentration with time are closely linked and little analysis or definition has been reported in open literature. However, knowledge of this behaviour is key to assist in defining the behaviour of the effluents created during airbag deployment and for quantifying human exposure for both vehicle occupants and those neutralising airbags at a vehicle's end of life.

Tables 14.3 shows summary data detailing the evolution of particle number concentration and size over the test duration, with an indication of variability between tests. Table 14.4 summarises data regarding the evolution of size segmented number concentration.

Airbag Type	Number concentration evolution	Particle size evolution
A: Solid Propellant	D+25s = Max. 2.37E+07 N/cc D+1200s = Min 1.89E+05 N/cc	Increase then reduction over time D+360s = 180-190nm D+720s = 180-195nm D+1200s = 160-182nm
B: Solid Propellant	D+16s = Max. 2.18E+07 N/cc D+1200s = Min. 4.67E+05 N/cc	Increase over time D+360s = 169-175nm D+720s = 182-190nm D+1200s = 200nm
C: Solid Propellant	D+2s = Max. 6.04E+07 N/cc D+1200s = Min. 1.46E+06 N/cc	Increase over time D+360s = 128-132nm D+720s = 138-143nm D+1200s = 146-155nm
D: Hybrid	D+6s = Max. 1.95E+07 N/cc D+1200s = Min. 9.21E+05 N/cc	Increase over time D+360s = 89-92nm D+720s = 110-112nm D+1200s = 127-130nm

Table 14.3: Particle number concentration and size evolution summary data (Note: D = time of deployment)

Airbag Type	Size segmented number concentration evolution
A: Solid Propellant	D+20s: 5-100nm dominant D+360s: 100-200nm dominant and 5-100nm reduced to lowest concentration D+1200s: 150-200nm dominant
B: Solid Propellant	D+20s: 5-100nm dominant D+360s: 100-200nm dominant and 5-100nm reduced to lowest concentration D+1200s: 150-250nm dominant
C: Solid Propellant	D+20s: 5-150nm dominant D+360s: 100-150nm dominant D+1200s: 100-150nm dominant
D: Hybrid	D+20s: 5-100nm dominant D+360s: 50-100nm dominant D+1200s: 100-150nm dominant

Table 14.4: Size segregated particle number concentration evolution summary data (Note: D = time of deployment)

The use of mean particle concentration and size measurement, as defined in test standards (SAE 2004; 2011a; Audi AG et al., 2001) and employed widely in studies reported in the literature, provides no information with regard to transient behaviour.

There are few options for the measurement of evolution of airbag effluent particle mass concentration detailed in the literature and these are limited to the use of sequential 5 minute gravimetric filter measurements (Wheatley et al. 1997; Gross et al., 1994; 1995; 1999; Schreck et al., 1995) and the use of a realtime aerosol monitor (Chan, 1989). The measurement of variability over time and the definition of a test duration in this study indicated that an analysis by 5 minute sequential gravimetric filter measurement is not able to provide a robust measurement with an acceptable degree of variability, unless samples were drawn for over 15 minutes. Such an approach is not suitable however, as the test duration would be extended to an unacceptable duration and not replicate exposure scenarios.

During Chan's 1989 study a realtime aerosol monitor was employed to define the evolution of total particle mass concentration and this system offered a response time of 8s. The DMS used in this research was able to offer a response time of 300ms and measured particle number concentration. The assessments of PM effluent by means of the DMS showed that particle concentration evolved rapidly and that a reduced response time during measurements would be favourable for comprehensive assessments of airbag effluents and this capability in combination with other advantages (Chapter 6) confirmed the suitability of the DMS for such an assessment, Tables 14.3 and 14.4.

The assessment of airbag PM effluents conducted within this research programme showed that initially after deployment a high concentration of PM effluent was generated and released into the test environment and subsequently reduced over time. Peak concentrations were reached in the first 25 seconds after deployment with an initial substantial reduction in concentration followed by a less pronounced and continuous reduction over the remainder of the test duration.

This behaviour is difficult to review in context of the literature due to a lack of comparable data, but appears comparable to that of the analysis conducted by Chan et al. (1989). The study by Chan et al. identified a high particle mass concentration appearing up to 60 seconds after deployment of the airbag and then a substantial reduction in the following 60 seconds, followed by a subsequent further reduction at a reduced rate over the remainder of the test. Chan et al., (1989) stated that the initial concentration and reduction consisted of '*large corn starch particles that settled out quickly'*. The behaviour of these larger particles is comparable to that of the particles measured during this research programme; however the measured particles were far smaller, with particle concentrations in the 5-200nm size range reducing quickly, Table 14.4. In this instance the reduction is therefore not likely to be associated with particle settling, with smaller particles remaining mobile for far longer (Baron, n.d.), but may more likely be associated with:

a) impaction of particles on the surfaces of the test environment
b) agglomeration of particles

The impaction of particles on the surfaces of the test environments, although not tested, most likely occurred due to the high pressure output of the inflation gases, forcing particles from the airbag cushion against the surfaces, yet an assessment to confirm such a theory would be required.

Whilst the likelihood of impaction was not proven in this research, the agglomeration of particles was identified by means of DMS and EM assessments. The DMS analysis showed that for all airbag PM effluents, particle GMD increased after deployment, with an initial rapid increase followed by a slower increase throughout the majority of the test. Assessing these changes in particle size, when related to concentration segregated into a number of smaller particle size ranges, provided further information regarding the PM effluents and the apparent particle agglomeration. In general this analysis showed that after the initial release of PM:

a) Particle concentrations in smaller particle size ranges (5-100nm) decrease
b) Particle concentrations in larger particle size ranges (100-300nm) increase

This analysis suggests that smaller particles are generated during the deployment of airbags and these agglomerate to produce groupings of particles that are measured as larger particles by the DMS. This particle grouping occurs due to Brownian motion or gravitational agglomeration, with Brownian agglomeration occurring when particles with random motion, collide with one another and join together. Gravitational agglomeration occurs when larger particles, commonly those larger than a micron (super-micron), settle quickly and capture smaller particles as they do so (Allen et al., 2001).

The indication from size and concentration data provided by the DMS, that the PM effluent is agglomerating is supported by the micrographs generated by EM and associated analyses (Chapter 13). These micrographs produced from samples collected 60 seconds after deployment, showed that at this measurement point particle agglomerates were present. The micrographs showed both super-micron particles appended by smaller particles and large groupings of smaller particle agglomerates, thus indicating both Brownian and gravitational agglomeration were responsible for the apparent changes in particle sizes and concentrations, measured by the DMS.

This data provides the first evidenced data to describe the evolution of airbag PM effluents and allows for more accurate exposure quantification and assessment for those exposed to these effluents either when disposing of airbags at a vehicle's end of life or post-collision for vehicle occupants.

14.4 Modelling PM effluents

The assessment of PM effluents with the DMS has allowed a mathematical model based on an exponential function to be defined that allows the proportion of the total particle number concentration in particular size ranges to be defined. Whilst mathematical models are well used to describe particle behaviours such as settling (Adetunji et al., 2009) and deposition and retention in the human body (ICRP, 1994) there are no apparent, comparable models used to describe characteristics of PM effluents from airbags in the nanoscale and as such this represents a novel approach in the field.

This has shown that a mathematical model can be used to accurately describe effluent PM characteristics and that each airbag using a differing propellant provides a distinct 'signature' that can be used to identify particular characteristics of airbag types. The modelling has not shown that each airbag can be identified from one another based on this size proportion data; however the propellant type used for each airbag can be. This assumption is confirmed by the lack of any notable difference in the model between airbags 'A' and 'B', which utilise the same propellant type and the clear difference between all other airbag and therefore propellant types.

The data provided by these models allows the concentration of particles of a particular size to be calculated for airbags and may be used in future studies that quantify exposure to airbag PM effluents in the nanoscale size range.

14.5 Morphological assessment

The assessment of particle morphology conducted by EM employed both SEM and TEM. These techniques provided supplementary information regarding particle size, concentration and morphological characteristics for particles in size ranges both above and below the measurement range of the DMS that was used for the great majority of the PM effluent assessment described in this thesis. The technique also identified the agglomeration of particles.

Airbag Type	Particle morphology	
	Size and concentration	**Characteristics**
A: Solid Propellant	Dominant: 30-150nm Lower concentration: 300-600nm and 2000nm	Spherical agglomerates
B: Solid Propellant	Dominant: 20-80nm	Spherical agglomerates
C: Solid Propellant	Dominant: 15-150nm Lower concentration: ~750nm and 500-1500nm	Spherical and rectangular agglomerates (~750nm)
D: Hybrid	Dominant: 2-40nm Lower concentration: 50-80nm and 200-500nm	Spherical agglomerates, 2-40nm and 50-500nm

Table 14.5: Particle morphology summary data

To allow analysis, particles were collected on filmed TEM grids used to intercept particles in a vacuum flow, from within the effluent test tank. With high particle concentrations being generated during deployment, a low sample vacuum flow rate of 3 litres per minute and short sampling durations were required to prevent high grid loading that would prevent analysis of particle characteristics. These durations were defined iteratively and were all below 1 minute, with some being substantially shorter for the higher particle concentration effluents. These short sampling durations and low vacuum flow rate requirements suggest that particle collection on TEM grids in the DMS, as demonstrated by Price (2009) would need to be conducted with substantial sample dilution to prevent grids from becoming overloaded. Comparable techniques to collect airborne PM particles upon TEM grid films are not limited to that demonstrated by Price

(2009), with collection on grids within cascade impactors also an option, although again efforts to reduce grid film loading would need to be employed.

For the assessment of airbag PM effluents the collection of particles on grids has not been described in the literature. The only documented method is sample collection with stubs coated with an adhesive or the use of adhesive films. These collection methods only allow assessment of particles with light microscopy or SEM and have been employed for the latter to characterise particles for forensic analyses (Marsh, 2011; Wyatt, 2011; Berk, 2009a; b). The aims of these studies generally differed to those of the study reported here, with the focus of most analyses in the literature being to compare airbag particle effluents to gunshot residue (GSR), thereby focusing on analysis of particles down to 1 micron in size (The FBI, 2011).

These studies therefore failed to assess or even identify particles in the sub-micron and nano-scale that formed the focus of the current research programme reported on in this thesis.

Initial assessment of particle size characteristics by TEM showed that the DMS provided accurate particle size measurements, within its measurement range capabilities and in agreement with the findings of Price et al (2009).

In addition to the identification of particle size and agglomeration characteristics, the assessment showed that, in general, there were similarities between the morphologies of particles emitted from each of the four subject airbags with the great majority of particles appearing generally spherical in nature.

14.6 Post-deployment vehicle ventilation

A lack of a coherent understanding and assessment method formed the stimulus for the research investigating in-vehicle airbag deployment and subsequent vehicle ventilation, during ELV treatment. Little quantification of the effect of ventilation on PM effluent concentration has been presented, although, varying recommendations regarding the process for airbag deployment and vehicle ventilation exist in the literature. Some state that airbags should be deployed outside of the test vehicle, whilst others provide options depending on the type and number of airbags to be deployed (IDIS, 2011; Mercedes Benz, 2002), and others remaining less clear regarding the method to be employed (SAE, 2010). There is little clear and cogent information detailing ventilation requirements, whether deployments are conducted within a vehicle or not. Mention is only briefly being made of the use of extraction systems, with usage requirements appearing to be backed up by little evidence (SAE, 2010). The use of extraction has only been observed at a state-

of-the-art facility in France (Re-Source Engineering Solutions, n.d.) and has not been observed in use in the UK and therefore the assessment did not consider stimulated ventilation and concentrated only on natural ventilation by opening of a test vehicle.

In addition, due to the sheer volume of airbags and other pyrotechnic devices from ELVs requiring neutralisation, and the ability for airbags to be deployed rapidly whilst in-situ, (Autodrain, 2012; Vortex Depollution, 2013), it is expected that neutralisation will nearly exclusively be conducted within vehicles. This therefore confirms the need for the testing in vehicles, initially without extraction, that has been undertaken within this research programme.

Tests conducted in vehicles showed that if a single front door of the test vehicle was opened 60 seconds after deployment; that particle concentration reduced to between 33% and 8% of the pre-ventilation concentration after a further 300s. After an additional 300s, number concentration had reduced to values of between 14% and 3%. These tests showed that particle concentration proportions and therefore absolute concentrations were significantly lower than those measured in the vehicle interior prior to ventilation.

14.7 Applicability to exposure scenario and data quality

An assessment at a small number of authorised treatment facilities was conducted by the author to understand the airbag neutralisation process at end of life depollution facilities. This provided key information regarding the task based exposure characteristics, yet without standardisation or guidance regarding these tasks it is unlikely to provide a comprehensive illustration of practice. Exposure to PM airbag effluents during ELV airbag neutralisation is likely to vary widely. However, in terms of re-entry and ventilation of an ELV after airbag deployment, the tests conducted and information provided indicates what is likely to be a worst case scenario for this exposure, with the vehicle remaining sealed during deployments and then ventilated soon after by opening a single door of the vehicle. The rationale is the same for existing effluent test tank and human exposure testing methodologies (SAE 2004; 2011a; Audi AG et al., 2001) where the likely worst case exposure scenario forms the basis of the test methodology.

Further applicability to the exposure scenario was also achieved by conducting tests not only in an effluent test tank but also in the interior of a vehicle to ensure any testing in purpose built test facilities replicates that of the actual exposure conditions with a vehicle.

Chapter 15

Conclusions

15.1 Introduction

Vehicle airbags have proved to be an effective element in reducing occupant injury and mortality risk during many types of collisions and are therefore widely used worldwide, with their use being legislated in some countries. When airbags are not deployed in collisions, they can reach the ELV waste stream and consequently, in many countries, must be neutralised or removed to minimise any health or environmental impact posed. In the EU end of life vehicle (ELV) legislation requires the neutralisation or removal or airbags and other energetic safety systems during the ELV depollution process. During this neutralisation process, airbags are deployed in vehicles remotely by operatives. After deployment the operatives return to the vehicles to continue depollution or retrieve deployment equipment. Consequently these processes repeatedly expose the operatives to a solid particle effluent produced when the airbags are deployed. This effluent is produced during the production of inflation gases by the deflagration of a propellant mixture.

Previous research regarding exposure to these effluents has focused only on the single-time exposure encountered after airbag deployment during a collision. However, the multiple exposures experienced by deployment operatives has acted as the stimulus for this research which conducted more expansive and diverse evaluation with contemporary equipment and methodologies than previously demonstrated. Therefore, the research presented within this thesis has contributed to an increase in knowledge in the field of airbag effluents and more specifically for solid particle effluents. In particular this research has provided information, not previously presented in the literature, regarding evaluation of test methodologies and characterisation of particle effluents in the sub-

micron and nano-scale size ranges. This will assist in characterising interactions with airbag effluents during ELV depollution and for post-collision exposures.

The main conclusions for each of the key investigation areas of this study are as follows.

15.2 Neutralisation quantification and scale of exposure

- The number of un-deployed airbags reaching EOL and requiring neutralisation in the UK alone was calculated at 6.5 million in 2012, an increase of 2.2 million from 2008. These airbags were required to be neutralised by approximately 1700 Authorised Treatment Facilities (ATFs) by operatives using simplistic deployment procedures to process large volumes of airbags.

15.3 Test methodologies

- Existing test methodologies used for airbag assessments in an effluent test tank are able to replicate the interior of an equivalently sized vehicle. Tests conducted in the test tank also resulted in lower inter-test variability than those conducted in the vehicle when measuring particle number concentrations. Test durations of at least 15 minutes are required to reduce variability to a consistently low level of approximately 6%.

15.4 Particle mass assessment:

- An assessment of effluent particle mass showed that the measured concentrations from tested airbags are in most instances considerably lower than those reported in the literature. Particle masses from airbags using a solid propellant inflator were considerably higher than for those using a hybrid inflator and in no case did concentration exceed the maximum specified limits for single-time, individual airbag, vehicle occupant exposures.

15.5 Particle size distribution

- Particle size calculated over the 1200s test duration ranged from 80nm to 135nm, depending on the airbag tested, with those using a solid propellant inflator, producing effluents with a mean particle size substantially higher than those produced by airbags using a hybrid inflator.
- The mean particle sizes obtained using the DMS were lower than those previously presented in the literature, (Chan et al., 1989; Gross et al., 1994; 1995; Ziegahn and

Nickl 2002), with >99% of particles emitted by tested airbags being smaller than 400nm.

- Time resolved particle size data showed that in all cases particle size increased considerably in the early stages after initial deployment (commonly after 60-360s) and then generally continued to increase throughout the test, albeit at a reduced rate. The smallest increases in size were identified for the airbag using a hybrid inflator.
- A unimodal particle size distribution was apparent for solid propellant airbags with the dominant mode arising between 135nm and 180nm. The hybrid airbag demonstrated a bimodal distribution with the primary mode at less than 100nm and the secondary mode at 20nm-25nm.
- The increase in size of particles emitted during deployments of airbags A, B and C was associated with an increase in relative humidity measured within the test tank, whilst temperature appears to stay relative stable throughout the test. This general trend does not appear to be replicated during tests of the emission from the hybrid airbag.

15.6 Particle concentration

- Mean particle number concentrations of between 2.05E+06 and 2.85E+06 were recorded. However, little data from comparable PM sources was defined in the literature in terms of number concentration and therefore simple associations were not easily drawn.
- Airbags utilising a solid propellant inflator produced higher PM concentrations than airbags using hybrid inflators.
- The length of time since deployment at which maximum concentration occurred varied from 2-21 seconds, with no clear difference found between the airbags using hybrid and solid propellant inflators.
- After the maximum particle concentration was attained, the concentration reduced over the remaining test duration at different rates depending on the airbag being tested. This reduction in concentration may well be associated with particle agglomeration or unintended sample loss; however the latter is unlikely due to the type of test environment employed.
- The concentration of smaller particles, in the nano-scale (<100nm) were initially greater than those in the higher size range of greater than 100nm. Over time the concentration of these smaller particles reduced whilst conversely the larger particles increase in concentration. This suggests that the smaller particles are agglomerating and thus an increase in concentration of larger particles is observed over time with a

reduction in smaller particles. This theory is supported by the particle size data that shows an increase in mean particle size in relation to time.

15.7 Mathematical modelling

- A mathematical model based on an exponential function was used to allow a distinct 'signature' to be defined for each of the tested airbags. The model defined the number concentration of particles of a particular size and consequently could be used to identify the likely exposure to particles of particular sizes for vehicle occupants after a collision and for ELV airbag deployment operatives.

15.8 Vehicle ventilation

- Tests conducted to replicate the ventilation of a vehicle after airbag deployment in an ELV situation identified that by opening one door of the test vehicle 60 seconds after deployment of a driver airbag, a significant drop in number concentration was measured in the first 300 seconds. After 600 seconds, the proportion of pre-venting particle concentration remaining dropped to between 14% and 3%, depending on the type of airbag being tested and other likely factors such as the air-exchange rate, although significant variability was identified.

15.9 Particle morphological assessment

- A method capable of capturing samples suitable for analysis by TEM and SEM was identified and assessment of micrographs showed that particle sizes defined from TEM and SEM correlate well to those measured with the DMS. In some instances particles were identified that were outside of the 5-1000nm measurement range of the DMS with large concentrations of particles as small as 2-3nm being identified, indicating that complimentary measurement methods should be used in combination to increase effective size resolution.
- The particles had the appearance of soot-like, combustion particles and these were nearly exclusively spherical and appeared commonly as agglomerates. The use of SEM identified that particles were collecting on top of one another and on the TEM grid surfaces and that both SEM and TEM should be used to robustly define effluent morphological characteristics.

The completion of the programme of study, as detailed in this thesis resulted in the achievement of objectives as defined in Chapter 1. However, as a consequence of the

scope and nature of this research, a number of areas of future work have been identified, to further increase knowledge in the field and these are detailed in Chapter 16.

Chapter 16

Suggestions for Future Directions

Whilst the presented research has substantially increased knowledge in the field of airbag effluent assessment and characterisation, there are clear opportunities to capitalise on the knowledge and novel material presented in this study, to provide even greater understanding of these effluents and human interactions with them and develop the presented ideas further.

- Whilst representative, the airbags selected for the focus of this research programme, represent, a relatively small sample size. Therefore to further increase the understanding and knowledge in the field it is recommended that other airbag types are assessed. This could include airbags that utilise inflators with different propellant compositions and masses, such as those in passenger and seat applications, along with smaller automotive pyrotechnics such as safety belt pre-tensioners and actuators.

- It is recommended that assessment of effluents from deployments of multiple airbags is conducted. Vehicles are now being equipped with multiple airbags which will soon reach end-of-life in larger volumes than they are currently. . Such an assessment may allow for the applicability of an additive type of assessment (where airbags are tested separately and spectral densities then combined) to be used to define 'vehicle airbag effluent concentrations'.

- To assist in defining any potential hazard to health posed by exposure to airbag effluents it would be beneficial to define other characteristics of the identified particles such as their composition, hygroscopicity, solubility and alkalinity which are all known to impact on a particle's propensity to illicit a human response.

- To provide greater information about the exposure situation it would be beneficial to undertake ventilation testing in a more controlled situation, with measurement of the air exchange rate and with varying the ventilation method by testing with more or less doors and windows being opened.

- With other characteristics of airbag particle effluents defined and further assessment of the exposure scenario, the presented data regarding particle concentrations may be applied to the two exposure scenarios of (a) post-collision exposures encountered after a vehicle collision and (b) the occupational exposure experienced during the process of ELV depollution, to assist in defining any risk associated with exposure to these effluents and any associated control measures that may be required.

- The assessment of particle morphologies has provided substantial novel data regarding airbag solid particle effluents and it is recommended that to capitalise on this, further assessments would consider defining any changes in particle morphology associated with time. This could be linked to DMS data such as that presented.

- It is possible that the use of TEM may be able to identify effluent particles from particular airbags or propellant types in a way not previously possible with SEM (Marsh, 2011; Wyatt, 2011; Berk, 2009a/b), as each of the airbags appeared to provide differing size and/or other physical characteristics and it is recommended that this is investigated further.

- The assessment of existing test methodologies has helped to define a robust set of requirements that should be adhered to when testing and characterising airbag effluents and in addition a new test protocol for measuring effluents. It is recommended that the methodologies are developed into a test procedure with limitations and requirements defined based on the further work suggested within this section.

Appendix A

Airbag consumption and un-deployed volume calculations

A1 Statistical analysis of vehicle parc and un-deployed occupant restraints: 2008-2012

To define the number of automotive occupant restraints requiring treatment within ELVs (in-line with EU Legislation) an analysis of passenger car sales, vehicle attrition, restraint fitment rates and likely consumption rates was conducted. Each of these stages required independent analyses of the data as defined within the following sections.

A1.1 UK Vehicle sales and occupant restraint fitment data

Passenger car sales in the UK have fluctuated between 1.95 million (1995) and 2.58 million (2003) over the last 15 years, (SMMT, 2010) whilst fitment of automotive pyrotechnic restraints has steadily increased. Occupant restraint fitment data provided by vehicle manufacturers (JATO, 2011) defined fitment rates for driver, passenger and knee airbags (DAB, PAB and KAB), front seat safety belt pre-tensioners (FBP) and driver and passenger anti-submarining airbags (DASA/PASA), Table A1.1. Data regarding restraints for rear seat positions and side impact and rollover protection were not readily available, therefore pyrotechnic restraint systems for rear seat positions were not considered in this review and side airbag (SAB) fitment has been estimated; based on lagged values for passenger airbags, which were thought to bear similarities in uptake.

Year	Estimated ELV mfg. year	DAB Fitment	PAB Fitment	FBP Fitment	KAB Fitment	PASA Fitment	DASA Fitment	SAB Fitment
2006	1993	0.652	0.020	1.510	0	0	0	0.004
2007	1994	0.693	0.035	1.560	0	0	0	0.008
2008	1995	0.738	0.061	1.611	0	0	0	0.016
2009	1996	0.785	0.105	1.663	0	0	0	0.030
2010	1997	0.835	0.180	1.718	0	0	0	0.057
2011	1998	0.889	0.311	1.774	0	0	0	0.108
2012	1999	0.946	0.536	1.832	0	0	0	0.204
2013	2000	0.976	0.665	1.882	0	0	0	0.420
2014	2001	0.996	0.786	1.928	0	0	0	0.575
2015	2002	0.996	0.850	1.932	0.006	0	0	0.660
2016	2003	0.998	0.911	1.946	0.012	0.006	0.006	0.842
2017	2004	0.999	0.940	1.956	0.019	0.006	0.006	1.015
2018	2005	0.999	0.962	1.964	0.029	0.007	0.007	1.165
2019	2006	0.999	0.987	1.974	0.048	0.015	0.015	1.427
2020	2007	0.999	0.988	1.976	0.097	0.014	0.014	1.564
2021	2008	0.999	0.985	1.972	0.130	0.010	0.010	1.708
2022	2009	0.999	0.998	1.996	0.204	0.020	0.016	1.924
2023	2010	0.999	0.999	1.998	0.274	0.015	0.014	1.974
2024	2011	0.999	0.999	1.998	0.344	0.015	0.014	1.976

Table A1.1: Occupant restraint fitment rates

From 1993 to 2002 the number of devices fitted to new vehicles is estimated to have doubled and tripled by 2011. Low fitment rates for anti-submarining airbags are associated with their use only being required for certain convertible vehicles.

A1.2 Vehicle attrition

Understanding the factors which contribute to a vehicle reaching its EOL and thus the average vehicle's lifespan allows for estimates of natural and premature vehicle attrition to be estimated. The age and proportion of vehicles reaching their EOL was defined from passenger car licensing data (DfT, 2011b). During years 0 to 4, after manufacture, some undefined variances in the number of vehicles licenced were identified and therefore data has been supplemented by values from a study by Morris and Crooks (2007). The proportional drop in licensed passenger cars (attrition) over 16 years is shown within Figure A.1.

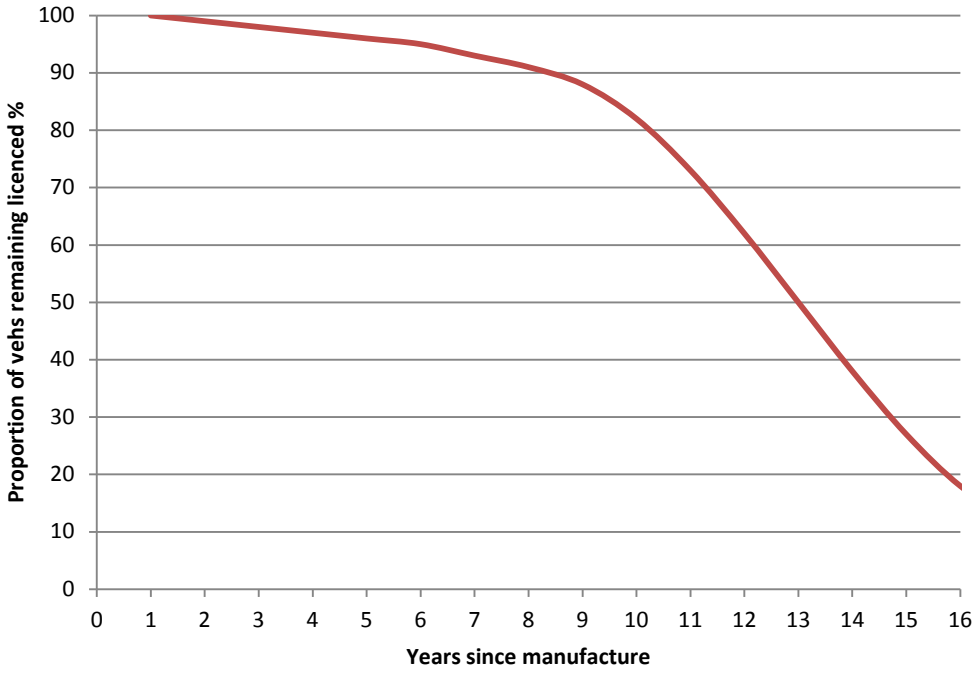

Figure A1.1: Passenger car attrition

A1.3 ELV causation factors

Vehicles reach their EOL for many reasons, yet can be simply classified as either 'premature' or 'natural' ELVs. Premature ELVs include those damaged in collisions, by fire, theft or other 'un-natural' reason, whilst natural ELVs are those that reach their EOL due to degradation over time. Analysis of each ELV category and their influence upon vehicle attrition, as defined within Figure A.1 follows.

A1.3.1 Premature ELV causation

Vehicles may reach the end of their life prematurely through unexpected events, such as collisions, theft, vandalism and fire damage. Collisions account for the greatest proportion of premature ELVs, (Morris and Crooks, 2007) whilst fires and natural occurrences although not easily quantified are expected to occur in comparatively small numbers and are therefore not considered further.

A1.3.2 Premature ELV collision severity and point of impact

As collisions account for the highest proportion of premature ELVs, collision severity and impact point from over two million collisions involving passenger cars (and taxis) in the UK were defined. Data was analysed from collisions where an injury was sustained and the collision was attended by, (or was subsequently reported to) the Police between 1998 and 2008 (DfT, 2012a; 2012b). This data identified that 50% of those collisions involved a frontal impact, 26% were rear impacts and 23% were side impacts (10% nearside and 13% offside). The remainder of those recorded collisions were those which involved a rollover or where no impact was recorded (2%).

This data was split further for each of the four identified categories (front, rear, side and other) into those collisions where occupants sustained a fatal, serious or slight injury. The data for these sub-categories is summarised below in Table A1.2. Of all collision types, 49% were frontal impacts and less than 1% of all collisions resulting in a fatal injury arose from a frontal impact.

	Impact side as a proportion of all injury collisions			
Injury severity	**Frontal impact %**	**Rear impact %**	**Side impact %**	**Other %**
Fatal	0.507	0.037	0.311	0.004
Serious	5.442	0.634	1.956	0.194
Slight/minor	43.540	25.279	20.231	1.850
Total	49.489	25.950	22.498	2.048

Table A1.2: Injury groups of impact direction UK, 1998-2008

Robust data regarding damage only incidents was not readily available, yet the Department for Transport (DfT) estimated that these accounted for an additional 2.45 million collisions in 2009 alone (DfT, 2009). For the purpose of this analysis it was assumed that 'damage only collisions' occurred in the same impact type proportions as

injury collisions. The use of this data and information from CCIS case reports (DfT, 2012) has allowed estimates of the likely severity of vehicle damage associated with the previously identified injury severity groups to be defined, Table A1.3.

Associated damage proportion	Injury Severity		
	Fatal	Serious	Slight
Severe	90%	15%	5 %
Moderate	9%	75%	20 %
Minor	1%	10%	75 %

Table A1.3: Injury severity and likely vehicle damage

For example, for fatal collisions it has been estimated that 90% will have resulted in severe vehicle damage, 9% in moderate damage and 1% in minor damage.

A1.3.3 Natural ELV causation

As vehicles age and their residual value drops, mechanical failure or body damage is increasingly likely to result in those vehicles reaching their EOL and therefore these are termed 'natural ELVs'. For this analysis the proportion of vehicles reaching their EOL 'naturally' was derived from a study by Morris and Crooks (2007). This data estimates that sixteen years after manufacture 73% of passenger cars would have reached their EOL 'naturally'.

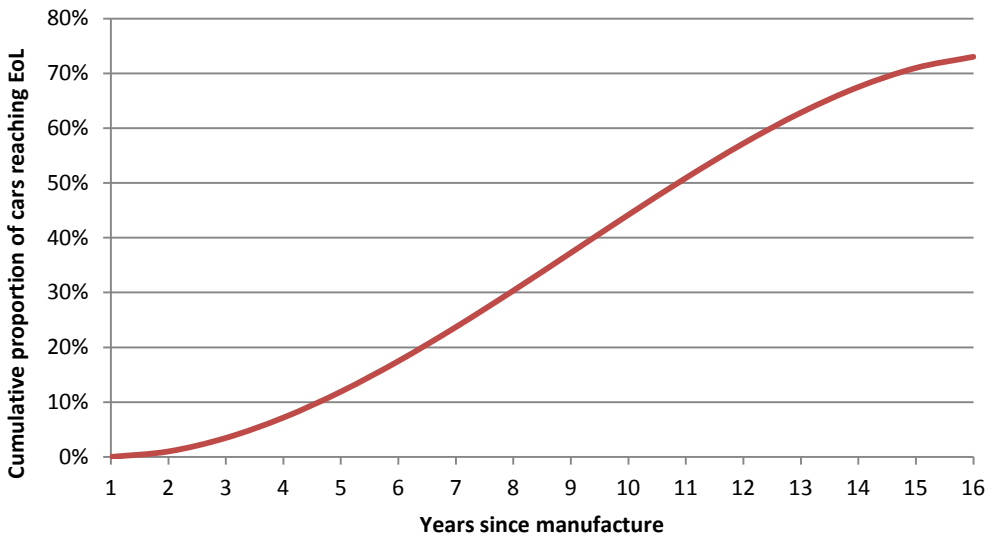

Figure A1.2: Natural passenger car attrition

A1.4 Summarised attrition causes

Using the previously identified data regarding impact point and severity in combination with data from Morris and Crooks (2007), causes of vehicle attrition have been defined, Figure A1.3. The proportional reduction of each impact type and severity is related to increasing 'natural' attrition.

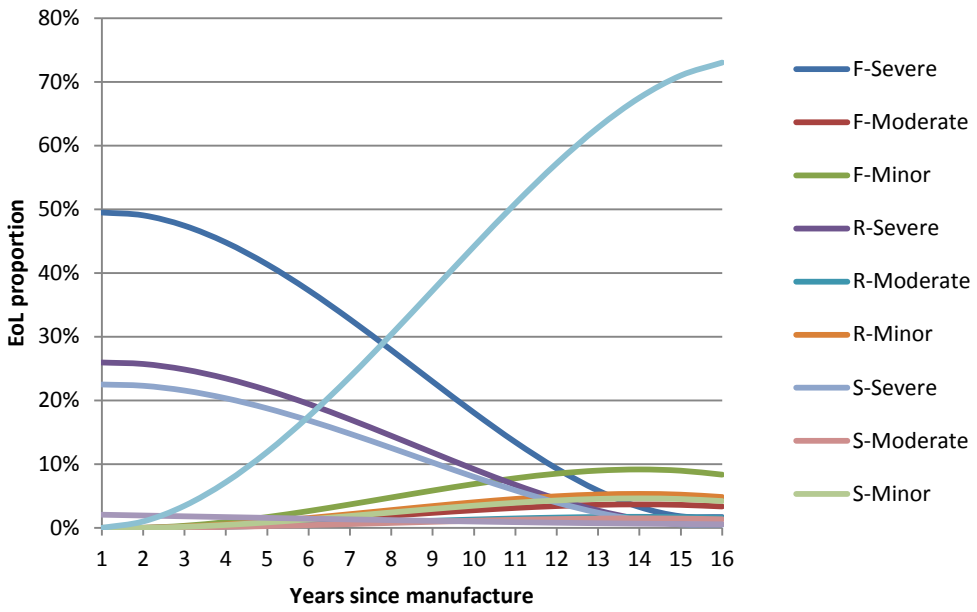

Figure A1.3: Summarised passenger car attrition

A1.5 Occupant restraint consumption rates

With the number of vehicles, causes of EOL and the likelihood of airbag and safety belt pre-tensioner consumption defined, the numbers of remaining live devices could be estimated. Consumption figures have been calculated by using estimates for each impact type and the likely front seat occupation values from national travel statistics. (Transport Scotland, 2012) This data indicated that journeys undertaken with a single occupant (driver) account for 61% of all passenger car usage, whilst those with a driver and front seat passenger account for 27%. For this analysis it was assumed that all systems are capable of defining seat occupancy and therefore only deploy components when a seating position is occupied. In addition, for side airbags it was assumed that the impact will only occur on the driver's side (occupied) and result in a single, side airbag deployment. Table A1.4 defines the proportion of each component type likely to remain after each collision type, i.e. in moderate frontal collisions a passenger airbag is likely to remain undeployed in 61% of collisions.

Impact severity and direction	Occupant restraint component proportion remaining							
	DAB	**PAB**	**SAB x2**	**FBP-DRV**	**FBP-FSP**	**DASA**	**PASA**	**KAB**
Sev. front	0.0%	61.0%	100.0%	0.0%	61.0%	0.0%	61.0%	0.0%
Mod. front	0.0%	61.0%	100.0%	0.0%	61.0%	0.0%	61.0%	0.0%
Min. front	50.0%	80.5%	100.0%	50.0%	80.5%	50.0%	80.5%	50.0%
Sev. rear	100.0%	100.0%	100.0%	100.0%	100.0%	100.0%	100.0%	100.0%
Mod. rear	100.0%	100.0%	100.0%	100.0%	100.0%	100.0%	100.0%	100.0%
Min. rear	100.0%	100.0%	100.0%	100.0%	100.0%	100.0%	100.0%	100.0%
Sev. side	100.0%	100.0%	50.0%	50.0%	80.5%	100.0%	100.0%	100.0%
Mod. side	100.0%	100.0%	50.0%	50.0%	80.5%	100.0%	100.0%	100.0%
Min. side	100.0%	100.0%	85.0%	50.0%	80.5%	100.0%	100.0%	100.0%
Rollover	0.0%	61.0%	61.0%	0.0%	61.0%	0.0%	61.0%	0.0%
Body/mech.	100.0%	100.0%	100.0%	100.0%	100.0%	100.0%	100.0%	100.0%

Table A1.4: Occupant restraints remaining at EOL

A1.6 Occupant restraints remainder

By considering vehicle attrition, causation and likely consumption estimates, the number of live automotive pyrotechnics remaining and requiring treatment within the ELV waste stream each year in the UK have been calculated, Table A1.5. These calculations were based solely upon the previously identified restraint system components for front seat positions.

Year	Undeployed automotive pyrotechnics (millions)
2008	4.28
2009	5.47
2010	5.38
2011	6.02
2012	6.50

Table A1.5: Undeployed automotive pyrotechnics remaining at EOL by year

Appendix B

Particulate Matter Exposure Limit Values

B1 Limit values specified in standards for airbag PM effluents:

Component	Limit value (mg/m3)	Notes
NaOH	5	
Copper (Dust and Smoke)	50	
Cobalt (Dust and Smoke)	10	
Iron Oxide (Dust and Smoke)	1250	Already limited by max. particle concentration limit
TiO2	2500	Already limited by max. particle concentration limit
ZrO2	25	
B2O3	1000	Already limited by max. particle concentration limit
CaO	12.5	

Table B1.1: Airbag effluent concentration limits (Audi AG et al., 2001)

Component	Exposure type	Concentration limit
Sodium hydroxide (NaOH)	STEL	2mg/m^3
Potassium hydroxide (KOH)	STEL	2mg/m^3
Calcium hydroxide (CaOH)	8 hour	5mg/m^3

Table B1.2: Occupational exposure limits - alkaline substances

	Long term exposure (8hr) limit	
	Inhalable	**Respirable**
HSE (UK)	10 mg/m^3	4 mg/m^3
OSHA	15 mg/m^3	5 mg/m^3
ACGIH	10 mg/m^3	3 mg/m^3

Table B1.3: Long term particle exposure limit values (NIOSH 1994; 1998)

Component	**Vehicle level limit**	
	SAE USCAR24	**AKZV-01**
Total particulate	125.0 mg/m^3	125.0 mg/m^3
Water soluble particulates	75.0 mg/m^3	75.0 mg/m^3
Water insoluble particulates	50.0 mg/m^3	50.0 mg/m^3
Sodium azide (NaN_3) particulate	1.43 mg/m^3	-
Sub 10 micron particulate	Fraction to be reported only	-

Table B1.4: Vehicle level particle limits, (SAE, 2004; 2011a; Audi AG et al., 2001)

Appendix C

Particle morphology sampling calculations

C.1 Particle morphology sampling calculations

Equation 7 details the attempt to numerically quantify the sampling duration for morphology testing to reduce high grid loading instances.

$$D = \frac{\boldsymbol{F}}{\left(\frac{\boldsymbol{F}}{\boldsymbol{L}}\right)\times(\boldsymbol{S}\times\boldsymbol{N}\times\boldsymbol{P})} \qquad \textbf{(Equation 7)}$$

Key:		
Sample line cross sectional area	mm^2	L
Grid area	mm^2	G
Film area	mm^2	F
Sampling flow rate	cc/s	S
Number concentration	N/cc	N
Mean particle area	mm^2	P
Sampling Duration	S	D
Area covered per second	mm^2	T

Table C1.1: Morphology sampling duration equation key

For these calculations it was assumed that particles would not collect upon one another on the grid film and that collection on grid films would be uniform. In addition it was assumed that the number of particles collected would be directly proportional to the area of the film as a proportion of the sampling tube cross sectional area.

Appendix D

Test tank design and construction

D.1 Test tank design and construction:

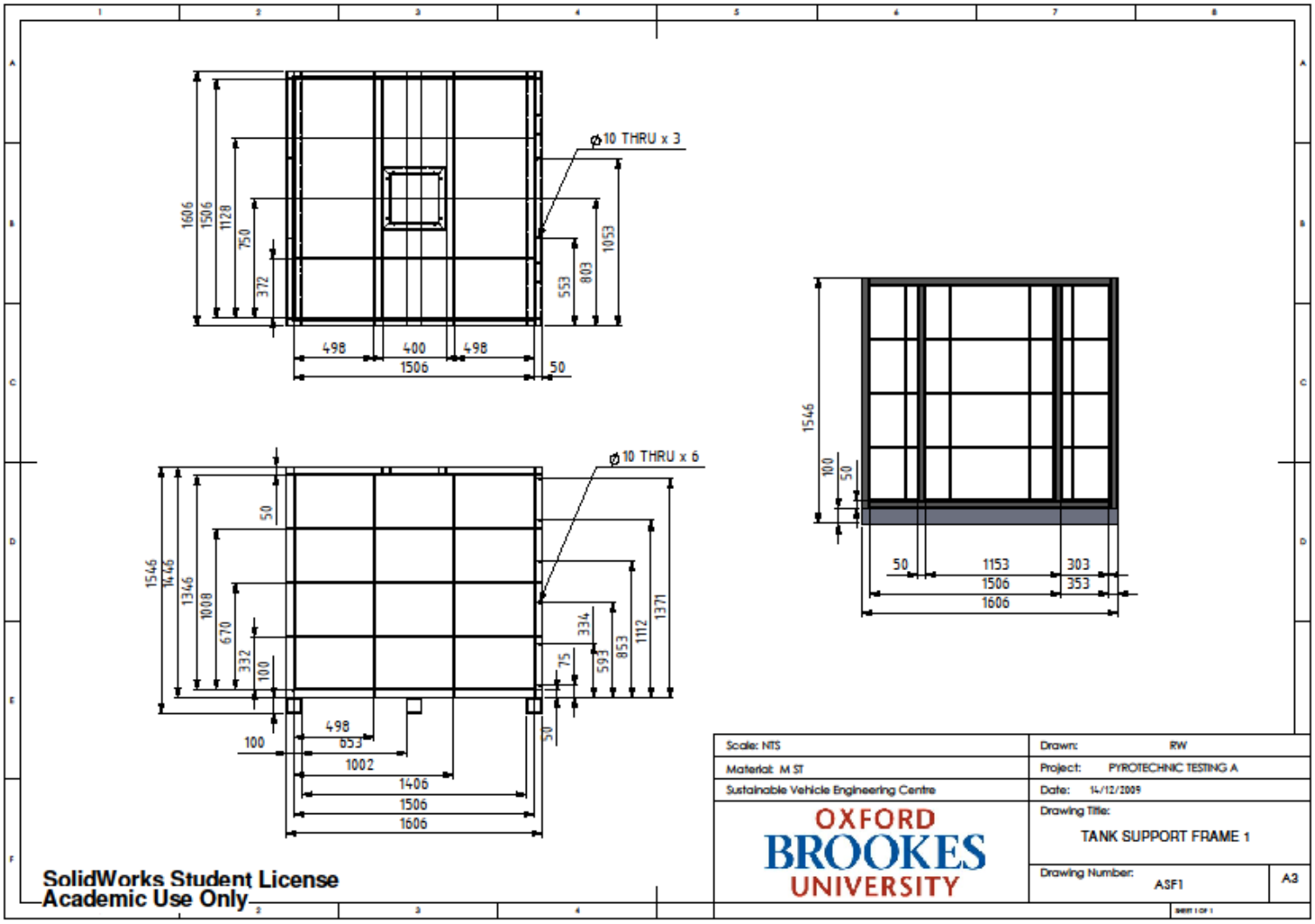
Ø10 THRU x 3
1606
1506
1128
750
372
553
803
1053
498
400
498
1506
50
Ø10 THRU x 6
1546
1446
1346
1008
670
332
100
50
75
334
593
853
1112
1371
100
498
653
1002
1406
1506
1606
50
1546
100
50
50
1153
303
1506
353
1606
SolidWorks Student License
Academic Use Only
Scale: NTS
Drawn: RW
Material: M ST
Project: PYROTECHNIC TESTING A
Sustainable Vehicle Engineering Centre
Date: 14/12/2009
OXFORD BROOKES UNIVERSITY
Drawing Title:
TANK SUPPORT FRAME 1
Drawing Number:
ASF1
A3

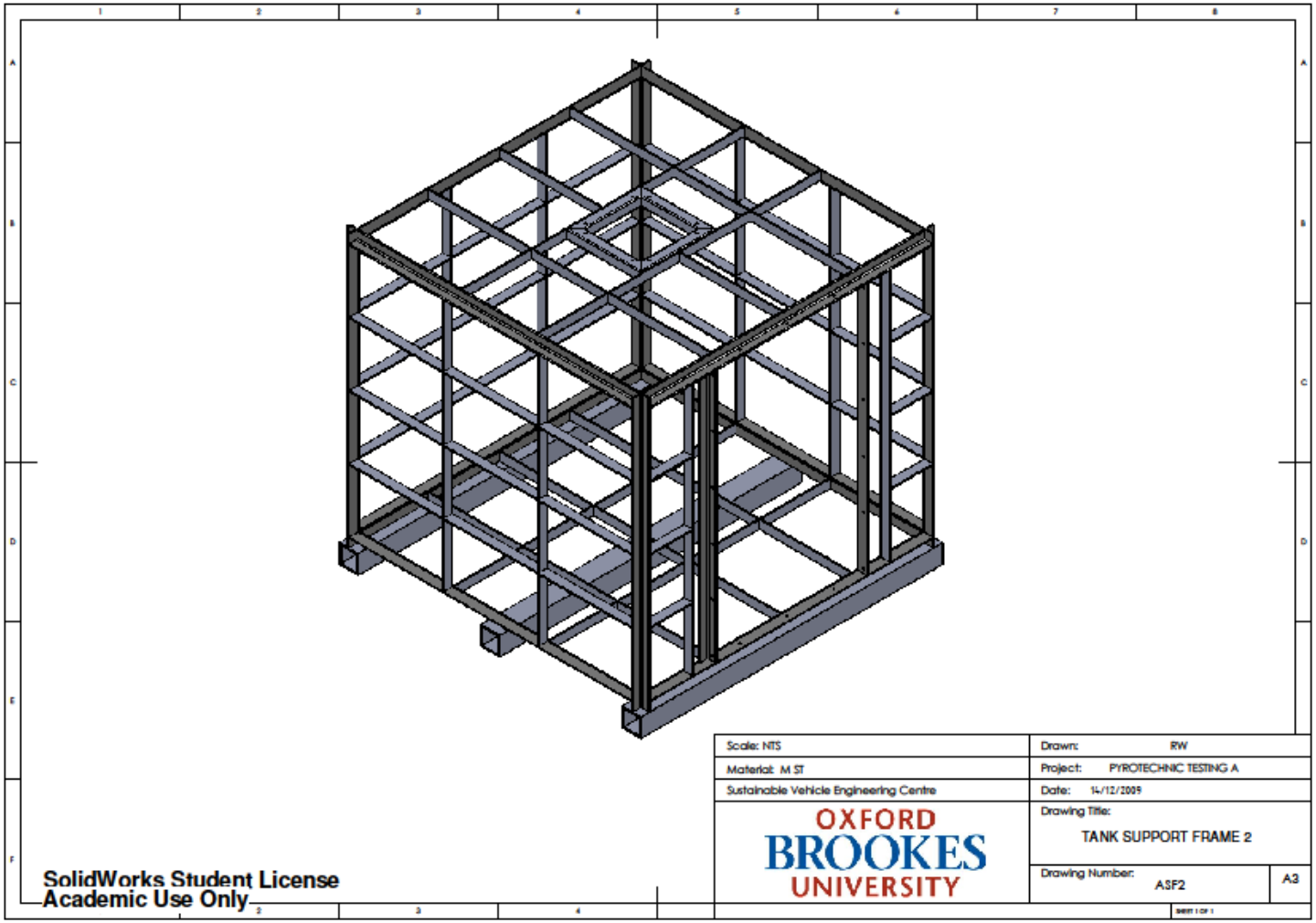

Figure D1.1: Test tank support frame

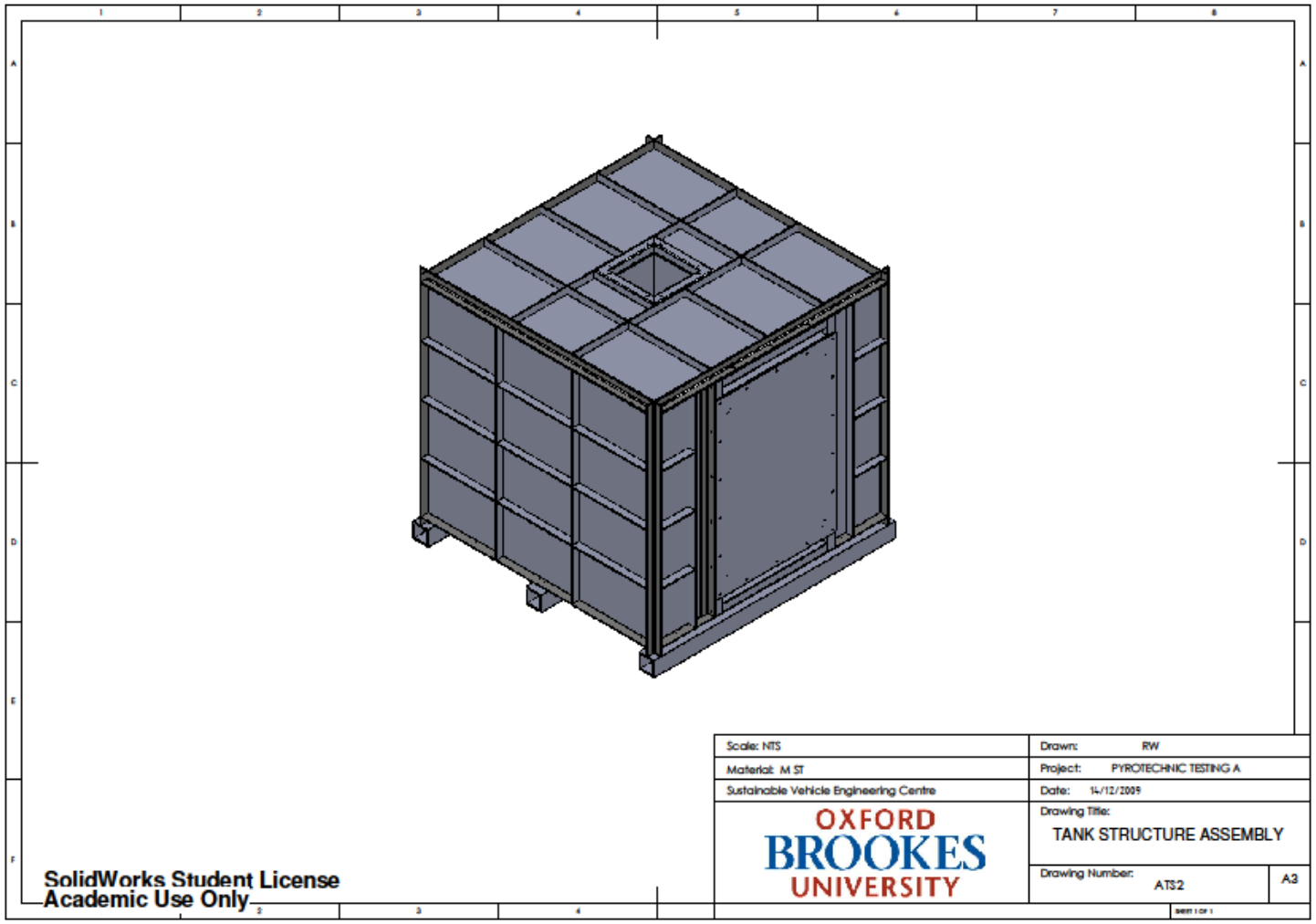

Figure D1.2: Test tank support frame

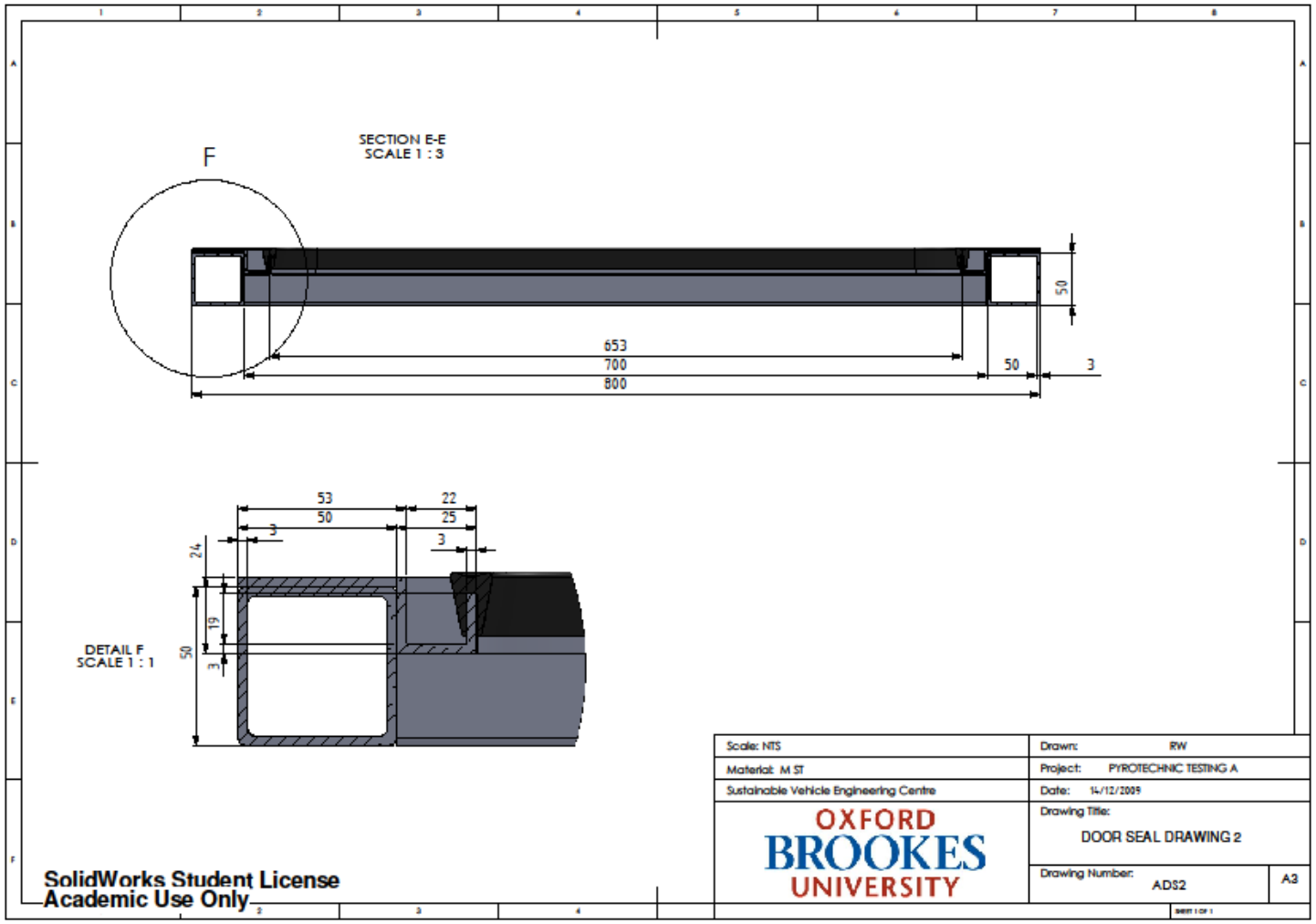

Figure D1.3: Test tank door seal detail

Figure D1.4: Test tank during construction 1

Figure D1.5: Test tank during construction 2

Figure D1.6: Test tank during construction 3

Figure D1.7: Test tank during construction 4

References

Adamson, I.Y.R., Prieditis, H., Vincent, R. (1999). Pulmonary toxicity of an atmospheric particulate sample is due to the soluble fraction', Toxicology and Applied Pharmacology, vol. 157, pp.43-50.

Adetunji, H., Pinto, L. M. M., Siddique, A. and Samuel, S. (2009). Potential occupational health risk from exposure to nano-scale particles from photocopiers - a pilot study. Revue Internationale sur l'Ingénierie des Risques Industriels. 2 (1): 15 – 27.

ARB (2002). Long-term health effects of PM 2.5: Recent Findings. [Online] Available: http://www.arb.ca.gov/research/health/healthup/may02.pdf.

ARC Automotive, Inc. (2009) Products, Automotive inflators, [Online], Available: http://www.arcautomotive.com/products.html [July 2011].

Aei (2007). [Online], Available: http://www.sae.org/automag/techbriefs/05-2007/1-115-5-18.pdf [May 2011].

Allen B. (2003). Opthalmic Care of the Combat Casualty: Textbooks of Military Medicine. Washington, USA. United States Government Printing.

Allen E, Smith P and Henshaw J (2001). A review of particle agglomeration. London, UK. AEA Technologies.

Assovskiy I.G, Chizhevskii O.T and Sergeev V.V (1997). Improvement of ballistic characteristics of gun propellants and charges using metallic additives. International Journal of Energetic Materials and Chemical Propulsion, vol. 4, issue 1-6.

Audi AG, BMW AG, Daimler Chrysler AG, Porsche AG und Volkswagen AG (2001). Arbeitskreis Zielvereinbarung, Pyrotechnische Rückhaltesysteme im Fahrwerk, AK-ZV 01, Arbeitskreis der Firmen.

Autodrain (2012). Airbag Tool [Online], Available: http://www.autodrain.net/products/air-bag-tool-product-page.php [March 2012].

Autoliv (n.d.). Seatbelt Pretensioners. [Online] Available: http://www.autoliv.com/ProductsAndInnovations/PassiveSafetySystems/Pages/Seatbelts/Pretensioners.aspx.

Automotive Systems Laboratory, Inc. (1995). Non-azide gas generating compositions with reduced toxicity upon combustion. U.S. Pat. 5,460,668.

Avetisian V, Berg P, Renz R and Karloff G (2006). Overmolded body for pyrotechnic initiator and method of molding same. U.S Pat. 7124688.

Banglmaier, R.F. & Rouhana, S.W. (2003). Investigation into the Noise Associated with Airbag Deployment: Part III – Sound Pressure Level and Auditory Risk as a Function of Inflatable Device, Annu Proc Assoc Adv Automot Med. vol. 47, pp. 25-50.

Barnes S.S, Wong W & Affeldt J.C (2012). A Case of Severe Airbag Related Ocular Alkali Injury. Hawaii J Med Public Health. Vol. 71, No. 8 pp.229–231.

Baron, P. (n.d.). Generation and Behavior of Airborne Particles (Aerosols), Division of Applied Technology. National Institute for Occupational Safety and Health Centers for Disease Control and Prevention. [Online], Available: http://www.cdc.gov/niosh/topics/aerosols/pdfs/aerosol_101.pdf [June 2012].

Bauberger, A. (2007). Pyrotechnic actuators for improved airbag adaptivity, Proceedings of the international pyrotechnic automotive safety symposium', Bordeaux, France, pp.32-42.

BBC (2010). Girl killed by inflating airbag during crash, [Online], Available: http://news.bbc.co.uk/1/hi/wales/8458944.stm [July 2011].

Berk, R.E. (2009a). Automated SEM/EDS analysis of airbag residue. I: Particle identification, Journal of Forensic Science, vol. 54, no. 1, pp. 60-69.

Berk, R.E. (2009b). Automated SEM/EDS analysis of airbag residue. II: Airbag residue as a source of percussion primer residue particles, Journal of Forensic Science, vol. 54, no. 1, pp. 69-76.

BMW (2013). Rescue manual, AG Munich, Germany [Online], Available: https://oss.bmw.de/rettungsleitfaden/en_Rescue_Manual_BMW_Mini.pdf [July 2013].

Boron Extrication (n.d.). Archives for list-of-vehicles-with-boron-and-uhss. [Online], Available: http://boronextrication.com/tag/list-of-vehicles-with-boron-and-uhss/ [January 2013].

Braver, E. R. & Kyrychenko, S.Y. (2004). 'Efficacy of side air bags in reducing driver deaths in driver-side collisions', American Journal of Epidemiology, vol. 159, no. 6, pp. 556-564.

British Standards Institution, (1993). BS EN 481:1993, BS 6069-3.5:1993 Workplace atmospheres. Size fraction definitions for measurement of airborne particles. BSI.

Brunekreef B and Holgate S.T (2002). Air pollution and health. The Lancet, vol. 360, issue 9341, pp.1233-1242.

Buzea, C., Pacheco Blandino, I.I., & Robbie, K. (2007). Nanomaterials and nanoparticles: Sources and toxicity, Biointerphases vol. 2, no. 4, pp. MR17 - MR172.

Camatini, M., Gualtieri, M. & Mantecca, P. (2011). Particles and health: State of the research, Polaris Research Center, Department of Environmental Science, University of Milano[Online], Available: http://www.aidic.it/aaas10/webpapers/69Camatini.pdf [July 2012].

Cambustion (2008). Cambustion application note DMS03. Sampling Engine Exhaust with the DMS500. [Online], Available: http://www.cambustion.com/sites/default/files/instruments/DMS/dms03v04.pdf [August 2010].

Cambustion (n.d.a). DMS instrument principle, DMS series principle, [Online], Available: http://www.cambustion.com/products/dms [February 2013].

Cambustion (n.d.b). DMS500 MkII Fast Engine Particulate Analyzer. [Online], Available: http://www.cambustion.com/products/dms500/engine [July 2012].

Cambustion. (n.d.c.) Fast response aerosol size measurements with the DMS500, [Online], Available: http://www.cambustion.com/products/dms500/aerosol [February 2013].

Carroll J.A, Cuerden R, Richards D, Smith S, Cookson R and Hynd D (2009). Matrix of serious thorax injuries by occupant characteristics, impact conditions and restraint type and identification of the important injury mechanisms to be considered in THORAX and

THOMO; Consisting of one main summary report and three annexes. European Commission DG RTD, Available http://www.biomechanics-coordination.eu/downloadables/Deliverables/COVER-D05-Annex%20I%20TRL-FINAL-Matrix%20of%20serious%20thorax%20injuries-24March2010.pdf

Caudle JM, Hawkes R, Howes DW, Brison RJ (2007). Airbag pneumonitis: a report and discussion of a new clinical entity. CJEM. Nov; 9(6):470-3.

CDX (2010). Auxiliary Systems: SRS Systems: Safety Systems. [Online] Available: http://www.cdxetextbook.com/auxil/srssystems/safety/seatbeltpretensioner.html

Chan, C.-Y. (2000). Fundamentals of crash sensing in automotive air bag systems. Warrendale, Pennsylvania, U.S.A. Society of Automotive Engineers, Inc. (SAE).

Chan, T.L., White, D.M. & Damian, S.A. (1989). Exposure characterization of aerosols and carbon monoxide from SIR, Journal of Aerosol science, vol. 20, pp. 657-665.

Choi, H.S., Ashitate, Y., Lee, J.H., Kim, S.H., Matsui, A., Insin, N., Bawendi, M.G., Semmler-Behnke, M., Frangioni, J.V. & Tsuda, A (2010). Rapid translocation of nanoparticles from the lung airspaces to the body, Nature Biotechnology. Vol. 28, pp. 1300-1303.

CITA (2002). Study 2. A test procedure for airbags. CITA.

Clarke S.W and Pavia D (1980). Lung mucus production and mucociliary clearance: Methods of assessment. Br. J. Clin Pharmac. Vol. 9, pp. 537-546

Clemo, K., Cross, G., & Morris, R. (2006). Report on recommended functional requirements including modelling and testing for smart restraint systems. PRISM Project Report R9/R10. [Online], Available: http://www.prismproject.com/08_R9R10_Merged_Final_Report.pdf [February 2013].

Conkling J.A and Mocella C.J (2011). Chemistry of Pyrotechnics: Basic principles and theory. FL, USA. CRC Press.

Conover K. (1992). Chemical burns from automotive air bag. Ann Emerg Med. Jun. 21(6)

Cox R.D (2013). Chemical Burns [Online], Available: http://emedicine.medscape.com/article/769336-overview [October 2013]

Cox, R.D., Balentine, J., VanDeVoort, J.T., Hirshon, J.M. & Halamka, J.D. (2013). 'Chemical burns', [Online], Available: http://emedicine.medscape.com/article/769336-overview [May 2013].

Cuerden, R. (2006). CCIS Accident Data Analysis, [Online], Available: http://www.trl.co.uk/files/general/2006-10-004-Topic.pdf [December 2012].

Cummings, P., McKnight, B., Rivara, F.P. & Grossman, D.C. (2002). Association of driver air bags with driver fatality: A matched cohort study, British Medical Journal, vol. 324, pp.1119–1122.

Cunningham, K., Brown, T.D., Gradwell, E. & Nee, P.A. (2000). Airbag associated fatal head injury: case report and review of the literature on airbag injuries, Journal of Accident and Emergency Medicine, vol. 17, pp. 139-142.

Davidson C.I, Phalen R.F and Solomon P.A (2005). Airborne Particulate Matter and Human Health: A Review. Aerosol Science and Technology, vol. 39, issue 8.

Dávila A, and Nombela M (2011). Development of a test tool to analyse airbag induced injuries. Paper number 11-0345. The 22nd ESV Conference Proceedings. The 22nd International Technical Conference on the Enhanced Safety of Vehicles (ESV) Washington, D.C., June 13-16

De Hartog, J.J., Hoek, G., Peters, A., Timonen, K.L., Ibald-Mulli, A., Brunekreef, B., Heinrich, J., Tiittanen, P., van Wijnen, J.H., Kreyling, W., Kulmala, M. & Pekkanen, J. (2003). Effects of fine and ultrafine particles on cardiorespiratory symptoms in elderly subjects with coronary heart disease: the ULTRA study, American Journal of Epidemiology,vol.157, pp.613–623.

De Vries S, Geerards AJM. (2007). Long-term sequelae of isolated chemical “airbag” keratitis. Cornea. 26(8):998–999.

DeCarloab, P.F., Slowikd, J.G., Worsnope, D.R., Davidovitsd, P. & Jimenezbc, J.L (2004). Particle morphology and density characterization by combined mobility and aerodynamic diameter measurements. Part 1: theory, Aerosol Science and Technology, vol. 38, no. 12, pp.A144 1185-1205.

Dekati (n.d.a). ELPI+ operating princliple [Online], Available: http://dekati.com/cms/elpiplus/operation [January 2012].

Dekati (n.d.b). ELPI+ specifications [Online], Available: http://dekati.com/cms/elpiplus/specifications [January 2012].

DfT (2009). Road Casualties Great Britain: 2009.London: Transport Statistics, The Stationery Office.

DfT (2010). Road Casualties Great Britain: 2010.London: Transport Statistics, The Stationery Office.

DfT (2011a). Strategic Framework for Road Safety. Making Roads Safer. Department for Transport.

DfT (2011b). Vehicle Licensing Statistics, Great Britain: Quarter 2 2011. Vehicle Licensing Statistics Quarterly Bulletin.

DfT (2012a). Road Casualties Great Britain: 2011.London: Transport Statistics, The Stationery Office.

DfT (2012b). Cooperative Crash Injury Study [May 2012].

DfT (2013). Certificate of Destruction Data: FOI Request [June 2013].

DfT (n.d.). Statistics at DFT, [Online], Available: https://www.gov.uk/government/organisations/department-for-transport/about/statistics [August 2011].

Diem, W. (2001) 'Anti-whiplash systems', AutoTechnology Vol. 1, No. 2, pp. 44-45.

Duma S.M, Rath A.L, Jernigan M.V, Stitzel J.D, Herring I.P (2005). The effects of depowered airbags on eye injuries in frontal automobile crashes. American Journal of Emergency Medicine, 23, 13–19.

Egerton R (2008). Physical Principles of Electron Microscopy: An Introduction to TEM, SEM, and AEM. NY, USA, Springer

Ellis, K.D., Minert, D.G., Saderholm, D.G. & Shaklik, B.M. (1998). Directional compressed gas inflator. U.S. Pat. 5826904 A.

Envco-Environmental Equipment (n.d.). Ambient (Non-Viable) Eight-Stage Cascade Impactors. [Online], Available: http://www.envcoglobal.com/catalog/product/stationary-pm-hardware/ambient-non-viable-eight-stage-cascade-impactors.html [January 2012].

Environment Agency (2012). Treatment facilities. [online] available http://www.environment-agency.gov.uk/business/topics/waste/143462.aspx

Epperly NA, Still JT and Law E. (1997). Supraglottic and subglottic airway injury due to deployment and rupture of an automobile airbag. Am Surg; 63: 979-81

EPSRC (n.d.). EPSRC Engineering instrument pool, [Online], Available: http://www.eip.rl.ac.uk/ [August 2012].

EuroNCAP (2009). Frontal impact testing protocol, Version 5.0. Euro NCAP (available from the Euro NCAP internet site: http://www.euroncap.com/files/Euro-NCAP-Frontal-Protocol-Version-5.0---0-808a8ef9-942b-4aed-a0c1-9d779b8b68f8.pdf).

EuroNCAP (2011). Test results: Jaguar XF. [Online] Available: http://www.euroncap.com/files/464_datasheet.pdf

EuroNCAP (2013). General questions about EuroNCAP [Online] Available: http://www.euroncap.com/Content-Web-Faq/b012b7f3-44f9-4755-94f9-a8642fd1402a/about-euro-ncap.aspx

EuroNCAP (n.d.). [Online], Available: http://www.euroncap.com/home.aspx [January 2011].

European Comission (2000). Directive 2000/53/EC of the European Parliament and of the Council of 18 September 2000 on end-of life vehicles

European Comission (n.d.). Vehicle: Safety design needs. [Online] Available: http://ec.europa.eu/transport/road_safety/specialist/knowledge/vehicle/safety_design_needs/cars.htm

Fernandez Espinosa, A.J., Ternero Rodriguez, M., Barragan de la Rosa, F.J. & Jimenez Sanchez, J.C. (2002). 'A chemical speciation of trace metals for fine urban particles', Atmospheric Environment, vol. 36, pp. 773-780.

Fisher Scientific (2004). Material Safety Data Sheet: Sodium Azide: 20960 [Online] Available: https://fscimage.fishersci.com/msds/20960.htm

Fogelzang A.E, Pimenov A.Y and Denisyuk A.P (1998). Mechanism of modifying ballistic properties of propellant formulations by fast-burning inclusions. Defence Science Journal, vol. 48, no. 4, pp.357-364

Ford (2012). Next-Generation Airbags on the All-New Ford Focus. [Online], Available: http://fordvideo.wieck.com/photos/Next-Generation-Airbags-on-the-All-New-Ford-Focus?query=focus+airbag [July 2013].

Ford (2013). Ford expands availability of rear inflatable safety belt to 2014 fushion.[Online], Available: https://media.ford.com/content/fordmedia/fna/us/en/news/2013/08/13/ford-expands-availability-of-rear-inflatable-safety-belt-to-2014.html [August 2013].

Frampton, R., Morris, R., Cross, G., & Page, M. (2005). Accident analysis methodology and development of injury scenarios. PRISM (Proposed Reduction of car crash Injuries

through improved SMart restraint development technologies) project report. [Online], Available: http://prismproject.com/R3_5_New_Images_Final.doc.pdf [June 2010].

Gao, N.P and Niu, J.L (2007). Modeling particle dispersion and deposition in indoor environments. Atmospheric Environment, Vol. 41, Issue 18, pp.3862-3876

Gault J.A, Vichnin M.C, Jaeger E.A and Jeffers J.B (1995). Ocular injuries associated with eyeglass wear and airbag inflation. J Trauma. Vol.38, no.4, pp.494–497.

Giordano, N. (2012). College Physics, Volume 1. Second Edition. USA. Cengage Learning.

Green, D.J., Mossi, D. G., Rink, K.K., Smith, B.W. (1999). Adaptive output fluid fueled airbag inflator. U.S. Pat. 5857699.

Grid-tech.com (n.d.). [Online], Available: http://www.grid-tech.com/catalog.htm [June 2010].

Gross KB, Haidar AH, Basha MA, Chan TL, Cwizdala CJ, Wooley RG and Popovich J. (1994). Acute pulmonary response of asthmatics to aerosols and gases generated by airbag deployment. Am J Respir Crit Care Med, Vol.150, pp.408-414

Gross KB, Kelly NA, Reddy S, Shah NJ and Grain TAK. (1999). Assessment of human responses to non azide effluents. 43rd Stapp Car Crash Conference Proceedings

Gross KB, Koets MH, D'Arcy JB, Chan TL, Wooley RG and Basha MA. (1995). Mechanism of induction of asthmatic attacks initiated by the inhalation of particles generated by airbag system deployment. J Trauma, Vol. 38, No. 4.

Gross, K.B., Haidar, A.H., Basha, M.A., Chan, T.L., Cwizdala, C.A., Wooley, R.G. & Popovich, J.R., J. (1994). Acute pulmonary response of asthmatics to aerosols and gases generated by airbag deployment, American Journal of Respiratory Critical Care Medicine, vol. 150, pp. 408-414.

Gross, K.B., Kelly, N.A., Reddy, S., Shah, N.J. & GRAIN, T.A.K (1999). Assessment of human responses to non azide effluents, 43rd Stapp Car Crash Conference, pp.365-376.

Hamaue, T., Takehara, H., Kameyoshi, H. & Mizuno, I. (2004). Seat belt retractor. U.S. Pat. 6722600.

Henry G.H. & Solverson, M.S (1995). Gas Generating Propellant. Pat. WO1995025709 A2.

Hetrick, J.W. (1952). Safety Cushion Assembly for Automotive Vehicles. U.S. Pat. 2649311 A.

Hickling, R. (1976). The noise of the automotive safety air cushion, Noise Control Engineering.

Hickling, R. (2002). Reducing impulsive sound due to airbag deployment in a passenger car. First Pan-American/Iberian meeting on acoustics, Cancun, Mexico.

Hinds, W.C. (1999). Aerosol technology: Properties, behavior, and measurement of airborne particles. Canada. John Wiley & Sons Inc.

Hollembeak, B. (2002). Automotive electricity and electronics (today's technician), Delmar Publishing.

Hollembeak, B. (2010). Today's Technician: Automotive Electricity and Electronics Classroom and Shop Manual Pack (Today's Technician: Automotive Electricity & Electronics), USA, Cengage Learning.

Home Office (2011). Crime in England and Wales 2010 to 2011. [Online], Available: https://www.gov.uk/government/publications/crime-in-england-and-wales-2010-to-2011 [December 2011].

HSE (2004). Health effects of particles produced for nanotechnologies. Merseyside, UK. HSE

HSE (2005). EH40/2005 Workplace exposure limits,Merseyside, UK. HSE.

HSE (2012). Working with substances hazardous to health: A brief guide to COSHH. Merseyside, UK. HSE

Huelke D.F, Moore J.L, Compton T.W, Rouhana S.W, Kileny P.R (1999). Hearing loss and automobile airbag deployments. Accid Anal Prev. vol.31, no.6, pp.789-92.

Hynd, D., Carroll, J.A., Richards, D., Wood, R. & Goodacre, O. (2011). Restraint system safety diversity in frontal impact accidents, Transport Research Laboratory.

ICRP (1994). Human Respiratory Tract Model for Radiological Protection, Ann. ICRP vol. 24, no. 1-3. [Online], Available: http://www.icrp.org/publication.asp?id=ICRP%20Publication%2066 [May 2010].

IDIS (n.d.). [Online], Available: http://www.idis2.com/ [January 2011].

IDIS (2011). Safe handling and neutralization of pyrotechnic devices in end of life vehicles. IDIS, Saarbruecken, Germany.

IIHS (1996). Status report. Vol. 31, No. 10 [Online], Available: http://www.iihs.org/externaldata/srdata/docs/sr3110.pdf [May 2010].

IIHS (n.d.). Highway safety topics. [Online], Available: http://www.iihs.org/iihs/topics [May 2011].

Image Systems (2012). TEMA Automotive. [Online] Available: http://www.imagesystems.se/image-systems-motion-analysis/products/tema-automotive.aspx

ISO (2009). ISO 15900:2009. Determination of particle size distribution -- Differential electrical mobility analysis for aerosol particles. ISO.

Jackson, E. (2012). SEDA USA. Discussion regarding in-vehicle deployment [email] (Personal communication, 2012)

Jaguar (2011). Jaguar safety,[Online], Available: http://www.jaguar.com/gl/en/xf/models_features/features/safety_security [October 2011].

JATO (2011). Restraint system fitment by year and sales volume, GB, 1998-2010. Troy, USA. JATO Analysis

JATO (n.d.). [Online], Available: http://www.jato.com/USA/Pages/Default.aspx [November 2012].

Kahane, C.J. (2006). An Evaluation of the 1998-1999 Redesign of Frontal Air Bags. Washington, USA. Department of Transportation.

Kelly, F.J (2003). Oxidative stress: its role in air pollution and adverse health effects. Occup Environ Med, Vol. 60, pp.612-616.

Kocbach Bolling, A., Pagels, J., Espen Yttri, K., Barregard, L., Sallsten, G., Schwarze, P.E. & Boman, C. (2009). Health effects of residential wood smoke particles: the importance of combustion conditions and physicochemical particle properties, Particle and Fibre Toxicology vol. 6, no. 29.

Kubota, N. (2002). Propellants and Explosives: Thermochemical Aspects of Combustion. Germany. Wiley.

Kulkarni, P., Baron, P.A. and Willeke, K. (2011). Aerosol Measurement: Principles, Techniques, and Applications, 3rd edition, John Wiley & Sons.

Larson, T.V. & Koenig, J.Q. (1994). Wood smoke: Emissions and non-cancer respiratory effects, Annual Review of Public Health, vol. 15, pp.133–156.

Lee, E.W. (1982). Sodium azide: bioavailability and metabolism in rats, GM Research Publication. GMR-4185.

Lewis University (1999). Material safety data sheet, Sodium azide[Online], Available: http://www.lewisu.edu/academics/biology/pdf/Sodium_Azide.pdf [June 2012].

Linderer, WM. (1953) 'Einrichtung zum schutze von in fahrzeugen befinlichen personen gegen verletzungen bei zusammenstoben', Deutsches Patentamt. Patentschrift. Nr: 816312, Classe: 63c, Gruppe: 70. [Online], Available: http://www.dpma.de/docs/service/klassifikationen/ipc/auto_ipc/de896312b.pdf [October 2011].

Linn W.S, Gong H, Clark K.W, Anderson K.R (2005). Evaluation of asthmatic volunteers' pulmonary responses to effluents from automotive airbags. Int. J. of Vehicle Design, 2005 Vol.38, No.4, pp.307 – 313.

Little, I.I. (1992). Airbag igniter having double glass seal. U.S. Pat. 5140906.

Machinery Lubrication (n.d.). The low-down on particle counters, [Online], Available: http://www.machinerylubrication.com/Read/351/particle-counters [December 2011].

Mackay, M., Hassan, A. M. & Hill, J. R. (1998). Current and future occupant restraint systems, Physical Medicine and Rehabilitation: State of the Art Reviews vol. 12, no. 1, pp. 29-38.

Marsh, L. (2011). Using dust from deployed airbags as trace material in automotive crimes, Trace Evidence Symposium, Missouri.

Mazieres J, Merault J.M, Borrel B, Barel P, Escamilla R and Didier A (2002). Acute bronchial constriction in a non-asthmatic patient provoked by airbag activation. Rev Mal Respir. 2002 Sep;19(4):537-8.

McCartt, A.T and Kyrychenko S.Y (2007). Efficacy of side airbags in reducing driver deaths in driver-side car and SUV collisions. Traffic Inj Prev, vol.8, pp.162-70.

McDonald R and Biswas P (2004). A methodology to establish the morphology of ambient aerosols. J. Air & waste Manage. Assoc. vol. 54, pp.1069-1078.

McFeely, W. J, Bojrab, D. I, Davis, K. G and Hegyi, D.F (1999). Otologic Injuries caused by Airbag Deployment, Otolaryngology-Head and Neck Surgery, vol. 121, pp.367-373.

Mercedes Benz (2002). Occupant Safety Systems. Mercedes Benz, USA.

Mertz, H. J. and Dalmotas, D. J. (2007). Effects of shoulder belt limit forces on adult thoracic protection in frontal collisions, SAE technical paper 2007-22-0015, Proceedings of the 51st Stapp car crash conference, U.S.A. Stapp car crash journal, 51. The Stapp Association, California, pp. 361-380.

Mitsubishi Motors (2007). Technology. [Online], Available: http://www.mitsubishi-motors.com/corporate/about_us/technology/review/e/pdf/2007/19e_11.pdf [December 2012].

Mittal M.K, Kallan M.J and Durbin D.R (2006). Breathing difficulty and tinnitus among children exposed to airbag deployment. Accid Anal Prev. Vol. 39, No. 3, pp.624-8.

Morris R and Crooks A (2007). Airbag disposal – Methods used across the industry in the UK, 2007 ipass conference, Bordeaux, France.

Morris, C.R., Zuby, D.S. & Lund, A.K. (1998). Measuring airbag injury risk to out-of-position occupants. Insurance Institute for Highway Safety. Canada, United States.NHTSA Enhanced Safety Vehicles 16 Conference. Paper Number 98-55-O-08.

Mueller, H. E., and Linn, B. (1998). Smart airbag systems, SAE technical paper 980558, Advances in Safety Technology, SP-1321, Society of Automotive Engineers Inc., Pennysylvania, pp. 161-163.

Mühlfeld, C., Gehr, P. & Rothen-Rutishauser, B (2008). Translocation and cellular entering mechanisms of nanoparticles in the respiratory tract, Swiss Med Weekly Vol. 138, No. 27-28, pp. 387-391.

Nazaroff W.W and Cass G.R (1989). Mathematical modeling of indoor aerosol dynamics. Environ. Sci. Technol. Vol. 23, Issue 2, pp.157-166.

New Star Environmental (2004). Eight Stage Non-viable Impactor. [Online] Available: http://www.newstarenvironmental.com/pdfs/8StageNV_brochure.pdf

NHTSA (1998). Federal Motor Vehicle Safety Standards and Regulations [Online] Available: http://www.nhtsa.gov/cars/rules/import/FMVSS/#SN208

NHTSA (2001a). Air bag technology in light passenger vehicles, [Online], Available: www.nhtsa.gov/DOT/NHTSA/NRD/AirBags/rev_report.pdf [March 2012].

NHTSA (2001b). Fifth/Sixth Report to Congress: Effectiveness of occupant protection systems and their use, NHTSA Report DOT HS 809 442. NHTSA.

NHTSA (2007). Lives saved in 2006 by restraint use and minimum drinking age laws, DOT HS 810 869. NHTSA, National Center for Statistics and Analysis. [Online], Available: http://www-nrd.nhtsa.dot.gov/Pubs/810869.pdf [January 2012].

NHTSA (2009a). Lives Saved Calculations for Seat Belts and Frontal Air Bags. DOT HS 811206. Washington, D.C., U.S.A.: U.S. Department of Transportation, National Highway Traffic Safety Administration, [Online], Available: http://www-nrd.nhtsa.dot.gov/pubs/811206.pdf [January 2011].

NHTSA (2009b). Lives saved in 2008 by restraint use and minimum drinking age laws, DOT HS 811 53. Washington, D.C., U.S.A.: U.S. Department of Transportation, National Highway Traffic Safety Administration, National Center for Statistics and Analysis.

NHTSA (2010). Lives saved in 2009 by restraint use and minimum drinking age laws, DOT HS 811 383. NHTSA, National Center for Statistics and Analysis. [Online], Available: http://www-nrd.nhtsa.dot.gov/Pubs/811383.pdf [January 2012].

NIOSH (1994). Manual of Analytical Methods, Fourth Edition Particulates not otherwise regulated, Total. Method 0500, Issue 2.

NIOSH (1998). Manual of Analytical Methods, Fourth Edition. Particulates not otherwise regulated, Respirable. Method 0600, Issue 3.

Nitrochemie Wimmis AG. (2005) High-performance propellants – for micro gas generators (MGG: pin-type, lead wire) and activators in the automotive industry. [Online], Available: http://www.nitrochemie.com/pdfdoc/Broschueren/Hochleistungsantriebe_fuer_Gasgeneratoren.pdf [June 2011].

NSW Centre for Road Safety. (n.d.). Side airbags, [Online], Available: http://roadsafety.transport.nsw.gov.au/stayingsafe/vehiclesafety/sideairbags.html# [June 2013].

Oberdörster, G., Maynard, A., Donaldson, K., Castranova, V., Fitzpatrick, J., Ausman, K., Carter, J., Karn, B., Kreyling, W., Lai, D., Olin, S., Monteiro-Riviere, N., Warheit, D. & Yang, H. (2005). Principles for characterizing the potential human health effects from exposure to nanomaterials: elements of a screening strategy, Particle and Fibre Toxicology, vol. 2, no. 8.

Office of Vehicle Safety Research. (1999). Updated review of potential test procedures for FMVSS no. 208, NHTSA, [Online], Available: www.nhtsa.gov/cars/rules/import/FMVSS [March 2012].

OSHA (2011). Standard 1910.134. Respiratory protection, personal protective equipment. [Online], Available: https://www.osha.gov/pls/oshaweb/owadisp.show_document?p_id=12716&p_table=standards [October 2012].

Ostiguy, C., Lapointe, G., Trottier, M., Ménard, L., Cloutier, Y., Boutin, M., Antoun, M. & Normand, C. (2006). Health effects of nanoparticles. Studies and research projects, IRSST [Online], Available: http://www.irsst.qc.ca/media/documents/pubirsst/r-469.pdf [May 2011].

NIOSH (1998). Particulates not otherwise regulated, respirable method 0600. NIOSH Manual of Analytical Methods (NMAM), Fourth Edition. No. 3. pp. 1-6. [Online], Available: http://www.cdc.gov/niosh/docs/2003-154/pdfs/0600.pdf [January 2012].

NIOSH (1994). Particulates not otherwise regulated total method 0500. NIOSH Manual of Analytical Methods (NMAM), Fourth Edition, no.2, pp. 1-3.

Pérez-Camarero E.R, De Cortazar J.L, Caudevilla C.J, Cabané J.M, Boleas M.E, Cilveti M.L (2000). Airbag lesions. Eur J Emerg Med. Vol. 7, no.2, pp.160.

Perotto, C. and Banes, L. (2002). Green propellant with high temperature stability for micro gas generators for automotive safety, Proceedings of the 29th International Pyrotechnics Seminar, pp.125-132.

Pietz, J.F. (1975). Method and composition for generating nitrogen gas. U.S. Pat. 3895098 A.

Poole, D.R. (1991). Azide-free gas generant composition with easily filterable combustion products. U.S. Pat. 5035757 A.

Pope, C.R., Burnett, M., Thun, E., Calle, D., Krewski, K., & G. Thurston, G (2002). 'Lung cancer, cardiopulmonary mortality, and long-term exposure to fine particulate air pollution', Journal of the American Medical Association, vol. 28, no. 9, pp. 1132-1141.

Price, P. (2009). Direct Injection Gasoline Engine Particulate Emissions. PhD Thesis. Oxford University.

Reed M.P (1994). Skin burns from airbag exhaust gas: laboratory experiments and mathematical modeling. Final report. UMTRI-94-24. Accessible at http://deepblue.lib.umich.edu/handle/2027.42/1073

Renault UK. (n.d.). Renault Restraint & Protection. Retrieved September 2, 2012, from Renault: www.renault.co.uk/about/safety/restraints.aspx

Renault. (2009). Renault and car safety, Anti-submarining airbag[Online], Available: http://www.renault.co.uk/about/safety/airbags.aspx [March 2013].

Re-Source Engineering Solutions. (n.d.) [Online], Available: http://www.indra.fr/re-source_engineering_solutions.html [May 2009].

Richardson, W.B., Rink, L.M. & Rink, K.K. (1997). Liquid-fueled inflator with a porous containment device. U.S. Pat. 5607181 A.

Richert, J., Coutellier, D., Götz, C. & Eberle, W. (2007). Advanced smart airbags: The solution for real-life safety?' International Journal of Crashworthiness vol. 12, pp.159-171.

Risto, P (2002). Assessing industrial pollution by means of environmental samples in the Kemi-Tornio region, Academic Dissertation to be presented with the assent of the Faculty of Science, University of Oulu, for public discussion in Raahensali (Auditorium L 10), Linnanmaa[Online], Available: http://jultika.oulu.fi/Record/isbn951-42-6870-9 [May 2012].

Ruzer L.S and Harley N.H (2012). Aerosols Handbook: Measurement, Dosimetry, and Health Effects, Second Edition. FL, USA. CRC Press

SAE (2004). USCAR24. Uscar Inflator Technical Requirements and Validation.Detroit, USA. SAE.

SAE (2010). J1855: Deployment of Electrically Activated Automotive Air Bags for automobile Reclamation. Detroit, USA. SAE.

SAE (2011a). J1794 SAE Restraint Systems Effluent Test Procedure (STABILIZED Aug 2011). Detroit, USA. SAE.

SAE (2011b). J1630: Airbag Module Deployment Test Procedure. Detroit, USA. SAE

SAE (1996). J1794 SAE Restraint Systems Effluent Test Procedure. Detroit, USA. SAE.

SMMT (2010). UK Car Top 10 Registrations from 1990-2009. SMMT Vehicle data.

SafetyNet (2009). Vehicle Safety. [Online] Available: http://ec.europa.eu/transport/road_safety/specialist/knowledge/pdf/vehicles.pdf [March 2010]

Schneidera, J., Weimera, S., Drewnicka, F., Borrmanna, S., Helasc, G., Gwazec, P., Schmidc, O., Andreaec, M.O. & Kirchnerd, U (2006) 'Mass spectrometric analysis and

aerodynamic properties of various types of combustion-related aerosol particles', International Journal of Mass Spectrometry, vol. 258, No. 1-3, pp. 37-49.

Schreck, R.M., Rouhana, S.W., Santrock, J., D'Arcy, J.B., Wooley, R.G., Bender, H., Terzo, T.S., DeSaele, K.H., Webb, S.R. & Salva, D.B. (1995). Physical and chemical characterization of airbag effluents, Journal of Trauma, vol. 38, no. 4, pp. 528-32.

Shaddix, C.R., Palotásb, A.B., Megaridisc, C.M., Choid, M.Y. & Yange, N.Y.C. (2005). Soot graphitic order in laminar diffusion flames and a large-scale JP-8 pool fire, International Journal of Heat and Mass Transfer, vol. 48, no. 17, pp. 3604-3614.

Shearer, S.A. & Hudson, J.R. (n.d). 'Fluid Mechanics: Stokes' Law and Viscosity' Measurement Laboratory. Investigation No. 3. Biosystems and Agricultural Engineering"

Shepich, T.J. (1990). OSHA Safety Hazard Information Bulletin on Automobile Air Bag Safety. United States Department of Labor, Occupational Safety and Health Administration. [Online], Available: https://www.osha.gov/dts/hib/hib_data/hib19900830.html [June 2012].

Sioutas, C. (1999). Evaluation of the measurement performance of the scanning mobility particle sizer and aerodynamic particle sizer, Aerosol Science and Technology Vol. 30, No. 1, pp. 84-92.

Smally A.J, Binzer A, Dolin S and Viano D (1992). Alkaline chemical keratitis: eye injury from airbags. Ann Emerg Med. vol. 21, no. 11, pp.1400–1402.

Starner, A. (1998). Airborne Particulates In Automotive Airbags, SAE Technical Paper 980645.

Steel, R.G.D, & Torrie, J.H (1960). Principles and Procedures of Statistics with Special Reference to the Biological Sciences. McGraw Hill, pp.187, 287.

Stein, J.D. (1999). Air bag and ocular injuries, Transactions of the American Ophthalmological Society, vol. 97, pp. 59–86.

Stein, S. (2005). Squeezing Blood Out of a Turnip – Why the Pharmaceutical Industry Struggles So Much With Impactor Data', AAPS ITFG Meeting -Applications And Calibration For Cascade Impaction.

Stellman J (1998). Encyclopaedia of Occupational Health and Safety: Volume I. Geneva, Switzerland. International Labour Office

Subash, M., Manzouri, B. & Wilkins, M. (2010). Airbag-induced chemical eye injury, European Journal of Emergency Medicine, vol. 17, no.1, pp. 22-3.

Sutphen, R.F. and Varner, R.W. (2003). Commercial Vehicle Accident Reconstruction and Investgation.Lawyers & Judges Publishing Co. Inc. p.313."

Swanson-Biearman B, Mrvos R, Dean B.S, Krenzelok E.P (1993). Air bags: lifesaving with toxic potential? Am J Emerg Med. vol. 11, no. 1, pp.38-39.

Takata (2013). Where are the airbags located? [Online] Available: http://www.takata.com/en/around/airbag06.html

The FBI (2011). FBI Law Enforcement Bulletin. The Current Status of GSR Examinations. [Online], Available: http://www.fbi.gov/stats-services/publications/law-enforcement-bulletin/may_2011/TheCurrentStatusofGSRExaminations [June 2013].

The Northern Echo (2012). Driver dies after breathing in airbag gases [Online], Available: http://www.thenorthernecho.co.uk/news/9730969.Driver_dies_after_breathing_in_airbag_gases/ [June 2012].

The University of Manchester. (n.d.a). Centre for Atmospheric Science. Condensation Particle Counters (CPC). [Online], Available: http://www.cas.manchester.ac.uk/restools/instruments/aerosol/cpc/ [July 2012].

The University of Manchester. (n.d.b). Centre for Atmospheric Science. Scanning Mobility Particle Sizer (SMPS). [Online], Available: http://www.cas.manchester.ac.uk/restools/instruments/aerosol/scanning/index.html [July 2012].

Tintinalli J. (2004). Emergency Medicine. Philadelphia: McGraw Hill.

Toyota (n.d.). Restraint device: Supplemental Restraint System (SRS) airbag[Online], Available: http://www.toyota-global.com/innovation/safety_technology/safety_technology/technology_file/passive/airbag.html [March 2010].

Transport Scotland. (2012). National Travel Survey: Scottish Results 2009/2010 [Online], Available: www.transportscotland.gov.uk/analysis/statistics/publications/nts-scottish-results-previous-editions

TRW Occupant Safety Systems. (2011). Occupant Safety Systems, [Online], Available: http://www.trw.com/sub_system/active_control_retractor_2 [February 2011].

TRW. (n.d.a). Frontal Airbags. [Online], Available: http://www.trw.com/occupant_safety_systems/airbags/frontal_airbags [August 2013].

TRW. (n.d.b). Load limiters. [Online], Available: http://www.trw.com/occupant_safety_systems/seat_belts/load_limiters [September 2012].

TSI (2010). Aerosol statistics lognormal distributions and dN/dlogDp, Particle Instruments. Particle Research. Application Note PR-001. USA.

TSI (n.d). Differential Mobility Analyzer 3081 [Online], Available: http://www.tsi.com/Differential-Mobility-Analyzer-3081/ [May 2012].

Tug, I.C. (2005). WP1: task 1.1: State of the art and patent search, Proposed Reduction of Car Crash Injuries Through Improved Smart Restraint Development Technologies, R1 T1.1 [Online], Available: http://www.prismproject.com/SOTA_Final.pdf [June 2010].

U.S Army Medical Department (n.d). [Online], Available: http://www.cs.amedd.army.mil/borden/ [July 2011].

Ulrich D, Noah E.M, Fuchs P & Pallua N (2001). Burn injuries caused by air bag deployment. Burns, Vol.27, No. 2, pp.196-9

United States Department of Labor. Occupational Safety and Health Administration. (n.d.) Occupational Exposure Limits (OELs). [Online], Available: https://osha.europa.eu/en/topics/ds/oel/members.stm [March 2012].

United States Department of Labor. Occupational Safety and Health Administration. (n.d.) Permissible Exposure Limits (PELs). [Online], Available: https://www.osha.gov/dsg/topics/pel/ [March 2012].

United States Environmental Protection Agency. (n.d) Particulate Matter, Health. [Online], Available: http://www.epa.gov/pm/health.html [May 2013].

University of Utah (n.d). Lecture 3. Brief Overview of Traditional Microscopes. College of Engineering. [Online], Available: http://www.eng.utah.edu/~lzang/images/Lecture_3_conventional-Microscope.pdf [January 2011].

US Dept. Energy (2010). Saab 9000. Compare Side-by-side: Specs [Online] Available: http://www.fueleconomy.gov/ [May 2011]

Vincent, J.H. (2007). Aerosol Sampling: Science, Standards, Instrumentation and Applications. England, John Wiley & Sons Ltd.

Vogel, H.J. (2007). Drug Discovery and Evaluation: Pharmacological Assays. New York. Springer.

VOI. (2010). Variable Output Inflators (VOI), [Online], Available: http://www.worldvoi.com/variable.shtml [September 2012].

VOI. (n.d.). Single-Stage Ampi Airbag Inflators.[Online], Available: http://www.worldvoi.com/single_stage.shtml [December 2010].

Volkswagen (2008). Research roadmap. [Online], Available: http://www.volkswagenag.com/content/vwcorp/info_center/en/themes/2008/06/research_roadmap_2008.html [October 2011].

Volvo (2009). Volvo's three point safety belt turns 50, [Online], Available: https://www.media.volvocars.com/global/en-gb/media/pressreleases/20115 [July 2013]

Volvo (2013). The all-new Volvo V40 – Pedestrian Airbag Technology, [Online], Available: https://www.media.volvocars.com/global/en-gb/media/videos/42391 [July 2013].

Vortex Depollution (2013). Airbag Deployment Tool [Online], Available http://www.vortexdepollution.com/products/vehicle-processing-equipment/air-bag-deployment-tool/air-bag-deployment-tool [January, 2013].

Vouitsis, E., Ntziachristos, L. & Samaras, Z. (2003). Particulate matter mass measurements for low emitting diesel powered vehicles: what's next? Progress in Energy and Combustion Science. vol. 29, Issue 6, pp. 635-672.

Wallis L.A & Greaves I (2002). Injuries associated with airbag deployment. Emerg Med J, Vol.19, pp.490-493

Wentzel, M., Gorzawski, H., Naumannc, K.H., Saathoff, H. & Weinbruch, S. (2003). Transmission electron microscopical and aerosol dynamical characterization of soot aerosols', Aerosol Science, vol. 34, pp. 1347-1370.

Wheatley AD, Sadhra S, Beach JR (1997). Exposure to toxic gas and particle phase pollutants evolved during deployment. Indoor and Built Environment, 1997, 6(3), 134-139.

White J.E, McClafferty K, Orton R.B, Tokarewicz A.C & Nowak E.S (1995) Ocular alkali burn associated with automobile air-bag activation. CMAJ. Vol. 153, no. 7, pp.933–934.

World Health Organization (1984). Evaluation of exposure to airborne particles in the work environment. Geneva, Switzerland. WHO.

World Health Organization (1999). Hazard Prevention and Control in the Work Environment: Airborne Dust. Geneva, Switzerland. WHO.

World Health Organization (2013). Health Effects of Particulate Matter. Copenhagen, Denmark. WHO.

Wyatt, J.M. (2011). Analysis of particles produced during airbag deployment by scanning electron microscopy with energy dispersive x-ray spectroscopy and their deposition on surrounding surfaces: a mid-research summary, Advanced Microscopy Technologies for Defense, Homeland Security, Forensic, Life, Environmental, and Industrial Sciences, vol. 803604.

Yi, S., Zhang, F., Qu, F. & Ding, W. (2012). Water-insoluble fraction of airborne particulate matter (PM(10)) induces oxidative stress in human lung epithelial A549 cells, Environmental Toxicology, [Electronic], Available: http://www.ncbi.nlm.nih.gov/pubmed/22331617 [June 2012].

Zheng, Z., Johnson, K.C., Durbin, T.D., Jung, H., Hu, S., Huai, T & Kittleson, D.B (2011). Particle mass and particle number emissions from a heavy-duty diesel vehicle under real-world driving conditions and a standard driving cycle, College of Engineering, Center for Environmental Research and Technology. University of California, Riverside.

Ziegahn, K. & Nickl, J. (2002). Airbag emissions: the quantification of gases, dust and acoustics in practice', 6th International Symposium and Exhibition on Sophisticated Car Occupant Safety Systems, Karlsruhe, Germany. Fraunhofer-Institut fuer Chemische Technologie (ICT).